

Dissertation
submitted to the
Combined Faculties for the Natural Sciences and for Mathematics
of the Ruperto-Carola University of Heidelberg, Germany
for the degree of
Doctor of Natural Sciences

presented by

Diplom-Chemikerin Florentine Wahl
born in Freiburg i. Br., Germany
oral-examination: March 3rd 2011

**Modified Oligonucleotides:
Investigations and Applications of the
Diels-Alderase Ribozyme**

Referees: Prof. Dr. Andres Jäschke
Prof. Dr. Stefan Wöfl

Acknowledgements

First and foremost I want to thank my supervisor Prof. Andres Jäschke, for giving me the opportunity to work in his research group, as well as for his constant support, encouragement and guidance during my thesis.

I am thankful to Professor Wölfl for accepting to review and co-examine this thesis. Furthermore I want to thank Prof. Fricker and Prof. Haefeli to who agreed to take part in my oral exam.

I owe sincere and earnest thankfulness to Dr. Roberto Fiammengo for mentoring me and for his support and friendship throughout all these years.

My thanks also go to Viola Funk and Karin Weiß, who supported me in any possible way. The personal of the IPMB, Heiko Rudy for everything he ever did help me with, Tobias Timmermann for acquiring NMR spectra and his support with computer problems, Besarta Ljaic and Sandra Suhm for their synthetic expertise, Steffi Dräger for her help.

Big thanks also go to my interns Michael Wrede, Helen Hagen, Michael Morgen and Michaela Stach for their excellent work.

Special thanks to Benjamin Strauss, Marie Winz, Dr. Roberto Fiammengo, Anna Wiesmayer, Dr. Alexander Niert and André Krause for proof-reading the manuscript.

Furthermore I want to thank my friends Dr. Bernd Sterling, Dr. Dave Smith and Martina Mechler for their invaluable support and especially Dr. Thomas Schultz for believing in me and make me believe in myself.

I am obliged to many of my colleagues - the present and past members of the Jäschke lab as well as the Helm group, who all helped me, contributed to this thesis and always created a good working atmosphere. Anna, for her help in the lab, as well with my terrace and the breaks spent together. Benjamin, for invaluable help during the last couple of months. Marie, for her advice. Sandeep, for great discussions and his support with my project. Armine and Martin, for introducing me into the world of biology. Matthias for his support. Ayan, for the good discussions. Juliane, André, Alex, Steffi K., Ankita, Surjendu, Hana, Steffi P., Marco, Salifu, Markus P., Felix, Madeleine, Michaela, Markus H., Mihaela ...

I am truly indebted and thankful to all my friends, who supported me during these years and helped me to get through the ups and downs of this thesis. Terje for the good times spent together.

My parents and my sister have always provided strong and consistent support. Without them I wouldn't be where I am now and I will forever be grateful for that.

For my family

Modified Oligonucleotides: Investigations and Applications of the Diels-Alderase Ribozyme.

1st Referee: Prof. Dr. Andres Jäschke

2nd Referee: Prof. Dr. Stefan Wöfl

The hypothesis of the origin of life was fundamentally changed by the discovery of catalytic RNA. The fascinating fact that RNA can function as a catalyst in the formation of carbon-carbon bonds, thereby creating enantiomeric centers and thus potential building blocks for life-sustaining structures, is of great importance to those who wish to understand biocatalytic processes. Ribozymes are generally identified by *in vitro* selection. Such an artificial ribozyme was utilized for the work presented in this dissertation; specifically, the Diels-Alderase ribozyme was the focus of the investigation. This ribozyme catalyzes a Diels-Alder reaction between anthracene and maleimide. The work presented herein revolved around modifications of oligonucleotides on different levels. Modification of RNA with organic moieties is indispensable for effective *in vitro* selection of such ribozymes.

This thesis consists of three parts. In the first, new pathways were established for the synthesis of modified guanosine monophosphates (GMPs). The ability of the enzyme T7 RNA polymerase to incorporate these modified GMPs during transcription priming coined the term initiator nucleotides. The syntheses of a substituted anthracene and aldehyde-modified initiator nucleotides connected with a flexible polyethylene glycol linker were realized in just three synthetic steps. The incorporation of the initiator nucleotides into short RNA transcripts was investigated, as well as their incorporation into an RNA library with a randomized region eligible for *in vitro* selection. Excellent incorporation rates up to 77% were obtained for the transcription into the RNA library. The reactivity of thereby modified RNA molecules was subsequently studied in chemical reactions. Whereas the anthracene derivative could be reacted in a Diels-Alder reaction, the aldehyde led to full conversion in the reaction with hydrazides.

In the second part of this thesis, the effect of divalent metal ions on the folding and stability of the Diels-Alderase ribozyme was studied in UV thermal denaturation experiments. Low concentrations of Mg²⁺ cations led to secondary structure stabilization of up to 85°C. Thermal denaturation studies of the wild-type ribozyme and comparison to mutants complement other ongoing investigations of the complex interplay of non-standard base pairs and triples in the ribozyme structure. While the wild-type ribozyme exhibited a significant stabilization in the presence of Mg²⁺ cations, a comparable stabilization of the mutants could not be observed. In accordance with the findings in other studies, the best interpretation of this effect on stability was that the mutants, despite their ability to form a pseudoknot structure, could not undergo further compaction.

In the third part of this thesis, the Diels-Alderase ribozyme, which causes a remarkable acceleration of the Diels-Alder reaction rate, was successfully used as a catalyst for fluorescently labeling oligonucleotides *in cis* and *in trans*. Investigations of the substrate specificity of the ribozyme revealed that only fluorescent maleimide dyes with five carbon atoms next to the dye were accepted as substrates. This distinct feature was utilized as a bioorthogonal labeling strategy for the Diels-Alder bioconjugation of anthracene-modified oligonucleotides with equimolar proportions of fluorescent dyes. A new dual orthogonal labeling strategy was achieved by using an iodoacetamide dye for the thiol modification and a maleimide dye for the anthracene modification within the same DNA strand. For the anthracene modification, the Diels-Alderase ribozyme was employed as a catalyst.

Modifizierung von Oligonukleotiden: Untersuchungen und Anwendungen des Diels-Alderase Ribozyms.

1. Gutachter: Prof. Dr. Andres Jäschke
2. Gutachter: Prof. Dr. Stefan Wöfl

Die Entdeckung, dass RNA katalytische Eigenschaften aufweist, beeinflusste die Hypothese über den Ursprung des Lebens fundamental. Für das Verständnis biokatalytischer Prozesse ist die faszinierende Tatsache, dass RNA die Bildung neuer Kohlenstoff-Kohlenstoff Bindungen katalysieren und dabei Stereozentren generieren kann von entscheidender Bedeutung. Die vorliegende Arbeit basiert auf der Erforschung und Anwendung eines solchen Ribozyms - des Diels-Alderase Ribozyms. Dieses Ribozym katalysiert die Diels-Alder Reaktion zwischen Anthracen und Maleimid. Ribozyme werden grundsätzlich durch *in vitro* Selektion identifiziert. Ein wichtiges, zentrales Thema dieser Arbeit ist die Modifikation und Funktionalisierung von Oligonukleotiden. Die Modifikation von RNA durch funktionelle Gruppen ist für die *in vitro* Selektion derartiger Ribozyme unverzichtbar.

Im ersten Teil der Arbeit wurden neue Synthesewege chemisch modifizierter Guanosinmonophosphate (GMP) untersucht. Die Fähigkeit des Enzyms T7 RNA-Polymerase während der Transkription GMP spezifisch als erste Base einzubauen, prägte dabei den Namen Initiatornukleotid. Die Darstellung eines Anthracen-Derivates und eines Aldehyds mit einem flexiblen Polyethylenglykol-Linker konnte in nur drei Syntheseschritten erreicht werden. Der Einbau der Initiatornukleotide in kurze RNA-Transkripte wurde ebenso wie der Einbau in eine für die *in vitro* Selektion geeignete RNA-Bibliothek mit randomisiertem Bereich untersucht und optimiert. Dabei konnten Inkorporationsraten bis zu 77% für den Einbau in die RNA Bibliothek erzielt werden. Anschließend wurde die Reaktivität der dabei modifizierten RNA Moleküle untersucht. Das Anthracen-Derivat konnte in einer Diels-Alder Reaktion umgesetzt werden, während der Aldehyd vollständig mit Hydraziden reagierte.

Im zweiten Teil wurde der Einfluss zweiwertiger Metallionen auf die Faltung und Stabilität des Diels-Alderase Ribozyms in UV-Denaturierungsexperimenten untersucht. Dabei konnte gezeigt werden, dass bereits geringe Konzentrationen von Mg^{2+} -Kationen in der Lage sind, die Sekundärstruktur bis 85°C zu stabilisieren. Studien zur thermischen Denaturierung des Wildtyps sowie Mutanten ergänzen andere laufende Studien zur Erforschung des komplexen Zusammenspiels ungewöhnlicher Basenpaarungen und Basentripel in der Ribozymstruktur. Obwohl beim Wildtyp eine signifikante Stabilisierung durch Mg^{2+} festgestellt wurde, konnte eine ebensolche Stabilisierung der Mutanten nicht nachgewiesen werden. In Übereinstimmung mit anderen Studien kann dies so interpretiert werden, dass die Mutanten, trotz ihrer Fähigkeit einen Pseudoknoten zu bilden, keine weiter Kompaktierung erfahren.

Im dritten Teil der Arbeit wurde das Diels-Alderase Ribozym, welches eine bemerkenswerte Reaktionsbeschleunigung hervorruft, erfolgreich als Katalysator für die Markierung von Oligonukleotiden mit Fluoreszenzfarbstoffen sowohl *in cis* als auch *in trans*, eingesetzt. Untersuchungen zur Substratspezifität haben gezeigt, dass nur Maleimide-Derivate mit fünf Kohlenstoffatomen zwischen Maleimid und Fluoreszenzfarbstoff als Substrat erkannt werden konnten. Dieses distinktive Merkmal konnte genutzt werden, um eine neue bioorthogonale Markierungsmethode für Anthracen-modifizierte Oligonukleotiden mit equimolaren Mengen an Fluoreszenzfarbstoffen zu schaffen. Eine neue zweifach orthogonale Markierungsmethode von Modifikationen im gleichen DNA-Strang konnte erzielt werden, indem für Thiol-Modifikationen Iodoacetamid- und für die Anthracen-Modifikation Maleimid-Fluoreszenzfarbstoffe verwendet wurden. Dabei wurde das Anthracen in einer Ribozym-katalysierten Diels-Alder Reaktion umgesetzt.

Table of contents

1	Introduction	5
1.1	The RNA world and ribozymes	5
1.2	<i>In vitro</i> Selection	6
1.3	The Diels-Alder reaction	7
1.4	Diels-Alder reactions in biocatalysis	9
1.5	The Diels-Alderase Ribozyme	11
2	Synthesis and applications of novel initiator nucleotides	13
2.1	Scientific background	13
2.1.1	Incorporation of initiator nucleotides with T7RNA polymerase	13
2.1.2	Anthracene derivatives	15
2.1.3	Aldehydes in bioconjugation reactions	15
2.1.4	Classic bioconjugation reactions	17
2.1.5	Classic organic reactions	18
2.2	Objectives	20
2.3	Results and Discussion	21
2.3.1	Synthesis of novel initiator nucleotides	21
2.3.2	Towards the <i>in vitro</i> selection of a novel Diels-Alder ribozyme	30
2.3.3	Incorporation and application of aldehyde containing initiator nucleotides	40
2.4	Conclusion	42
3	Thermal denaturation studies of the Diels-Alderase ribozyme	45
3.1	Scientific background	45
3.1.1	Metal ions in ribozyme folding and catalysis	45
3.1.2	The Diels-Alderase ribozyme	47
3.1.3	UV melting curves	49
3.1.4	Practical considerations of determining UV denaturation	49
3.2	UV denaturation of the Diels-Alderase ribozyme	50

3.2.1	Comparison of the Diels-Alderase wild-type with two mutants: U17C and U17iC	53
3.3	Conclusion and Discussion	55
4	Bioorthogonal and orthogonal labeling of oligonucleotides	57
4.1	Scientific background	57
4.1.1	Bioorthogonal labeling	57
4.1.2	Fluorescent labeling of oligonucleotides	58
4.1.3	Thiol modification	61
4.1.4	Disulfide reducing reagents	61
4.1.5	Maleimides	62
4.1.6	α -Haloacetamides	63
4.1.7	Diels-Alder reaction as tool for bioconjugation	63
4.1.8	The Diels-Alderase ribozyme	64
4.1.9	Anthracene as substrate	65
4.2	Objectives	66
4.3	Results and Discussion	67
4.3.1	Synthesis of anthracene modified oligonucleotides	67
4.3.2	Dipartite Diels-Alder ribozyme assay	68
4.3.3	Synthesis of DY 649 C ₅ -maleimidocaproic acid hydrazide	71
4.3.4	Diels-Alderase ribozyme-catalyzed labeling <i>in trans</i>	73
4.3.5	Dual orthogonal labeling of DNA with maleimides	78
4.3.6	Dual orthogonal functionalization of DNA with two different dyes	81
4.3.7	Analytical data of post-synthetically modified oligonucleotides	83
4.3.8	Important aspects of the labeling conditions	84
4.4	Conclusion	89
5	Conclusion and Outlook	91
5.1	Synthesis and applications of novel initiator nucleotides	91
5.2	Thermal denaturation studies of the Diels-Alderase ribozyme	93
5.3	Bioorthogonal and orthogonal labeling of oligonucleotides	94
6	Experimental section	97
6.1	Molecular biological techniques	97

6.1.1	General methods	97
6.1.2	Detection of nucleic acids	100
6.1.3	Determining the concentration of nucleic acids	102
6.1.4	Radioactive labeling with ^{32}P phosphor	103
6.1.5	PCR (Polymerase Chain Reaction)	104
6.1.6	Primer extension	106
6.1.7	<i>In vitro</i> T7 transcription	107
6.1.8	Diels-Alder reaction of the 2,3 dimethyl anthracene modified RNA	108
6.1.9	Deprotection of the aldehyde modified RNA and reaction with hydrazide	108
6.1.10	Melting curves	109
6.1.11	Automated solid-phase synthesis of oligonucleotides	110
6.1.12	High-performance liquid chromatography of oligonucleotides	112
6.1.13	Mass spectrometry of oligonucleotides	113
6.1.14	Fluorescent dyes	114
6.1.15	Flourescent labeling reactions of oligonucleotides	117
6.2	Synthetic procedures	120
6.2.1	General	120
6.3	Synthetic procedures for compounds of chapter 2	121
6.3.1	Synthetic procedures of the initiator nucleotides	121
6.3.2	Analysis of the initiator nucleotides	145
6.3.3	Alternative procedures towards the synthesis of initiator nucleotides	146
6.4	Synthetic procedures for compounds chapter 4	161
6.5	Oligonucleotides, buffers and material	168
6.6	List of Abbreviations	173
6.7	Appendix	177
7	Bibliography	181

1 Introduction

1.1 The RNA world and ribozymes

The question of the origin of life is one of the oldest questions of mankind and one of the most difficult to address in biology. The term “RNA World” was first used by Gilbert in 1986,^[1] even though the idea of an RNA based world as a hypothetical origin in the evolution had been suggested long before by Sir Francis Crick.^[2] When Gilbert established the term RNA world solely cleavage and ligation of phosphodiester bonds by RNA were known, but his hypothesis inspired and is still inspiring scientists all over the world to seek proof of an RNA world.

In 1982 Cech *et al.*^[3, 4] discovered RNA sequences that were able to cleave and rejoin the phosphate esters between their own nucleotides. This self-splicing RNA provided the first example of a catalytically active site formed by a ribonucleic acid.^[5] Independently, Altmann and co-workers^[6] found that RNase P is an RNA, processing endonuclease cleaving precursors of tRNA and releasing 5'-precursor sequences and mature tRNA.^[7, 8] Since then a number of other natural ribozymes have been discovered. The most prominent ribozymes are group I and II self splicing introns,^[9] encompassing the *Tetrahymena* ribozyme that was originally discovered by Cech, the hammerhead ribozymes,^[10] the hairpin ribozyme,^[11] the small self-cleaving Varkud satellite (VS)^[12] or the hepatitis delta virus ribozyme (HDV).^[13] Ribozymes can either catalyze a reaction *in cis*, meaning the ribozyme modifies itself, or *in trans* non-selfmodifying. These ribozymes, mostly discovered by the *in vitro* selection methodology, could turn out to be the missing link between a formerly RNA dominated world to today's protein-dominated world.

In 1993 Crick wrote “It may turn out that we will eventually be able to see how this RNA world got started. At present, the gap from the primal 'soup' to the first RNA system capable of natural selection looks forbiddingly wide.”^[14] Even though some years have passed and the discovery of new natural and artificial ribozymes has led to a further understanding of this hypothesis, more fundamental research into the function and application of ribozymes may eventually lead to hints that may further support the hypothesis of an RNA world.

1.2 *In vitro* Selection

The progress in the discovery of new ribozymes is mainly due to the technique of *in vitro* selection, independently developed by Joyce, Szostak and Gold in 1990. This technique enables to screen libraries of up to 10^{15} different nucleic acid molecules for a distinct functionality.^[15] This method is known as *in vitro* selection,^[16] *in vitro* evolution^[17] or SELEX, an acronym standing for Systematic Evolution of Ligands by EXponential enrichment.^[18] With this technique large libraries of randomized nucleic acids have been screened successfully for catalytic activity^[19-26] and screened for binding to small molecules or proteins.^[27-33] RNA and DNA molecules that can bind small molecules are called aptamers. After two decades of *in vitro* selection ribozymes have proven that they are indeed potent catalysts. Ribozymes are capable of catalyzing a broad spectrum of chemical reactions with good catalytic rate enhancement. An overview over some *in vitro* selected ribozymes are given in table 1.

Table 1: Examples for artificial ribozymes obtained by *in vitro* selection.

Reaction	Reference	Reaction	Reference
RNA cleavage	[34]	Aminoacylation	[35, 36]
RNA ligation	[20, 37]	Aldol-reaction	[38]
Phosphoester cleavage	[39, 40]	Diels-Alder reaction	[41, 42]
Phosphoester transfer	[43, 44]	Michael addition	[45]
Phosphorylation	[46]	Formation of an amide bond	[47] ^a
Peptide bond formation	[26, 48]	Cleavage of an amide bond	[49]
Self-capping	[50]	Formation of an urea bond	[51]
RNA polymerization	[52]	Nitrogen alkylation	[53]
Aldehyde reduction	[54]	Sulfur alkylation	[55]
Alcohol dehydrogenation	[56]	Porphyrin metalation	[57]
Acyl transfer	[58, 59]	Claisen condensation	[60]

^a Contains 5'-substituted uridine analogs that are essential for catalysis.

The general procedure of the *in vitro* selection methodology starts with a chemically synthesized DNA pool with a randomized region, flanked by two constant regions consistent of the primer binding sites and a T7 RNA polymerase promoter (figure 1). This DNA pool is to be amplified in a preparative scale PCR to gain several copies of each sequence. After T7 RNA polymerase transcription the obtained RNA pool is employed in the reaction it should catalyze, or exposed to the molecule it should bind. Subsequently active or binding sequences

are separated by affinity chromatography. The obtained RNA sequences are reverse transcribed into DNA, amplified by PCR and again transcribed into RNA to re-enter the selection cycle. Generally 5 to 10 rounds of selection should suffice to enrich the reactive sequences.^[15, 61]

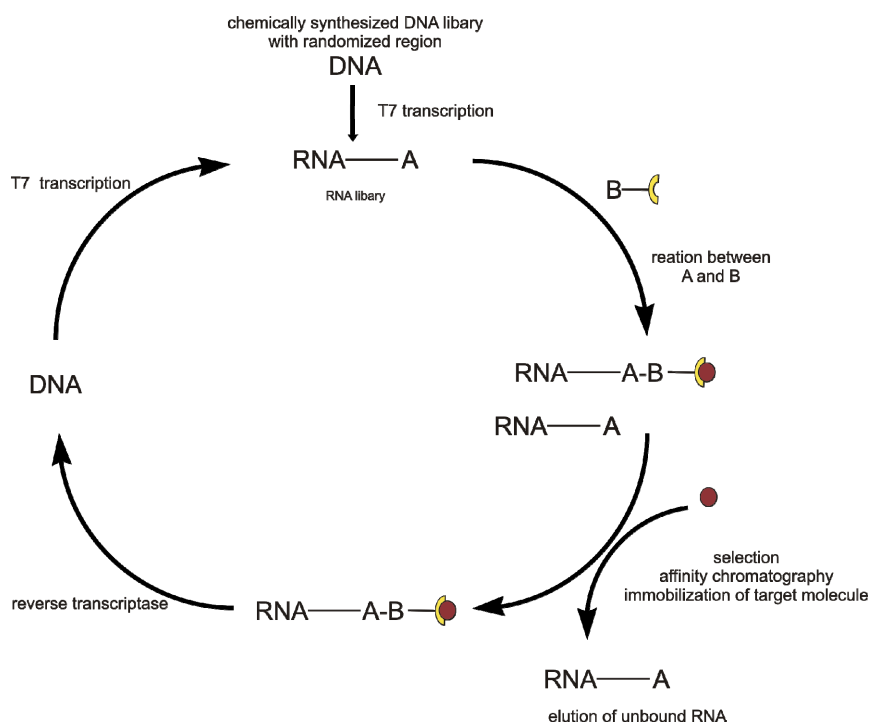
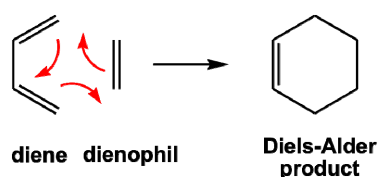


Figure 1: General selection scheme for the *in vitro* selection of reactive RNA sequences.

1.3 The Diels-Alder reaction



Scheme 1: The Diels-Alder reaction.

The Diels-Alder reaction is one of the most important reactions in organic chemistry. It was named after Otto Diels and Kurt Alder, who first described the reaction in 1928^[62] and were awarded the Nobel Prize in 1950 for their research on [4 + 2] cycloadditions. In one step two new carbon-carbon bonds are formed in a chemoselective manner and a six-membered ring is created (scheme 1). This cycloaddition between the diene and the dienophile is concerted, requiring the arrangement of the frontier orbitals.^[63, 64]

The reactivity of the Diels-Alder reaction depends on the energy difference between the HOMO (highest occupied molecular orbital) and LUMO (lowest occupied molecular orbital). The lower the energy difference between the two molecular orbitals the lower is the energy of the transition state of the Diels-Alder reaction (figure 2).

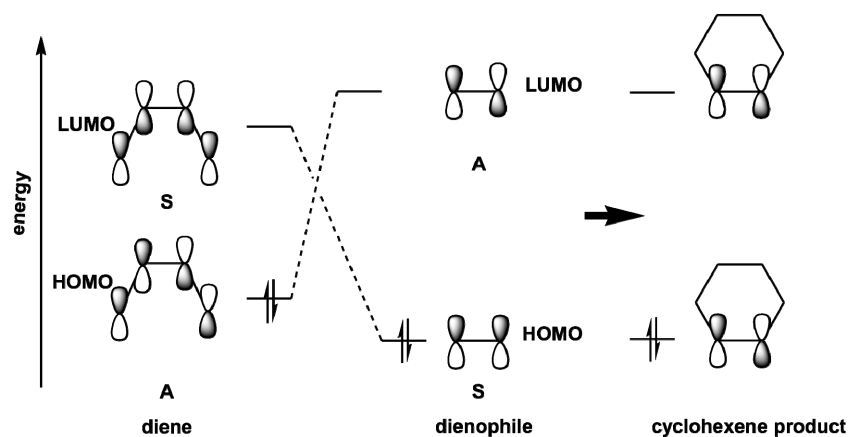
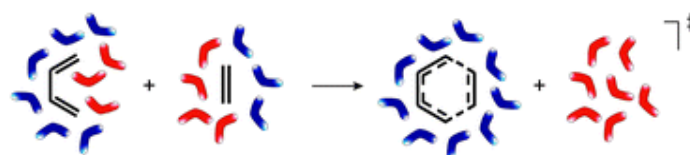


Figure 2: The Diels-Alder reaction. The dienophile reacts with a diene to form a six-membered cyclohexene. Three π -bonds in the substrates are converted into two σ -bonds and a new π -bond in the product. Molecular orbitals (S = symmetrical, A = asymmetrical) are shown according to the Woodward-Hoffmann rules. For clarity only the HOMO π -electrons are shown. Adapted from Tarasow *et al.*^[65]

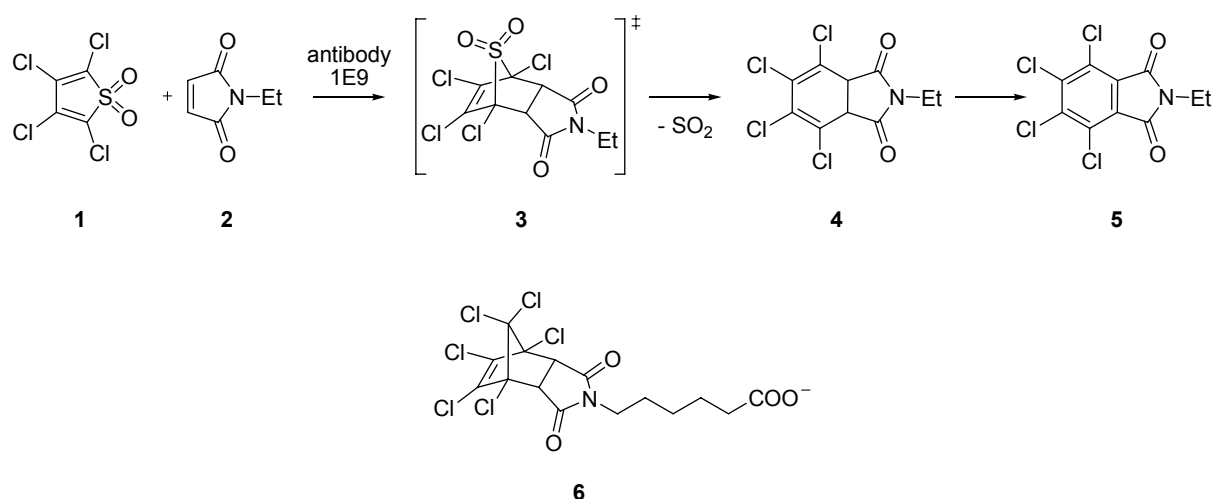
Since the discovery of the Diels-Alder reaction studies using water as a solvent have been undergoing.^[66] Woodward and co-workers reported a change in the endo-exo selectivity for the Diels-Alder reaction between furan and maleic acid in water.^[67] Eggelte *et al.* reported the first reaction rate acceleration for Diels-Alder reactions in aqueous media.^[68] However, it was not until the landmark paper by Breslow *et al.* in 1980^[69] that the acceleration of the Diels-Alder reaction in water had been recognized in the scientific society. Breslow and Rideout attributed the acceleration to an entropy-driven hydrophobic effect (scheme 2).^[69]



Scheme 2: Illustration of the hydrophobic hydration shells around the diene, dienophile and the Diels-Alder product. The red hydration shells are released into the solution during the reaction. Adopted from Otto *et al.*^[70]

1.4 Diels-Alder reactions in biocatalysis

Following the fundamental principles of Pauling,^[71] Jencks proposed in 1969 that complementarity between the active site and the transition state of an enzyme contributes significantly to enzymatic catalysis; therefore, the construction of an antibody to a hapten, resembling the transition state of a reaction should lead to such an enzyme. A transition state analogue provided by the antibody should stabilize the transition state and therefore cause an acceleration of the reaction.^[72] The first proof of this principle was provided by Schulz and Lerner^[73-75] studying esterase antibodies. The first catalytic Diels-Alder reaction had been demonstrated in 1989 by Hilvert *et al.* with the antibody 1E9.^[76, 77]



Scheme 3: Antibody 1E9 catalyzes the Diels-Alder reaction between tetrachlorothiophene dioxide **1** and *N*-ethylmaleimide **2**. The reaction proceeds in two steps: the intermediate **3**, which eliminates sulphur dioxide to give the product **4**, undergoing air oxidation to form *N*-ethyl tetrachlorophthalimide **5**. The Antibody 1E9 was raised against the hexachloronorbomene derivative **6** as structural analogue of the transition state.^[78]

The chemical structure of many natural products suggests an involvement of a Diels-Alder reaction, but so far in most of these pathways a Diels-Alderase was illusive. For a long time three enzymes were believed to act as Diels-Alderases.^[79, 80] The solanapyrone synthase,^[81] the lovastatin nonaketide synthase (LNKS), and the macrophomate synthase.^[82] Studies of the macrophomate synthase suggested the involvement of a Diels-Alder reaction, but in fact the reaction seems to proceed *via* a sequential Michael-aldol pathway.^[83-85]

Computational studies have led to designed enzymes catalyzing a Diels-Alder reaction.^[86, 87] Recently Baker and co-workers have indeed selected an enzyme catalyzing an intermolecular Diels-Alder reaction of the diene 4-carboxybenzyl *trans*-1,3-butadiene-1-carbamate and the

dienophile *N,N*-dimethylacrylamide (figure 3).^[88] Employing an algorithm of the modelling program RosettaMatch^[89] the transition state and its stabilization in the catalytic pocket was simulated and subsequently libraries of protein scaffolds were scanned to find applicable candidates. An initial scan of 10^{19} protein scaffolds identified about 10^6 possible active sites in proteins. By further optimizing this modelling approach the proteins were limited to a manageable number of 84 proteins. These 84 proteins were then expressed within *E. coli*. After engineering, 50 stable proteins remained and were then tested for catalytic activity in the Diels-Alder reaction. Only two of these enzymes actually showed catalytic activity. Further modified, these enzymes show strong selectivity for the substrates and compared with the metal catalyzed reaction the novel enzymes are only one magnitude slower. In principle, 8 different isomers could result in this Diels-Alder reaction, out of which four are produced during the uncatalyzed reaction. Remarkably, the engineered enzyme only catalyzes the reaction of one specific isomer.

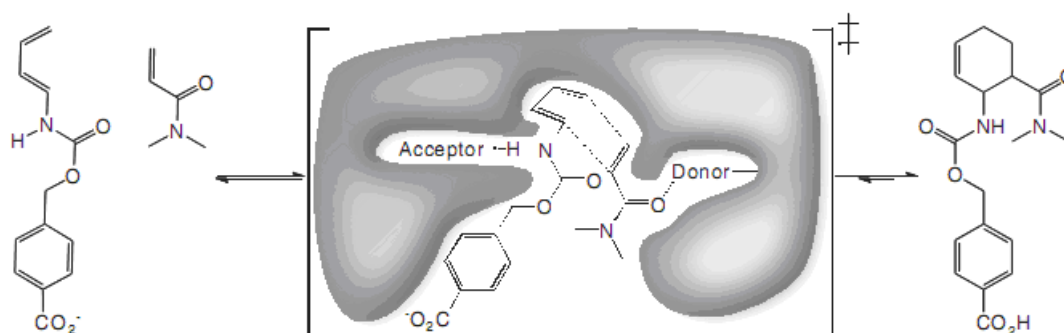


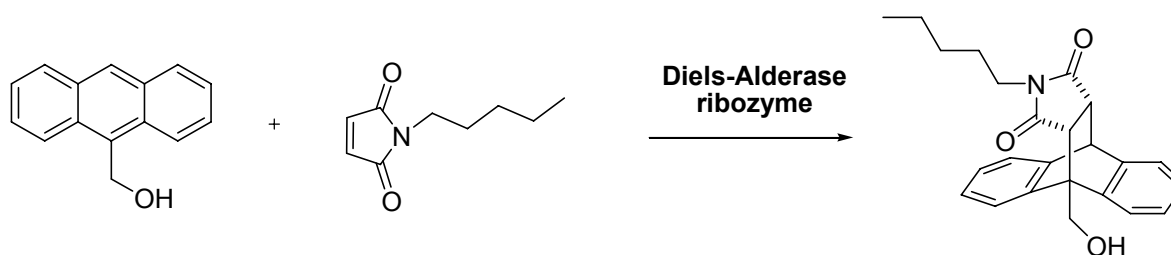
Figure 3: The Diels-Alder reaction - diene and dienophile undergo a pericyclic [4 + 2] cycloaddition to form a chiral cyclohexene ring. The image also shows the designed target active site, with hydrogen bond acceptors and donors activating the diene and dienophile and a complementary binding pocket holding the two substrates in an orientation optimal for catalysis. Adapted from Siegel *et al.*^[88]

Not only antibodies and proteins are able to catalyze Diels-Alder reactions. Nucleic acids are also capable of accelerating Diels-Alder reactions. The first artificial ribozyme was published by Tarasow and Eaton, this ribozyme however is dependent on the presence of pyridine and copper ions.^[42] This ribozyme was only active if covalently attached to one of the reactants and therefore is not really a true catalyst. The first true Diels-Alder ribozyme was selected by Jäschke and co-workers. This Diels-Alder ribozyme provides the basis for the present work and shall be elaborated further in the next chapter.

Not only ribozymes for the catalysis of Diels-Alder reactions have been selected, Silverman and co-workers reported a deoxyribozyme that can catalyze the Diels Alder reaction as efficiently as the reported ribozymes.^[22, 90]

1.5 The Diels-Alderase Ribozyme

Seelig and Jäschke selected a Diels-Alderase ribozyme, catalyzing the carbon-carbon bond formation between an anthracene derivative and a maleimide.^[91] This ribozyme is able to catalyze a multiple turnover reaction, with an acceleration of up to 20 000 fold with high enantio-selectivity. It is the first true Diels-Alderase ribozyme and capable of performing the Diels-Alder reaction between the free reactants (scheme 4).



Scheme 4: Diels-Alderase ribozyme catalyzed reaction between 9-hydroxymethyl anthracene and *N*-pentylmaleimide.

Rational design and ribozyme engineering lead to the identification of a minimal motif consisting of 49 nucleotides.^[41] The secondary structure motif consists of 3 helices (helix I-III), and an asymmetric internal loop, composed of a pentanucleotide UGCCA, and a hexanucleotide AAUACU, and a formally single stranded 5'-end (figure 4). Mutation analysis identified highly conserved structural elements to be part of the formally single stranded regions. The nucleotides G₁, G₂, A₃, G₄, U₈, U₁₀, C₁₁ and U₂₀ are highly conserved while the sequence of the helices I and III are variable as long as the strands are complementary to each other. A strong conservation was found for helix II, both in length and purine/pyrimidine pattern. Mismatches in this region lead to a total loss of catalytic activity.^[92]

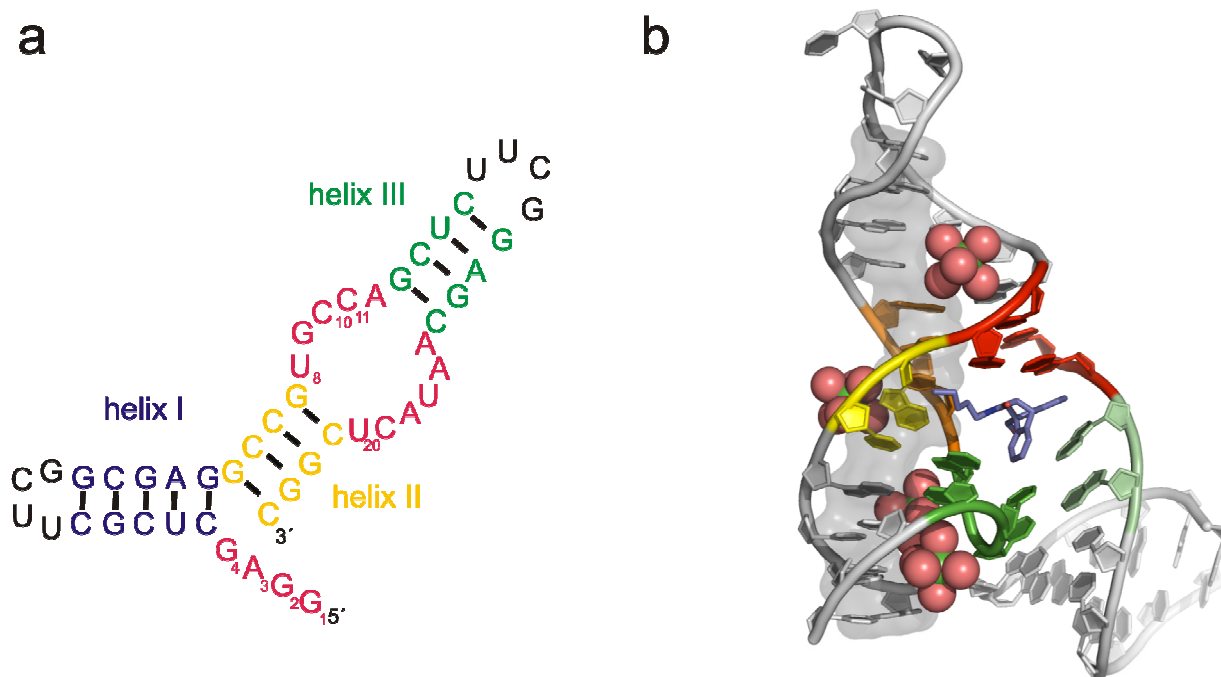


Figure 4: **a:** Secondary structure of the Diels-Alderase ribozyme minimal motif. **b:** X-ray structure of the Diels-Alder ribozyme with co-crystallized reaction product (blue) in the catalytic pocket.

The complex three-dimensional structure of the Diels-Alderase ribozyme had been predicted by mutational analysis^[92] and was later confirmed by crystal structures of the ribozyme.^[93] The ribozyme adopts a λ -shaped fold of its three helices in which stems II and III stack coaxially, with stem I abutting the active site.^[94] The 5' end of the RNA bridges helical stems III and I, generating a complex nested pseudoknot topology. The pseudoknot architecture presents a preformed hydrophobic pocket, precisely complementary to the reaction product.^[93]

The minimal motif of the ribozyme could be converted into a two- and three-stranded system by formally cleaving the two tetraloops. The bipartite system consists of an unmodified 38mer and an anthracene-tethered 11mer, while the tripartite version consists of a 24mer an 18mer and the tethered 11mer.^[92, 95] Both constructs show a similar catalytic activity to the 49mer minimal motif. All versions of the Diels-Alder ribozyme can catalyze the reaction *in cis* and *in trans* between the free ligands. The benefit of a reaction catalyzed *in trans* is that a huge variety of different substrates could be investigated as potential substrates. Stuhlmann *et al.* showed that the ribozyme tolerates several substitutions on both substrates, except in the 2- and 3-position of anthracene.^[96] The significance of the above mentioned results will be explicitly discussed in chapter three and four.

2 Synthesis and applications of novel initiator nucleotides

2.1 Scientific background

2.1.1 Incorporation of initiator nucleotides with T7RNA polymerase

The structural and mechanistic studies of RNA biochemistry greatly depend on the incorporation of modified nucleotides. Nucleotides that bear a modification at the phosphate backbone or at a base can either be introduced randomly or at a specific site. If the desired RNA sequence is short enough (max. 40 nt), chemical synthesis is the simplest solution. For long RNA sequences a combination of chemical synthesis and RNA ligation has to be employed.^[97]

An efficient possibility for site-specific 5'-modification of RNA is transcription initiation priming. Nucleotides lacking a 5'-triphosphate are unavailable for incorporation during elongation of the RNA molecule. Due to their ability to initiate transcription reactions they are named initiator nucleotides.^[98] RNA polymerase binds specifically at the promoter sequence of the double stranded DNA and starts the transcription with the nucleoside triphosphates present in the reaction mixture. As the modified nucleoside monophosphate can only be incorporated at the 5'-end, each transcribed RNA sequence can only carry a single modification. Transcription priming naturally leads to mixed populations of modified and unmodified RNA sequences, because not every RNA strand is primed with a GMP. To produce as much modified RNA as possible the concentration of the modified nucleotide has to be high as compared to the unmodified nucleotide, albeit this usually has the effect of lower transcription efficiencies. Therefore the concentration of 5'-modified nucleotide over unmodified nucleoside triphosphate has to be optimized carefully.

Modified nucleotides have been used as initiators to prime *in vitro* RNA transcription for quite a while.^[99] Initiator nucleotides can be divided in dinucleotides and guanosine monophosphate (GMP) derivatives modified with an organic moiety. The transcription initiation with commercially available guanosine derivatives like adenylyl-(3'-5')-guanosine (ApG) and cytidylyl-(3'-5')-guanosine (CpG) has been utilized to create a free 5'-hydroxyl group, which is then available for subsequent RNA radioactive end-labeling with [γ -³²P] ATP using T4 RNA polymerase or polynucleotide kinase.^[100] Fluorescein, carboxytetramethylrhodamine (TAMRA) or biotin ApG are nowadays common modifications

in chemical oligonucleotide synthesis. Guanosine-5'-*O*-(1-thiomonophosphate) (GMP α S) is commercially available, and can e.g., be derivatized with photochemical groups such as p-azidophenacyl bromide^[101] and has been used to select ribozymes by Famulok or Suga and co-workers.^[54, 59]

Except of the above-mentioned, the variety of chemically modified initiator nucleotides that have been described in literature is limited. For the synthesis of 5'-amino and 5'-thiol modified initiator nucleotides a series of synthetic routes have been published earlier.^[102-104]

5'-Thiol modified RNA can be used for the selection of ribozymes catalyzing e.g. a Michael addition, while 5'-amino modified RNA may be used for the selection of an amide synthase.^[102] Recently, Pfander and Jäschke developed an initiator nucleotide with an aldehyde modification which was then amino- or hydrazine-derivatized.^[105] Furthermore, Famulok and co-workers introduced a photocleavable initiator nucleotide with a ketone functionality^[106] and fumaramide-derivatized guanosines as Michael acceptors.^[45] Tri-Link recently brought 5'-biotin and 5'-amino-GMP respectively AMP to the market.^[107] All initiator nucleotides mentioned above have been synthesized by the modification of guanosine monophosphate. A slightly different approach has been pursued by Huang and co-workers who introduced modified adenosine monophosphates but the scope of modified AMPs for transcription priming is still less common, because it requires a different T7 promoter.^[108-110]

The research group of Prof. Jäschke has a long-standing interest in the *in vitro* selection of novel catalytic RNA sequences. For that purpose, initiator nucleotides with polydisperse polyethylene glycol linkers have been synthesized for the selection of a Diels-Alder ribozyme.^[111] The anthracene tethered initiator nucleotide described by Seelig *et al.* is the only published example of a modified GMP with a polydisperse linker. Polydisperse linkers, in this context, have the advantage over monodisperse polyethylene glycol linkers that the same modification is at disposal with many different linker lengths creating a library of RNA molecules. This diversity increases the chances to successfully select a catalytically active sequence. Notwithstanding the fact, that due to their molecular-weight non-homogeneity, the synthesis of polydisperse initiator nucleotides is by far more demanding than the synthesis of monodisperse compounds.

2.1.2 Anthracene derivatives

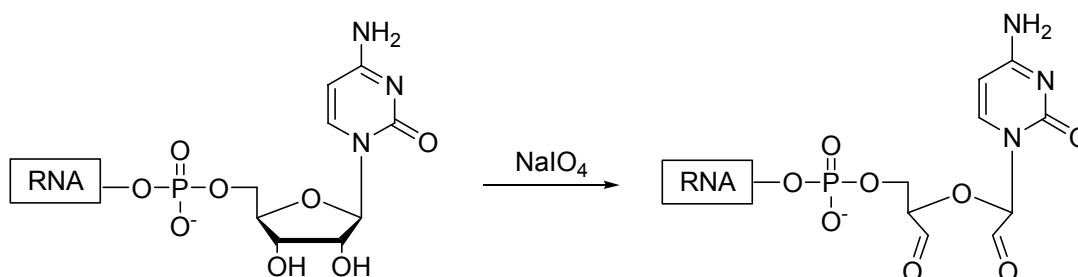
The usefulness of site-specific modifications with anthracene for oligonucleotide synthesis will elaborately be illustrated in chapter four.

The main purpose of anthracene-modified initiator nucleotides has so far been the *in vitro* selection of Diels-Alderase ribozymes^[41] or studies of folding, the reaction mode or allosteric activation of the same.^[112]

2.1.3 Aldehydes in bioconjugation reactions

Aldehydes are highly reactive and therefore periodate oxidation has found widespread application, especially in carbohydrate and protein biochemistry. For RNA, this technique is less common,^[113] but can be used in the same manner for cross-linking,^[114] fluorescent labeling^[115] and biotinylation.^[116] In their native state, proteins, peptides and nucleic acids contain no naturally occurring aldehyde residues. On the other hand, aldehydes are one of the most reactive and most versatile functional groups known to chemists. Therefore establishing new and straightforward strategies to introduce aldehydes into oligonucleotides is of utmost interest.

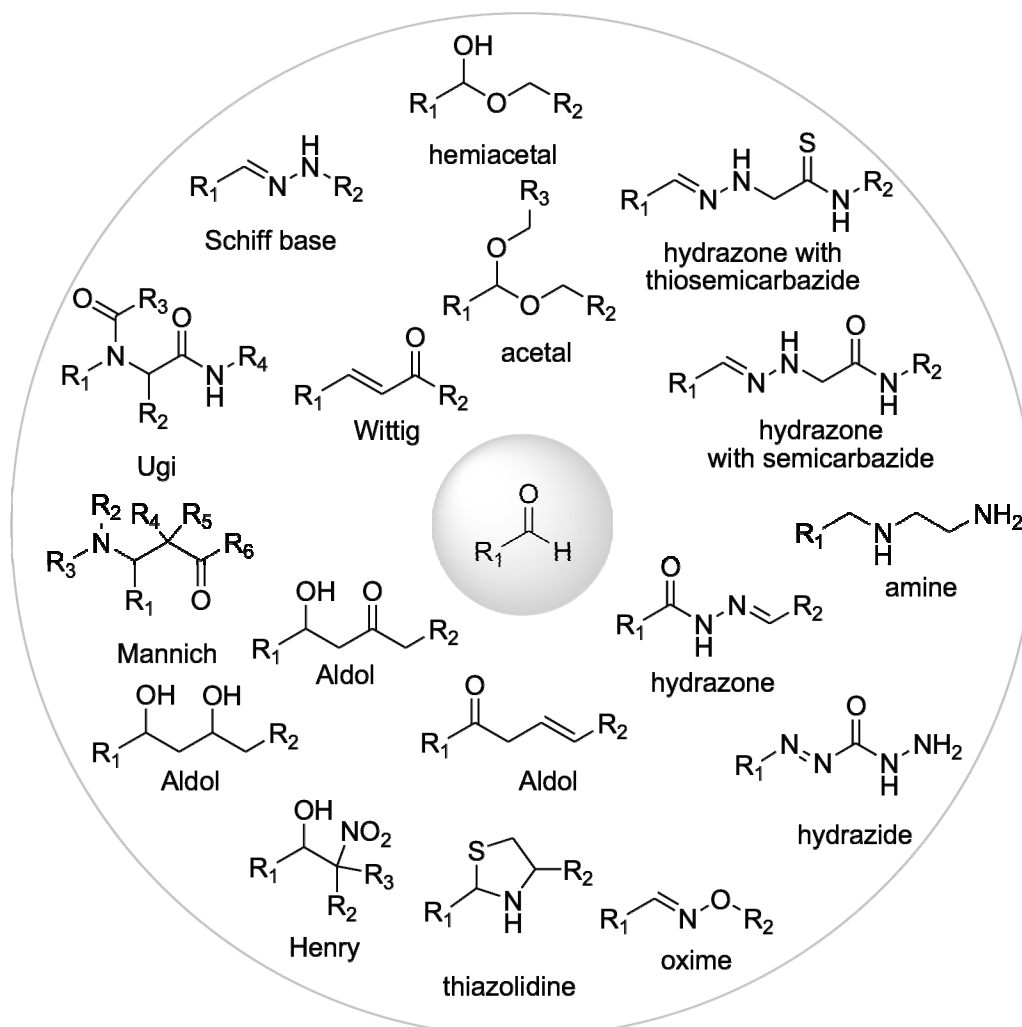
The most common method for introducing aldehydes and ketones into polysaccharides and glycoproteins is the oxidation of vicinal diols by periodate.^[117] The vicinal diols of ribose in RNA nucleotides can also be cleaved with periodate,^[118] allowing the addition of a 3'-end label to RNA.^[119] DNA lacking a 2'-diol can not be oxidized with periodate (scheme 5). DNA however, can be partially depurinated to form aldehydes for further labeling or cross-linking.^[120] Silverman and co-workers identified a deoxyribozym, which can depurinate its 5'-terminal guanosine nucleotide using periodate as a cofactor.^[121]



Scheme 5: Periodate oxidation of a 3'-cytidine.

Back in 2003 Glen Research launched the first aldehyde modifier as a phosphoramidite for the 5'-end modification of DNA in automated oligonucleotide synthesis, but is yet far from being a standard modification in custom oligonucleotide synthesis. Three synthetic procedures for the synthesis of aldehyde-modified phosphoramidites for the 5'-end modification of DNA have been published so far.^[122] The introduction of an aldehyde moiety by T7 RNA transcription and subsequent conjugation reactions have been described by Pfander *et al.*^[105]

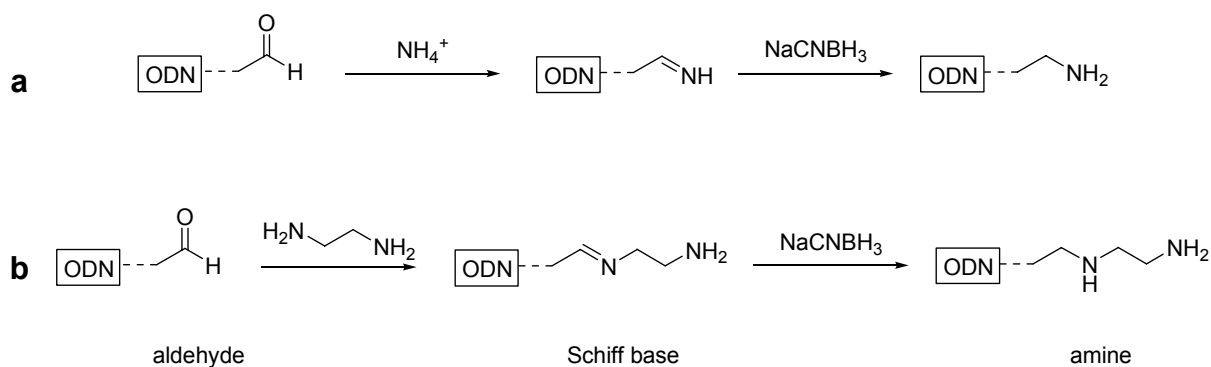
Scheme 6 illustrates reactions that are possible with aldehydes in aqueous solution. An uncountable number of other reactions are possible with aldehydes and presumably many will sooner or later find their way into bioconjugation, protein and nucleic acid chemistry.



Scheme 6: Reaction products of aldehydes that have been demonstrated in water with DNA, RNA, PNA or peptides.

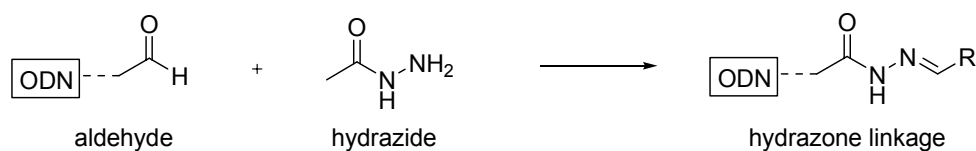
2.1.4 Classic bioconjugation reactions

The most important bioconjugation of aldehydes is the reaction with primary and secondary amines to form Schiff bases. The Schiff base formation is relatively labile, because it is a reversible reaction and can be hydrolyzed easily. Therefore a subsequent reduction stabilizes the conjugation product (scheme 7). This technique has recently been employed extensively in the pioneering work on DNA-templated organic synthesis and DNA-templated peptide nucleic acids (PNA) oligomerization by Liu and co-workers.^[123-125]



Scheme 7: The aldehyde can be aminated with ammonia (**a**) or a diamine (**b**) to form a Schiff base in the presence of sodium cyanoborohydride as a reducing agent, to produce an amine modification.

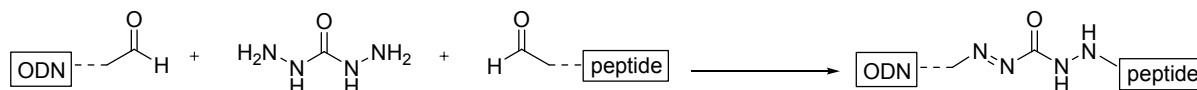
The second most important reaction is the modification of aldehydes with hydrazide or bis-hydrazide compounds. Aldehydes spontaneously react with hydrazides to form a hydrazone linkage (scheme 8). The hydrazone bond is a type of Schiff base, but the linkage between a hydrazide and an aldehyde is more stable than the linkage between an aldehyde and an amine. Further stabilization can be achieved under reductive conditions.



Scheme 8: Aldehydes and hydrazides form a hydrazone linkage.

The hydrazone linkage formed from a hydrazine and an aldehyde is much more stable than the bond formed between a hydrazide and an aldehyde.^[126] Furthermore, the reactivity of hydrazines exceeds the reactivity of hydrazides by far, but up to today most commercially available tags and cross-linking reagents are only available as hydrazides. The selection of

commercially available hydrazides ranges from immobilization tags like biotin hydrazide, hydrazide activated streptavidin or hydrazide-terminated magnetic beads, to fluorescent dyes, and proteins. Containing a hydrazide group at both ends homo-bifunctional hydrazides can be used as cross-linking reagents (scheme 9).



Scheme 9: Bis-hydrazides can be used to transform an aldehyde into a terminal hydrazide group.

Further reactions for bioconjugation with aldehydes are the formation of acetals, hydrazone formation with semicarbazides and thiosemicarbazides, thiazolidine or oxime linkage.

2.1.5 Classic organic reactions

Initiator nucleotides provide excellent tools for the *in vitro* selection of ribozymes. In the last couple of years many organic reactions have found their way into protein and nucleic acid chemistry. Herein, a short summary over a selection of possible organic reactions with aldehydes in biomolecules will be given.

The aldol reaction has found widespread application in DNA-templated synthesis^[127, 128] and Famulok and co-workers have reported the *in vitro* selection of an aldolase ribozyme. In their case the aldehyde moiety was the substrate while the RNA was modified by a photocleavable ketone initiator nucleotide.^[106] Fan *et al.* reported that double-stranded DNA can be used as a catalyst to facilitate the Henry reaction (nitro-aldol reaction) of several different substrates.^[129]

The Wittig reaction is possibly the most popular method to create carbon-carbon double bonds. Recently it was found that the Wittig reaction is accelerated in water and that ylides and aldehydes can be stabilized in water. Water was found to enhance the reactivity in Wittig reactions due to its ability to stabilize the polar transition state, a phenomenon that a nonpolar medium is less capable of.^[130] Liu and co-workers have implemented a DNA-templated Wittig reaction with excellent yields and short reaction times.^[131] McKee *et al.* recently reported three sequential DNA-templated Wittig reactions.^[132]

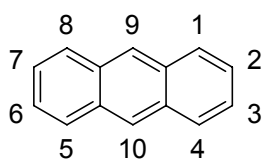
Two multi-component reactions of which one of the components is an aldehyde have to be mentioned in this context. The Ugi condensation, also known as the Ugi four-component reaction, usually refers to the reaction between a carbonyl compound, an amine, an

isocyanide, and a carboxylic acid.^[133, 134] The Ugi reaction is like the Wittig reaction accelerated in water^[135] and has been applied in peptide synthesis^[136] and labeling of PNA monomers.^[137]

The Mannich reaction, well known to organic chemists, is the condensation of an iminium ion, formed *in situ* from an aldehyde with an amine and an enolizable carbonyl. Almost one century after its discovery Francis and co-workers described the first bioconjugation application.^[138]

2.2 Objectives

From previous studies by Stuhlmann *et al.*^[96] it is known that the Diels-Alder ribozyme selected for anthracene and maleimide has strict limitations to its tolerated substrates. We envisioned it should be possible to select a different ribozyme motif, able to form a bigger binding pocket and thus able to catalyze the Diels-Alder reaction between 2,3-dimethylantracene and maleimide derivatives. The original Diels-Alderase ribozyme does not tolerate any substituents in the 2 and 3 position of anthracene (scheme 10)



Scheme 10: IUPAC nomenclature for anthracene.

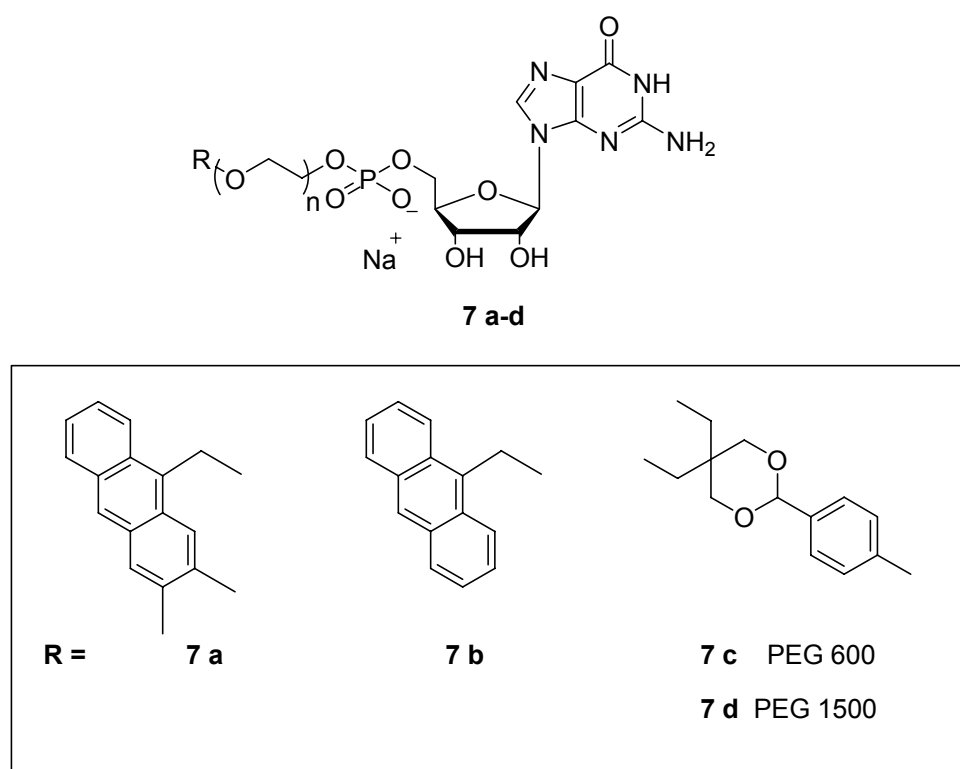
The aim was to develop a synthetic approach for the synthesis of novel initiator nucleotides and implement it for the synthesis of 2,3-dimethylantracene, as well as for non-substituted anthracene, to make it easily accessible for studies of the existing Diels-Alderase ribozyme. Furthermore, the incorporation into RNA during T7 RNA polymerase transcription was to be studied with a short DNA template and a DNA pool with a randomized region to study the availability for a possible *in vitro* selection.

Anthracene is mainly employed in Diels-Alder reactions. Aldehydes on the other hand are extremely reactive and versatile molecules that can be used for a countless number of organic reactions, respectively bioconjugations and therefore are extremely useful for the introduction of many functionalities into nucleic acids. In cases where the distance is critical polydisperse polyethylene glycol linkers are highly advantageous. Therefore, aldehyde modified initiator nucleotides with different linker lengths are attractive compounds. The synthesis of initiator nucleotides with aldehyde functionalities will be designed, realized and subsequently the incorporation into RNA will be studied. After incorporation studies the reactivity of the resulting modified RNA has to be determined.

2.3 Results and Discussion

2.3.1 Synthesis of novel initiator nucleotides

The initiator nucleotides **7a-d** (scheme 11) were synthesized establishing new synthetic procedures.

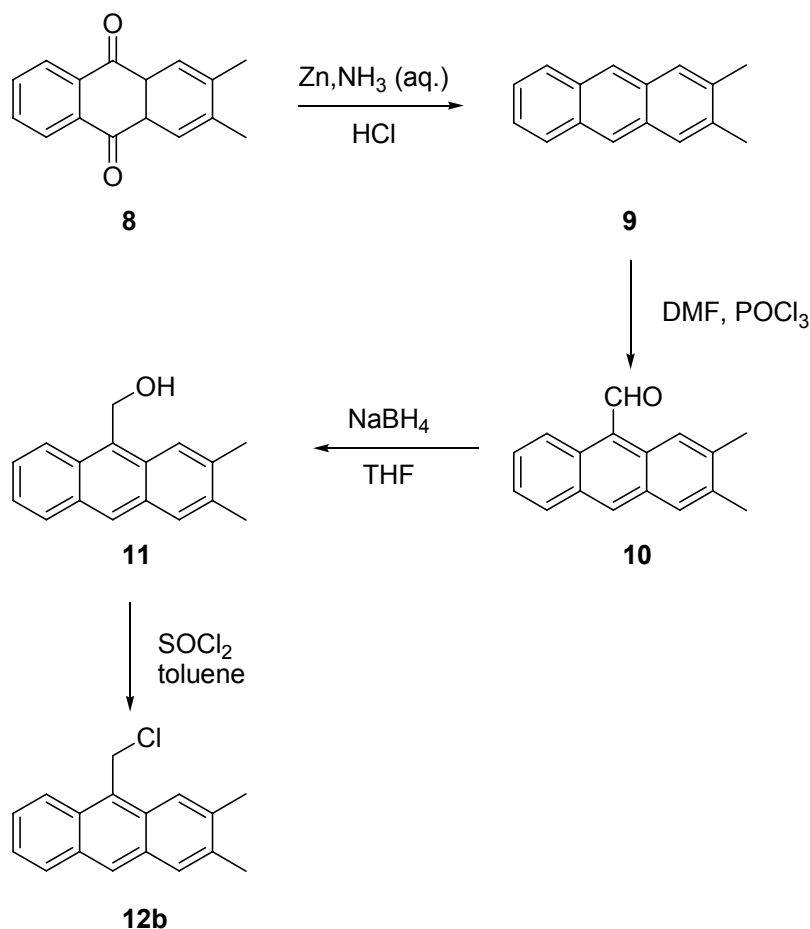


Scheme 11: Initiator nucleotides **7 a-d**.

Even though the polydisperse polyethylene glycol compounds are here linguistically described as a single compound it has to be pointed out that each PEG compound consists of several compounds, identical in their functional groups or modifications, but different in the number of ethylene glycol units.

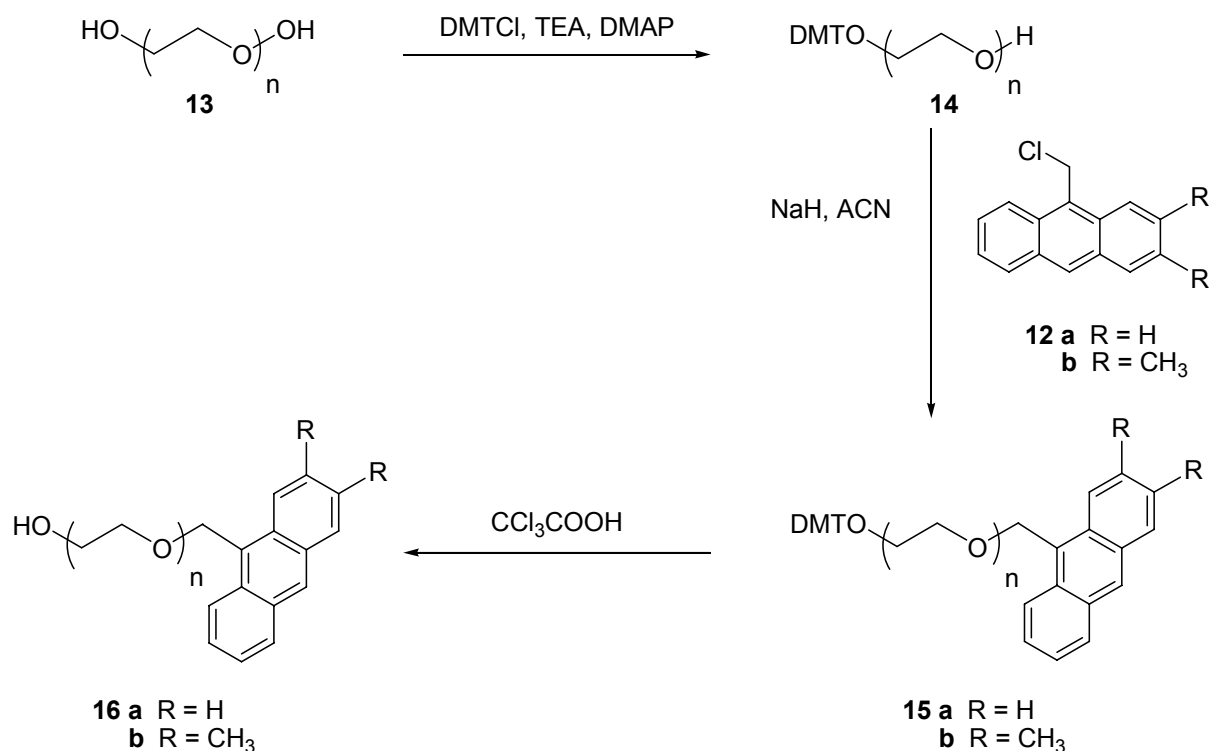
2.3.1.1 Synthetic procedures to anthracenyl initiator nucleotides

For the synthesis of the 9-(chloromethyl)-2,3-dimethyl anthracene bearing initiator nucleotides **7a-b** a synthetic procedure to 9-(chloromethyl)-2,3-dimethyl anthracene had to be established **12** (scheme 12).



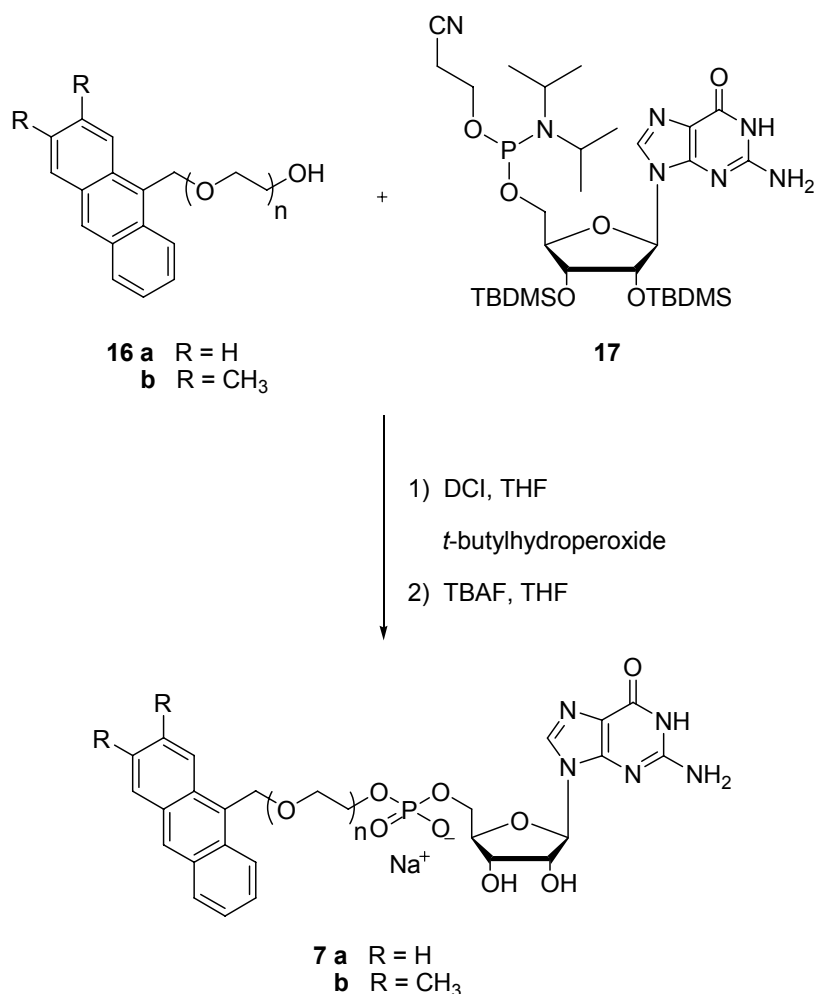
Scheme 12: Preparation of 9-(chloromethyl)-2,3-dimethyl anthracene.

The synthesis of 9-(chloromethyl)-2,3-dimethylanthracene **12b** starts from the commercially available 2,3-dimethylanthraquinone **8**. 2,3-Dimethylanthraquinone was reduced with granular zinc and aqueous ammonia in an autoclave and later treated with hydrochloric acid. Purification turned out to be rather difficult and after flash chromatography on silica and displacement only 28% 2,3-dimethylanthracene **9** could be obtained. In a Vilsmeier-Haak reaction anthracene could exclusively be formylated at the 9-position with a yield of 95%, similar to a procedure described for non substituted anthracene.^[139] 2,3-dimethylanthracene-9-carbaldehyde **10** was reduced with sodium borohydrate to yield 92% of the corresponding alcohol **11** and was further reacted with thionyl chloride and without further purification 94% of 9-(chloromethyl)-2,3-dimethyl anthracene **12b** was obtained.



Scheme 13: Synthesis of (anthracen-9-yl-methoxy)-polyethylen glycol **16a** and 2-((2,3-dimethylantracene-9-yl)-methoxy)-polyethylene glycol **16b**.

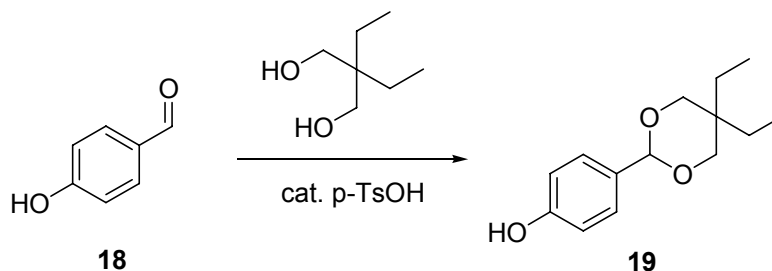
PEG 600 was selectively mono-protected with 4,4'-dimethoxytrityl (DMT) according to the procedure published by Fiammengo *et al.* for hexaethylene glycol.^[140] PEG 600 was dissolved in acid free dichloromethane with 4-dimethylaminopyridin (DMAP) as activator and triethylamine to deprotonate the hydroxyl group. In a dichloromethane solution DMT-Cl was added very slowly during several hours *via* a syringe pump. An excess of PEG and the slow addition of DMT-Cl prevent a di-protection. Traces of di-protected product could be eliminated by purification over silica. Mono-protected PEG 600 **14** was obtained in a yield of 75%. In an S_N2-reaction the free hydroxyl group of the DMT-protected polyethylene glycol was deprotonated with sodium hydride and either reacted with 9-(chloromethyl)anthracene to form the bifunctional PEG with DMT and anthracene **12a** or reacted with 9-(chloromethyl)-2,3-dimethylantracene **12b** to form the corresponding derivative. For anthracene a yield of 46% was achieved while for 2,3-dimethylantracene 75% of the pure product was obtained after flash chromatography. The DMT protecting group was removed by exposure to 3% trichloro acetic acid in DCM for five minutes. After purification over silica 82% of (anthracen-9-yl-methoxy)-polyethylene glycol **16a** and 84% of 2-((2,3-dimethylantracene-9-yl)-methoxy)-polyethylene glycol **16b** were obtained.



Scheme 14: Synthesis of initiator nucleotides **7a** and **b**.

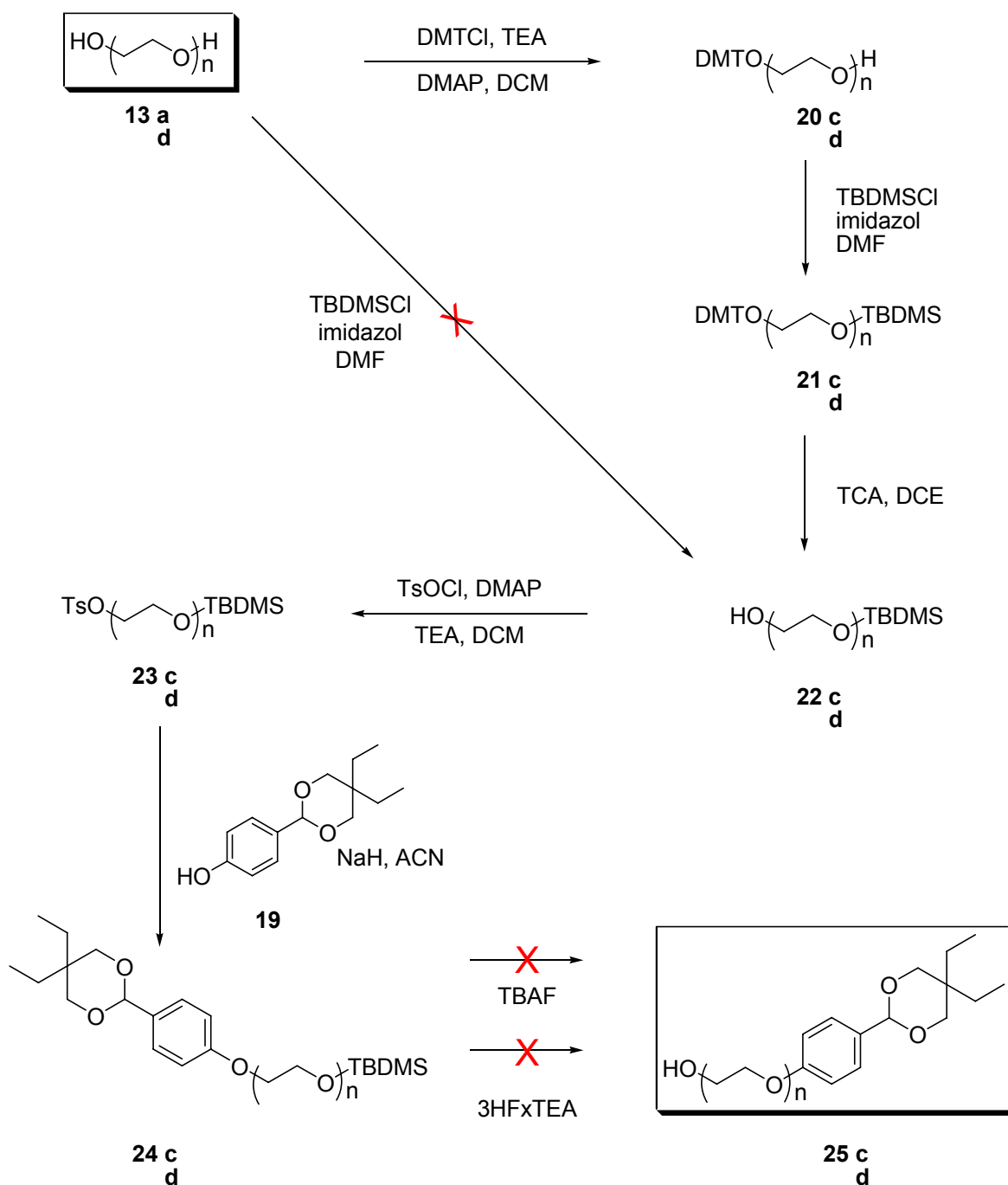
2',3'-bis TBDMS-protected guanosine was synthesized from unprotected guanosine according to literature.^[141] The corresponding 5'-O-phosphoramidite was prepared in 88% yield using 2-cyanoethyl-*N,N*-diisopropylchlorophosphoramidite for phosphitylation. This synthesis can be achieved without protection of the nucleobase.^[142] As reported in literature no *N*-phosphitylation during phosphoramidite coupling with imidazolium activators was observed.^[143] The initiator nucleotides **7a** and **7b** were synthesized the anthracene modified polyethylene glycol compounds **16a** and **16a** and 2,3-bis-(*t*-butyldimethylsilyl) guanosin-5-O-(β -cyanoethyl-*N,N*-diisopropylphosphor-amidite) **17** in the presence of 4,5-dicyanoimidazole (DCI). After 1 h the reaction was quenched by the addition of *t*-butylhydroperoxide. The solvent was removed and the guanosine intermediate directly deprotected from the TBDMS protection groups on the 2'-and 3'-hydroxyl and the β -cyanoethyl by the addition of tetra-*n*-butylammonium fluoride (TBAF). Purification was carried out *via* reverse phase column chromatography, followed by ion exchange and a second reverse phase column chromatography.

2.3.1.2 Novel aldehyde containing initiator nucleotides



Scheme 15: Protection of 4-hydroxybenzaldehyde.

Commercially available 4-hydroxybenzaldehyde **18** was protected as an acetal in a *p*-toluenesulfonic acid catalyzed reaction. General organic synthetic procedures for the acetal protection of aldehydes require the removal of the formed water to push the equilibrium to form more acetal. The azeotropic distillation with a water trap did not shift the equilibrium towards the desired product. When performed with one equivalent potassium carbonate the conversion observed by TLC was only 50%. In another approach, two equivalents of dry magnesium sulfate lead to a similar conversion. Notably, the performance of the reaction without any auxiliary agents made the workup easiest and after purification on silica 62% of the protected aldehyde **19** was obtained.



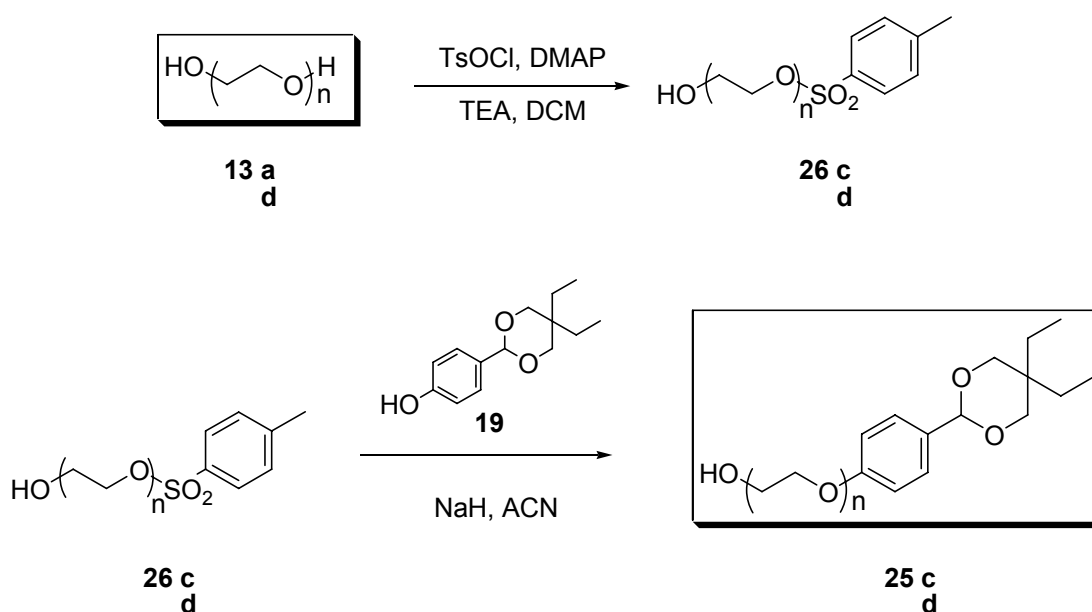
Scheme 16: First synthetic strategy to polyethylene glycol-*p*-toluolsulfonat.

All compounds represented in scheme 16 were purified on silica by flash chromatography. Reaction conditions for tosylation are not compatible with DMT as a protecting group. DMT would be cleaved off during the tosylation and bis-tosylated PEG compounds would be the consequence. For that reason it was decided to use TBDMS as a protection group instead. To ensure that only mono-protected PEG was available for subsequent reactions, DMT-protected PEG was prepared as described earlier.

The remaining free hydroxyl group was then protected with TBDMS-Cl under standard conditions. After purification bis-protected PEG 600 **21c** was obtained with a yield of 76%, while the yield for PEG 1500 **21d** was 70%. The deprotection of DMT resulted in the mono TBDMS protected PEG compounds in a moderate yield of 50% for PEG 600 **22c** and 78% for PEG 1500 **22d**. Subsequent tosylation with *p*-toluenesulfonyl chloride in the presence of TEA as a base and 4-dimethylaminopyridine (DMAP) as a catalyst was successfully carried out to yield 87% clean product for PEG 600 **23c** and 75% for PEG 1500 **23d**. Nucleophilic substitution by the protected aldehyde **19** yielded 60% for PEG 600 **24c** and 99% for PEG 1500 **24d**.

Surprisingly, deprotection from the TMDMS protection group failed. Neither TBAF, nor hydrogen fluoride in triethylamine lead to the liberation of the aldehyde modified polyethylene glycol. An acid catalyzed deprotection was not possible because the acetal protected aldehyde is acid labile and the latter is only deprotected after incorporation into RNA *via* T7 transcription. This synthetic route was not persevered any further; however it could be useful for non acid labile modifications.

Having experienced the above mentioned problems with protecting groups not being removable after a multistep synthesis, we were curious if we could accomplish a direct activation by mono-tosylation of the polydisperse polyethylene glycol substrates, PEG 600 and PEG 1500.

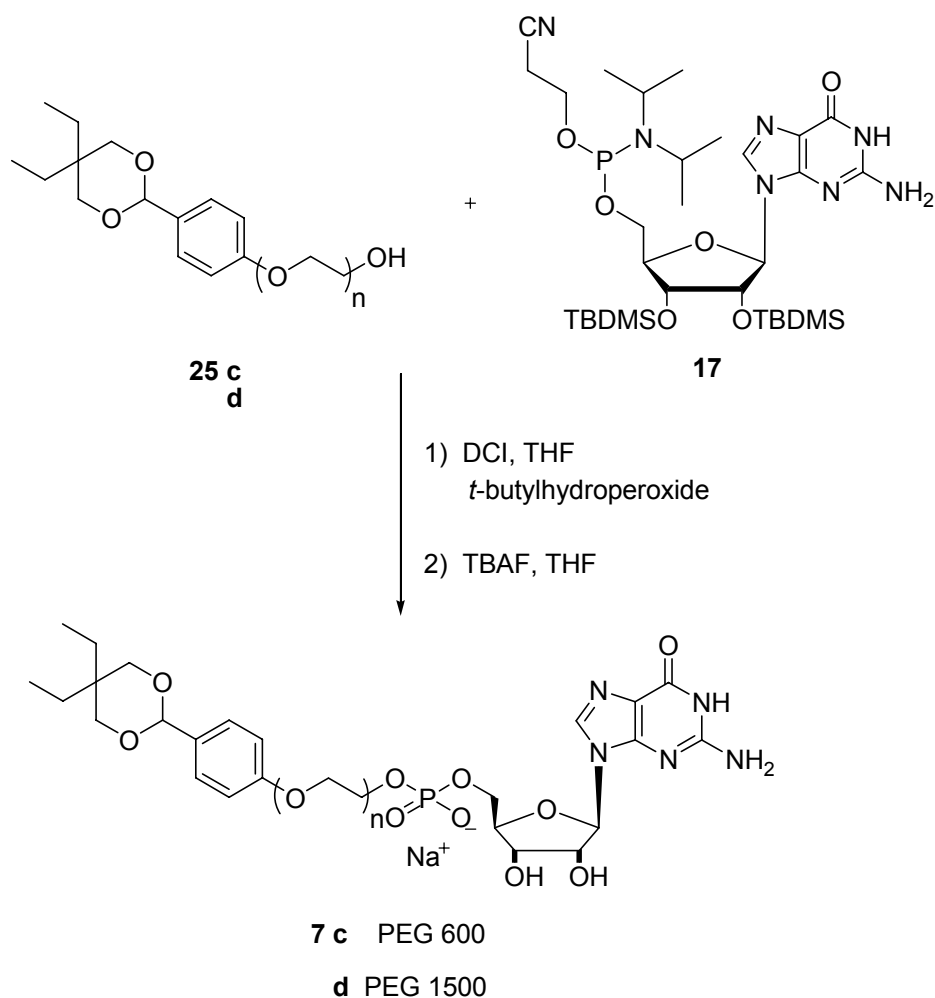


Scheme 17: Second synthetic strategy to polyethylene glycol *p*-toluenesulfonate and subsequent substitution.

Mono-functionalization of symmetrical diols has been of high interest in organic synthesis, but the scope of selective reactions is still very limited. Mono-tosylation of polyethylene glycols is the key step to all kinds of hetero-bifunctional PEG derivatives. Synthetic procedures for the mono-tosylation of short monodisperse polyethylene glycol have been reported, but many of the approaches are rather exotic, like the montmorillonite catalyzed,^[144] or silver (I) mediated combined with potassium iodine catalyzed mono-tosylation.^[145-149] A more simple approach had been reported for di-, tetra- and hexaethylene glycol.^[103, 150, 151] *p*-Toluenesulfonyl chloride was added to the polyethylene glycol with pyridine as base, the product had to be purified by column chromatography, in some cases even twice on normal silica and RP-C₁₈ silica.

The mono-tosylation was achieved by a slow addition of *p*-toluenesulfonyl chloride in DCM in the presence of the catalyst 4-dimethylaminopyridine and TEA. PEG is commercially available and relatively inexpensive and was therefore used in ten-fold excess over the *p*-toluenesulfonyl chloride. After tosylation the mono-tosylated product was separated from the excess PEG simply by extraction. While PEG alone is extracted into the aqueous phase, the mono-tosylated PEG remains in the organic dichloromethane phase. Mono-tosylated PEG 600 **26c** was obtained in a yield of 74% and PEG 1500 **26d** in a yield of 96%. The absence of bis-tosylated or non-tosylated PEG could unambiguously be ensured by MALDI-TOF MS analysis. Commonly, the tosyl function is easily hydrolyzed in the presence of water. However, the tosylated polyethylene glycol could be stabilized over a long period of time if the residual water was removed directly after the synthesis by coevaporation with toluene. The activation of polyethylene glycol by tosylation allows their modification with basically all hard nucleophiles in an S_N2 reaction.

The aldehyde-functionalized PEGs were obtained from 4-(5,5-diethyl-1,3-dioxan-2-yl) phenol **19**, which was first deprotonated with sodium hydroxide in ACN and refluxed with the mono-tosylated PEG for two days. After silica purification 47% of aldehyde mono-functionalized PEG 600 **25c** and 80% and of PEG 1500 **25d** were available for subsequent synthesis of the initiator nucleotide.



Scheme 18: Synthesis of initiator nucleotides **7c** and **d**.

The initiator nucleotides **7c** and **d** were synthesized from the aldehyde mono-functionalized polyethylene glycols and 2,3-bis-(*t*-butyldimethylsilyl)guanosin-5-O-(β -cyanoethyl-*N,N*-diisopropylphosphoramidite) **17** in the presence of DCI. After the addition of *t*-butyl hydroperoxide the solvent was removed and the guanosine intermediate directly deprotected. While for the anthracene derivative initiator nucleotides a relatively small excess of TBAF was sufficient to deprotect the guanosine, for the aldehyde initiator nucleotides six equivalents TBAF and prolonged reaction times were necessary. Purification of the initiator nucleotides was carried out by reverse phase column chromatography, ion exchange and a second reverse phase column chromatography.

2.3.1.3 Analytically of polydisperse polyethylene glycols

The easiest way to analyze polydisperse polyethylene glycols is MALDI-TOF MS analysis. In all cases, a Gaussian set of highly resolved peaks representing the distribution of PEG molar masses was produced. For PEG 600 chain lengths from 7 to 19 PEG units were observed and the highest intensity was assigned to $n = 13$, while for PEG 1500 the chain lengths varied from 17 to 40 with 27 giving the most intense signal.

It is also generally known that the quantitiveness of MALDI-TOF MS strongly depends on the process of ionization.^[152] However, the purity of the synthesized compound and the absence of side products can absolutely be proven, as no other masses have been observed.

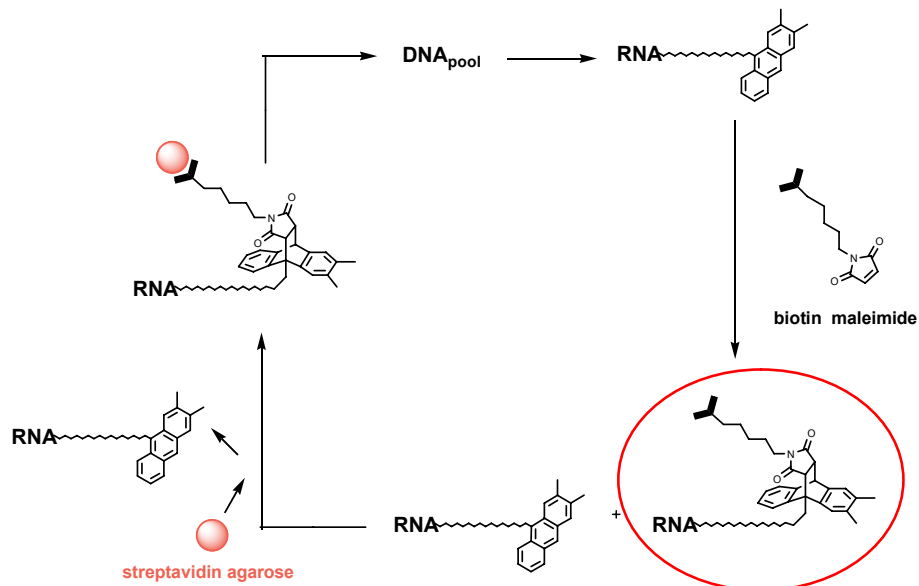
Synthetic polymers usually contain alkali metal cations as impurities from chemicals, solvents or glassware. Even during MS analysis alkali cation, impurities still remaining in the mass spectrometer, form adducts and the attachment of these cations, with Na^+ being the most common one, are observed.^[153] Modeling studies showed that alkali cations are coordinated to available oxygen sites along the backbone.^[154]

In the present work for polyethylene glycols with higher masses in MALDI-TOF MS analysis the main signal observed is not only just the adduct of one alkali cation, but combinations of either two alkali cations or mixtures of two different alkali cations. Shimada *et al.* had shown that additions of alkali cations mainly take place for the cation with the smallest ionic radius. During synthesis Li^+ was never present in any of the reactions, but residual Li^+ in the spectrometer from preceding samples was coordinated by the PEG compounds.^[155] Alkali cation adducts were observed with a increasing length of the polyethylene glycol, especially for PEG 1500 adducts of different cation combinations were measured. To prove that indeed the described product had been obtained the initiator nucleotides were later analyzed by high resolution ESI mass spectrometry. The integrity of the product was evidenced with absolute accuracy.

2.3.2 Towards the *in vitro* selection of a novel Diels-Alder ribozyme

The so called direct *in vitro* selection of a Diels-Alderase ribozyme, was first described by Seelig and Jäschke.^[41] For the selection of a true catalyst the substrate has to be tethered to the RNA library. The polymer linker attaches the anthracene substrate to the RNA, but after a Diels-Alder reaction with a maleimide derivative the RNA itself remains unaltered. After incubation, the RNA library is covalently attached to anthracene and therefore an anchoring

functionality has to be introduced during this reaction to allow for separation of the reactive from the unreactive species. Biotin maleimide is commercially available and thus the reactive species can easily be separated *via* biotin - streptavidin interaction on a solid support.

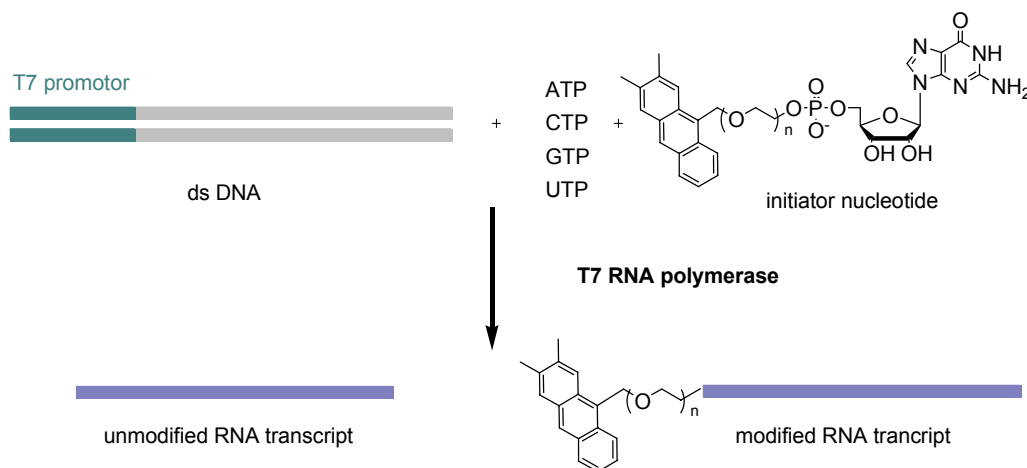


Scheme 19: Selection scheme for the *in vitro* selection of a Diels-Alderase ribozyme catalyzing a Diels-Alder reaction between 2,3-dimethylantracene and biotin maleimide.

The selection scheme for a possible *in vitro* selection of a Diels-Alderase ribozyme (scheme 19) proceeds from the RNA library, created by T7 RNA polymerase (RNAP) transcription starting from a DNA pool. During the transcription 2,3-dimethylantracene is incorporated into the RNA library by the enzyme T7 RNAP. The subsequent Diels-Alder reaction between 2,3-dimethylantracene and biotin maleimide creates two species. The desired sequences, which catalyze the Diels-Alder reaction and the ones where no reaction has taken place. The two species are partitioned on streptavidin agarose, while the RNA where no Diels-Alder reaction has taken place passes through the streptavidin agarose columns, the species now carrying biotin remain on the column. The retained RNA is eluted, reverse transcribed, amplified by PCR and again transcribed into RNA in the presence of an initiator nucleotide and re-introduced into the selection cycle. Noteworthy, other options than streptavidin for the separation of reacted and unreacted species e.g., separation on bead are available.

2.3.2.1 T7 RNA polymerase transcription

During transcription initiation the 5'-modified guanosine monophosphate is selectively incorporated at the 5'-end of the transcript (scheme 20).



Scheme 20: 5'-Modification of RNA with 2,3-dimethylanthracene *via* initiator nucleotide priming during T7 RNAP transcription.

For the initial experiments on the incorporation and reactivity of the initiator nucleotide a dsDNA template was used that transcribes into a 25 nt long RNA. Polydisperse polyethylene glycol based initiator nucleotides consist of many compounds with a molecular weight difference of 44.03 g mol^{-1} . This is naturally the case for the transcribed RNA, several different RNA molecules originate from one sequence, all set apart by the difference of one polyethylene glycol unit. These differences in molecular weight exceed the resolution of PAGE analysis and therefore the modified transcribed RNA does not appear like a sharp band but rather like a smear. For the 25mer the resolution was still acceptable if analysis was performed by 20% denaturing PAGE (figure 5).

The reaction was carried out using $0.2 \mu\text{M}$ template, 4 mM ATP, CTP and UTP, 0.35 mM GTP and 4 mM initiator nucleotide **7a**. For better visualization the transcription was performed with $[\alpha\text{-}^{32}\text{P}]\text{-CTP}$.

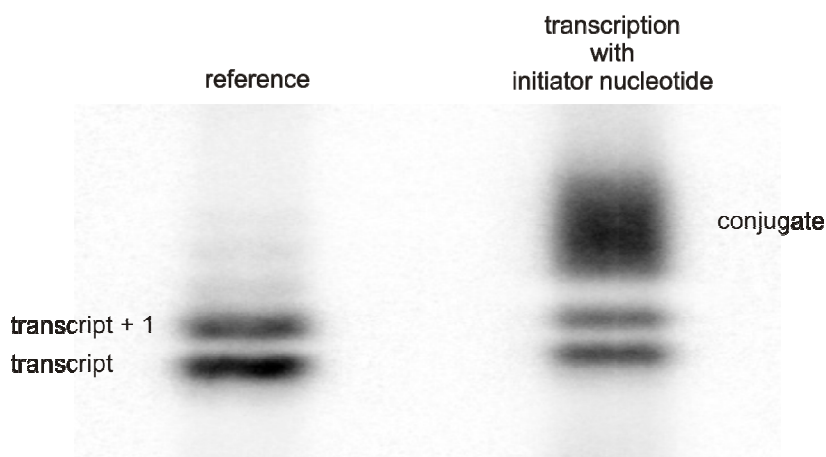


Figure 5: Transcription initiation of a 25-mer DNA template with the 2,3-dimethylantracene initiator nucleotide **7a**. 20% PAGE gel, autoradiography.

T7 RNA polymerase in general suffers from 3'-end heterogeneity of the RNA transcripts, meaning it has the tendency to append one or two and sometimes even more non-templated nucleotides.^[156, 157] For the 25mer these elongated sequences were observed, which in some cases resulted in a slight superimposition of the observed bands of the conjugate.

The incorporation rate was determined by HPLC and autoradiography to be 71% and the mass was confirmed by MALDI-TOF MS analysis (figure 6).

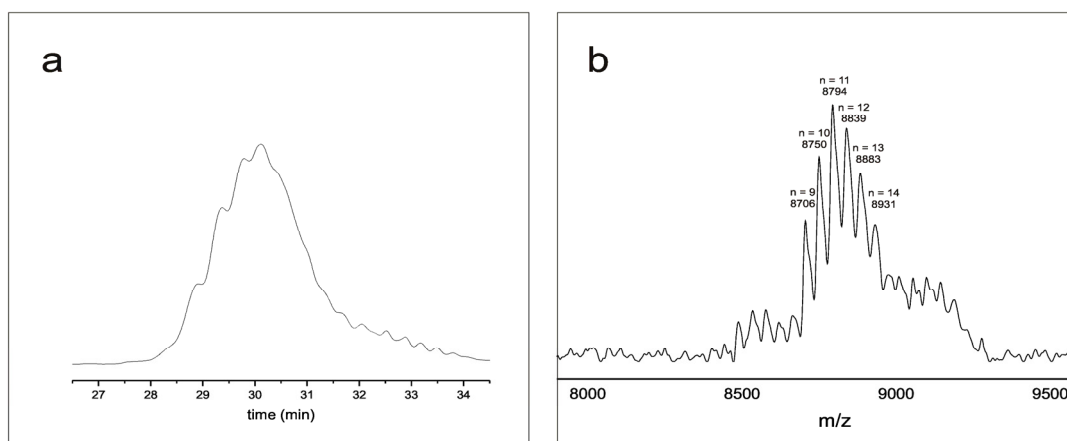


Figure 6: a: HPLC diagram at 260 nm of the polydisperse 2,3-dimethylantracene initiator nucleotide after incorporation into the 25mer RNA transcript. **b:** MALDI-TOF MS analysis: here the signal also shows that the polydisperse initiator nucleotide was incorporated. For $n = 11$ a mass of 8794 m/z was observed, which confirms the calculated mass of 8792 m/z for $[M+H]^+$.

2.3.2.2 Evaluation of the reaction conditions

To evaluate the reaction conditions of the Diels-Alder reaction between RNA tethered 2,3-dimethylantracene and biotin maleimide (see scheme 19) the reaction was performed with the above described model-transcript.

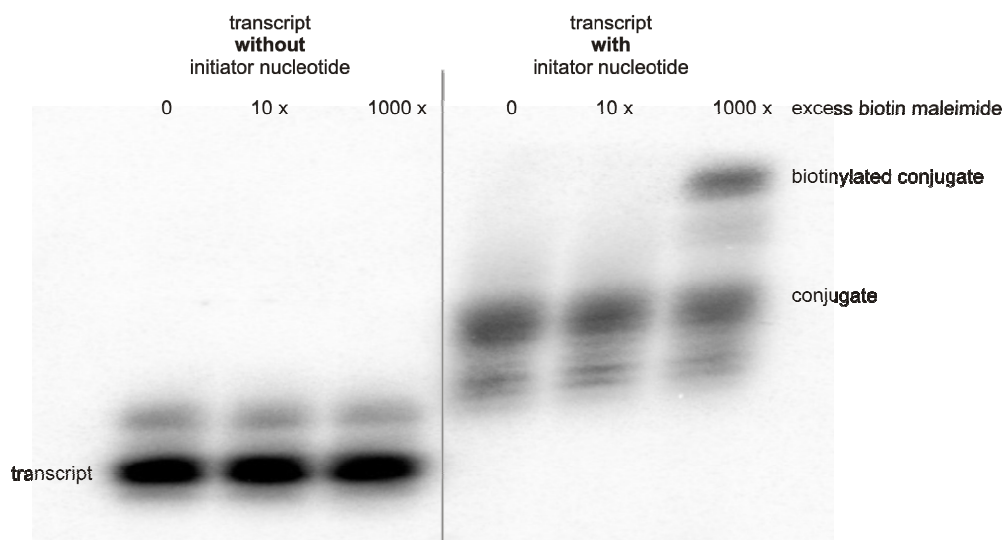


Figure 7: Diels-Alder reaction between RNA tethered 2,3-dimethylantracene and biotin maleimide. While the transcript without initiator nucleotide showed no reactivity with biotin maleimide the transcript with incorporated 2,3-dimethylantracene reacted with an 1000 fold excess of biotin maleimide. Analysis by autoradiography of a 20% PAGE.

In the first cycles of an *in vitro* selection the biotin maleimide has to be present in excess to enrich all sequences, even those that show moderate or low catalytic activity. The determination of the background rate is important to distinguish catalysts with low to moderate efficiency from good catalysts. In an initial experiment the conversion of the transcript was compared to the conversion of the transcript with the incorporated 2,3-dimethylantracene initiator nucleotide. Only if incubated over night with a 1000 fold excess of biotin maleimide a reaction product could be observed. The unmodified transcript showed no reactivity with biotin maleimide even at a 1000 fold excess and incubation over night (figure 7).

It was established that the new 2,3-dimethylantracene initiator nucleotide can be incorporated into a short model transcript and subsequently reacted with biotin maleimide. As a next step the incorporation into an RNA library with a randomized region should be tested. To accomplish this task the library had to be generated as described in the following section.

2.3.2.3 Generation of an RNA library

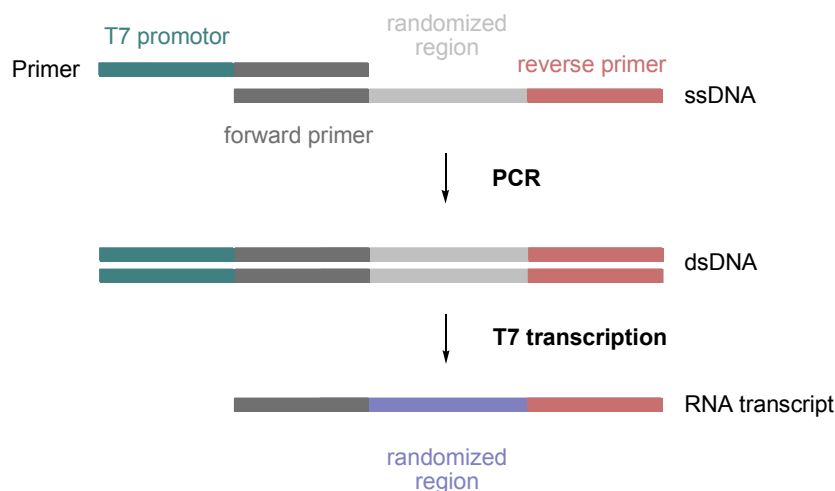


Figure 8: Generation of an RNA library with randomized region. The promoter sequence is essential for the recognition of the DNA template by RNAP. A polymerase specific promoter sequence can be appended to the dsDNA template during PCR by application of a primer containing this sequence. The dsDNA template can then be transcribed into RNA.

An RNA library was synthesized beginning from a DNA pool with a randomized region (figure 8). A DNA pool with a randomized region is the key feature to provide the huge complexity necessary to *in vitro* select catalytic species. Mathematically the limitation of this complexity is reached if the randomized region is only 25 base pairs long. If all four bases are randomly incorporated at all positions and every sequence is only represented once a complexity of $4^{25} \sim 10^{15}$ would be reached.^[15] 25 base pairs are too short to form the three-dimensional structures that are necessary for binding or forming a catalytic pocket in an active RNA structure. Therefore longer randomized regions provide better exit criteria for a successful *in vitro* selection. A 70 nucleotide long randomized region was chosen, flanked by the conserved regions, thus the resulting ssDNA template was 109 nucleotides long.

5'-GGA GCT CAG CCT TCA CTG C- N₇₀-GGC ACC ACG GTC GGA TCC AC-3'

From a 1 μ mol scale DNA synthesis 16.70 nmol DNA were obtained, equating to a pool complexity of 1.01×10^{16} . But even after purification not all templates can be amplified. To assess the complexity of the generated pool, primer extension with a radioactively labeled primer was performed. Only 24% of the pool could be amplified to full length product, resulting in an excellent pool complexity of 3.3×10^{15} .

2.3.2.4 Optimization of the PCR reaction

The two primers used for the PCR of this DNA pool are standard primers in our laboratory and have been named primer A and primer B. Primer A contains a promoter sequence which is added to the double stranded DNA during PCR (see figure 8). The addition of a promoter is indispensable for T7 polymerase recognition and thus transcription into RNA. In the case of the 109mer the addition of the promoter sequence leads to a 128 nucleotides long dsDNA template after PCR. For that reason primer A is 38 nt long while primer B only consists of 20 nucleotides, resulting in different optima for hybridization during PCR. This problem could partially be overcome by the use of higher primer B concentrations during PCR.

After several optimizations of the template concentration, annealing temperature, magnesium ion concentration and number of PCR cycles a preparative PCR was carried out with prolonged annealing and elongation steps in every cycle. In a pool with high complexity only one or very few copies of each sequence are represented and therefore long elongation steps are essential for the amplification of all sequences. Unspecific product formation could be avoided by performing only 6 PCR cycles. Repetitive cycles did not improve the product formation considerably, but two side product bands with a length of around 180 and 210 base pairs were formed.

The optimal PCR conditions were determined to be a template concentration of 0.2 μM , 10 μM primer A, 15 μM primer B, 0.2 mM concentration of all NTPs and the use of 4 mM magnesium chloride. For the preparative PCR a total volume of 55 mL was partitioned into several 96 well plates and after PCR combined again and purified by phenol extraction.

2.3.2.5 Transcription initiation with the DNA library

The transcription of the DNA library has first been studied without the initiator nucleotide.

The highest yield in terms of oligonucleotide multiplication was obtained with 4 pmol dsDNA template. Several transcription buffer systems and MgCl_2 concentrations were tested and 40 mM Tris buffer at pH 8.1 containing 22 mM Mg^{2+} , 0.1 mM spermidine and 0.01% Triton X-100 were determined to be the best conditions for the transcription of the DNA pool.

For the incorporation of the initiator nucleotide into the RNA library the concentration of the initiator nucleotide and of GTP was varied while the three other NTPs were kept constant at 4 mM. The use of a high concentration of NTPs had been shown to yield the highest amount of RNA transcript.^[158]

For the transcription of the DNA library with the 2,3-dimethylantracene initiator nucleotide incorporation rates up to 77%, determined by HPLC (figure 9), could be achieved. Unfortunately the transcription was considerably inhibited by the initiator nucleotide. Low transcription yields were linked to the presence of the initiator nucleotide. The transcription was carried out with 0.35 mM GTP and 4 mM initiator nucleotide. In the reference reaction no initiator nucleotide was present. If the initiator nucleotide would not cause inhibition of the T7 RNAP similar yields for the transcription with and without initiator nucleotide would be the case. However a decoupled RNA yield was observed in the absence of the initiator nucleotide (figure 9).

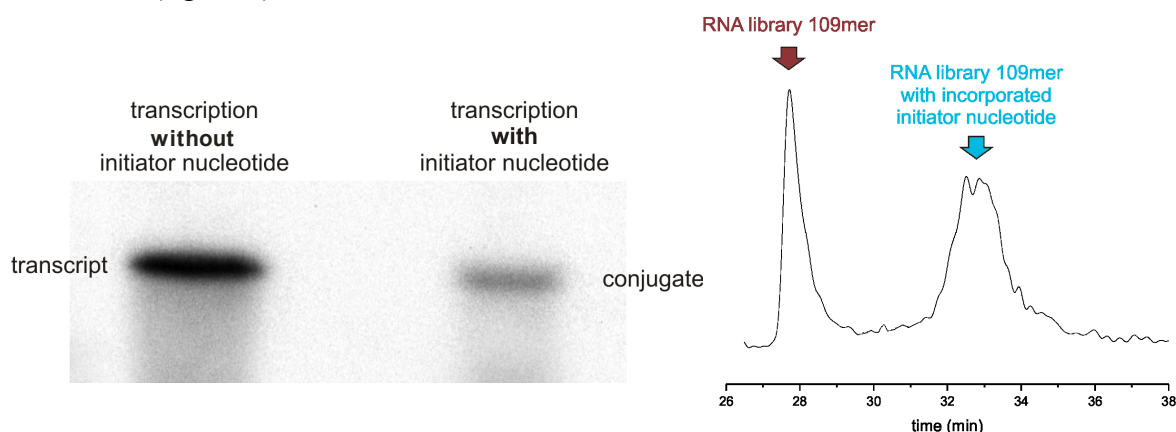


Figure 9: Transcription initiation without and with 2,3-dimethylantracene initiator nucleotide, using 0.35 mM GTP and 4 mM initiator nucleotide. Analysis by autoradiography of 12% denaturing PAGE and incorporation rate determination *via* HPLC detection of the ^{32}P signal.

The overall yield could be improved by inverting the ratio between GTP and initiator nucleotide, using 4 mM GTP and 1 mM initiator nucleotide. However, the incorporation rate dropped below 10%, which resulted in less conjugation product than using 0.35 mM GTP and 4 mM initiator nucleotide. Furthermore this experiment (figure 10) again showed that the 2,3-dimethylantracene initiator nucleotide has an inhibiting effect on the T7 RNAP enzyme.

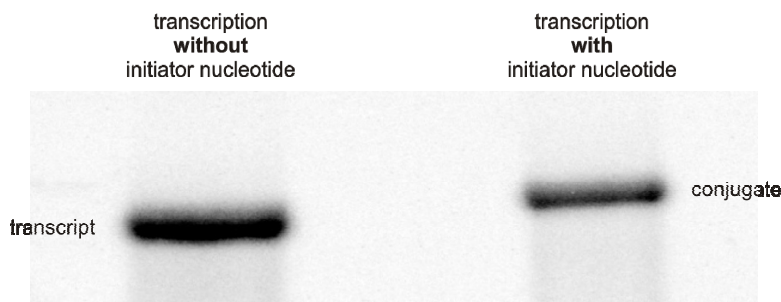


Figure 10: Transcription initiation without and with 2,3-dimethylantracene initiator nucleotide, using 4 mM GTP and 1 mM initiator nucleotide. Analysis by autoradiography of 8% PAGE.

Anthracene derivatives are known to readily react with oxygen upon exposure to light to form the corresponding epidioxyanthracenes, or sometimes described as photoperoxides.^[159, 160] Therefore elevated temperatures and exposure to light have to be avoided, because loss of the aromaticity of the anthracene would make a Diels-Alder reaction impossible.

The enzyme T7 RNAP is usually used at 37°C or higher temperatures. The stability of the initiator nucleotide and the anthracene derivative were investigated under conditions analogous to the conditions of the transcription. The initiator nucleotide was incubated in transcription buffer for four hours and the integrity of the initiator nucleotide was confirmed by HPLC analysis before incubation, after two and four hours at 37°C (figure 11). The initiator nucleotide remained unaltered and no epoxide formation was observed. Furthermore, this experiment allowed the conclusion that for the initiator nucleotide no decomposition accrued over the period of four hours at a temperature of 37°C. Low incorporation yields can therefore not be linked to decomposition of the initiator nucleotide.

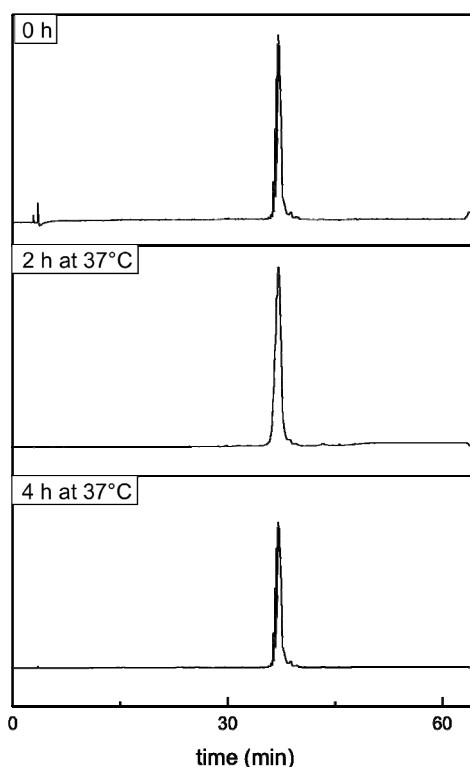


Figure 11: HPLC at 260 nm at different time points after incubation of the initiator nucleotide in transcription buffer at 37°C.

Further approaches to improve the yield of the conjugated RNA library were investigated. These approaches included elongated reaction times, the use of commercially available transcription kits or the addition of a so called booster mix, containing NTPs and additional

initiator nucleotide in buffer supplemented with T7 RNAP, after two hours, followed by continuous transcription for another two hours. T7 RNAP has a DNase and RNase function, which can be inhibited by an excess of NTPs during the transcription, the addition of a booster mix thus does not only provide more material for the transcription, but also inhibits the nuclease function of the RNAP.^[161] Commonly, residual salt from the preparation of the DNA template can be responsible for low transcription yields.^[113] To eliminate this aspect the template was desalted before transcription and the initiator nucleotide was purified *via* a second ion exchange and a third reverse phase column chromatography. But the inhibition of the transcription of the DNA library in the presence of the initiator nucleotide bearing 2,3-dimethylanthracene could not be overcome.

However, the fact that an incorporation rate of 77% could be achieved during RNAP transcription with a DNA library with a 109 nucleotide long sequence is quite noteworthy.

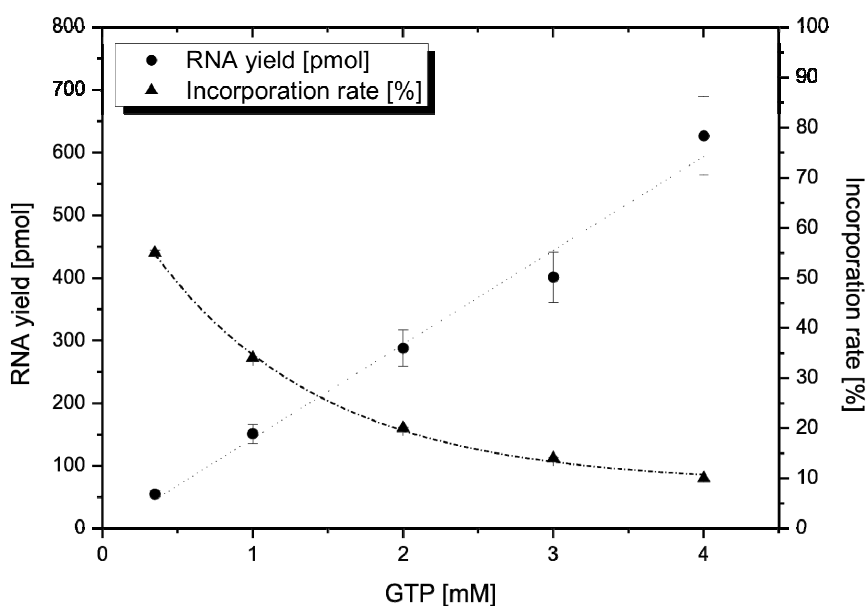
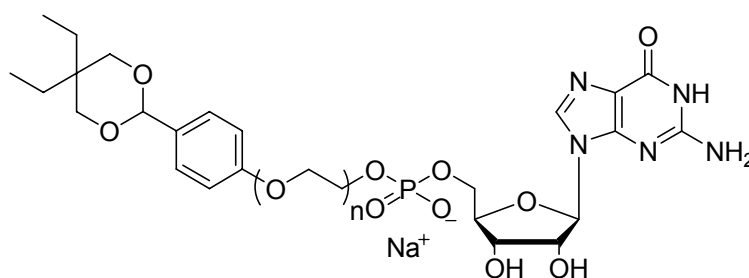


Figure 12: Enzymatic incorporation of the initiator nucleotide (1 mM) *via* T7 RNA polymerase transcription (2 h reaction time) of the 109 nt dsDNA library, varying the GMP concentration.

2.3.3 Incorporation and application of aldehyde containing initiator nucleotides

In section 2.3.1.4 a short and efficient synthetic approach to the synthesis of polydisperse aldehyde-modified initiator nucleotides was developed (scheme 21). The incorporation and reactivity of the aldehyde-modified initiator nucleotides will be tested and is described herein.



7 c PEG 600
d PEG 1500

Scheme 21: Aldehyde modified initiator nucleotides.

Initiator nucleotide **7c** with n_{PEG} varying from 7–19 was synthesized from PEG 600, while the initiator nucleotide with PEG 1500 **7d** resulted in a distribution of $n_{\text{PEG}} \sim 17$ –41 (figure 13).

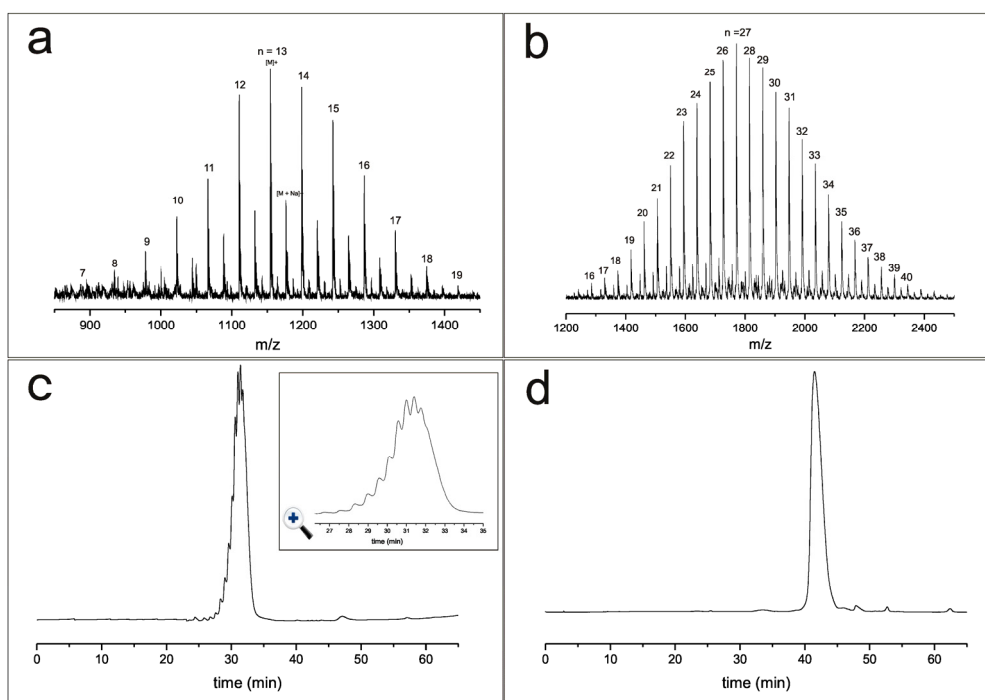


Figure 13: Illustration of the differences between the initiator nucleotide with PEG 600 **7c** and PEG 1500 **7d**. **a:** MALDI TOF MS of initiator nucleotide **7c**; **b:** MALDI TOF MS of initiator nucleotide **7d**; **c:** HPLC detection at 260 nm of initiator nucleotide **7c**; **d:** HPLC detection at 260 nm of initiator nucleotide **7d**.

room temperature the reaction was analyzed *via* PAGE and a gel shift for the biotinylated conjugate was observed. Notably, full conversion could be observed for the reaction between the aldehyde-modified initiator nucleotide and the hydrazide (figure 15).

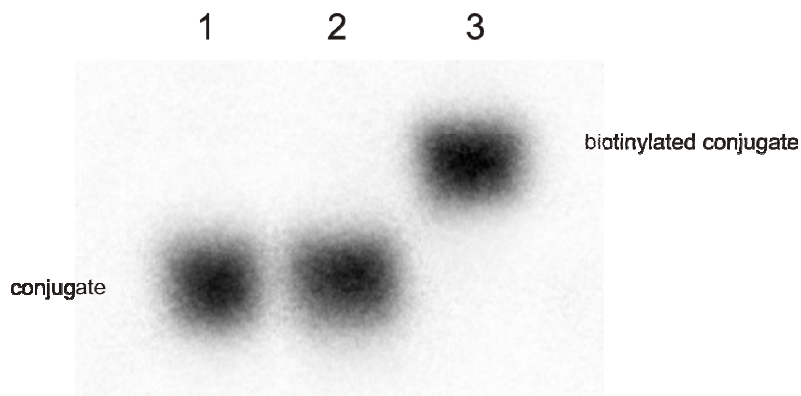


Figure 15: Lane 1: conjugate protected aldehyde. Lane 2: conjugate deprotected aldehyde. Lane 3: conjugate aldehyde deprotected and reacted with biotin hydrazide. 12% PAGE, autoradiography scan.

2.4 Conclusion

The 5'-end modification of RNA could be achieved co-transcriptionally by transcription priming using T7 RNAP and initiator nucleotides with either a benzaldehyde organic moiety or 2,3-dimethylantracene. For the transcription of short oligonucleotides no inhibition of the enzyme T7 RNAP was observed. The initiator nucleotide bearing 2,3-dimethylantracene could be incorporated into a 109 nucleotide long RNA library with a randomized region with an incorporation rate of 77% although diminished total yields were observed. For the aldehyde modified initiator nucleotide an incorporation rate of 52% could be observed. Hydrophilic moieties are known to result in lower incorporation efficiencies than hydrophobic moieties.^[140]

The reactivity of the incorporated initiator nucleotides was confirmed. After transcription the anthracene modified RNA was biotinylated in a Diels-Alder reaction with biotinmaleimide, while the aldehyde-modified RNA was biotinylated employing a biotin-hydrazide. Full conversion for the formation of the hydrazone was observed.

The synthesis of polydisperse initiator nucleotides could considerably be improved. For the synthesis of polydisperse initiator nucleotides with an anthracene moiety a very clean and rather short synthetic route could be established. Originating from the anthracene derivative

and the TBDMS protected guanosine monophosphate the synthesis could be achieved in only five steps. Furthermore, a novel synthetic pathway, *via* a mono-tosylated polyethylene glycol compound, was established and demonstrated for the aldehyde modified initiator nucleotide presenting a superior synthetic strategy for the incorporation of many highly functional organic modifications into RNA. The mono-tosylated polyethylene glycol represents the key step to a vast variety of organic modifications in RNA. The tosyl-activated PEG can be reacted in an S_N2 reaction with a multitude of nucleophiles. Furthermore, the synthesis of such initiator nucleotides can be achieved in only three synthetic steps.

3 Thermal denaturation studies of the Diels-Alderase ribozyme

3.1 Scientific background

3.1.1 Metal ions in ribozyme folding and catalysis

The discovery that RNA molecules do not only carry genetic information, but can also have catalytic activity and thus require a defined structure, has led to a new understanding of the structures and mechanisms of folding. Like proteins, RNA adopts complex three-dimensional structures for the precise presentation of chemical moieties that are essential for its function as biological catalyst, translator of genetic information and structural scaffold.^[162] The most important parameter in folding and shape of single-stranded nucleic acids is complementary Watson-Crick base pairing *via* hydrogen bonding. Even though RNA molecules usually consist of single strands, RNA molecules contain linear runs that are complementary to other runs elsewhere in the molecule. This way RNA can form double-stranded regions. Further important nucleotide interactions as part of tertiary interactions are intra- or intermolecular interactions based on canonical and non-canonical base pairs, pseudoknots, water bridges, and interactions with metal ions.^[113]

The structure of oligonucleotides, either free or in complex with metal ions or specific ligands, can be analyzed using various experimental methods, like X-ray crystallography, cryo-electron microscopy, NMR, structure-specific probes, RNA engineering, mass spectrometry and thermal denaturation. A good explanation on structure, folding and function of an oligonucleotide is generally obtained from a combination of experimental setups.

Using UV spectroscopy, thermal denaturation experiments can be utilized to determine the stability of RNA secondary and tertiary structures and are informative about the hierarchy and dynamics of RNA folding. Thermal denaturation of RNA complements other techniques, such as crystallography, NMR, CD spectroscopy or probing experiments.^[163]

Two distinct functions of metal ions are essential for ribozymes. Divalent cations provide stabilization for the structural folding of RNA and can be required for chemical reactions. Pyle described the RNA molecule as an extended polyanion that is not easily packed into its catalytically active form without substantial charge neutralization between the interacting strands.^[164] Cations therefore neutralize the charge in folded RNA molecules. It was suggested that divalent cations bind to specific sites, and thus form a metal ion core in RNA

equivalent to the hydrophobic core in proteins. This way the core folds the secondary structure into the required tertiary structure.^[165, 166] The tertiary structure is the three-dimensional organization, which is relevant for the biological function of RNA molecules.

RNA contains a number of ligands for metal coordination, mainly due to the phosphate oxygens, 2'-hydroxyls, base carbonyls and transition-state oxyanions, which preferentially coordinate hard alkaline earth metals ions such as Mg^{2+} . Magnesium ions are generally hexahydrated and are coordinated in an octahedral geometry, whereas coordination numbers greater than six are common for Ca^{2+} . The Mg^{2+} cation has a low affinity to nitrogen ligands and basically no affinity for sulphur. Transition metals such as Mn^{2+} can be coordinated by ribonucleic oxygens as well as the nitrogens in the ring of the bases.^[167] Other common transition metals like Zn^{2+} and Cd^{2+} exhibit a similar behaviour as Mn^{2+} .^[168]

With one negative charge per nucleotide (located at every phosphate of the phosphodiester back bone) the negative charge density of RNA is extremely high. These negative charges would repel each other, but that repulsion is greatly diminished when each phosphate is surrounded by a cloud of small cations. Due to their high charge density and their negative electrostatic potential all nucleic acids accumulate concentrated cation atmospheres, which extend over a distance of several Ångström.^[169] Simplified, the interaction of RNA with cations can be divided into two major categories. One interaction is diffuse, meaning that the ions remain entirely hydrated and are only affected by the electrostatic potential of the RNA. The other is chelating and characterized by direct contacts between the RNA and the metal ions.^[170] Chelating metal ion binding sites have been identified for a number of RNA molecules in X-ray crystal structures.

For a long time it was believed that ribozymes only fold and catalyze reactions in the presence of divalent metal ions. The hammerhead, the hairpin and the VS ribozyme were the first ribozymes reported to have catalytic activity in the absence of divalent metal ions.^[171] However, monovalent metal ions have to be applied at molar concentrations (non-physiological) for folding, activity, and stabilization of the structure. Nevertheless, they can not compete with the catalytic activity observed in the presence of divalent metal ions.^[172]

As for structural concerns, the pseudoknot RNA from Beet Western Yellow Virus (BWYV) is possibly the most prominent example of a pseudoknot structure stabilized by monovalent cations. The crystal structure revealed four putative coordination sites for alkali metal cations.^[173] UV denaturation experiments showed that the RNA could entirely be stabilized up to high temperatures by sodium cations alone.^[174]

3.1.2 The Diels-Alderase ribozyme

Various analytical techniques have been employed to study the structural and mechanistic properties of the Diels-Alderase ribozyme.^[92, 93, 175, 176]

The Diels-Alderase ribozyme was found to require divalent metal ions such as Mg^{2+} , Mn^{2+} or Ca^{2+} for folding into its three-dimensional structure, but it has to be pointed out that, unlike many other ribozymes the Diels-Alder ribozyme does not involve metal ions in the catalytic process.

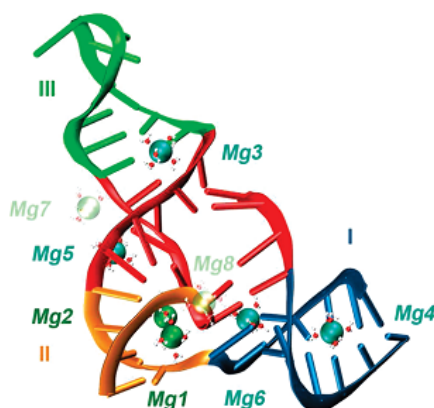


Figure 16: Crystal structure of the Diels-Alderase ribozyme. Mg stands for magnesium ions indicated in green. Latin numbers indicate the helices I-III. Figure adapted from Berezniak *et al.*^[177]

The Diels-Alderase ribozyme is stabilized by eight Mg^{2+} cations (figure 16). Mg1 and Mg2 contribute most to the structural scaffold of the catalytic pocket, while Mg3-Mg6 stabilize the λ -shaped RNA structure. Mg7 and Mg8 mediate contacts between RNA molecules in the crystal lattice, but these magnesium ions are not coordinated to the ribozyme in solution.^[177]

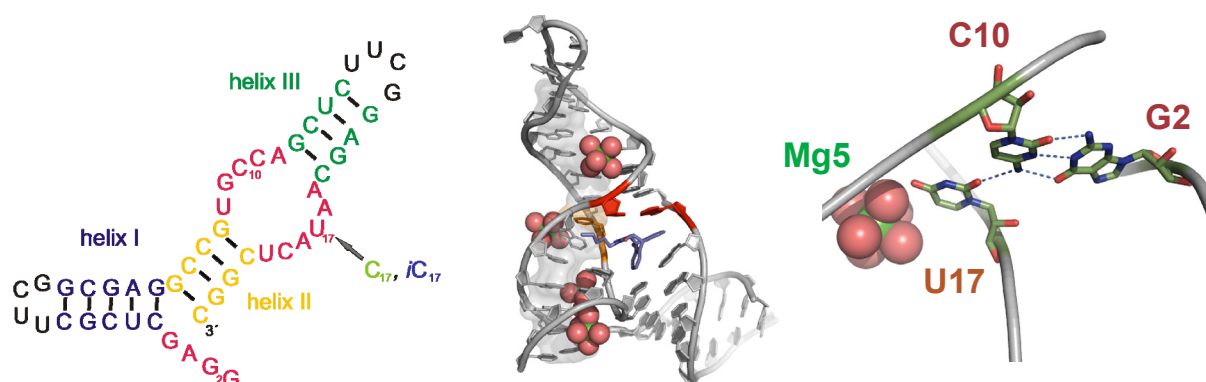
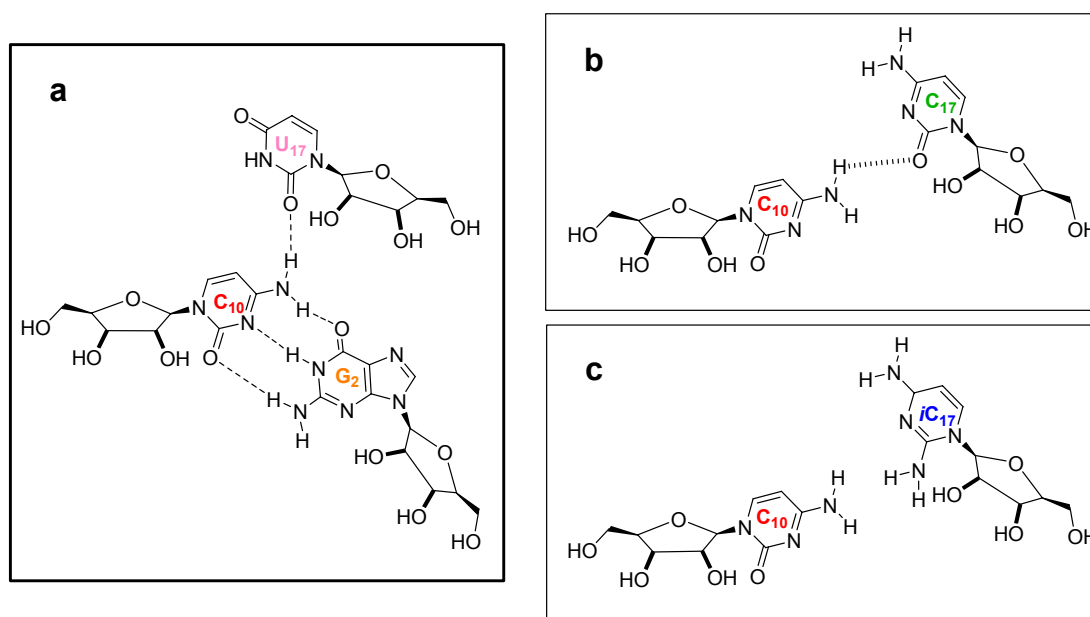


Figure 17: Two and three dimensional structure of the Diels-Alderase ribozyme; the three bases involved in this triple are indicated.

In the following, light will be shed on a particular structural element of the Diels-Alderase ribozyme. A tertiary interaction of three bases in the heart of the binding pocket: the tertiary interaction of the U17 base with the pseudoknot base-pair C10-G2 was first identified in the X-ray crystallographic structure and has proven to be absolutely essential. These triple bridging bases facilitate the cross-strand junction of the pseudoknot, stacking interaction with the neighbouring bases and one magnesium ion number five (figure 17) which stabilizes this junction point. Furthermore these bases are part of the central H-bonding network forming the binding pocket of the ribozyme.



Scheme 23: **a:** the base triple G2 – C10 – U17 (wild-type) **b** and **c:** mutants (C10 – C17 and C10 – iC17). Hydrogen bonding disrupted.

Atomic mutagenesis has been utilized to selectively perturb these bonds and illustrate the functional relevance of the interaction between U17-O2 and C10-HN4. To gain further insight into this triple base pair an U17C and an U17*i*C mutant (scheme 23) ribozyme have been compared to the wild type.

A comparison in reactivity between the wild-type ribozyme and these mutants showed that both mutants fold into a pseudoknot structure, but can not undergo further compactation. While the U17C mutant shows a factor three decreased activity, the U17*i*C mutant is entirely inactive.^[178] Furthermore the dienophile is activated by two weak H-bonds related to that triple (U17-2'OH and G9-HN2 vs. dienophile-O). This H-bonding network contributes to the stabilization of the transition state and is therefore crucial for the catalytic activity. Lead (Pb²⁺) probing also showed that the U17*i*C mutant has no affinity to the Diels-Alder product.^[179]

3.1.3 UV melting curves

The temperature induced transition between the native and denatured state of nucleic acids can conveniently be observed by UV absorbance. The absorbance *versus* the temperature profile is referred to as a UV absorbance melting curve and the midpoint of this transition is called the melting temperature (T_m) of the analyzed nucleic acid. T_m corresponds to the temperature at which half of the sample is folded and half is unfolded.^[180] As the temperature increases the ratio of molecules in a denatured state increases. The native state and the denatured state of the nucleic acid exhibit different absorptivities,^[181] enabling to monitor this change in absorption as the process of melting and the disruption of the structural elements of the nucleic acid.^[182]

3.1.4 Practical considerations of determining UV denaturation

The choice of buffer is an extremely important aspect when it comes to performing reliable UV thermal denaturation studies. Among the most important considerations are the pK_a and its temperature dependency, the buffer capacity, and the compatibility with divalent metals.^[183] Table 2 lists some of the most common buffers for UV denaturation experiments.

Table 2: Buffers used for UV thermal denaturation studies.

Buffer	pK_a (25°C, I = 0.1 M)	$\Delta pK_a/\Delta T$ (°C ⁻¹)	Compatible with divalent ions	Reference
Sodium cacodylate	6.27	-0.0015	Yes	a
Sodium phosphate	7.20	-0.0028	No	a
TrisHCl	8.06	-0.028	No	a
MOPS	7.20	-0.015	Yes	b, c
HEPES	7.55	-0.014	Yes	a

a [183], b [184], c [185]

The optimized buffer for the Diels-Alderase ribozyme consists of 30 mM Tris·HCl (pH 7.4), 300 mM NaCl and 80 mM MgCl₂.^[111] Unfortunately Tris·HCl buffer has a huge temperature dependency of the pK_a . The most commonly used phosphate buffer, consists of a mixture of monobasic dihydrogen phosphate and dibasic monohydrogen phosphate,^[186] but can not be used, because it sequesters divalent ions such as Mg²⁺, Mn²⁺, Cd²⁺ or Ca²⁺. The MOPS buffer is often used for thermal denaturation studies, even though its pK_a is known to be temperature

dependent.^[182, 187] Initial experiments considering different buffers showed that MOPS has a high temperature dependency and pH changes from 7.0 to 6.2 if heated from 25°C to 80°C were observed. While sodium cacodylate showed best results and was therefore used throughout all melting experiments. One has to keep in mind that all buffers contain cations, e.g. a 25 mM sodium cacodylate buffer contains 25 mM Na⁺ cations, which naturally contribute to the stability of the RNA.

3.2 UV denaturation of the Diels-Alderase ribozyme

The aim was to study secondary and tertiary interactions of the Diels-Alderase ribozyme wild-type as well as the two mutants U17C and U17iC. In previous studies the mutant 17iC mutant, in which the H-bonding network is disrupted, was entirely inactive, while the C17 mutant, that is still capable to form an H-bond, only showed a catalytic activity of 30% as compared to the wild-type.^[178] The magnesium ion Mg²⁺ is in close proximity to this base-triple (figure 17) and therefore studies of the thermal stability in dependency on the Mg²⁺ ion concentration may lead to further insight on this interaction.

A UV/Vis spectrophotometer equipped with a Peltier block temperature-controller was utilized to determine the melting curves at 260 nm. Heating and cooling cycles in the temperature range of 15-90°C were measured in 25 mM sodium cacodylate buffer with a temperature gradient of 0.5°C/min. The melting curves itself were obtained from plotting the normalized melting temperatures vs. the absorbance at 260 nm. The interesting structural information however, was extracted from a plot of the first derivative of the absorbance vs. the temperature.

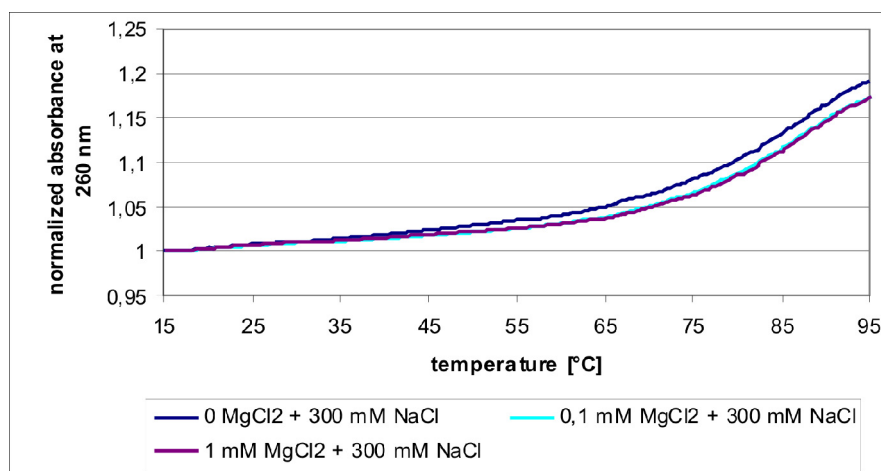


Figure 18: Absorption of the wild-type at different MgCl_2 concentrations in the presence of 300 mM NaCl.

Figure 18 presents the melting curve of the wild-type ribozyme in the presence of 300 mM NaCl as present in the commonly used buffer for the Diels-Alderase ribozyme. A good stabilization of the structure can already be extracted from this plot.

Looking at the first derivative of UV denaturation curves the first peak in the low temperature range can be attributed to the opening of the tertiary structure. For the opening of the secondary structure much higher temperatures are required (figure 19).^[113] Each independently folding element therefore has its own T_m . Thermal denaturation studies of the Diels-Alderase ribozyme (wild-type) in the presence of 300 mM NaCl (99.999% pure NaCl) showed that the structure is entirely stabilized. The melting temperature of the Diels-Alderase ribozyme in the presence of high concentrations of Na^+ was found to be at 86°C ($\pm 0.2^\circ\text{C}$) and independent from the Mg^{2+} concentration. The opening of the tertiary structure was observed at 65°C ($\pm 0.2^\circ\text{C}$).

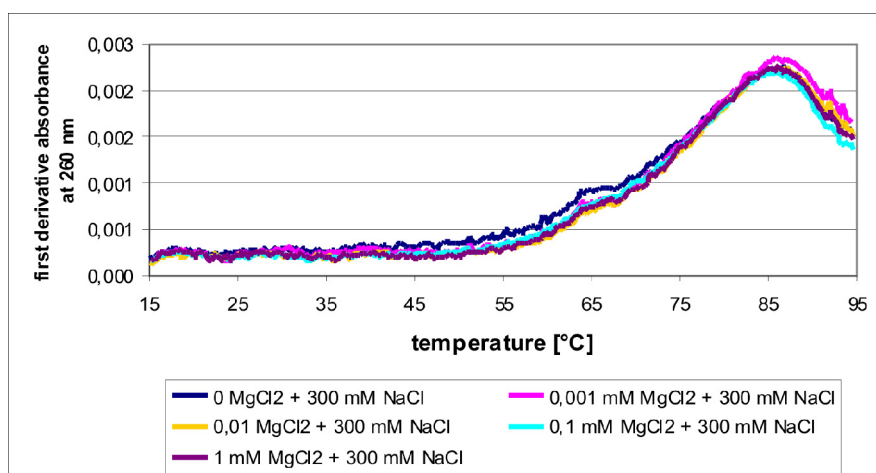


Figure 19: UV denaturation curves of the Diels-Alderase ribozyme in the presence of 300 mM NaCl. First derivative of the absorption plotted vs. the temperature.

In the presence of 300 mM NaCl (figure 19) the entire structure was stabilized and additional stabilization with divalent metal cations could not be monitored with thermal denaturation experiments. If further stabilization would be possible, e.g. with higher concentrations of monovalent or divalent metal cations it can not be monitored by thermal denaturation experiments. Therefore, further thermal denaturation experiments were carried out in the absence of Na^+ cations to study denaturation behaviour in dependency on the presence of EDTA and divalent metal ions, respectively Mg^{2+} cations.

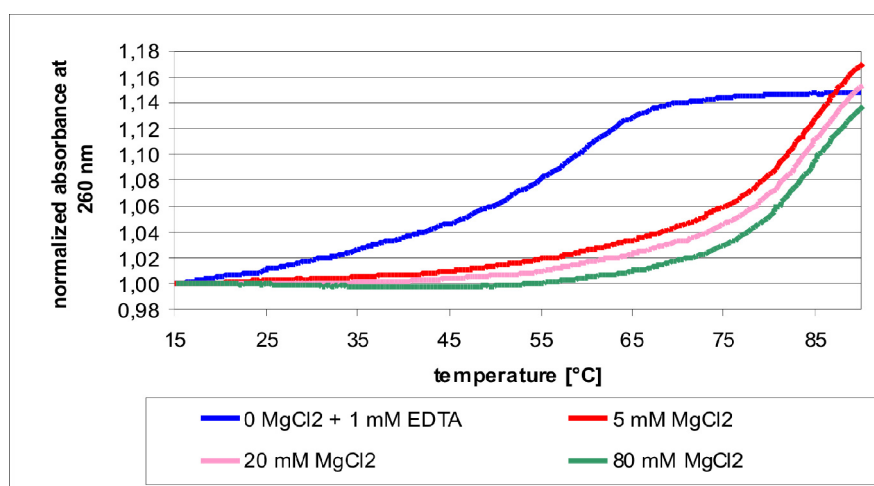


Figure 20: Absorption of the wild-type at different MgCl_2 concentrations respectively with EDTA.

If EDTA was added to trap traces of divalent ions (figure 21), the structure of the Diels-Alderase ribozyme was found to be destabilized and the melting temperature was shifted by 26°C from 83°C ($\pm 0.2^\circ\text{C}$) to 57°C ($\pm 0.2^\circ\text{C}$).

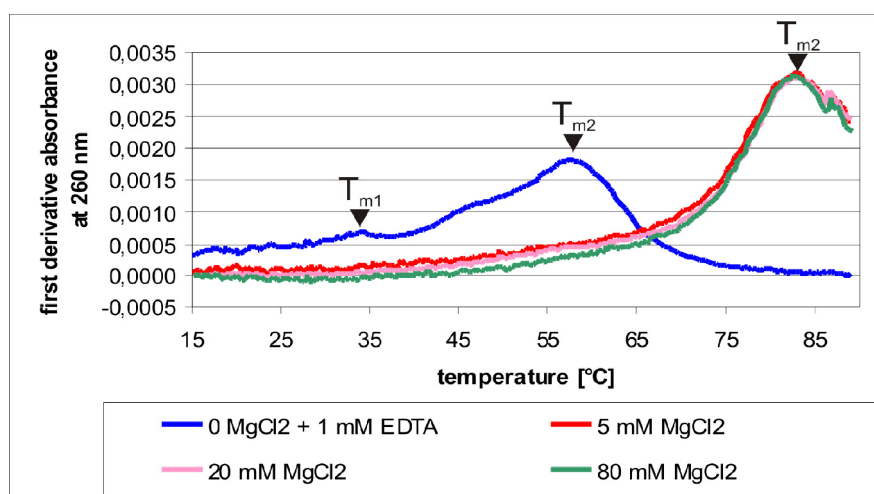


Figure 21: Absorption of the wild-type at different MgCl_2 concentrations. T_{m1} indicates the opening of the tertiary structure and T_{m2} the opening of the secondary structure.

The addition of 5 mM MgCl₂ was already sufficient to fully stabilize the Diels-Alderase ribozyme (figure 21).

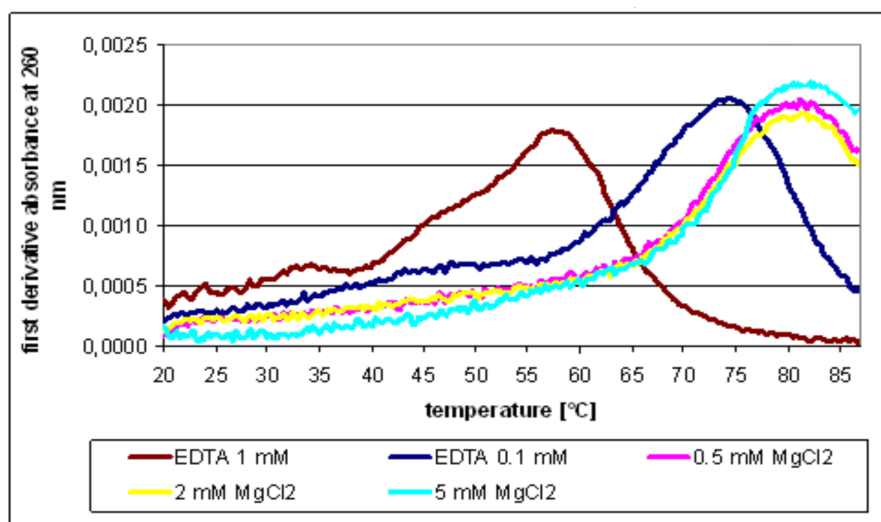


Figure 22: Absorption of the wild-type at different MgCl₂ concentrations respectively with EDTA.

In dependency of the EDTA concentration, the opening of the tertiary structure (T_{m1}) was observed at different temperatures, while the addition of Mg²⁺ significantly stabilized the tertiary structure (figure 22, table 3). Buffer solutions generally contain impurities of divalent metal ions, the difference in the melting temperature between 1.0 and 0.1 mM EDTA can be seen as a reflection of the divalent metal ions present in the buffer solution.

Table 3: T_m values of the Diels-Alderase ribozyme in the presence of different MgCl₂ and EDTA concentrations. T_{m1} opening of the tertiary structure; T_{m2} opening of the secondary structure.

MgCl ₂ / EDTA	T_{m1} [°C]	T_{m2} [°C]
1 mM EDTA	33	57
0.1 mM EDTA	44	74
0.5 mM MgCl ₂	-	80
2 mM MgCl ₂	-	80
5 mM MgCl ₂	-	83

3.2.1 Comparison of the Diels-Alderase wild-type with two mutants: U17C and U17*i*C

In a series of measurements the wild-type, the U17C mutant and the U17*i*C mutant have been compared at different magnesium chloride concentrations.

Initial experiments showed that the opening of the secondary structure for the mutants occurs at similar temperatures of the wild-type. For further experiments the mutants were

investigated at temperatures up to 60°C. The interesting transition observed in UV denaturation experiments is T_{m1} , the opening of the tertiary structure and this transition occurs below 60°C.

Mg^{2+} ion concentrations between 0.1 mM EDTA and 2 mM showed no considerable difference between the wild-type and the mutants. As an example the comparison between the wild-type and the mutants at 0.2 mM $MgCl_2$ is shown (figure 23, for details see appendix). At an Mg^{2+} concentration of 5 mM a significant difference between the mutants was monitored, the stabilization of the wild-type lead to a lower absorption (figure 24 and 25).

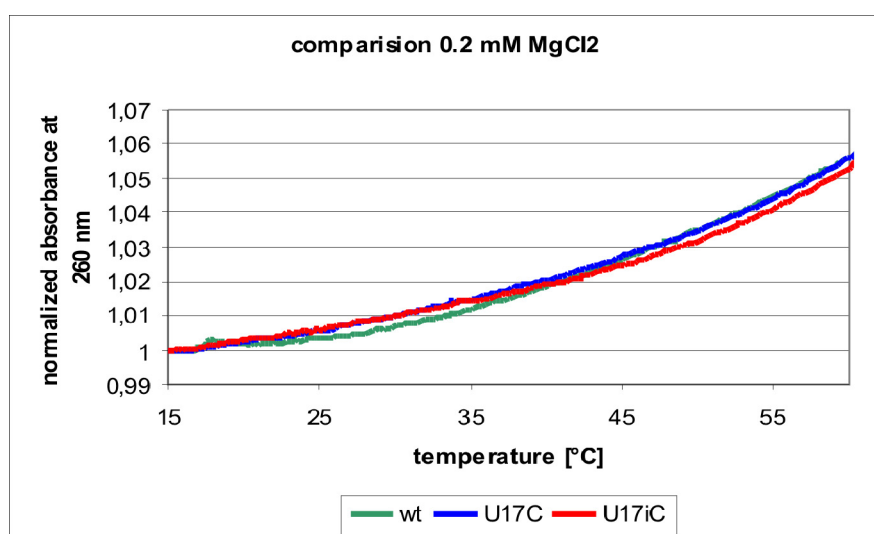


Figure 23: Comparison between the wild-type and the U17C and C17iC mutant at 0.2 mM $MgCl_2$, plotted as a function of the normalized absorption vs. the temperature.

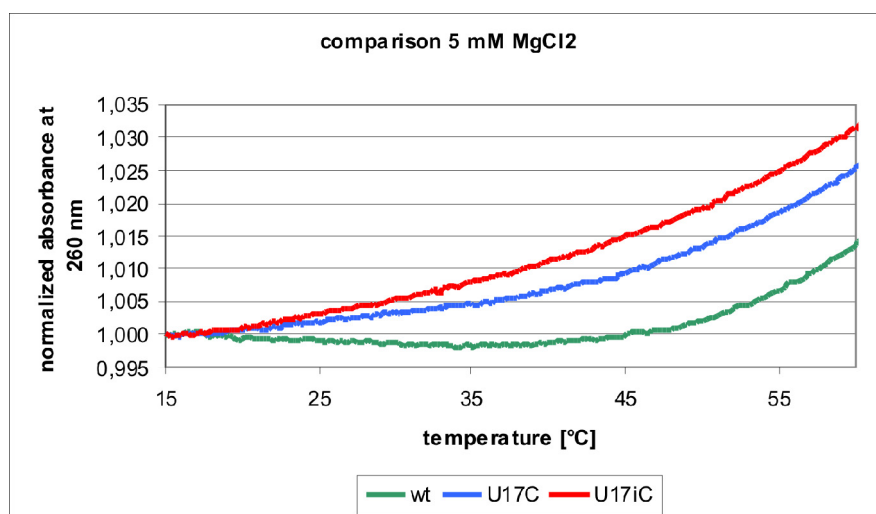


Figure 24: Comparison between the wild-type and the U17C and C17iC mutant at 5 mM $MgCl_2$, plotted as a function of the normalized absorption vs. the temperature.

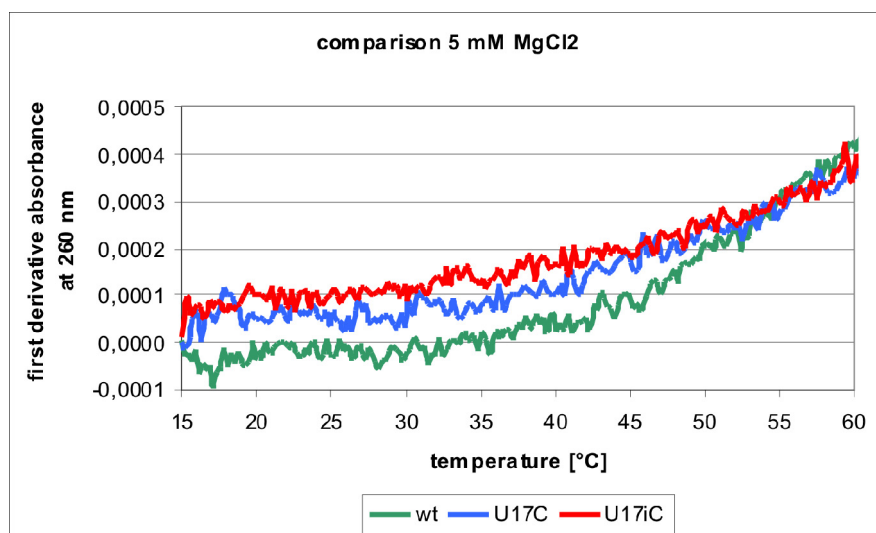


Figure 25: Stabilization of the tertiary structure; Comparison between the wild-type and the U17C and C17iC mutant at 5 mM MgCl₂; first derivative of the absorption vs. the temperature.

3.3 Conclusion and Discussion

In a single-molecule fluorescence resonance energy transfer study Kobitski *et al.* found three different states in the Mg²⁺ dependent folding of the (wild type) Diels-Alderase ribozyme. These states were assigned as the unfolded, the intermediate and the folded state. The intermediate state shows a very strong Mg²⁺ dependency on the compaction of the ribozyme structure. These single-molecule studies further showed that in the absence of MgCl₂ the unfolded state has the highest population and with an increasing Mg²⁺ concentration the transition from the intermediate state to the folded state is clearly evident. The Mg²⁺ dependent midpoint transition to reach the fully folded structure occurs around 5 mM MgCl₂.^[175]

These results are in accordance with our UV denaturation experiments. No significant difference could be observed between the wild-type and the two mutants U17C and U17iC at concentrations below 5 mM MgCl₂. With increasing Mg²⁺ concentration an increase in stabilization of the ribozymes could be observed. Both the wild-type and the mutants were equally stabilized, while at an Mg²⁺ ion concentration of 5 mM a significant increase in stabilization of the wild-type could be observed, while the mutants were not further stabilized. Other experiments have shown that the mutants can form the pseudoknotted structure but can not undergo further compaction.^[175] The missing H-bond provides a good explanation why the U17iC mutant can not undergo this compaction. The U17C mutant on the other hand can

participate in the H-bonding network. However, it is yet not entirely understood why this mutant only shows 30% catalytic activity.^[178] The assumption is that the U17C mutant can not bind the Mg^{2+} ion number five as tightly as the wild-type is substantiated by the finding in the here presented thermal denaturation experiments. The fact that mutant U17C, can form a pseudoknot, but can not be further compacted by the association of the magnesium ion number five would explain why it only shows a catalytic activity of 30%.

The G-C rich structure of the helix I and III of the Diels-Alderase ribozyme suggested a high melting temperature. With these thermal denaturation studies it could be shown that it is indeed extremely stable at temperatures up to 85°C. The secondary structure is stabilized by the addition of relatively low amounts of divalent metal ions. The good stabilization observed for the Diels-Alderase ribozyme is in conformity with thermal data observed for other RNA molecules forming pseudoknot structures.^[163, 188]

4 Bioorthogonal and orthogonal labeling of oligonucleotides

4.1 Scientific background

4.1.1 Bioorthogonal labeling

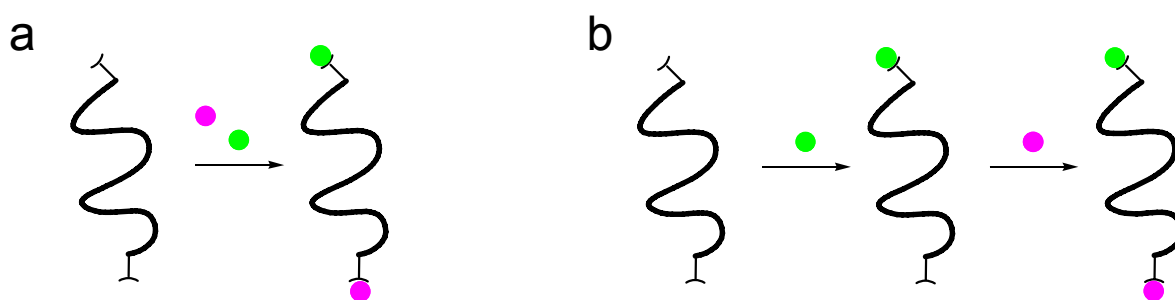
The possibility to use covalent chemistry to label biomolecules has become an essential tool and has significantly contributed to a greater understanding of chemical and biological systems. These labels serve for visualization, for studying the nature, structure or behavior of the biomolecule, for diagnostic analytics, for identification or quantification, for purification or for conjugation of the biomolecule to a surface or other biomolecules.

A bioorthogonal reaction can be defined as a chemical transformation between two functional groups that takes place selectively within complex biological samples.^[189] Bioorthogonal functionalities are incorporated into biological molecules like proteins, amino acids, or nucleic acids. After the integration of these tags into a biomolecule the desired label or biophysical probe is attached in a bioorthogonal reaction. In contrast to the number of chemical modifications in biomolecules the scope of bioorthogonal labels is still limited, because not many chemical reactions fulfill the requirements of bioorthogonal strategies.

Bertozzi *et al.* characterized the challenges an organic chemist has to face when designing a bioorthogonal labeling strategy. A bioorthogonal reaction can be identified from the repertoire of a chemical text book, by first removing all reactions that are sensitive to water; second, removing all the reactions that are redox sensitive; third, reactions that require temperatures above 37°C, pressure or high concentrations. Further limitations are functionalities that can be digested by cellular enzymes and all reagents that are cytotoxic. The remaining reactions are potential bioorthogonal reactions.^[190]

Bioorthogonal reactions for the modification of biomolecules with two different labels are of paramount interest. The applications mentioned above for labeled biomolecules can thereby be combined. In nucleic acid chemistry dual fluorescently labeled probes have found particular recognition. They provide access to diagnostic detection^[191, 192] or structural investigations especially employing FRET (Förster resonance energy transfer) techniques.^[193, 194]

In an ideal case of bioorthogonal labeling of biomolecules the tags and the labels are so specific that the labeling can be performed in a “one-pot reaction” (scheme 24a). If the specificity and selectivity of either the tags or the labels is not high enough, the labeling has to be performed in two subsequent steps (scheme 24b). In this case the single-labeled biomolecule has to be purified after the first step to ensure selectivity for the second label.



Scheme 24: Cartoon representation of the technique of dual bioorthogonal labeling of oligonucleotides with fluorescent dyes, **a:** ideal scenario: a “one-pot-reaction” **b:** two step labeling reaction.

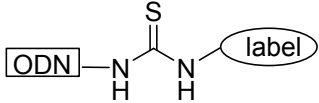
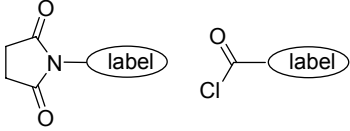
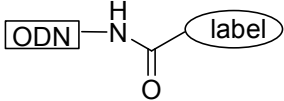
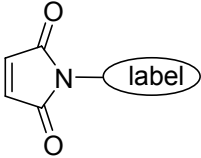
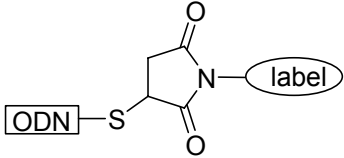
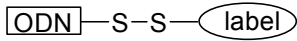
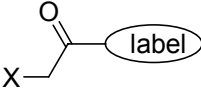
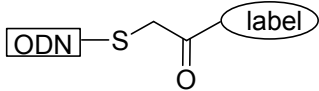
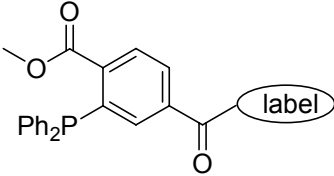
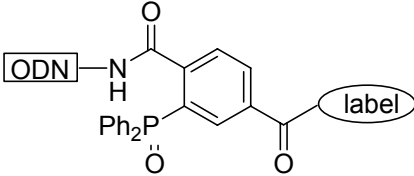
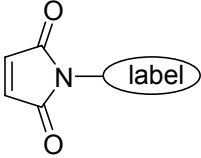
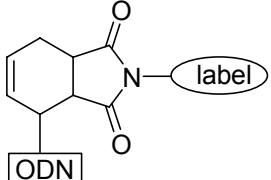
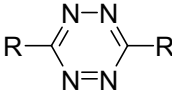
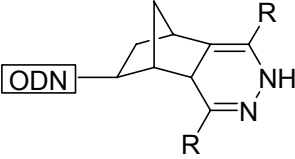
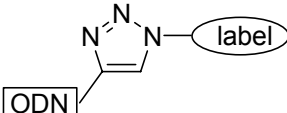
4.1.2 Fluorescent labeling of oligonucleotides

In the following, some important achievements in fluorescent labeling of oligonucleotides will be discussed, with focus on 5'-end modifications.

While enzymatic DNA and RNA synthesis is carried out from the 5'- to the 3'-end, chemical synthesis of oligonucleotides follows the 3'- to 5'-direction. Therefore, modification of chemically synthesized oligonucleotides at the 5'-end is accomplished making use of chemically modified phosphoramidites. However, modification at the 5'-end is in general limited to the selection of available phosphoramidites. Some fluorescent dyes are commercially available as phosphoramidites for automated DNA synthesis, but these dyes are basically limited to fluorescein derivatives. Fluorescein was the first fluorescent dye discovered,^[195] and is therefore well studied and many derivatives are known, but fluorescein dyes also suffer from the effect of photo-bleaching.^[196] Recently, phosphoramidites with rhodamine, Cy3 and Cy5 dyes, as well as phosphoramidites with Cy-dye-like structures have become commercially available, but many of these dyes are sensitive to the conditions required for the removal of the base protecting groups during chemical oligonucleotide synthesis. To combine high yield automated synthesis and fluorescent labeling for many dyes special base-labile phosphoramidite monomers are required.^[197] Even though this method is

the easiest way to large amounts of fluorescently labeled oligonucleotides the limitations in the use of fluorescent dye phosphoramidites are obvious and undeniable. When it comes to chemical synthesis of modified RNA molecules the limitations are even considerably larger.^[198] A post-synthetic approach can overcome most of these limitations. Small reactive groups are introduced into DNA or RNA during oligonucleotide synthesis, which can then be conjugated to the desired functional molecule in a bioorthogonal manner after oligonucleotide synthesis and deprotection.^[199] These chemical modifications are introduced into the desired oligonucleotide in the form of phosphoramidites, but in general these molecules are small and much more stable as compared to the direct introduction of fluorescent dyes. Furthermore, these small molecules are non reactive with nucleic acids but are highly reactive organic molecules. The beauty of this approach is that, depending on the modification, several different types of functional tags can be conjugated to the oligonucleotide. Table 4 provides an overview over common post-synthetic modifications of oligonucleotides.^[113, 200]

Table 4: Common post-synthetic labeling reactions.

Modification	Label	Conjugation product
$\text{ODN}-\text{NH}_2$ Amines	$\text{S}=\text{C}=\text{N}-\text{label}$ Thiocyanates	
	 Active esters and acyl chloride	
$\text{ODN}-\text{SH}_2$ Thiols	 Maleimides	
	$\text{R}-\text{S}-\text{S}-\text{label}$ Disulfides	
	 Haloacetamides	
$\text{ODN}-\text{N}_3$ Azides Staudinger ligation		
$\text{ODN}-\text{diene}$ Dienes Diels-Alder reaction	 Dienophiles (maleimide)	
$\text{ODN}-\text{dienophile}$ Inverse electron demand Diels-Alder reaction		
$\text{ODN}-\text{alkyne}$ Alkynes Huisgen reaction	N_3-label	

4.1.3 Thiol modification

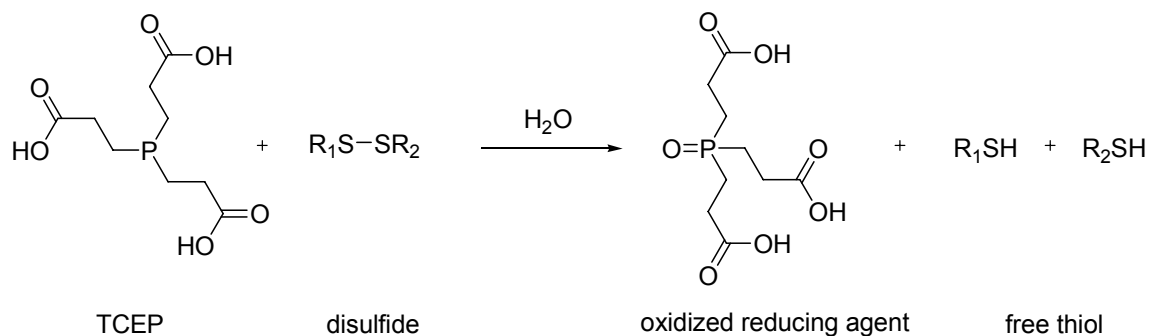
The variety of natural thiol-containing biomolecules ranges from cysteine, glutathione, to coenzyme A to peptides, enzymes, and membranes. Therefore, thiol-modifications have a longstanding history in biochemistry.^[201] An SH functional group is generally referred to as either a thiol group or a sulfhydryl group.

Aliphatic thiols are easy to alkylate and are the most active group found in cells. This is caused by the large dipole moment, nucleophilicity, and the vacancy in the d orbital of the thiol group.^[202] Because of this reactivity thiol-containing phosphoramidites, for oligonucleotide synthesis (so called thiol-modifiers) are commercially available and have found widespread application.^[203, 204] Consequently, a large number of reagents are available for the bioconjugation to sulfhydryl groups, of which the most common ones are maleimides, haloacetyl and halide derivatives, aziridines, acryloyl derivatives, thiol-disulfide exchange reagents, and dative bond-formation reagents with metal surfaces. For this thesis, only maleimides and α -haloacetamides are of greater importance and shall be discussed in detail in chapter 4.1.5 and 4.1.6.

4.1.4 Disulfide reducing reagents

Thiol modified oligonucleotides can form inter- or intramolecular disulfide bonds and are often still protected by disulfide bonds after synthesis. Therefore, prior to any site-specific reaction the disulfides need to be reduced. For this purpose commonly used reductants are β -mercaptoethanol (ME), dithiothreitol (DTT), and tris(2-carboxyethyl)phosphine (TCEP). ME cleaves disulfides in a reaction that proceeds *via* a mixed disulfide, meaning that two molecules of reducing reagent are necessary to reduce one disulfide bond. DTT itself has two free thiol groups and forms a very stable cyclic disulfide as oxidation product and therefore can be used in lower concentrations.

TCEP was first synthesized by Levinson *et al.* in 1969^[205] and employed for the reduction of disulfide bonds in proteins by Rüegg *et al.* in 1977.^[206] As compared to other phosphines TCEP is resistant to oxidation, non-volatile, odorless, and exhibits a much higher reactivity and stability than DTT or ME. Despite these seemingly excellent properties this phosphine fell into oblivion until 1991 when Burns *et al.*^[207] found a way to synthesize large quantities of TCEP. Only after that Pierce Chemical Co started to market the product in 1992.^[208] The reduction of a disulfide bond with TCEP is shown in scheme 25.

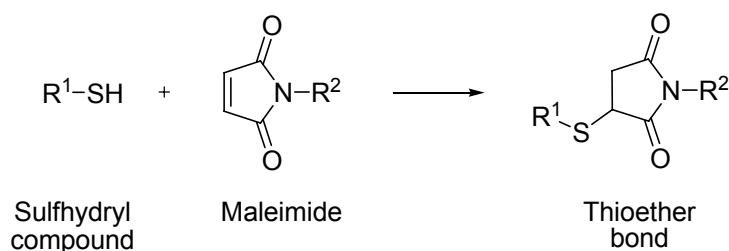


Scheme 25: Reduction of a disulfide bond with TCEP.

TCEP has an outstanding stability in water and shows no reactivity towards other functional groups present in proteins or nucleic acids. The advantage of TCEP over DTT is clearly that excess TCEP does not have to be removed by dialysis prior to the actual reaction. Standard labeling protocols do not include the removal of excess TCEP before the reaction. However, a few publications report that TCEP does, against common belief, react with molecules used for bioconjugation.^[209-211]

4.1.5 Maleimides

Maleimides are derivatives of the maleic anhydride and an amine derivative. The double bond of the maleimide undergoes alkylation with thiol groups to form stable thioether bonds (scheme 26) or can serve as a dienophile in the Diels-Alder reaction. The Diels-Alder reaction will be further discussed in chapter 4.1.7.

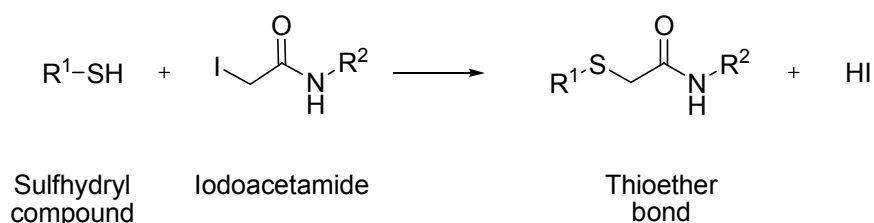


Scheme 26: Reaction of a sulfhydryl compound with a maleimide.

Maleimides are widely used in bioconjugation especially in the bioconjugation of proteins. Therefore, almost any desirable label is available as maleimide. The scope of commercially available maleimides ranges from fluorescent dyes, to proteins, and antibodies to hetero-bifunctional cross-linkers.

4.1.6 α -Haloacetamides

α -Haloacetamides are reactive towards several functional groups present in biomolecules, amine groups being the least, and thiols the most reactive. α -Haloacetamides are known for all halogens. Iodine presents the most reactive α -haloacetamide, followed by bromine, chlorine, and fluorine, which is almost unreactive towards all functional groups. Iodoacetamides are typically used as blocking reagents for thiol groups in protein chemistry.^[126] Commercially available dyes are almost exclusively synthesized as the iodoacetamide. For that the term iodoacetamide will be used equivalent with the term α -haloacetamide. The reaction between an iodoacetamide and a thiol group forms a stable thioether bond (scheme 27).



Scheme 27: Reaction of a sulfhydryl compound with iodoacetamide.

4.1.7 Diels-Alder reaction as tool for bioconjugation

The Diels-Alder reaction between a diene and a dienophile reacting in a [4+2] cycloaddition is a powerful tool for post-synthetic bioconjugation. The fact that the Diels-Alder reaction is accelerated in water makes the Diels-Alder reaction a perfect fit for bioconjugation.^[212-214] Maleimides are widely used in many types of bioconjugation reactions and therefore are the most popular dienophiles for Diels-Alder reactions. A huge variety of maleimide derivatives is commercially available: virtually any fluorescent dye, biotin maleimides, antibody maleimide conjugates, surface immobilized maleimides, proteins e.g. maleimide-HRP (horseradish peroxidase), or maleimide-alkaline phosphatase.

The first bioconjugation via Diels-Alder reaction had been described by Seelig and Jäschke, who selected a ribozyme for the Diels-Alder cycloaddition between anthracene and a maleimide.^[41]

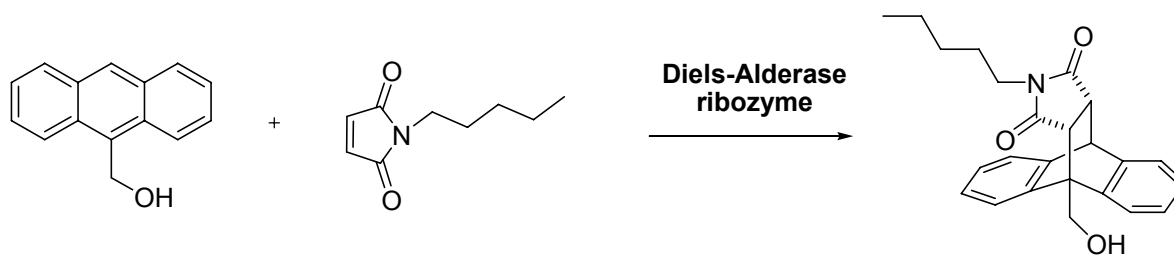
A number of Diels-Alder reactions for the modification of proteins and peptides^[215, 216] have been reported in the recent years among others e.g., conjugations of oligonucleotides to

peptides^[217-219] or the ligation of oligonucleotides *via* Diels-Alder reaction.^[220] A rather limited number of oligonucleotide modifications with small tags have been reported so far.^[221] Up to today fluorescent labeling of oligonucleotides *via* Diels-Alder reaction has so far only been reported by very few authors. Hill *et al.* reported the 5'-end modification of oligonucleotides with cyclic and acyclic hexadienes and the subsequent Diels-Alder reaction with maleimides.^[221] While most maleimides used by Hill *et al.* reacted easily with the diene within 30 min, and not more than two equivalents of functionalized maleimide were required, the modification with fluorescent dyes appeared much more demanding. After 20 h reaction time and by the use of twelve equivalents of fluorescein maleimide a labeled product could be detected. Graham *et al.* reported the labeling reaction of an internally diene modified 20mer with fluorescent dyes. Apart from difficulties in distinguishing the products from each other, their approach seems to be more efficient than the above mentioned, but still requires 30% v/v acetonitrile and elevated temperatures for four hours.^[222] The use of organic solvents and elevated temperatures during labeling reaction prevents the use of this strategy for sensitive biomolecules.

In summary, a number of examples for the Diels-Alder reaction mediated bioconjugation have been reported in the last couple of years. However, so far only very few authors have described an efficient Diels-Alder bioconjugation of fluorescent dyes to oligonucleotides. The general picture that can be drawn from these reports shows that labeling of oligonucleotides by Diels-Alder reaction can be very efficient, but is extremely dependent on the type of label. Dyes seem to be the least efficient labels. The Diels-Alder reaction is a promising tool for bioconjugation of small molecules to nucleic acids and the addition of a suitable catalyst could be a way to overcome the abovementioned problems.^[200]

4.1.8 The Diels-Alderase ribozyme

A ribozyme that catalyzes the Diels-Alder reaction between tethered anthracene and biotin maleimide was selected by Jäschke and co-workers.^[41] In the selection the anthracene-modified RNA acted as a ribozyme and substrate at the same time, thus modifying itself in a reaction catalyzed *in cis*. Furthermore, this ribozyme was also found to accelerate the Diels-Alder reaction of the free reactants in a true catalytic manner *in trans* (scheme 28).



Scheme 28: Ribozyme-catalyzed reaction between 9-hydroxymethyl anthracene and *N*-pentylmaleimide.

4.1.9 Anthracene as substrate

In the landmark paper by Sauer *et al.* the reactivity of dienes towards maleic anhydride in Diels-Alder reactions was investigated and two major findings support the choice of anthracene as a diene.^[223]

- I. The reactivities of cyclic and quasi-cyclic dienes considerably exceed the reactivities of acyclic dienes. Electron-donating substituents on the diene usually accelerate the reaction.
- II. The k_2 values of anthracene derivatives are influenced to a high degree by substituents in the 9- and 10 position.

Even though these experiments were carried out in dioxane the results are comparable to water as solvent, as the influence of the substituents on the energetic properties of the π -system is independent from the solvent.

However, previously published results on modification of biomolecules *via* Diels-Alder reaction have, with two exceptions have not employed anthracene as a diene. So far the first and only successful description of a Diels-Alder bioconjugation with anthracene as a substrate was described by Seelig and Jäschke in 1999.^[41]

Recently, Overkleeft and co-workers reported the labeling of endogenously expressed enzymes based on the Diels-Alder ligation and reported that among the investigated dienes the anthracenyl modified biomolecule was unable to undergo Diels-Alder ligation.^[189]

4.2 Objectives

The ever-expanding demand for new and better fluorescent labeling techniques for biomolecules, and the broad but still limited scope of labeling methods for oligonucleotides, has prompted an interest in an investigation into the Diels-Alder bioconjugation of oligonucleotides. Knowing that the Diels-Alderase ribozyme is able to accelerate the cycloaddition between an anthracene and maleimide in a true biomolecular fashion the aim was to investigate whether the Diels-Alderase ribozyme could be utilized as “machinery” for fluorescent labeling reactions of oligonucleotides.

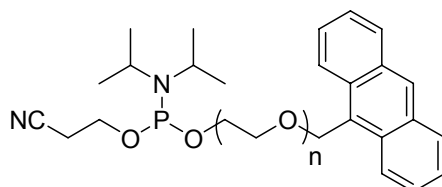
Investigating the following steps one after another the idea was to find a bioorthogonal method to fluorescently label oligonucleotides with the Diels-Alderase ribozyme. Since dual labeled fluorescent probes are of paramount interest it will also be investigated if a dual orthogonal labeling strategy can be developed.

The objectives for this investigation are:

- I. Can the Diels-Alderase ribozyme catalyze the fluorescent labeling of oligonucleotides *in cis*?
- II. Can the Diels-Alderase ribozyme catalyze the post-synthetic fluorescent labeling of a functionalized DNA *in trans*?
- III. Is it possible to develop a bioorthogonal labeling strategy exploiting the substrate specificity that has been reported for the Diels-Alderase ribozyme earlier?
- IV. How can a dual orthogonal labeling strategy employing the Diels-Alderase ribozyme be developed and implemented?

4.3 Results and Discussion

4.3.1 Synthesis of anthracene modified oligonucleotides



27 a n = 4 (ATEG)

b n = 6 (AHEG)

Scheme 29: 9-Anthracenylmethyl tetraethylene glycol (ATEG) phosphoramidite **27a** and 9-anthracenylmethyl hexaethylene glycol (AHEG) phosphoramidite **27b**.

An efficient way to synthesize short oligonucleotides bearing an anthracene modification is the coupling of 2-(anthracen-9-ylmethoxy)ethyl 2-cyanoethyl diisopropylphosphoramidite (scheme 29) with different PEG linkers at the 5'-end, as a last coupling step in automated oligonucleotide synthesis. For this purpose two of these molecules **27a** and **b** have been synthesized, differing in the length of the glycol linker, according to published procedures.^[95] This approach has been utilized to synthesize oligonucleotides ORN1, ODN2, ODN5, ODN6 and ODN8. The oligonucleotides were purified by preparative HPLC and integrity was determined by mass spectrometry (table 4).

Table 4: Oligonucleotides, HPLC and mass analysis.

ODN	Type	Sequence	t _R [min]	[M+H] calculated	[M+H] observed
ORN1	RNA	5' - AHEG GGA GCU CGC CC - 3'	23.4 ^c	4019.59	4018.5 ^b
ODN2	DNA	5' - AHEG GGA GCT CAG CCT TCA CTG C-3'	37.7	6300.27	6300.4 ^a
ODN3	DNA	5' - GTA CAG TCT GAA GTG - 3'	18.8	4630.81	4630.5 ^a
ODN4	DNA	5' - CAC TTC AGA CTG TAC - 3'	19.1	4511.96	4511.8 ^b
ODN5	DNA	5' - AATEG GTA CAG TCT GAA GTG - 3'	36.3	5079.46	5079.7 ^a
ODN6	DNA	5' - AHEG GTA CAG TCT GAA GTG - 3'	37.3	5165.02	5166.1207 ^b
ODN7	DNA	5' - SH C₆ GTA CAG TCT GAA GTG - 3'	24.0	4830.09	4832.0 ^a
ODN8	DNA	5' - AHEG GTA CAG TCT GAA GTG C₃SH -3'	37.3	5335.14	5336.0263 ^b

^a MALDI-TOF MS – measured in the positive mode, ^b high resolution ESI MS – measured in the negative mode.

Unless indicated otherwise HPLC gradient O1 was used; ^c gradient O2 (chapter 6.1.12).

4.3.2 Dipartite Diels-Alder ribozyme assay

The dipartite Diels-Alderase ribozyme construct consists of two hybridized RNA strands. A 38mer forming the catalytic pocket and an 11mer (figure 26). The 11mer can be modified with anthracene polyethylene glycol and serves as substrate. In this case the catalytic reaction will proceed *in cis*.

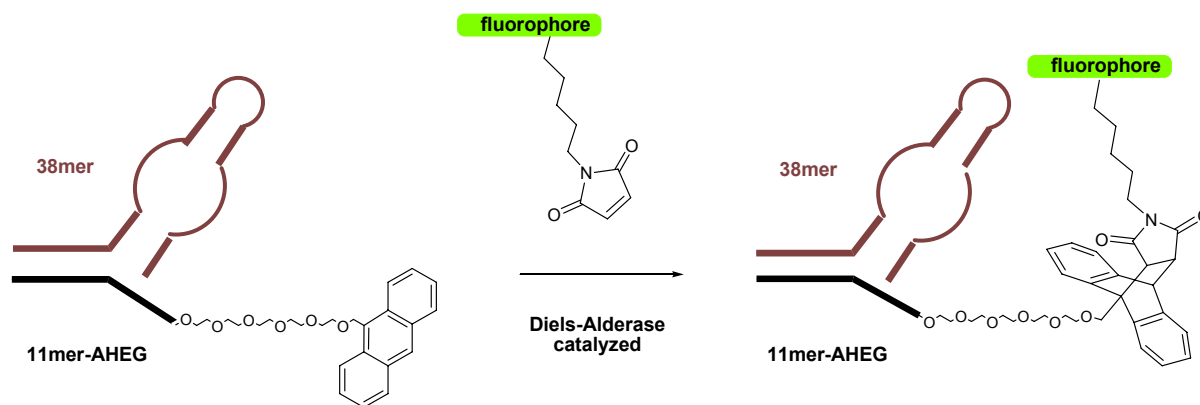
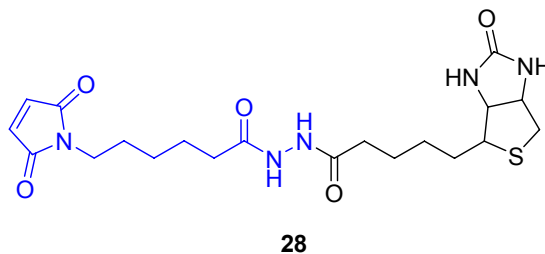


Figure 26: Dipartite Diels-Alderase ribozyme assay; **b:** Diels-Alder reaction catalyzed by the dipartite Diels-Alderase ribozyme.

The Diels-Alderase ribozyme has rather strict requirements regarding the structure of the diene and the dienophile. The main restriction of the Diels-Alderase ribozyme is that it only catalyzes the Diels-Alder reaction between the original substrates it was selected with: anthracene and maleimide derivatives. During the selection of the Diels-Alderase ribozyme biotin maleimide **28** (scheme 30) has been used and indeed maleimidocaproic acid and *N*-pentylmaleimide are among the best substrates for the ribozyme.^[41, 96]

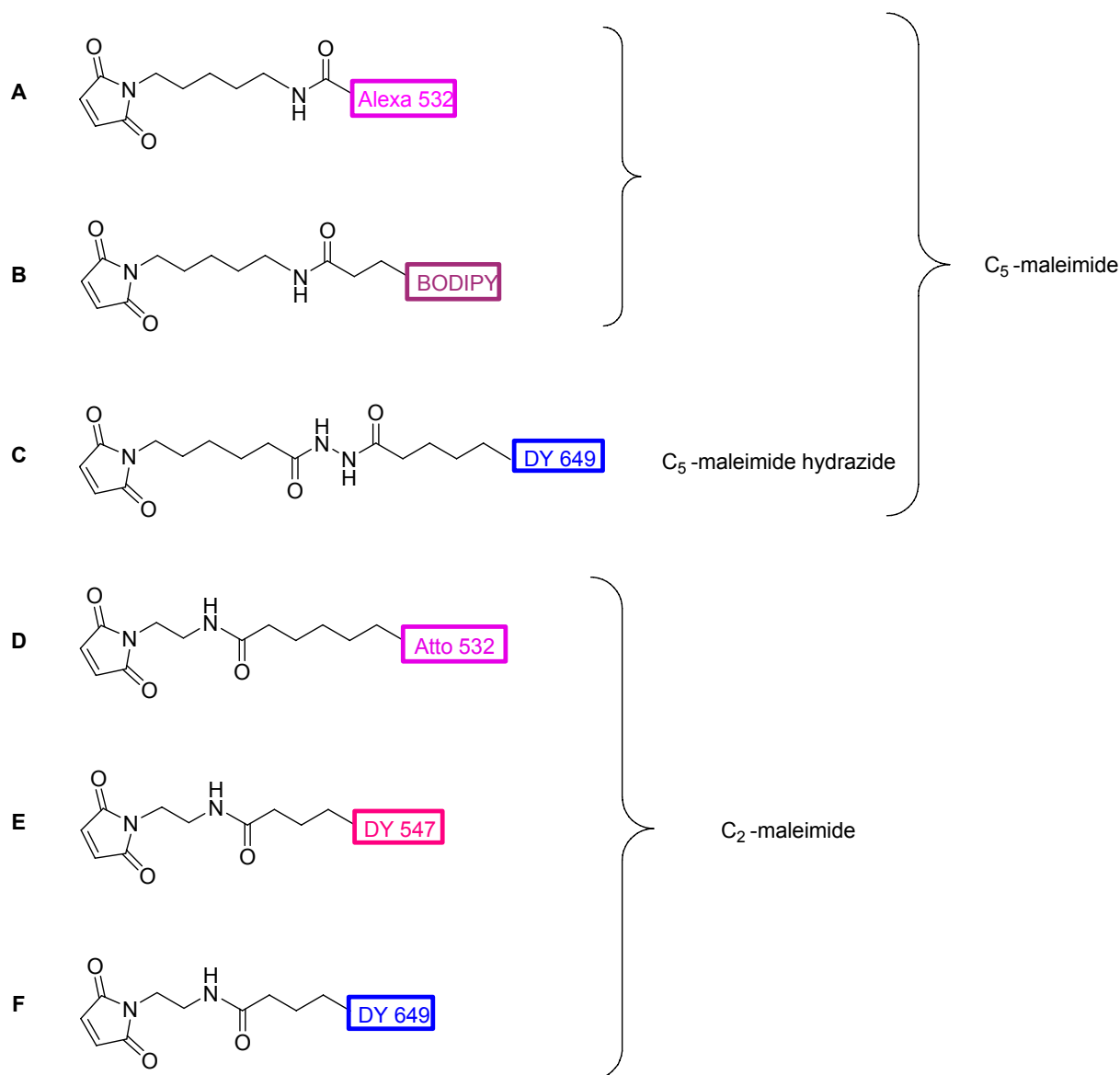


Scheme 30: Chemical structure of biotin maleimide; in blue maleimidocaproic acid hydrazide.

Now, the challenge was to find out if these restrictions in substrate specificity could be extended to fluorescent maleimide dyes. It was expected that the Diels-Alderase ribozyme would catalyze the reaction with maleimides connected with five carbon atoms long linkers,

while maleimides with shorter linkers should be less efficient substrates for the Diels-Alderase ribozyme.

Most commercially available fluorescent maleimides have a linker length of two carbon atoms (C_2 -maleimide) next to the amide bond connecting the dye to the maleimide. Very few maleimide dyes with a linker of five carbon atoms (C_5 -maleimide) are available. Scheme 31 gives a schematic overview of all the dyes, which were used for this work. Detailed information and chemical structures of the dyes are given in the experimental section.



Scheme 31: Maleimide dyes with C_2 - and C_5 -linkers. All maleimides with five carbon atoms next to the amide bond are subsumed as C_5 -maleimides (A-C). The linkers of the commercially available C_5 -maleimides Alexa Fluor 532 (A) and BODIPY (B) are different from the self synthesized hydrazide C_5 -maleimide (C), which will be introduced in chapter 4.3.3. All C_2 -maleimides (D-F) are commercially available.

For the catalyzed Diels-Alder reaction *in cis*, the 38mer and the 11mer RNA anthracene-conjugate (ORN1) were hybridized in a ratio of 1:2. The 11mer-AHEG (ORN1) was doped with [32 P]-pCp labeled 11mer-AHEG to visualize the difference between modified and unmodified 11mer in a gel shift assay.

The ribozyme clearly showed the expected selectivity towards the C₅-maleimide. For the C₂-maleimide dyes, no conversion was observed (figure 27). However, the reactivity of the C₅-maleimide dye is also dependent on the nature of the dye. For the C₅-maleimide Alexa Fluor 532 dye 20% product formation was observed, while only 12% Diels-Alder product was formed with the C₅-maleimide BODIPY dye. This is possibly due to its chemical structure and solubility. The Alexa Fluor 532 dye bears two sulfonate groups and has a good solubility in water, whereas the BODIPY dye is poorly soluble in water.

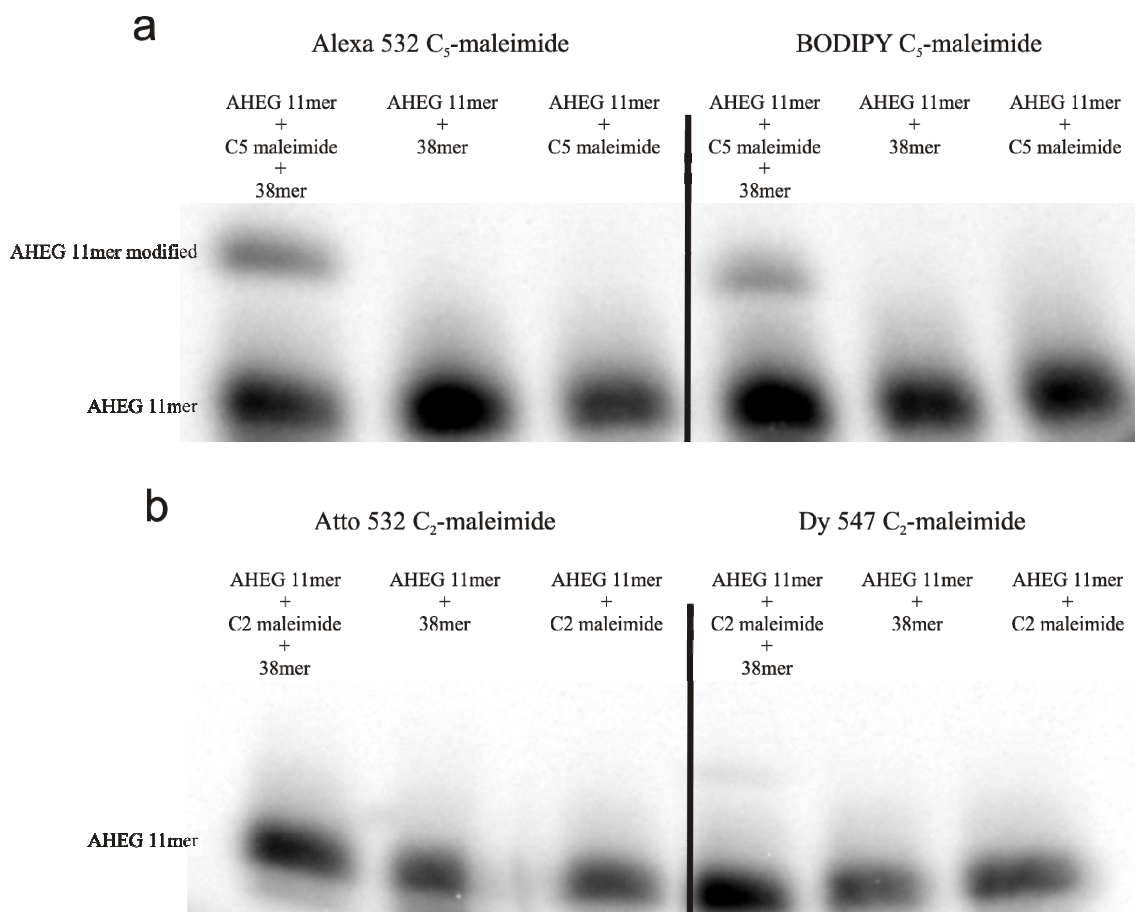
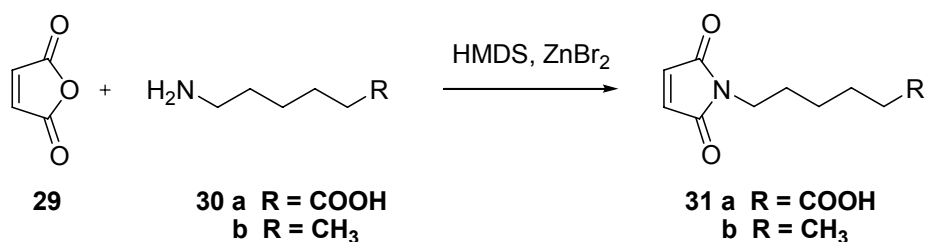


Figure 27: Comparison of C₂- and C₅-maleimide. Conjugation of ORN1 in the dipartite Diels-Alderase ribozyme assay. Reaction time 30 min. 38mer (0.2 μM) and ORN1 (0.1 μM), doped with α³²-pCp labeled ODN2, all dyes 50μM. The gel shift assay with autoradiography showed that for C₅-maleimide dyes (**a**) a labeling reaction took place, while with C₂-maleimide dyes (**b**) no Diels-Alder product formation was observed. For each dye the controls were performed without dye (middle) and without 38mer = uncatalyzed (right).

With this experiment it was demonstrated that the Diels-Alderase ribozyme only tolerates C₅-maleimide as substrates. No conversion was observed for maleimides with a C₂-linker.

Against the backdrop of the results by Stuhlmann *et al.*^[96] and the selectivity observed in the dipartite Diels-Alder assay (figure 27) a fluorescent dye with a C₅-maleimidocaproic acid hydrazide was synthesized.

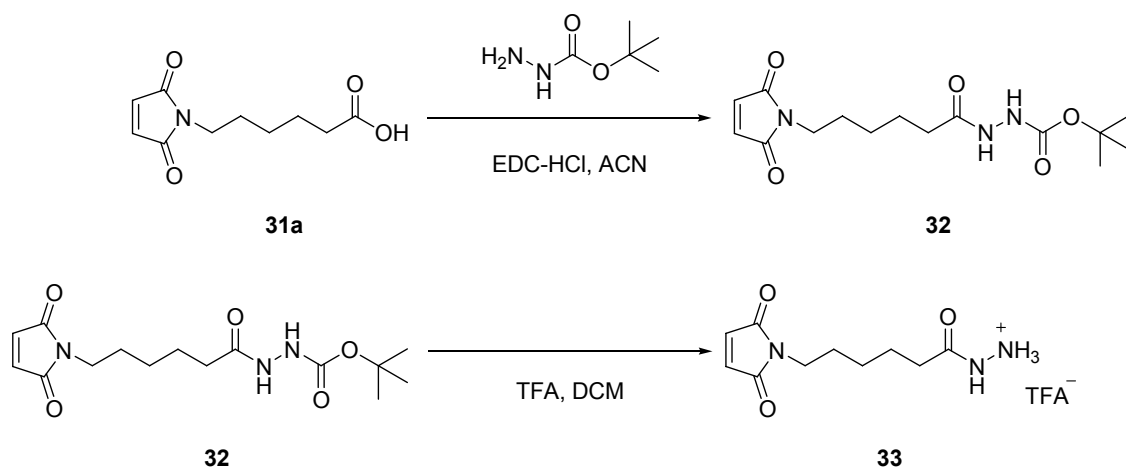
4.3.3 Synthesis of DY 649 C₅-maleimidocaproic acid hydrazide



Scheme 32: Synthesis strategy for maleimide derivatives.

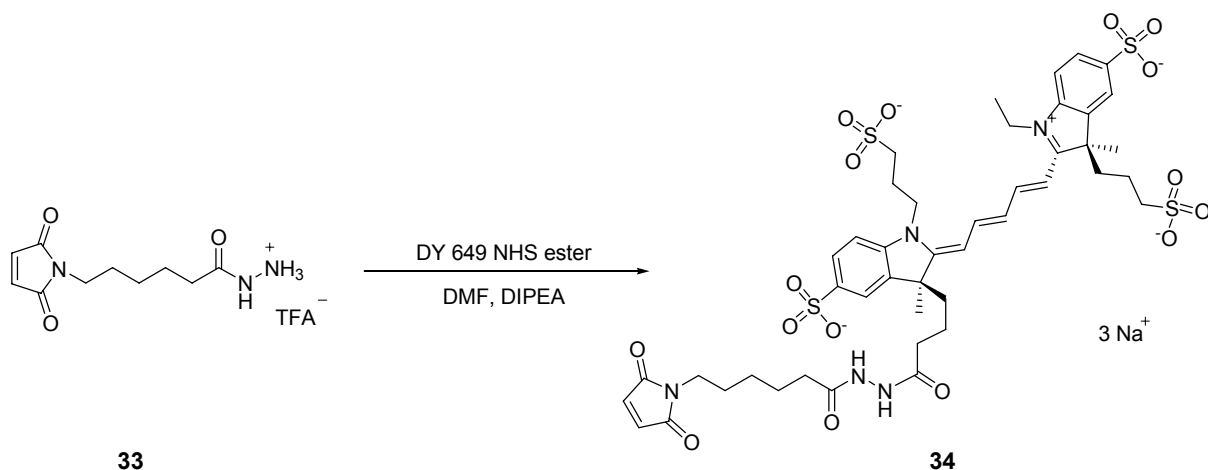
The general way how maleimide derivatives are obtained is the simple addition of the desired amine to maleic anhydride in acetonitrile. An attempt to synthesize maleimidocaproic acid *via* this route failed, because too many side products were formed. Based on the initial work of Vorbrueggen^[224] the use of hexamethyldisilazane (HMDS) and zinc bromide as Lewis acid (scheme 32) to initiate the reaction provides a superior route to synthesize maleimide derivatives in good yield and purity.^[225] Maleimidocaproic acid **31a** was obtained from maleic anhydride **29** and 6-aminocaproic acid **30a** by initiation of the reaction with HMDS/ZnBr₂ under reflux for three hours and subsequent stirring over night.^[226] The product could be purified by column chromatography to result in a clean product in 74% yield.

N-Pentylmaleimide **31b** is used in all kinds of Diels-Alderase ribozyme assays, thus the above described synthetic procedure was extended to the synthesis of *N*-pentylmaleimide. The synthesis and quality of the product could be improved significantly as compared to common procedures. For reaching a purity that is compatible with biological assays purification by flash chromatography was carried out and yellow crystals (82%) were obtained. For biological assays the purity is extremely important. HPLC analysis confirmed a purity of 99.8%.



Scheme 33: Synthesis of 6-maleimidocaproic acid hydrazide.

6-Maleimidocaproic acid **31a** was stirred with *tert*-butyl carbazate in the presence of *N*-ethyl-*N'*-(3-dimethylaminopropyl)carbodiimide hydrochloride (EDC-HCl) in acetonitrile at room temperature for 17 h. The product was further purified by silica chromatography and pure Boc-protected 6-maleimidocaproic acid hydrazide **32** was obtained in a yield of 61%. Deprotection was carried out with 10% trifluoroacetic acid (TFA) in dichloromethane, to yield 93% 6-maleimidocaproic acid hydrazide **33**. DY 649 NHS ester was purchased from Dyomics and incubated with 6-maleimidocaproic acid hydrazide **33** in DMF in the presence of Hünig's base (*N,N*-diisopropylethylamine (DIPEA)) as a proton scavenger for 36 hours at 25°C. DY 649 C₅-maleimidocaproic acid hydrazide **34** was obtained in good yield and was purified by semi-preparative HPLC.



Scheme 34: Synthesis of DY 649 C₅-maleimidocaproic acid hydrazide.

The use of DY 649 C₅-maleimidocaproic acid hydrazide for labeling of oligonucleotides will be introduced in chapter 4.3.4.1.

4.3.4 Diels-Alderase ribozyme-catalyzed labeling *in trans*

In contrast to the Diels-Alderase ribozyme catalyzed reaction *in cis* that has been discussed so far, the aim of this thesis was to employ the Diels-Alderase ribozyme as a catalyst for post-synthetic modification of various oligonucleotides. For the reaction *in trans*, the reaction partners are free in the solution. The maleimide is connected to the fluorescent dye and the anthracene is tethered to the target oligonucleotide. Figure 28 explains how the functionalization of oligonucleotides is accomplished catalyzed by the Diels-Alder ribozyme.

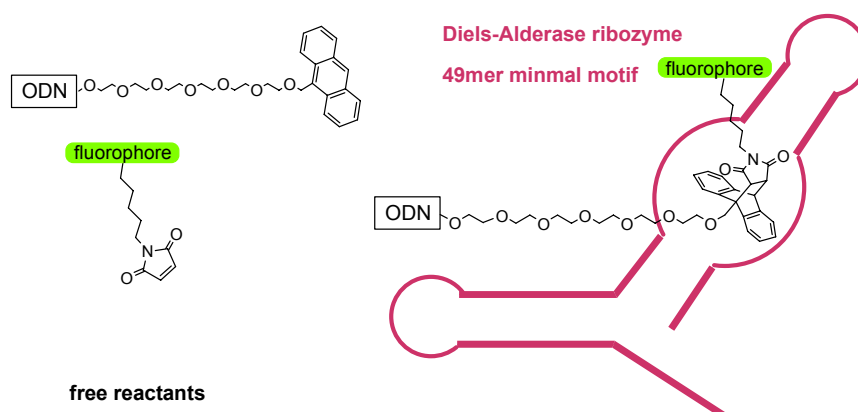


Figure 28: Schematic model of a Diels-Alder reaction between anthracene and maleimide catalyzed by the Diels-Alderase ribozyme *in trans* in the catalytic pocket of the 49 nucleotide long minimal motive of the Diels-Alder ribozyme.

For fluorescently labeling oligonucleotides *in trans* with the Diels-Alderase ribozyme DNA sequences were synthesized as introduced in chapter 4.3.1. An important technique for the introduction of small molecules into DNA, which has not been mentioned yet, is the extension of modified primers. This technique facilitates the chemical synthesis of long modified DNA strands. For that reason a DNA 19mer-AHEG sequence was synthesized, which had earlier been utilized to serve as a forward primer in PCR, where it is extended to yield long DNA products. The first seven bases of this DNA 19mer-AHEG (ODN2) can be aligned with the first seven bases of the Diels-Alder ribozyme.

Notably, the radioactive 3'-end labeling of DNA (ODN2) with [^{32}P]-pCp could be accomplished with T4 RNA ligase.

For the reaction with Alexa Fluor 532 no gel shift could be observed. It was therefore concluded that the labeling reaction was not successful (figure 29). The reason is probably that interactions like base pairing of ODN2 with the Diels-Alderase ribozyme prevent the anthracene from entering the catalytic pocket.

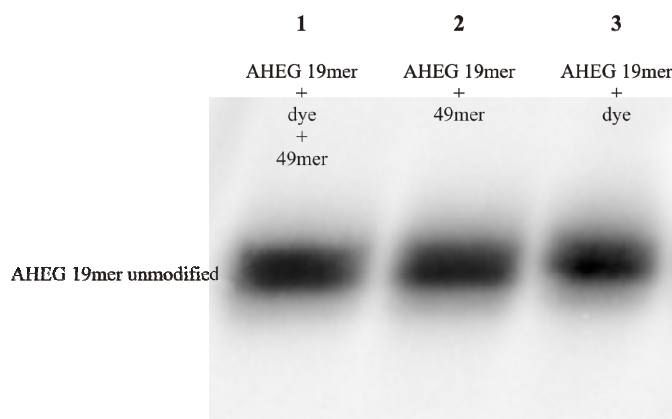


Figure 29: Labeling reaction of ODN2 (AHEG 19mer) with Alexa Fluor 532 C₅-maleimide. Conjugation of ODN2 *in trans* Diels-Alder assay. Reaction time 30 min, autoradiograph. **Lane 1:** ODN2 reaction with Alexa Fluor 532 C₅-maleimide catalyzed by the 49mer Diels-Alderase ribozyme. **Lane 2:** ODN2 without Alexa Fluor 532 C₅-maleimide. **Lane 3:** uncatalyzed background reaction of ODN2 with Alexa Fluor 532 C₅-maleimide.

Consequentially, an oligonucleotide that cannot hybridize with the Diels-Alderase ribozyme in any way and could not form any hairpins was designed. Oligonucleotides ODN8 and ODN9 were synthesized. Both share the same sequence but differ in the number of ethylene glycol units in the spacer between the anthracene and the 5'-end of the oligonucleotide. ODN5 was modified with anthracene tetraethylene glycol (ATEG), while ODN6 was modified with anthracene hexaethylene glycol (AHEG).

It was also decided to desist from further labeling the oligonucleotides with [³²P]-pCp, because the 3'-labeling reaction with [³²P]-pCp is not very efficient, neither for RNA nor DNA. Therefore, only doping of the oligonucleotides during the reaction is possible and not very practical, because the radioactively labeled oligonucleotide and the non-radioactive oligonucleotide have a different mobility in PAGE. For further experiments, visualization by fluorescent imaging and SYBR Gold staining was considered sufficient, as the amount of DNA in the assays was high enough for detection by staining.

ODN5 and the Alexa Fluor 532 C₅-maleimide were mixed in a 1:1 ratio and the Diels-Alderase ribozyme added as a catalyst. Even though the reaction was performed at high concentrations no significant labeling was observed even after reaction times up to two hours (figure 30). Thermal denaturation studies (appendix) showed that ODN5 and ODN6 have exactly the same melting temperature. The best interpretation of this effect is that the short linker hinders the anthracene to enter the catalytic pocket.

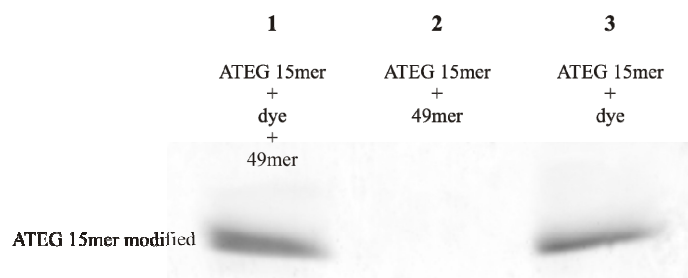


Figure 30: Labeling reaction of ODN5 (ATEG 15mer (tetraethylene glycol)) with Alexa Fluor 532 C₅-maleimide. Reaction time 2 h. Fluorescent imaging 532 nm. **Lane 1:** ODN5 reaction with Alexa Fluor 532 C₅-maleimide catalyzed by the 49mer Diels-Alderase ribozyme. **Lane 2:** ODN5 without Alexa Fluor 532 C₅-maleimide. **Lane 3:** uncatalyzed background reaction between ODN5 and Alexa Fluor 532 C₅-maleimide.

The oligonucleotide synthetically modified with anthracene hexaethylene glycol (AHEG) was first tested with Alexa Fluor 532 C₅-maleimide and a clear difference between the ribozyme-catalyzed and uncatalyzed Diels-Alder bioconjugation was detected (figure 31).

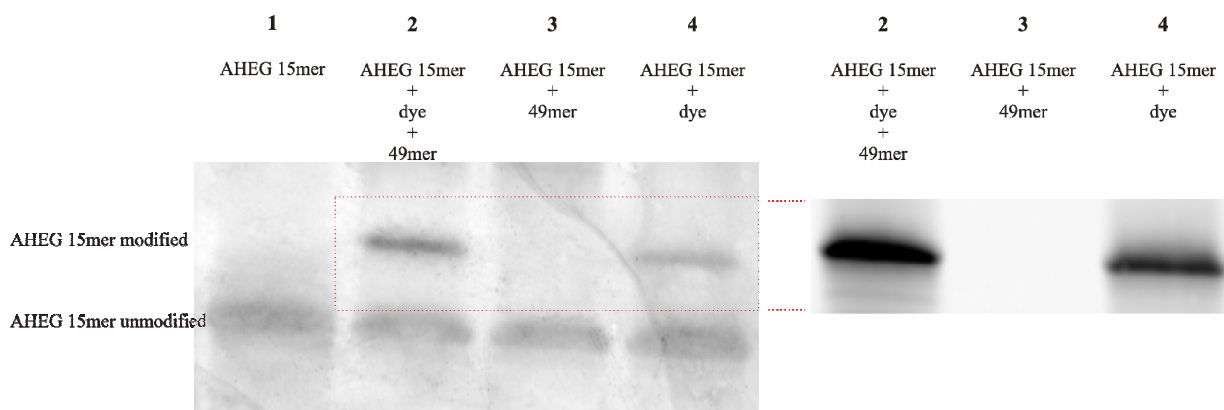


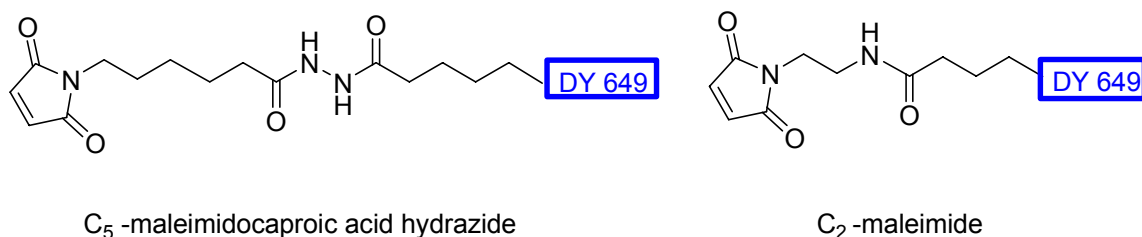
Figure 31: Labeling reaction of ODN6 (AHEG 15mer (hexaethylene glycol)) with Alexa Fluor 532 C₅-maleimide. Conjugation of ODN6 *in trans* Diels-Alder assay. Reaction time 30 min. **Left:** SYBR Gold stained; **right:** fluorescent scan 532 nm. **Lane 1:** ODN6. **Lane 2:** ODN6 reaction with Alexa Fluor 532 C₅-maleimide catalyzed by the 49mer Diels-Alderase ribozyme. **Lane 3:** ODN6 without Alexa Fluor 532 C₅-maleimide. **Lane 4:** uncatalyzed background reaction of ODN6 with Alexa Fluor 532 C₅-maleimide.

The data show that in the presence of the Diels-Alderase ribozyme the labeling reaction is significantly improved. The most important result is that no notable difference was observed if the dye was used in a five-fold excess as compared to a 1:1 ratio. The determinant in this reaction is the presence of the Diels-Alderase ribozyme. This finding is promising, because fluorescent dyes are expensive and the ability of catalyzing the reaction while keeping the amount of dye as low as possible is of great interest.

Optimization of the labeling efficiency was carried out using Alexa Fluor 532 C₅-maleimide. An extensive set of different concentrations and different excess ratios of dye over the oligonucleotide were tested. A well detectable labeling reaction took place if 7 mol% Diels-Alderase ribozyme was used. Best results were observed if the labeling took place in a 1:1 ratio of oligonucleotide and dye in the presence of 14 mol% Diels-Alderase ribozyme as a catalyst. Labeled oligonucleotides were observed after 10 min reaction time and a moderate yield of fluorescently labeled oligonucleotides was obtained after 30 min. Best results were achieved after 2 h reaction time. A prolongation of the reaction time over night did not improve the yield significantly. However, the labeling efficiency could not be improved above 20% as determined by SYBR Gold staining, followed by analysis with the software Image Quant.

4.3.4.1 Direct comparison of C₂-maleimide *versus* C₅-maleimide for Diels-Alder labeling reaction

Earlier studies have shown that biotin maleimide, the original substrate, the Diels-Alderase ribozyme was selected with, and maleimidocaproic acid are among the best substrates for the Diels-Alderase ribozyme.^[41, 96] To investigate the influence not only of the linker length but also the heteroatoms in the linker a dye with maleimidocaproic acid hydrazide **34** was synthesized (chapter 4.3.3).



Scheme 35: DY 649 C₅-maleimidocaproic acid hydrazide and DY 649 C₂-maleimide.

Fluorescent dyes are rather big molecules and their character and behavior in solubility is very much dependent on their structure and charge, thus reactivities of different dyes can not be compared directly.

Having synthesized the DY 649 as C₅-maleimidocaproic acid hydrazide a direct comparison to the commercially available DY 649 C₂-maleimide could be investigated (scheme 35). The

reactions were performed in parallel and additionally the influence of the Diels-Alderase ribozyme as catalyst was investigated (figure 32).

The reaction was performed in a 1:1 dye to oligonucleotide ratio, in the concentrations that had earlier been determined to be optimal for the labeling reaction catalyzed by the Diels-Alder ribozyme. The progression of the reaction was investigated after 30 min and after two hours and is shown in figure 32. An overview over the labeling yields obtained by analysis with Image Quant from figure 32 is given in table 5.

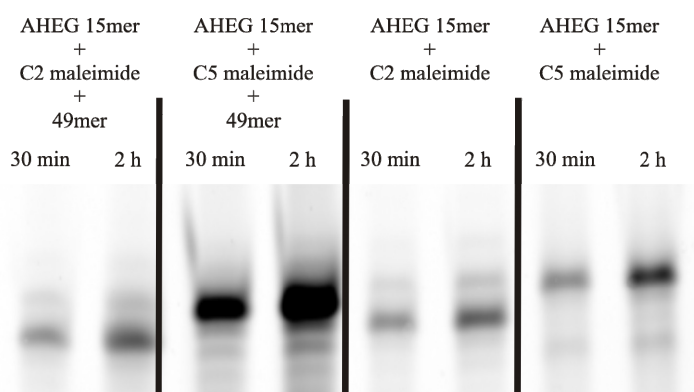


Figure 32: Direct comparison of C₂- and C₅-maleimide. Conjugation of ODN6 (AHEG 15mer) with DY 649 C₂-maleimide and DY 649 C₅-maleimidocaproic acid hydrazide. Reaction time 30 min and 2 h. Fluorescent imaging at 610 nm. **Lane 1:** Diels-Alder ribozyme-catalyzed reaction with C₂-maleimide. **Lane 2:** Diels-Alder ribozyme-catalyzed reaction with C₅-maleimide. **Lane 3:** uncatalyzed reaction with C₂-maleimide. **Lane 4:** uncatalyzed reaction with C₅-maleimide. Table 5 summarizes the results of gel analysis with ImageQuant.

Table 5: Direct comparison of reaction yields achieved with C₂- and C₅-maleimide.

		30 min	2 h
catalyzed	C ₂ -maleimide	1.8%	3.6%
	C ₅ -maleimide	13.2%	24.0%
uncatalyzed	C ₂ -maleimide	1.7%	2.5%
	C ₅ -maleimide	2.1%	4.6%

For the C₂-maleimide dye only a slight background reaction was observed and even the addition of the Diels-Alder ribozyme did not constitute a difference. In contrast, for the C₅-maleimide hydrazide a significant difference between the catalyzed and uncatalyzed reaction was observed. Without the addition of the Diels-Alder ribozyme the labeling efficiency does not differ much from the labeling efficiency with the C₂-maleimide. If the reaction was catalyzed with the ribozyme a five-fold increase in labeling efficiency could be observed as compared to the uncatalyzed reaction. This experiment demonstrates the catalytic selectivity of the Diels-Alder ribozyme. Having demonstrated that the Diels-Alderase ribozyme only

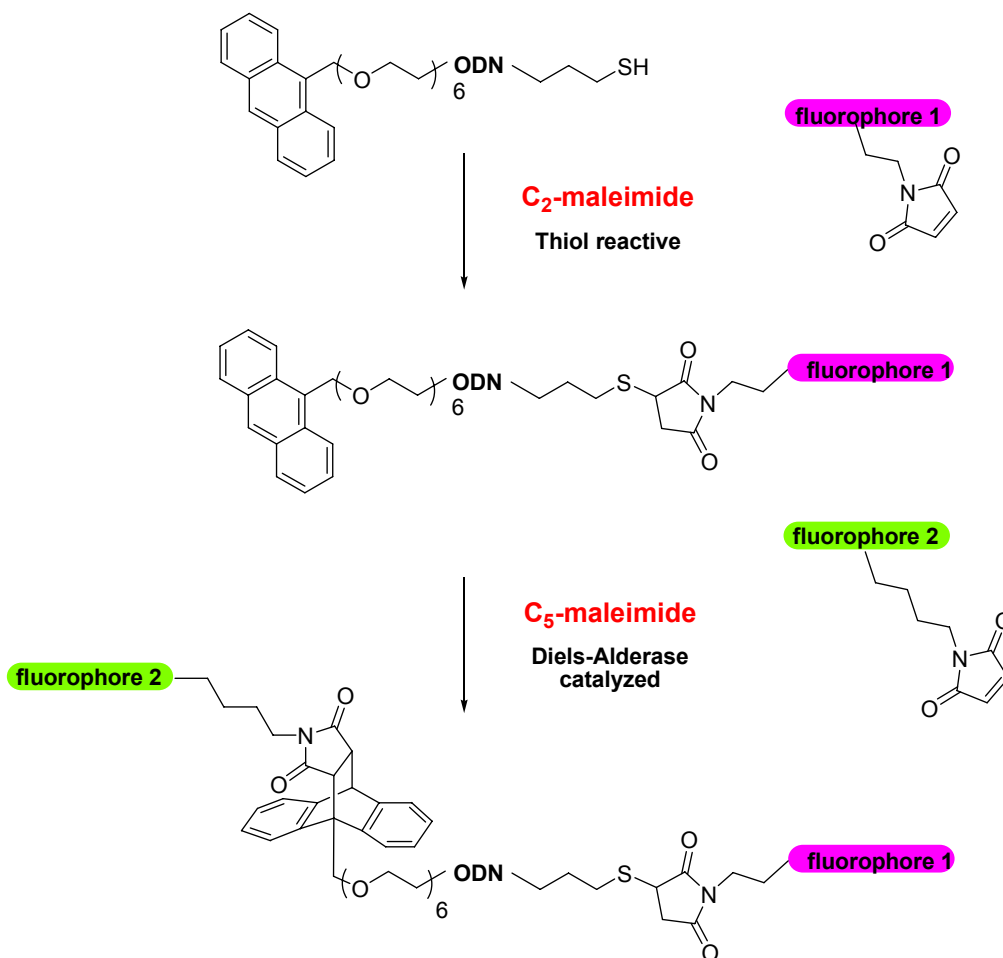
catalyzes the labeling reaction with C₅-maleimide fluorescent dyes originated in the idea to exploit this finding for a novel dual-bioorthogonal labeling strategy and shall be discussed in the following.

4.3.5 Dual orthogonal labeling of DNA with maleimides

Inspired by the selectivity observed for labeling of a DNA strand tethered to anthracenylmethyl hexaethylene glycol (ODN6) with C₅-maleimide fluorescent dyes *via* a ribozyme-catalyzed Diels-Alder reaction, it was conceived that this selectivity could be exploited for a novel dual, orthogonal labeling strategy. It was demonstrated that the Diels-Alderase ribozyme provides a possibility for selective labeling of oligonucleotides with C₅-maleimides but not C₂-maleimides. Thiolated biomolecules are typically appropriate for the modification with maleimides and since most maleimide dyes are commercially available as C₂-maleimides this approach was the corollary.

An oligonucleotide was therefore modified with anthracene hexaethylene glycol at the 5'-end and a sulfhydryl moiety at the 3'-end (ODN8), which should then be labeled with two maleimide fluorescent dyes with different linker lengths.

Conception was that the thiol modification could first be labeled with a C₂-maleimide, whereas the anthracene remains unmodified until a C₅-maleimide is added along with the Diels-Alder ribozyme as a catalyst (scheme 36). Even in the presence of the Diels-Alderase ribozyme no significant Diels-Alder reaction of C₂-maleimide dyes with the anthracene was observed as shown in the previous chapter. Therefore no removal of the C₂-maleimide dye should be necessary for the second labeling step, the ribozyme-catalyzed Diels-Alder reaction with the C₅-maleimide dye.



Scheme 36: Proposed dual orthogonal labeling strategy exploiting the selectivity of the Diels-Alderase ribozyme for C₅-maleimides over C₂-maleimides. In a first step the sulfhydryl group is selectively labeled with a C₂-maleimide carrying fluorophore 1 (magenta) and subsequently, without removal of the dye, anthracene is selectively labeled with C₅-maleimide fluorophore 2 (green) catalyzed by the Diels-Alder ribozyme.

4.3.5.1 Investigations on fluorescent labeling of thiolated oligonucleotides with maleimides

For the optimization of the thiol labeling reaction with C₂-maleimide fluorescent dyes the same 15mer sequence with a thiol-modification was synthesized. For practical reasons (easier to synthesize) a thiol modification at the 5'-end, containing a C₆ spacer between the last base and the sulfur atom, was chosen (ODN7).

All reactions were carried out with 10 pmol of thiolated oligonucleotide. Standard protocols for the labeling of thiol modifications in biomolecules recommend a 20 to 40 fold excess of the maleimide dye over the biomolecule to ensure maximal yields for the labeling reaction. The influence of different dye excesses were tested. The anthracene modified oligonucleotide (ODN6) was always investigated in parallel under the same conditions to determine if a

labeling with a C₂-maleimide could be accomplished selectively only for the thiol modified oligonucleotide ODN7.

If less than a 10 fold excess of dye was used no significant labeling of the sulfhydryl group was observed and with an excesses of 10 and above the Diels-Alder reaction was as fast as the thioether bond formation between the maleimide and the thiol (figure 33). Selectivity could not be achieved adequately, because the maleimide dye had to be used in excess for thiol alkylation with maleimides. Under these conditions, the background reaction between the free anthracene-modified oligonucleotide and the C₂-maleimide dye in solution was too high.

Kinetic measurements showed that the Diels-Alder reaction is already too prominent after five minutes. Typically modification of thiolated probes is achieved either during 2 h at 25°C or over night at 4°C. Performance of the labeling reaction at 4°C could also not decrease the rate of the Diels-Alder reaction to achieve a selective labeling reaction on the thiol modification without modifying the anthracene as well.

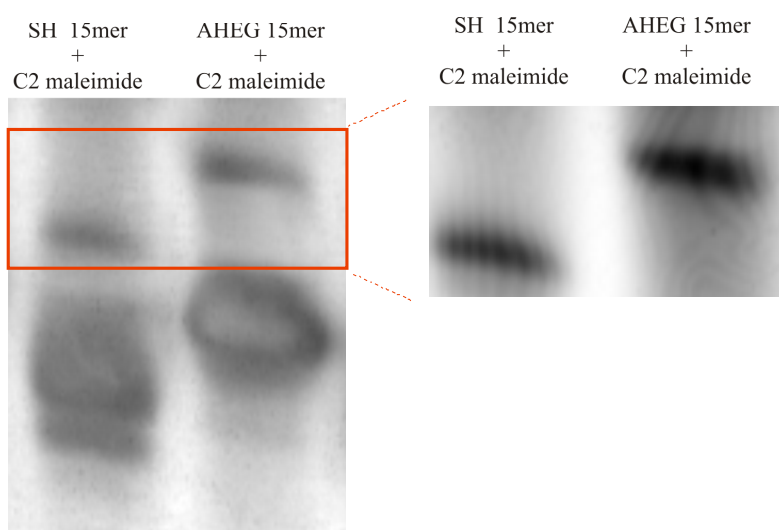


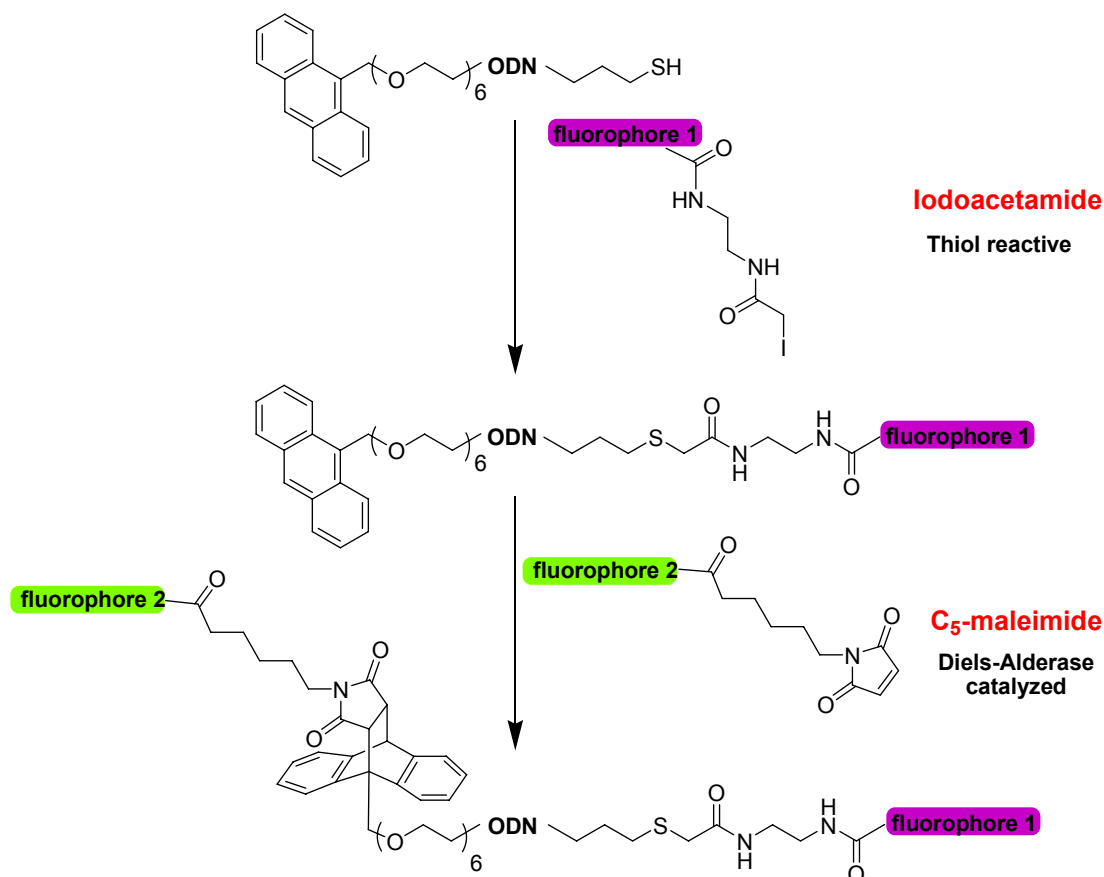
Figure 33: Thiol labeling compared with the reactivity of the anthracene towards maleimides. ODN8 (SH 15mer) and ODN7 (AHEG 15mer) reacts with Atto 532 C₂-maleimide (20 fold excess), reaction time 2 h at 25°C. **A:** SYBR Gold stained: the lower bands represent the unreacted product, the upper bands the fluorescently labeled oligonucleotides. Labeling efficiency was estimated with ImageQuant to be ~ 10%. **B:** fluorescent scan (532 nm).

A problem that has to be addressed, arises from the preceding disulfide cleavage with TCEP. It was observed that TCEP does react with maleimides, and if no excess of maleimide was used, the side reaction between maleimide and TCPE had a significant influence on the labeling efficiency. This will be discussed in detail in chapter 4.3.10.2.

It was concluded that the orthogonal labeling of the thiol modification could not be accomplished in the presence of an anthracene. Therefore, a different labeling strategy to perform a dual, orthogonal labeling of the bi-functional oligonucleotide had to be developed.

4.3.6 Dual orthogonal functionalization of DNA with two different dyes

As mentioned in the introduction, a less common, but still very efficient method to modify thiol-containing biomolecules is the use of α -haloacetamides. Unfortunately the variety of iodoacetamides, being the most common α -haloacetamide, commercially available is nowhere near the variety of commercial maleimide dyes. Additionally, iodoacetamides are much more demanding in synthesis, extremely apolar and less stable than maleimides. Apart from that no reactivity towards anthracene was expected and therefore they were chosen to be used in a dual, orthogonal labeling of the oligonucleotide ODN8 (scheme 37).



Scheme 37: Dual, orthogonal labeling of ODN8. In a first step the sulfhydryl group is selectively labeled with fluorophore 1 (purple). Anthracene is labeled with C₅-maleimide fluorophore 2 (green) catalyzed by the Diels-Alder ribozyme. As fluorophore 1 Atto 590 iodoacetamide was employed and fluorophore 2 Alexa Fluor 532.

The reactivity of the iodoacetamide dye towards the mono-functionalized oligonucleotides ODN7 and ODN6 was again investigated in parallel. Labeling of the thiol-modification of ODN7 with Atto 590 iodoacetamide was performed according to standard protocols with a 20-fold excess of the iodoacetamide dye. Figure 34 shows that the thiolated oligonucleotide (ODN7) was fluorescently labeled with iodoacetamide while the anthracene modified oligonucleotide (ODN6) stayed entirely unaltered even incubated with a 20-fold excess of iodoacetamide dye.

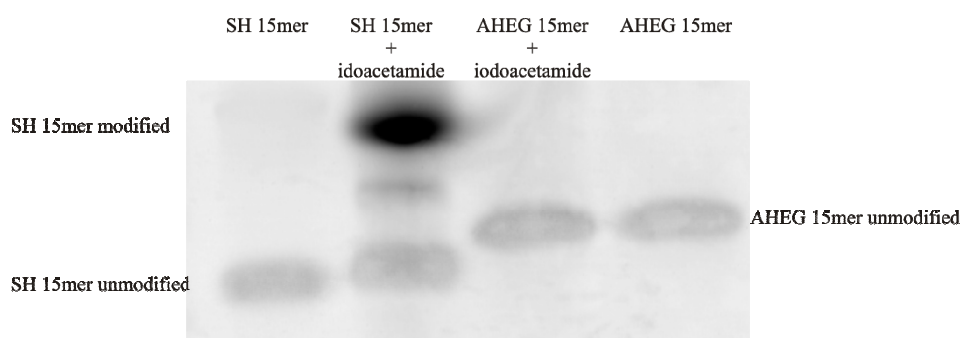


Figure 34: Thiol labeling with Atto 590 iodoacetamide, compared with the reactivity of the anthracene. SH 15mer (ODN8) and AHEG 15mer (ODN7) Atto 590 iodoacetamide (1mM), Reaction time 2 h. SYBR Gold stained.

Iodoacetamide dyes are poorly soluble in aqueous buffer. While the Atto 590 dye is known to be well soluble in water the iodoacetamide derivative is absolutely insoluble in water. In a heterogeneous solution no labeling reaction could be detected. Therefore, 20% ethanol had to be added to solubilize of the dye and thereby facilitate the desired labeling reaction. From previous studies it is known that the Diels-Alder ribozyme has no significant activity at ethanol concentrations above 10%.^[95] For that reason the dual orthogonal labeling had to be performed in two consecutive steps. After evaporation of the ethanol, removal of excess dye and unlabeled oligonucleotide was carried out by gel purification. A purification step in-between the two labeling steps is also advantageous due to the fact that the disulfide reducing agent TCEP is removed and will not compete with the anthracene for the maleimide in the second labeling step.

The dual orthogonal labeling of ODN8 was carried out in two steps. Labeling of the 3'-thiol modification was carried out as described above and the Diels-Alderase ribozyme catalyzed labeling was performed as described in chapter 4.3.4. Figure 35 shows the PAGE of the dual orthogonal labeled oligonucleotide.

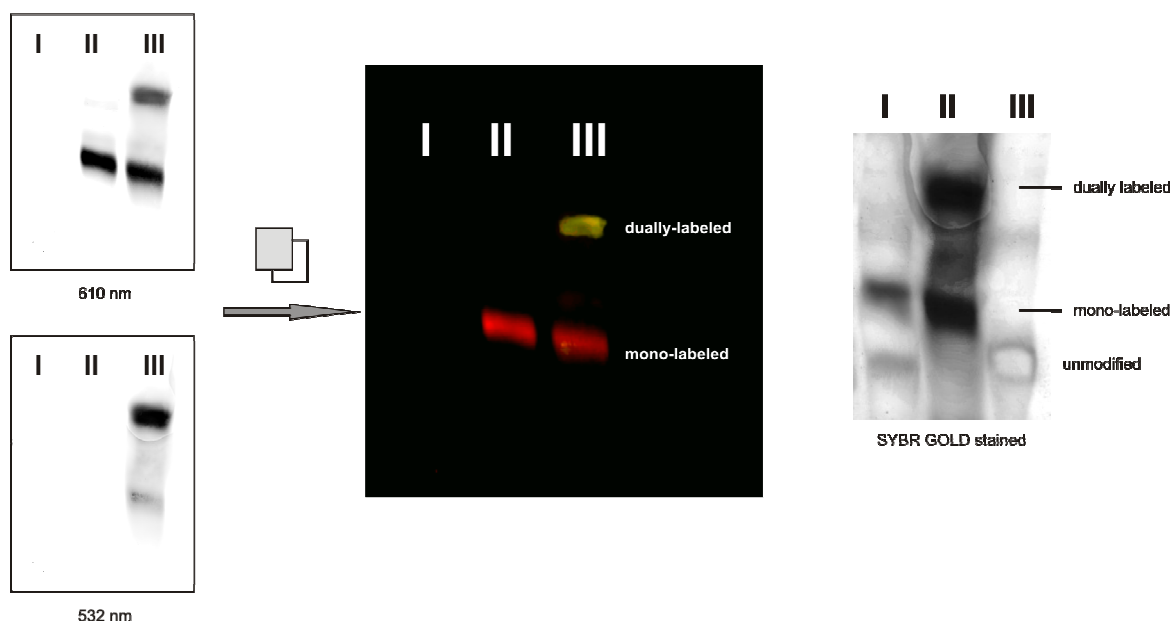


Figure 35: Dual orthogonal labeling of ODN8. For the Atto 590 dye the best wavelength for imaging is 610 nm (red), while the Alexa Fluor dye is imaged at 532 nm (green). The fluorescent scan in the middle shows the overlaid images of the scans at 610 nm and 532 nm (left). On the right the SYBR Gold scan of the same PAGE is shown. **I:** ODN8 labeled with Iodoacetamide. **II:** ODN8 labeled with iodoacetamide and maleimide. **III:** ODN8 unmodified (in the SYBR Gold stain over stained, therefore the band appears white).

4.3.7 Analytical data of post-synthetically modified oligonucleotides

Here analytical data of selected modified oligonucleotides are presented.

Table 6: Selective analytical data of labeled oligonucleotides. MALDI-TOF mass analysis

ODN	Modified ODNs	$[M+H]^+$ calculated	$[M+H]^+$ observed
ODN9	ODN6 Alexa Fluor 532 C ₅ maleimide	5956.20	5957.8
ODN11	ODN7 Atto 590 Iodoacetamide	5560.44	5558.1
ODN12a	ODN8 Atto 590 Iodoacetamide	6088.38	6086.0 ^a
ODN12	ODN8 Atto 590 Iodoacetamide and Alexa Flour 532 C ₅ maleimide	6856.28	6857.8

^a calculated for $[M+Na]^+$

4.3.8 Important aspects of the labeling conditions

4.3.8.1 Purification after bioconjugation

For labeling reactions of biomolecules the dye is usually used in a 20 to 40 fold excess. The purification of the labeled molecules from the dye excess is in general dependent on the nature of the dye. In protein biochemistry and also for larger oligonucleotides size exclusion techniques or dialysis provide an efficient way to remove excess dye. For short oligonucleotides there are no such standard protocols. Several different approaches to remove the excess dye and purify the labeled oligonucleotide were investigated. Phenol extraction or chloroform extraction and isopropanol or lithium perchlorate precipitation were not satisfactory, because the dye was not removed entirely. Direct injection of the reaction mixtures to HPLC was not sufficient. Even low amounts of unreacted dye caused high background fluorescence and, depending on the dye and the emission spectra, clear interpretation of the labeling was not possible. A similar problem was observed if the reaction mixture was directly loaded on a preparative denaturing PAGE, where the free dye masked all other signals.

Another possibility is the use of commercial dye removal kits. These kits are usually used to remove excess dye in sequencing reactions and therefore it has to be pointed out that dye terminator kits are designed for longer oligonucleotide sequences. The DyeEx 2.0 Spin Kit from Qiagen provides separation *via* gel filtration according to molecular weight. The drawback of this kit is that a maximum volume of 20 μ L can be loaded and therefore larger sample volumes had to be evaporated or lyophilized and adjusted to the required volume. With the radioactively labeled 11mer the elution efficiency and the reproducibility of this system was investigated. The amount of RNA was determined *via* Cherenkov counting before and after DyeEx application (table 6). Additionally, the samples were analyzed by denaturing PAGE and the loss of labeled and unlabeled oligonucleotide visualized by autoradiography (as example figure 36 is shown for Alexa Fluor 532 C₅-maleimide) and analyzed with ImageQuant.

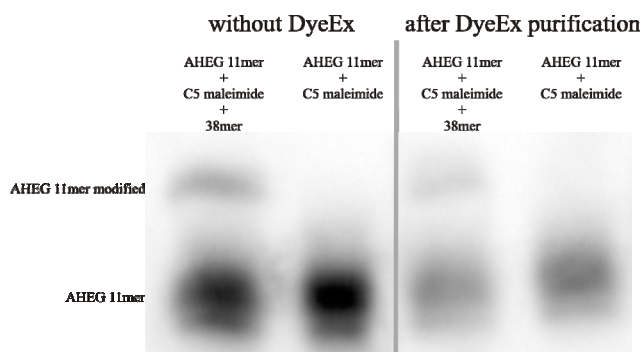


Figure 36: Elution efficiency of labeled and unlabeled oligonucleotides by autoradiography.

As shown in figure 36 and the actual loss of short oligonucleotides is rather high. However, the fact that the same amount of labeled and unlabeled RNA stays on the gel-filter material made DyeEx a valuable tool for the removal of unreacted dye. If handled correctly, the reproducibility of dye removal with this particular kit is very high and the elution efficiency is ~30% for short oligonucleotides.

Another advantage of DyeEx purification after labeling is that the reducing reagent TCEP is also removed from the reaction mixture. If the dye and the excess of TCEP was not removed from the reaction solution prior to PAGE analysis, higher background fluorescence was observed, along with as well as an abnormal shape of the bands. Abnormal elution behavior of TCEP containing probes has been reported previously.^[209] For all reaction mixtures except the labeling with iodoacetamide DyeEx was used.

The benefit of the Atto 590 iodoacetamide being entirely insoluble in aqueous solutions is that there is no need to remove the excess dye through DyeEx. As the insoluble dye does not penetrate the polyacrylamide matrix, it can easily be removed from the loading pockets after the PAGE. It can even be recovered by organic extraction, followed by HPLC purification.

4.3.8.2 TCEP as reducing reagent

As introduced earlier, TCEP is marked as the ideal reagent for the reduction of disulfide bonds prior to any labeling reaction.^[227] The advantages of TCEP over other reducing reagents are not only that, in contrast to ME and DTT just a single molecule TCEP is required to reduce one disulfide bond, but also that the molecule does not have any thiol functionality and therefore does not compete with the thiol group of the oligonucleotide during the labeling reaction. Supposedly it has no reactivity toward other molecules. For that reason, common knowledge is that there is no need to remove TCEP from the reaction mixture before labeling. In contradiction to this belief a few authors observed a competitive reaction between the

TCEP and the maleimide. The reactivity of TCEP towards these molecules is usually masked by the huge excess of dye over the reducing agent.^[228] In protein biochemistry common protocols recommend a 10-fold excess of reducing reagent over the thiol and a 20 to 40 fold excess of dye over the thiol.

In this study, the thiolated oligonucleotides could not be detected if they were not reduced prior to analytical measurements like HPLC and mass spectroscopy. In gel electrophoretic analysis, if not treated with a reducing reagent, the main band was associated with the dimers linked via disulfide. Apart from the disulfide linked dimer many bands were visible (figure 37) if the oligonucleotide was not treated with TCEP. Figure 37 shows that if the dye is used in a 1:1 ratio with TCEP no labeling could be observed, while for the reaction mixture without TCEP a faint band was observed corresponding to the fluorescently labeled oligonucleotide. These findings are in agreement with Getz *et al.*. Labeling myosine with a fluorescent maleimide they found that a labeling reaction took place in the presence of TCEP, albeit with a lower efficiency than if no reductant was added at all.^[211] For proteins, reducing reagents can be removed *via* dialysis or gel filtration, even though Shafer *et al.* found that TCEP elutes, despite its low molecular weight together with small proteins and can therefore not be removed entirely.^[209] For short oligonucleotides like the 15mer it is exceptionally difficult to remove TCEP before labeling. Gel elution of short oligonucleotides is demanding and precipitation is not very efficient. Common protocols for disulfide cleavage of oligonucleotides recommend bulk reduction in 1 mg scale. For optimization of the labeling reactions only 10 pmol or even smaller amounts of oligonucleotide were used, which made it impossible to remove reducing agent prior to the labeling reaction. Da Pieve *et al.* recently reported similar problems for the reduction of thiol modified short aptamers. They observed very low conjugation efficiencies in the presence of TCEP.^[229] For future labeling reactions of thiols with maleimides options like immobilized TCEP should be investigated in order to improve the labeling procedure.

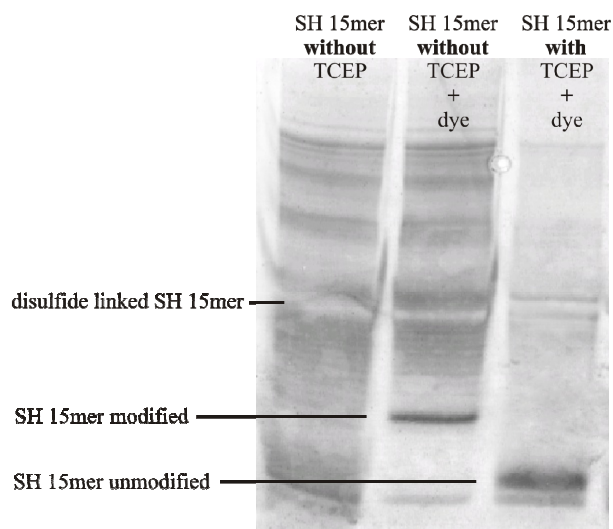


Figure 37: Reduction of ODN7 with TCEP. SYBR Gold stained. **Left:** ODN7 without TCEP treatment many bands are visible. **Middle:** No TCEP treatment, but after the addition of Atto 532 maleimide in a 1:1 ratio fluorescently labeled ODN7 was observed. **Right:** ODN7, TCEP and Atto 532 maleimide were used in a 1:1:1 ratio, no labeling reaction could be observed.

4.3.8.3 Investigation of the reaction between maleimides and TCEP

As discussed in the previous paragraph, there are hardly any reports about the reactivity of TCEP with maleimides and common labeling protocols state that TCEP shows no reactivity towards maleimides. Hence, no investigation about the mechanism or the undesired products has been reported, so far. To confirm that there is indeed a competitive reaction taking place between the maleimide dyes and TCEP a set of experiments was designed. Equimolar amounts of TCEP and a maleimide derivative were mixed in water and the resulting product was analyzed by NMR and mass spectrometry. To keep the reaction conditions as close as possible to the actual reaction, *N*-pentylmaleimide was chosen as maleimide. The ^1H -NMR spectrum of the reaction product was compared with the spectra of the pure reactants in the same solvent.

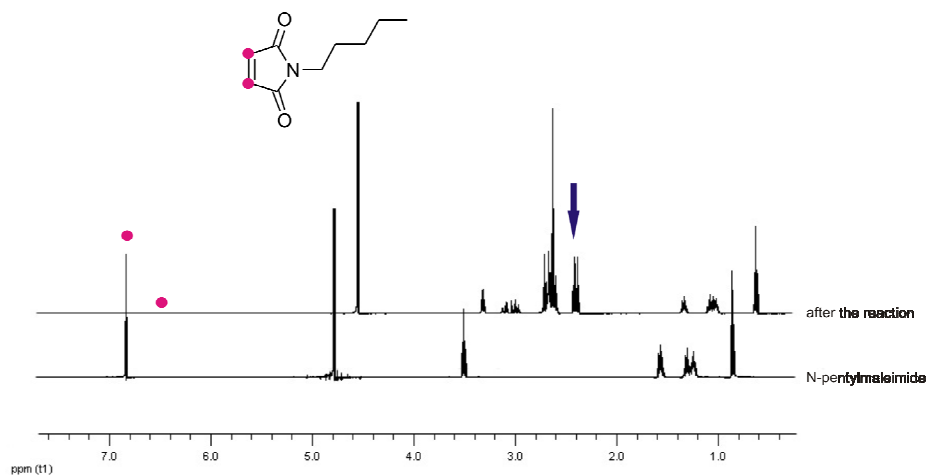


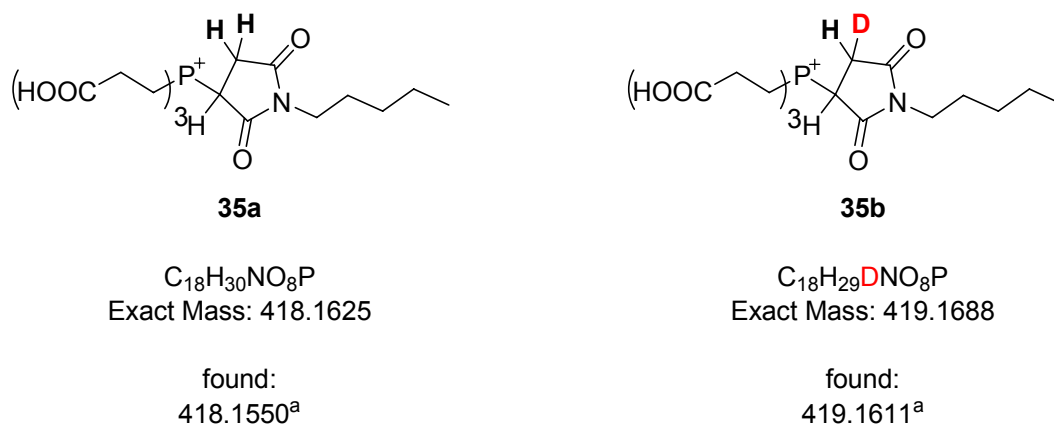
Figure 38: ^1H NMR spectrum of *N*-pentylmaleimide before and after the reaction with TCEP in water. The signal for the vinylic protons of *N*-pentylmaleimide disappears during the reaction. The blue arrow indicates the signal generated for the newly incorporated protons.

Before the reaction the vinylic protons of *N*-pentylmaleimide showed a chemical shift of 6.84 ppm. After the reaction the signal for the vinylic protons could not be observed any more. This experiment shows that double bond had been reduced to a single bond.

To examine whether the protons come from the solvent water, the same reaction was again performed in D_2O . The chemical shift of 2.64 ppm (figure 35) indicated with a blue arrow could be assigned to the protons of the reduced double bond. If the reaction was performed in D_2O , this signal was not visible, because deuterium does not give a signal in ^1H NMR, proving that the protons originate from the solvent water.

In the phosphorus NMR a shift of the signal was observed. This shows that TCEP (15.8 ppm) was bound to the former vinylic bond of the maleimide (39.12 ppm) after the reaction. To prove that the shift is not just due to oxidation of the phosphine, the phosphine was oxidized with hydrogen peroxide and analyzed (56.64 ppm).

After the reaction between TCEP and maleimide a stable product was isolated. High resolution mass analysis was performed and the proposed reaction products and observed masses are illustrated in scheme 38.



Scheme 38: Reaction performed in H₂O results in product **35**, if performed in D₂O the mass observed (^a HR-ESI MS) is exactly associated with one deuterium incorporated at the reduced vinylic bond.

As shown above TCEP does, against common belief, react with maleimides in a 1:1 ratio. For the modification of thiolated oligonucleotides with maleimides, TCEP should be removed from the reaction before addition of the maleimide or an excess of the dye over TCEP has to be applied.

4.4 Conclusion

The site-specific covalent labeling of oligonucleotides catalyzed by the Diels-Alderase ribozyme was demonstrated successfully *in cis* and *in trans*, showing high substrate specificity. Only maleimides with a C₅-linkage between the maleimide and the fluorescent dye were tolerated as substrates, while for fluorescent maleimide dyes with a C₂-linkage next to the dye no acceleration by the Diels-Alderase ribozyme was observed. Labeling with decent efficiencies was observed after 10 min with equimolar amounts of fluorescent dye. The synthesis of a C₅-maleimidocaproic acid hydrazide dye could be accomplished. With this maleimide dye a decent labeling efficiency of 24% could be obtained.

A dual orthogonal labeling strategy exploiting the substrate specificity of the Diels-Alderase ribozyme could not be achieved by employing two maleimide dyes with different linker lengths between the dye and the maleimide. For the modification of oligonucleotides with fluorescent dyes an excess of dye was required and thus the Diels-Alder background reaction of the anthracene with the C₂-maleimide dye was too prominent.

Iodoacetamide showed no reactivity towards anthracene and could therefore be utilized to fluorescently label the thiolated functionality. In a second step anthracene could be labeled with a maleimide fluorescent dye to provide a bis-fluorescently labeled oligonucleotide.

Notably, the labeling strategy employing the Diels-Alderase ribozyme is truly bioorthogonal. The modification of the thiolated oligonucleotide is basically also bioorthogonal, as long as it is studied with oligonucleotides. As mentioned earlier in the cell many thiol modifications are present. More importantly, in the labeling reaction providing the bis-fluorescently labeled oligonucleotide both reactions are orthogonal to each other, meaning that both reactions are independent.

Valuable insight into the labeling of thiol modified oligonucleotides was gained investigating the reactivity of TCEP with maleimides. It was demonstrated that the reaction between TCEP and a maleimide leads to a stable product. This finding is important to improve post-synthetic modification of thiolated oligonucleotides as well as for other biomolecules.

5 Conclusion and Outlook

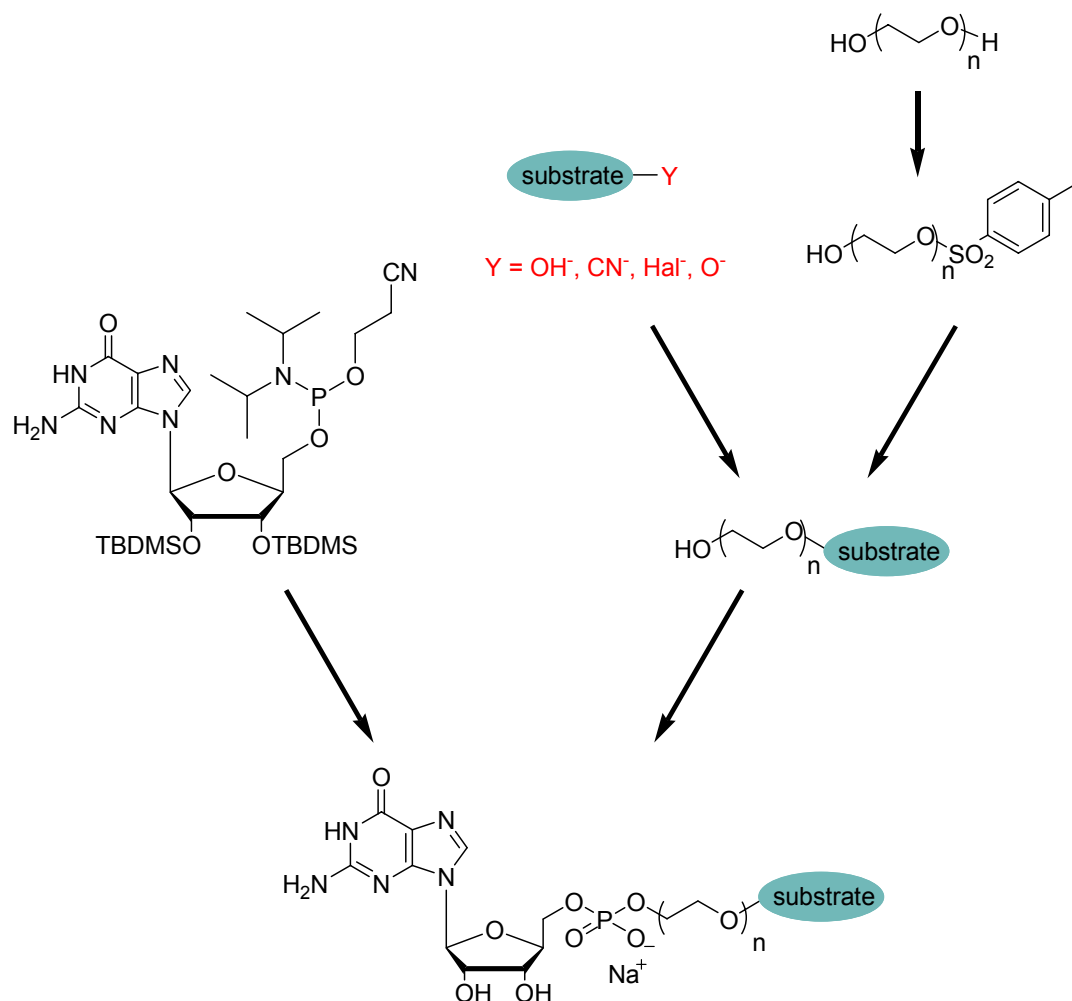
The center piece of the presented work is a small ribozyme which catalyzes the Diels-Alder reaction between an anthracene and a maleimide with multiple turnover and high enantioselectivity.^[93] In the course of this work, different approaches have been pursued successfully to explore and understand the complex mechanisms of function and action of the Diels-Alderase ribozyme. Furthermore, novel approaches for the enzymatic and chemical modification of oligonucleotides were developed.

5.1 Synthesis and applications of novel initiator nucleotides

The ability of the DNA-dependent T7 RNA polymerase to selectively incorporate modified guanosine monophosphates at the 5'-end can be used for the introduction of organic moieties into RNA during transcription. For the *in vitro* selection of ribozymes this technique is of utmost interest. The use of polydisperse polyethylene glycol linkers for the synthesis of modified guanosine monophosphates is more demanding than the synthesis of initiator nucleotides with monodisperse polyethylene glycol, but creates a library of different molecules. This is especially important for applications where the distance is critical.^[230]

In the work presented here, the routes and methods of polydisperse initiator nucleotide synthesis were considerably improved. A very clean and short synthetic route was established for the synthesis of polydisperse initiator nucleotides that contain an anthracene moiety. The synthesis could be achieved in only five steps by starting from the anthracene derivative and the TBDMS-protected guanosine monophosphate. Furthermore, the novel synthetic procedures established for the aldehyde modified initiator nucleotide present a superior synthetic strategy, only requiring three synthetic steps.

Two key intermediates establish a vast variety of possibilities (scheme 39). One intermediate is the TBDMS-protected guanosine phosphoramidite. The other and even more relevant intermediate is the mono-tosylated polyethylene glycol, which may be used in a multitude of reactions that involve modified initiator nucleotides. It is reasonable to assume that the activation of such alcohols with tosyl enables the modification with virtually any organic moiety, because it can be reacted with any hard nucleophile in an S_N2 reaction.



Scheme 39: Synthetic strategy for the preparation of a variety of initiator nucleotides. Tosylated polyethylene glycol represents the key intermediate to a vast number of possible organic modifications.

The modification of RNA with an aldehyde is enormously versatile and can be used for simple post-synthetic modifications such as the reductive amination with a fluorophore or an anchoring group for the immobilization of RNA. Reductive amination can also provide a convenient method to introduce small molecules for the selection of aptamers.^[231] In the past this approach has been utilized with amine modified oligonucleotides, possibly due to the lack of direct aldehyde modifications on RNA. The number and stability of small molecules bearing amino modifications available, further increases the versatility of the described aldehyde modifications. Furthermore, the initiator nucleotide presented here can be used as the basis for *in vitro* selections of many different ribozymes catalyzing diverse chemical reactions, for instance an aldol reaction or a Wittig reaction.

The 5'-end modification of RNA was achieved co-transcriptionally by transcription priming using the enzyme T7 RNAP with initiator nucleotides containing a 2,3-dimethylanthracene or a benzaldehyde modification. For the transcription of a short DNA template full activity of T7

RNAP was observed in the presence of the initiator nucleotides. The initiator nucleotide bearing a 2,3-dimethylantracene moiety was incorporated into a 109 nucleotide long RNA library that contained a randomized region, at a respectable incorporation rate of 77%, although diminished total yields were observed. The aldehyde modified initiator nucleotide was incorporated at a rate of 52%. Hydrophilic moieties are known to result in lower incorporation efficiencies than hydrophobic moieties,^[140] which coincides with the results presented here, the anthracene-modification being more hydrophobic than the benzaldehyde modification.

The reactivity of the modified RNA molecules was subsequently studied in chemical reactions. While the anthracene derivative could be reacted in a Diels-Alder reaction, the aldehyde was fully converted in the reaction with biotinhydrazide.

5.2 Thermal denaturation studies of the Diels-Alderase ribozyme

Due to its complexity, it is necessary to utilize a combination of experimental methods to elucidate structure, folding and function of catalytic RNA. Thermal denaturation experiments were employed to determine the stability of secondary and tertiary structures. The wild-type as well as mutants of the Diels-Alderase ribozyme were investigated in thermal denaturation studies to complement other approaches such as X-ray crystallographic studies,^[93] lead-probing,^[179] or smFRET.^[175] The G-C rich structure of the Diels-Alderase ribozyme suggested a high melting temperature and indeed, it was not surprising that even low concentrations of divalent metal ions lead to a stabilization of the secondary structure up to 85°C.

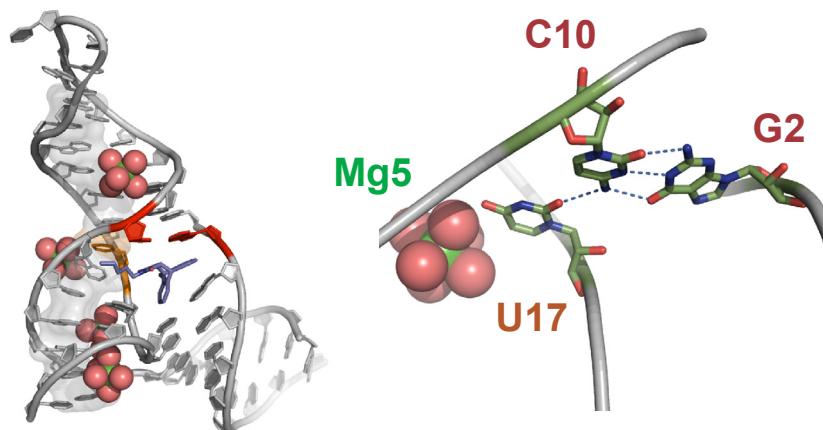


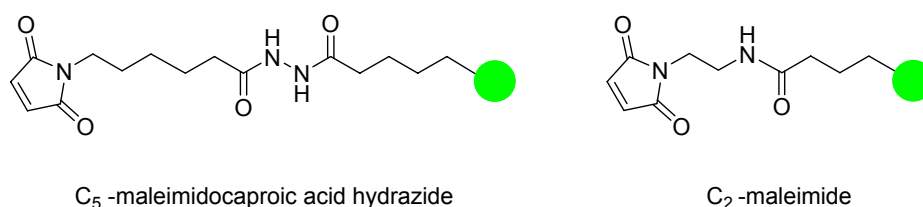
Figure 39: Three dimensional structure of the Diels-Alderase ribozyme; the base triple.

Further insight into one of the complex interaction characteristic of the Diels-Alderase ribozyme was gained by investigating the thermal denaturation behaviour of two mutants when compared with the wild-type. The base triple G2–C10–U17 (figure 39) has been shown previously to be relevant for catalysis. A mutant 17UiC in which the H-bonding network is disrupted, was entirely inactive, while the 17UC mutant, that is still capable of forming the H-bond, only showed a catalytic activity of 30% as compared to the wild-type.^[178] In the thermal denaturation experiments, both the wild-type and the mutants were equally stabilized at a Mg^{2+} ion concentration up to 5 mM. At 5 mM ion concentration, a significant increase in stabilization of the wild-type was observed, while the mutants were not further stabilized. These results are in good agreement with previous studies and indicate that the mutants can fold and form the pseudoknotted structure but cannot undergo further compaction. In agreement with this, smFRET measurements had also shown that at an Mg^{2+} ion concentration of 5 mM the Diels-Alderase ribozyme molecule had adopted its fully folded structure.^[175]

5.3 Bioorthogonal and orthogonal labeling of oligonucleotides

In the third part of this thesis, a novel application of the Diels-Alderase ribozyme is described in which the ribozyme is utilized as a catalyst for fluorescent labeling of oligonucleotides.

In summary, the site-specific covalent labeling of oligonucleotides catalyzed by the Diels-Alderase ribozyme was achieved and high substrate specificity was demonstrated. The structure of the active site of ribozyme allowed only for maleimides with a C_5 -linkage between the maleimide and the fluorescent dye to be used as substrates. Fluorescent maleimide dyes with a C_2 -linkage next to the dye were not recognized as substrates.

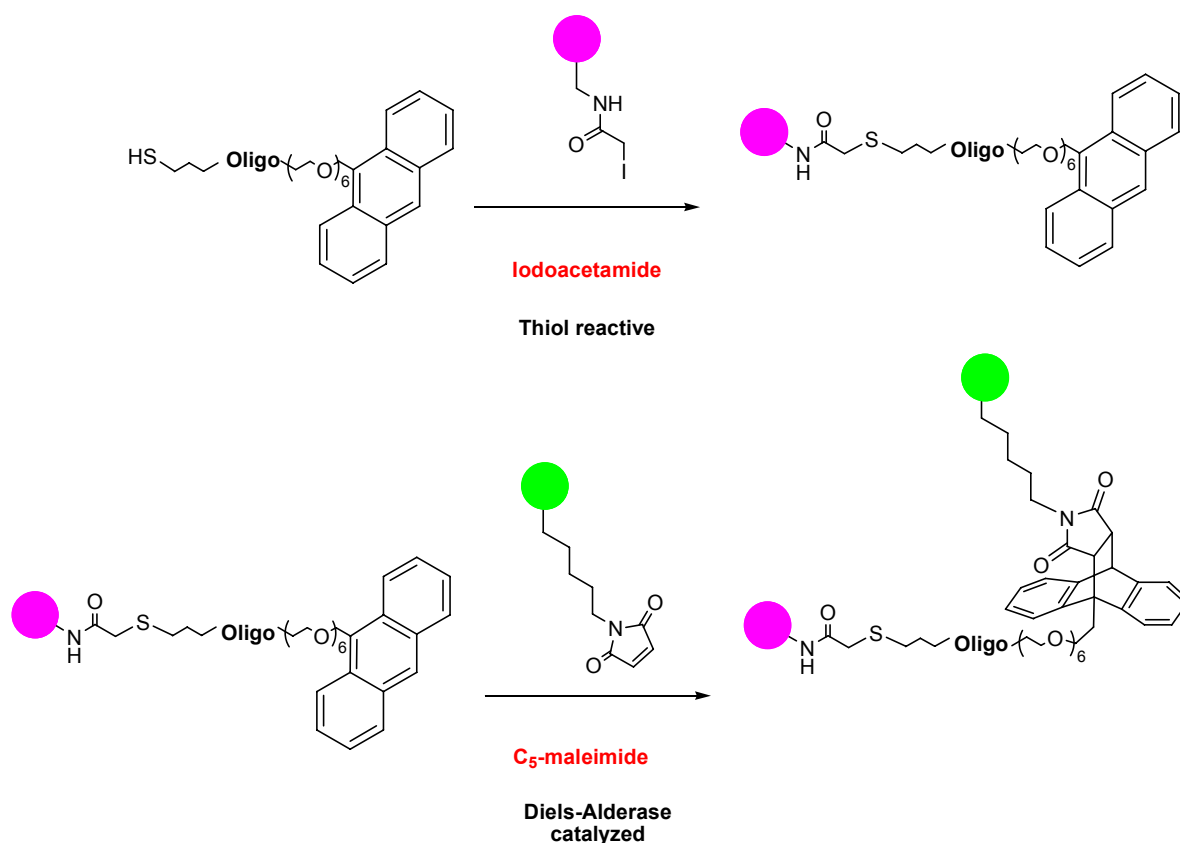


Scheme 40: C_5 -maleimidocaproic acid hydrazide and commercially available C_2 -maleimide.

A strategy for the synthesis of fluorescent dyes with a C_5 -maleimidocaproic acid hydrazide linkage (scheme 40) was established that provides a route to better substrates than the

commercially available C₅-maleimide dyes. An acceptable labeling efficiency of 24% could be achieved with this maleimide. It is noteworthy that so far only one attempt to utilize an anthracene as a diene for the Diels-Alder bioconjugation with fluorescent dyes has been reported and no conversion had been observed.^[189] Moreover, it was reported that the Diels-Alder bioconjugation can be very efficient, but is extremely dependent on the type of label and fluorescent dyes seemed to be the least efficient labels.^[221, 222]

Weisbrot and Marx recently expressed the need for a catalyst to improve the Diels-Alder cycloaddition as a tool for DNA bioconjugation.^[200] Having demonstrated that the Diels-Alderase ribozyme is able to catalyze the reaction between an anthracene tethered oligonucleotide and a fluorescent maleimide dye *in trans*, it would be an interesting task to extend this approach and conjugate anthracene-modified oligonucleotides to other labels, as well as other biomolecules, such as proteins and peptides.



Scheme 41: Illustration of the orthogonal labeling strategy for dual fluorescently labeled probes.

In addition, a new method for labeling one DNA probe with two different fluorescent dyes was developed. An anthracene modification and a thiol modification within the same DNA strand were selectively labeled with two different fluorescent dyes (scheme 41).

It was demonstrated that an anthracene modified oligonucleotide does not react with iodoacetamide. However, the thiol group could selectively be modified and labeled with an iodoacetamide dye. In a second step the novel method to fluorescently label anthracene in a Diels-Alderase catalyzed reaction with fluorescent maleimide dyes was employed to provide a unique labeling strategy to dual fluorescent labeled probes. In conclusion, the two reactions are orthogonal to each other and provide a strategy for dual labeling of oligonucleotides with fluorescent probes.

6 Experimental section

6.1 Molecular biological techniques

6.1.1 General methods

Fine chemicals for molecular biology and spectroscopic experiments were purchased in the highest commercially available purity. Water was purified by Mill-Q Synthesis A10 (Millipore, Billerica, Massachusetts, USA). All buffers and solutions were sterilized *via* steriflip® Milipore 22 µm filters.

Gel electrophoretic methods

Separation of nucleic acids *via* gel electrophoretic methods is based on the different migration of molecules with different charges and masses in an electrical field. The migration depends on the electric field and the connectivity of the gel matrix. As gel matrix commonly agarose and polyacrylamide is used.

Agarose gels

Agarose gel electrophoresis is a standard method for separation, identification and isolation of nucleic acids. By varying agarose concentration, gel pore size can be controlled to separate nucleic acids in a wide range of sizes. For special applications high resolution agarose, an intermediate melting agarose, is available for nucleic acids up to 1000 nt but with a resolution in the range of single base pairs. As DNA ladder GeneRuler™ Ultra Low Range and 100 bp DNA Ladder (Fermentas, St. Leon-Rot) were used. Nucleic acids have been separated on 2-3% agarose gels, 1 x TBE buffer, during 25 min, with 120 V. For staining Ethidium bromide was added to the agarose gel during preparation, documentation was carried out on a AlphaImager (Alpha Innotech Corporation, San Leonardo).

Denaturing polyacrylamide gel electrophoresis (PAGE)

PAGE has been used for detection and purification of nucleic acids. The denaturing conditions of PAGE analysis are mild and conserve secondary and tertiary structures of nucleic acids.

Oligonucleotides have been separated on 8- 20% polyacrylamide gels. The gel solution has been prepared with Rotiphorese® Ready-to-Use Gel Solutions containing sequencing gel concentrate, sequencing gel diluent and sequencing gel buffer). After the addition of ammonium persulfate (APS (1% (w/v)), as a radical donator and *N,N,N',N'*-tetramethylethylenediamine (TEMED (0.1% (v/v)) as catalyst for the formation of free radicals in the presence of ammonium persulfate and is thus used as an enhancer for the polymerisation. Vertical gels have been produced between two glass plates silanized with 2% dichlorodimethylsilane in chloroform. The layer thickness was 0.4 mm for analytical gels and 1.0 mm for preparative gels.

The conditions for the separation on PAGE gels varied depending on the percentage of the gel and the length of the oligonucleotides to be separated. Loading buffer (1 x TBE-buffer, 90% formamide) containing the two dyes xylenecyanol and bromphenol blue help monitoring the migration behavior of nucleic acids. Visualization of PAGE analysis was done by phosphor imaging (GE Healthcare, Munich), staining with SYBRGold or ethidium bromide and imaging with Typhoon (GE Healthcare, Munich) and UV shadowing and imaging by an AlphaImager (Alpha Innotech Corporation, San Leandro).

For the analysis of fluorescent labeled oligonucleotides a loading buffer without xylenecyanol was used to reduce the background. Xylenecyanol has UV absorption of λ_{max} 615 nm. Bromphenol blue was allowed to run out of the gel or cut off in the scan.

Elution of nucleic acids from electrophoretic gels

Elution of nucleic acids from either PAGE or agarose gels are based on diffusion. The desired nucleic acids had been excised from the gel, cut into as small pieces as possible. 500 μL ammonium acetate 0.5 M were added, mixed at 20°C and 650 rpm over night on a benchtop thermo shaker. The solutions were filtered over 45 μm Spin columns (Nanosep® MF, PALL® Life Science, Darmstadt) to remove small gel pieces and the nucleic acids precipitated as described below. Alternatives are elution kits, e.g. MinElute PCR Purification Kit or RNeasy

MinElute Cleanup Kit (Qiagen, Hilden). Best elution efficiencies were achieved by elution with ammonium acetate.

Precipitation of nucleic acids

The method of choice for precipitation of nucleic acids depends on the size and the desired purity of the nucleic acids.

Precipitation with ethanol or isopropanol

After elution from the gel the nucleic acids in ammonium acetate (0.5 M) have been vortexed with a 2 fold excess of ice-cold ethanol or isopropanol and stored at -80°C for at least 30 min, or -20°C over night. The cold samples were centrifuged at -5°C, 13 000 rpm for at least 45 min. *E. coli* tRNA (10 µg/µl) was used as a precipitation aid for very short oligonucleotides. The supernatant was removed and the pellet dried in a centrifugal vacuum concentrator.

Precipitation with lithium perchlorate

For short nucleic acids (10 to 25 nt) best yields have been observed by precipitation with lithium perchlorate.

After elution from the gel the nucleic acids in ammonium acetate (0.5 M) have been vortexed with a 10 fold excess of a lithium 2% lithium perchlorate in acetone and centrifuged at r.t., 10000 rpm for 40 min. The residual acetone was evaporated, the pellet dissolved in 20 µL water followed by desalinization on a NAP-5 column and removal of the water in a centrifugal vacuum concentrator.

Purification of nucleic acids with organic solvents

Separation of nucleic acids between organic solvents is an easy way to remove proteins from the reaction mixture. While nucleic acids remain in the water phase proteins separate into the organic phase. Phenol has a denaturing effect on the proteins while chloroform mostly helps to separate the organic phase from the aqueous phase. An equivalent volume phenol/chloroform (1:1) was added to the reaction mixture and vortexed well. Separation of the two phases was accelerated by centrifugation at rt, 15000 rpm for 5 min (for Eppendorf tubes MIKRO 120, Hettich. Separation in Falcon or Greiner tubes in an Eppendorf centrifuge

5804 R at rt, 9000 rpm for 5 min). The organic layer was removed and the procedure repeated as described above. The aqueous layer was then transferred to a clean tube and the remaining phenol removed by diethyl ether extraction (centrifugation r.t., 15000 rpm for 5 min for Eppendorf tubes MIKRO 120, Hettich. Separation in Falcon or Greiner tubes in an Eppendorf centrifuge 5804 R at rt, 9000 rpm for 5 min). The organic layer was removed and the nucleic acids precipitated from the aqueous solution as described above.

6.1.2 Detection of nucleic acids

Autoradiography

For detection and evaluation of radio labeled nucleic acids phosphor image screens (*Imaging Screens*, GE Healthcare, Munich) were used. The gels were wrapped into plastic foil, radioactive paper, used as markers and the imaging screens exposed in a X-ray cassette. Exposure time was dependent on the amount of radioactivity of the sample. For read out of the screens Typhoon 9400 (GE Healthcare, Munich) was used. The data was edited and quantified with ImageQuant 5.2 (GE Healthcare, Munich) and IQ Tools (GE Healthcare, Munich).

Fluorescence detection

Fluorescent labelled nucleic acids were analyzed with Typhoon 9400 (GE Healthcare, Munich). Typhoon 9400 provides 457/488/532/633 nm excitation, the different lasers are given in table 7. The wavelength for imaging was tailored to the fluorescence spectra (excitation and emission) of the dyes. The data was edited and quantified with ImageQuant 5.2 (GE Healthcare, Munich), IQ Tools (GE Healthcare, Munich) or ImageJ 1.42q (National Institutes of Health, USA).

Table 7: Lasers in Typhoon 9400.^[232]

Light	Laser type	Wavelength
red	10 mW Helium neon laser	632.8 nm
green	20 mW solid state doubled frequency SYAG laser	532 nm
blue	30 mW argon ion laser	488 (20 mW), 547 nm (4 mW)

Staining

Ethidium bromide staining was mostly used for detection of nucleic acids on agarose gels while for PAGE gel analysis SYBRGold staining was the method of choice.

Ethidium bromide

Ethidium bromide is an intercalating fluorescent reagent which changes its emission spectra after binding to nucleic acids and can easily be detected with UV light. Ethidium bromide was added to the agarose solution before casting the gels, 5 μ L bromide solution (1%) per 100 mL 2% agarose solution. Readout on AlphaImager (Alpha Innotech Corporation, San Leandro).

SYBR[®] Gold

SYBR[®] Gold nucleic acid gel stain is an unsymmetrical cyanine dye that exhibits fluorescence enhancement upon binding to nucleic acids. PAGE gels were stained by agitating in 1 x TBE buffer with 10-20 μ L SYBR[®] Gold stock solution for 30 min. The fact that excitation maxima for the dye-nucleic acid complex is around 495 nm and the emission maxima at \sim 537 nm makes the Typhoon 9400 (GE Healthcare, Munich) the perfect readout. Images were recorded at 488 nm.

UV-shadowing

UV-shadowing allows the detection of nucleic acids without any treatment; however large amounts (> 1.0 nmol) of nucleic acids are necessary as compared to above mentioned methods. The gels were covered in plastic and placed on fluorescent TLC plates. Exposed to UV light (254 nm) the oligonucleotides quench the fluorescence and are visible as dark shadows. Documentation of the readout can be carried out with the AlphaImager (Alpha Innotech Corporation, San Leandro).

6.1.3 Determining the concentration of nucleic acids

Photometric determination

Concentrations of oligonucleotides were determined by UV measurements on a Nanodrop ND-1000 (PeqLab, Erlangen). For nucleic acid quantification, the Beer-Lambert equation is modified to use an extinction coefficient with units of ng-cm/ml. Using this extinction coefficient gives a manipulated equation: $c = (A * e)/b$

c: (nucleic acid concentration [ng/μL]), **A:** (absorbance in AU), **e** (wavelength-dependent extinction coefficient in [ng-cm/μL]), **b:** (path length [cm]).

The generally accepted extinction coefficients for nucleic acids are:

dsDNA: 50 ng-cm/ul

ssDNA: 33 ng-cm/ul

RNA: 40 ng-cm/ul

To assess the purity of DNA and RNA the ratio of absorbance at 260 nm (λ_{\max} nucleic acids) and 280 nm (λ_{\max} proteins) is used. A ratio of ~1.8 is generally accepted as “pure” for DNA; a ratio of ~2.0 is generally accepted as pure for RNA. If the ratio is appreciably lower in either case, it may indicate the presence of protein, phenol or other contaminants that absorb strongly at or near 280 nm.^[233]

Amount radio labeled nucleic acids

The amount of RNA transcribed *via* T7 RNAP with [α -³²P] could be determined after PAGE purification and precipitation. An aliquot typically of 1 μL was taken from the reaction mixture and the radioactivity determined by Cerenkov-counting (LS 6500, Beckman Coulter, Krefeld). The concentration could be determined by the following equation.

$$\text{Incorporation rate } \alpha\text{-}^{32}\text{P} [\%] = \frac{\text{radioactivity RNA [cpm]}}{\text{total radioactivity [cpm]}}$$

$$\text{amount RNA [nmol]} = \frac{\text{incorporation rate} * \text{concentration CTP } [\mu\text{M}] * \text{reaction volume } [\mu\text{L}]}{\text{number of cytidine in RNA transcript}}$$

$$\text{number of RNA-transcripts for each DNA-template} = \frac{\text{amount transcribed RNA [mol]}}{\text{amount DNA template [mol]}}$$

6.1.4 Radioactive labeling with ^{32}P Phosphor

5'-labeling *via* kinase reaction

The enzyme T4 Polynucleotide kinase, short T4 PNK, catalyzes the transfer of the γ -phosphate from ATP to the 5'-OH group of oligonucleotides or nucleoside 3'-monophosphates.^[234] The reaction was incubated on a thermo shaker at 37°C for 30 min. PAGE purified, eluted and precipitated as described.

Table 8: 5'-Labeling of oligonucleotides with $[\gamma\text{-}^{32}\text{P}]\text{-ATP}$.

Chemicals	Volume [μL]	Final
Oligonucleotide	1	0.1 nmol
Buffer A 10x	2	1 x
$[\gamma\text{-}^{32}\text{P}]\text{-ATP}$	3	
T4 PNK 10 U/ μL	1	10 U
H ₂ O	13	
Σ	20	

Radioactive labeling *via* ligation

The enzyme T4-RNA-ligase catalyzes the esterification of a RNA 3'-hydroxyl group with a 5'-phosphate group of another molecule (RNA or ribonucleotide) in the presence of ATP.^[235] The 3'-prime end of RNA was labeled with Cytidin-3'-(5'- ^{32}P)-bis-phosphat $[\text{}^{32}\text{P}]\text{-pCp}$.^[236] The reaction was incubated in a thermo mixer at 16°C for 20 h, purified on a 20% PAGE as described. After elution the labeled RNA was precipitated with 100 μL *E. coli* tRNA (10 $\mu\text{g}/\mu\text{l}$) as a precipitation aid and centrifuged over night (13000 rpm, -5°C). Interestingly DNA could also be labeled according to the same protocol.

Table 9: 3'-Labeling of RNA with [³²P]-pCp.

Substance	Volume [μ L]	Final
Oligonucleotide 10 μ M	2	20 pmol
Ligation buffer for T4 RNA ligase	2	yx
ATP 10 mM	1	0.5 mM
[³² P]-pCp	10	100 μ Ci
T4 RNA ligase 10 U/ μ L	2	20 U
DMSO	2	10% (v/v)
H ₂ O	1	
Σ	20	

6.1.5 PCR (Polymerase Chain Reaction)

PCR is an *in vitro* method for the exponential amplification of DNA sequences.

GenTherm Taq Polymerase, buffer (10x, without MgCl₂), MgCl₂ and dNTP solutions (100 mM) were purchased from Rapidozym (Rapidozym, Berlin, Germany). GenTherm DNA-Polymerase, is a recombinant 5'-3'-DNA-polymerase, originally from *Thermus aquaticus*, expressed in E. coli without 3'-, 5'-exonuklease activity. Primer A and primer B were synthesized by IBA (Göttingen, Germany).

Table 10: Protocol for analytical PCR.

Chemicals	Volume [μ L]	Final	Step	Temperature [°C]	Time [min:sec]
PCR buffer (10x)	20	1x	1	94	5:00
dsDNA pool (10 μ M)	0.4	0.02 μ M	2	92	1:00
MgCl ₂ (50 mM)	16.0	4 mM	3	54	1:00
dNTP Mix (25 mM)	1.6	0.2 mM	4	72	1:30
Primer B (100 μ M)	3.0	1.5 μ M	5	5 times to step 2	
Pimer A (100 μ M)	3.0	1.5 μ M	6	72	8:30
Taq polymerase	4	0.1 U/ μ L	7	End	
H ₂ O	152	-			
Σ	200				

Analysis of analytical PCR reaction products was performed on agarose gels, purification either with QIAquick PCR Purification Kit (Quiagen, Hilden) or *via* preparative PAGE.

Preparative scale PCR

Table 11: Protocol for preparative PCR. Volumes for a master mix.

Chemicals	Volume [mL]	Final	Step	Temperature [°C]	Time [min:sec]
PCR buffer (10x)	1.920	1x	1	92	03:00
ssDNA pool (14.2 μ M)	0.261	0.2 μ M	2	92	02:00
MgCl ₂ (50 mM)	1.536	4 mM	3	54	06:00
dNTP Mix (25 mM)	0.150	0.2 mM	4	72	10:00
Primer B (100 μ M)	2.88	15 μ M	5	5 times to step 2	
Primer A (100 μ M)	1.920	10 μ M	6	End	
Taq polymerase	10.159	0.1 U/ μ L			
H ₂ O	8.0832	-			
Σ	19.200				

The master mix for the preparative PCR was prepared in three 50 μ L Falcon tubes each containing 19.2 mL master mix. All compounds were added, except the Taq polymerase and the DNA template, and the master mix was kept on ice. Taq polymerase and the template were added right before partitioning the reaction into 200 μ L batches in a 96 well plate. The master mix was transferred into reservoirs and with a multi channel pipette transferred into a 96 well plate. Purification of the PCR products from the preparative scale reaction were purified by phenol extraction.

6.1.6 Primer extension

Primer extension is used to assess how much of an ssDNA pool is amplified to full length product. The primer B was labeled with [γ - ^{32}P] ATP at its 5' end. The reaction was analyzed on a 12% PAGE.

Table 12: Protocol for primer extension.

Chemicals	Volume [μL]	Final
PCR buffer 10x	10.0	1x
^{32}P labeled primer B (31 μM)	1.0	0.25 μM
primer B (100 μM)	1.0	0.6 μM
ssDNA template (76.9 μM)	1.0	1 μM
MgCl_2 (50 mM)	8.0	4 mM
dNTPs (each 100 mM)	1.0 of each dNTP	10 μM
Taq DNA polymerase (0.1 U/ μL)	2.0	
H_2O	73.0	
Σ	100	

Table 13: Temperature protocol for primer extension in a single PCR cycle.

Temperature [$^{\circ}\text{C}$]	Time [min]
94	4:00
50	60:00
End	

6.1.7 *In vitro* T7 transcription

T7 RNA polymerase utilizes the transcription of dsDNA templates into the complementary RNA sequence. The enzyme was isolated from *E. coli* BL21 (DE3) cells with a cloned gene encoding T7 RNA polymerase.^[156]

Table 14: Standard protocol T7 transcription.

Chemicals	Volume [μ L]	Final
Transcription buffer (10x)	5.0	1x
GTP (25 mM)	0.7	0.35 mM
ATP (100 μ M)	2.0	4 mM
CTP (100 μ M)	2.0	4 mM
UTP (100 μ M)	2.0	4 mM
Template (2 μ M)	5.0	0.2 μ M
Initiator nucleotide (17.2 mM)	11.8	4 mM
DTT (100 mM)	5.0	10 mM
BSA (1 mg/ml)	2.0	50 μ g/mL
[α - ³² P] CTP (10 μ Ci/ μ L)	2.0	
T7 RNA polymerase	1.25	
H ₂ O	11.25	
Σ	50	

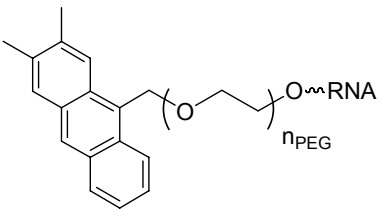
After preparing the reaction mixture an aliquot of 1 μ L was taken and stored aside to later be able to determine the concentration of the transcript. The transcription was incubated at 37°C for 2-4 h in a water bath. After 2 h more enzyme was added and incubated for another 2 h at 37°C. The transcription was stopped by the addition of loading dye (1 x TBE-buffer, 90% formamide, xylene cyanol and bromphenol blue) and either directly loaded on a gel or stored at -80°C.

During the optimization of the T7 transcription all substances were varied, except the buffer, BSA and DTT. Additionally in some cases a so called booster mix was added after 2 h and incubated for other 2 h.

Table 15: Booster mix for a T7 transcription of 50 μL .

Chemicals	Volume [μL]
Transcription buffer (10x)	4.0
GTP (25 mM)	0.35
ATP (100 μM)	1.0
CTP (100 μM)	1.0
UTP (100 μM)	1.0
Initiator nucleotide (17.2 mM)	5.9
T7 RNA polymerase	1.25

Table 16: MALDI-TOF mass analysis for transcribed RNA with initiator nucleotide.

	n_{PEG}	Calculated $[\text{M}+\text{H}]^+$	Found
Transcript = 5'-GG AGC UCA GCC UAC GAG CCU GAG CC-3'		8249	8254
Conjugate	9	8704	8706
	10	8748	8750
	11	8792	8794
	12	8836	8839
	13	8880	8883
	14	8924	8931

6.1.8 Diels-Alder reaction of the 2,3 dimethyl anthracene modified RNA

Initiator nucleotide **7b** was incorporated during T7 RNAP transcription. The purified conjugate (20 pmol) was dissolved in water and PBS buffer and biotin maleimide was added in a 10 respectively 1000 fold excess. The reaction was incubated in a thermo shaker over night at 25°C and 650 rpm and directly loaded on a 20% PAGE.

6.1.9 Deprotection of the aldehyde modified RNA and reaction with hydrazide

Initiator nucleotide **7c** was incorporated during T7 RNAP transcription. The purified conjugate (20 pmol) was dissolved in water and the aldehyde functionality deprotected by treatment with 2% trifluoroacetic acid in water for 10 min at r.t., leaving the RNA entirely intact. The reaction was quenched by the addition of 3.6 μL 1 M NaHCO_3 solution. 2.67 μL

0.4 M sodium acetate buffer were added to adjust the pH to 5.5. Biotin hydrazide was added in a 1000 fold excess and the reaction incubated for 4 h at r.t on a thermo shaker at 750 rpm. The RNA was precipitated to remove the biotin hydrazide excess by lithium perchlorate precipitation and analyzed on a 12% PAGE.

6.1.10 Melting curves

Thermal denaturation experiments of nucleic acids are an important method to observe temperature dependent conformational changes. Heating of a molecule leads to a change in absorbance and therefore reflects the conformational change.

Melting experiments are used to determine the hybridization between oligonucleotides or different regions within an oligonucleotide and are therefore valuable in primer design. Further secondary and even tertiary structure of DNA and RNA molecules and it may also be used to study the binding of specific targets to oligonucleotides.

RNA solutions were prepared by mixing the RNA stock solution in buffer and the addition of magnesium chloride and/ or sodium chloride solutions respectively EDTA was added. The concentration of the RNA was adjusted to an OD of 0.5. In general the OD range should be between 0.3 and 0.6. For the Diels-Alderase ribozyme this is equivalent to ~ 10 µg of RNA. After addition of all components the solutions were degassed in an ultrasonic bath for 10 minutes. The samples were transferred into Teflon-stoppered quartz cuvettes and dependent on the attempted maximum temperature sealed with additional Teflon tape. All samples were overlaid with 2-3 mm silicon oil to prevent evaporation of the buffer.

As a buffers sodium cacodylate 25 mM (magnesium phosphate 25 mM or MOPS 25 mM) adjusted to a pH of 7.0 were used.

Melting curves were recorded at 260 nm with a Cary 100 Bio-UV7Vis Spectrometer (Varian, Darmstadt) and cuvettes (Cary UV MICRO CELL 0.9 mL, Varian, Darmstadt (cuvettes produced by Starna) with a path length of 10 mm. UV absorption was recorded as a function of the temperature. First the samples were heated with a heating rate of 5°C/min and kept at maximum and minimum temperature for 5 minutes to ensure proper folding with the present cations. For the analysis the RNA samples were then heated at a rate of 0.5°C/min from 15-95°C (or 15-65°C) and absorbance readings were collected every 0.1°C. The data for denaturation (15-95°C) were collected as well as the data for renaturation (95-15°C). This

process was repeated twice. If no degradation of the oligonucleotides takes place the first and second recording can exactly be overlaid.

The data was analyzed with MS Excel according to the following procedure

- I. The ordinate scales of the curves were normalized to concentrations of 1 A260 unit at 15°C.
- II. The normalized absorbance data was smoothed using the moving average over 10 data points.
- III. First derivative of the absorbance *versus* temperature data (dA/dT) were obtained and T_m was determined as the maximum of the first derivative.

During the entire measurement the sample changer was purged with nitrogen gas to avoid water condensation in the machine or on the cuvettes.

Optical density (OD) = $\log_{10} (I_i / I_t)$ where I_i = Intensity of incident light, I_t = Intensity of transmitted light. One OD unit (ODU) (sometimes also called AU (absorption unit)) is defined as the amount of sample that gives an UV absorbance at 260 nm of 1, if the sample is dissolved in 1 mL volume and measured in a cuvette with a path length of 1 cm.

6.1.11 Automated solid-phase synthesis of oligonucleotides

Solid phase DNA and RNA synthesis was performed on an Expedite 8909 automated synthesizer by Applied Biosystems. The synthesis was performed using standard phosphoramidite chemistry.^[237, 238]

As a solid support dC CPG (*t*-butylphenoxyacetyl, TAC controlled pore glass) (40 $\mu\text{mol/g}$, 500 Å) and β -cyanoethyl-phosphoramidites containing base-labile TAC-protecting groups were purchased from Proligo. For modification at the 5'-end modified polyenglykol- β -cyanoethylphosphoramidites were prepared (see synthetic procedures).

The 2'-hydroxyl group was protected as a *t*-butyldimethylsilylether. Standard reagents employed in DNA solid-phase synthesis (deblocking reagent - dichloroacetic acid in DCM, activator - dicyanoimidazole, oxidizing reagent - iodine in THF/H₂O, and capping reagent *t*-butyl-phenoxyacetanhydride in acetonitrile), as well as acetonitrile (water content ≤ 10 ppm) were purchased from Proligo and Sigma Aldrich Fine Chemicals.

Solid-phase synthesis of ODNs was performed on 1 μmol scale synthesis, usually leaving the terminal 4,4'-dimethoxytrityl (DMT) group on. The phosphoramidites were used prepared as 0.067 M (DNA monomers), and 0.1 M (RNA monomer) acetonitrile solutions over activated molecular sieve. The standard protocols provided by Applied Biosystems were optimized to reduce the consumption of the amidites and reduce the time for the coupling.

The Oligonucleotides were cleaved of the solid support by incubation in ammonia at 55°C over night. The solid support was washed with EtOH (3x500 μL), the combined aqueous and ethanol containing solution was extracted with chloroform (3x1 mL) and evaporated on the lyophilizer. Oligonucleotides were dissolved in 1 mL Millipore water and the modification rate was determined by integration of the HPLC spectra. For purification the oligonucleotides were filtered through a 0.22 μm membrane filter, purified by preparative HPLC, collected, lyophilized and diluted again in water. The integrity of the oligonucleotides was determined by analytical HPLC and mass spectrometry.

Table 17: Protocol for 1 μ mol scale solid-phase DNA/ RNA synthesis (Adenosine (dA/ rA) cycle).^[a]

step	Function	mode ^[b]	amount [puls]	time [s]	description
Deblocking	144 /*Index Fract. Coll	NA	1	0	"Event out ON"
	0 /*Default	WAIT	0	1.5	"Wait"
	38 /*Diverted Wsh A	PULSE	15	0	"Flush system with Wsh A"
	141 /*Trityl Mon. On/Off	NA	1	1	"START data collection"
	16 /*Dblk	PULSE	20	0	"Dblk to column"
	0 /*Default	WAIT	0	20	"Default"
	16 /*Dblk	PULSE	40	40	"Deblock"
	38 /*Diverted Wsh A	PULSE	60	0	"Flush system with Wsh A"
	141 /*Trityl Mon. On/Off	NA	0	1	"STOP data collection"
	38 /*Diverted Wsh A	PULSE	20	0	"Flush system with Wsh A"
	144 /*Index Fract. Coll.	NA	2	0	"Event out OFF"
Coupling	1 /*Wsh	PULSE	8	0	"Flush system with Wsh A"
	2 /*Act	PULSE	5	0	" Flush system with Act"
	19 /*C + Act	PULSE	5	0	"Monomer + Act to column"
	19 /*C + Act	PULSE	3	24	"Couple monomer"
	2 /*Act	PULSE	3	24	"Couple monomer"
	19 /*C + Act	PULSE	2	16	"Couple monomer"
	2 /*Act	PULSE	3	24	"Couple monomer"
	0 /*Default	WAIT	0	20	"Default"
	1 /*Wsh	PULSE	7	56	"Couple monomer"
	1 /*Wsh	PULSE	21	0	"Flush system with Wsh A"
Capping	12 /*Wsh A	PULSE	20	0	"Flush system with Wsh A"
	13 /*Caps	PULSE	8	0	"Caps to column"
	12 /*Wsh A	PULSE	9	23	"Cap"
	12 /*Wsh A	PULSE	21	0	"Flush system with Wsh A"
Oxidizing	15 /*Ox	PULSE	35	0	"Ox to column"
	0 /*Default	WAIT	0	20	"Default"
	12 /*Wsh A	PULSE	60	0	"Flush system with Wsh A"
Capping	13 /*Caps	PULSE	7	0	"Caps to column"
	12 /*Wsh A	PULSE	45	0	"End of cycle Wash"

^[a] Deblocking reagent = dblk, acetonitrile = Wsh, WshA, activator = Act, capping reagents = Caps, oxidizer = Ox.

^[b] 1 PULSE = 16 μ L.

6.1.12 High-performance liquid chromatography of oligonucleotides

HPLC analyses were performed on an Agilent 1100 Series HPLC system equipped with an diode array detector using a Phenomenex® Luna 5 μ m C18 column (4.6 \times 250 mm) and eluting with a gradient of buffer A and buffer B at 1 mL/min flow-rate. Preparative HPLC was performed using Phenomenex® Luna 5 μ m C18 column (15.0 \times 250 mm) and eluting with a gradient of buffer A and buffer B at 5 mL/min flow-rate.

The following gradient was used:

Gradient O1:

Time [min]	Buffer B [%]
0	10
10	10
30	30
45	100
50	100

Gradient O2:

Time [min]	Buffer B [%]
0	0
15	30
30	100
35	100
40	0

6.1.13 Mass spectrometry of oligonucleotides**Sample preparation**

Oligonucleotides were either dissolved in 10 μ M water or in 0.1 M TEAA pH 7.0 to a final concentration of 10 μ M (100 pmol) and desalted using Millipore C₁₈ ZipTips. The C₁₈ resin was first wetted by using 50% aqueous acetonitrile solution (2 x 10 μ L) and then equilibrated with 0.1 M TEAA pH 7.0 (3 x 10 μ L). The oligonucleotide was bound to the resin letting the entire 10 μ L sample solution pass through the resin in the filter tip (10 x). The salts were removed by washing the resin first with water (3 x 10 μ L) and 0.1 M TEAA pH 7.0 (3 x 10 μ L). A clean vial with 4 μ L of 50% acetonitrile/water was used to elute the oligonucleotides by aspirating and dispensing the solution (5-10 x).

MALDI TOF mass analysis

The samples for analysis were prepared using the dried droplet method with the following matrix solutions: **1)** 6-aza-2-thiothymine/ diammonium hydrogen citrate in 1:2 v/v water/ acetonitrile (detection in negative mode); **2)** 3-hydroxy-picolinic acid/ diammonium hydrogen citrate in 2:1 v/v water/ acetonitrile (detection in positive mode).

HR-ESI MS analysis

HR-ESI mass spectra were recorded in the negative mode on a Bruker MicroTOF-QII. The samples were diluted 1:5 in 25mM piperidine/ imidazole (25% Water / 75% ACN). The oligonucleotide solutions were introduced into the ion source with a syringe pump at flow rates of 3 to 4 μ L/min. For each measurement, up to 128 scans were averaged to improve the

signal-to-noise ratio. Data processing was performed using the software DataAnalysis 4.0 SP1.

6.1.14 Fluorescent dyes

All dyes have been purchased from Invitrogen Life Technologies (Carlsbad, California, USA), Atto-Tec (Siegen, Germany) or Dyomics (Jena, Germany). DY 649 Hydrazide maleimide has been synthesized from the commercially available Dyomics DY 649 NHS ester and maleimido caproic acid hydrazide, after HPLC purification a stock solution was prepared in EtOH and stored at -20°C. Commercially available dyes have been used without further purification. All dyes were diluted in DMSO and the stock solution was always stored at -20°C in their original vial but protected from light with aluminium or optically opaque boxes. Dilutions were always stored in dark brown reaction vials. For iodoacetamides DMSO should be avoided, because iodoacetamides might get oxidized in DMSO. Therefore the Atto 590 iodoacetamide stock solution was dissolved in anhydrous DMF.

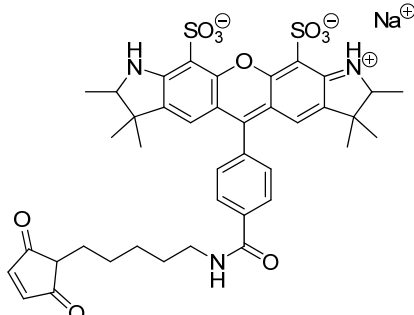
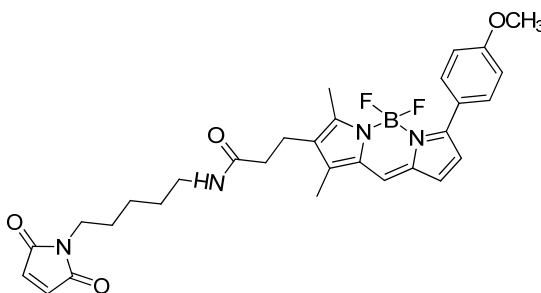
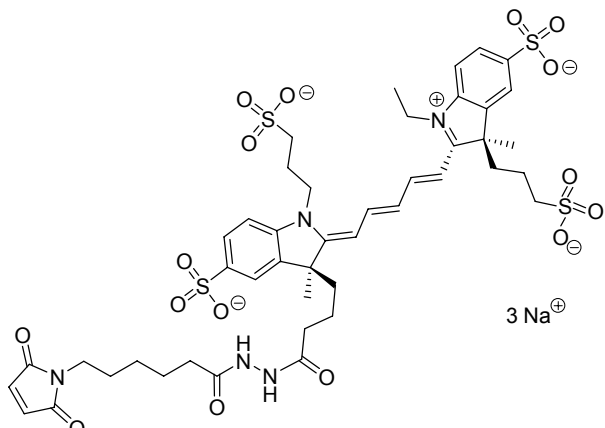
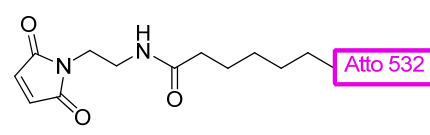
BODIPY TMR C₅-maleimide and Atto 532 maleimide are poorly soluble in water, while Atto 590 iodoacetamide is absolutely insoluble in water or any type of buffer. Alexa Fluor® 532 C₅-maleimide and all applied Dyomics dyes are extremely well soluble in water respectively aqueous buffer systems.

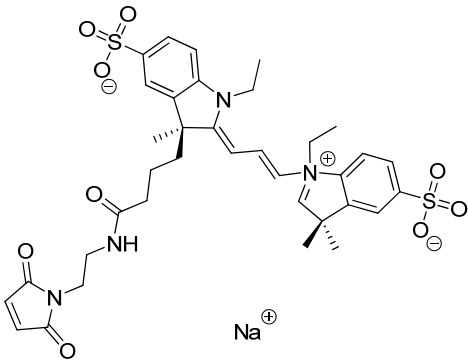
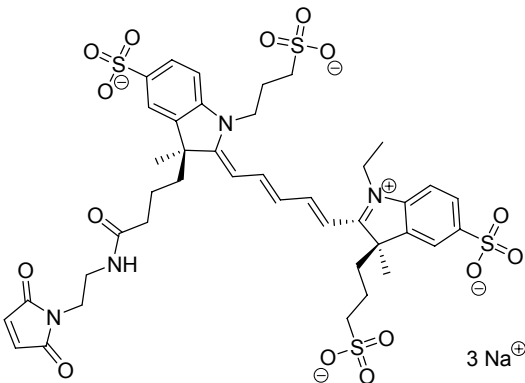
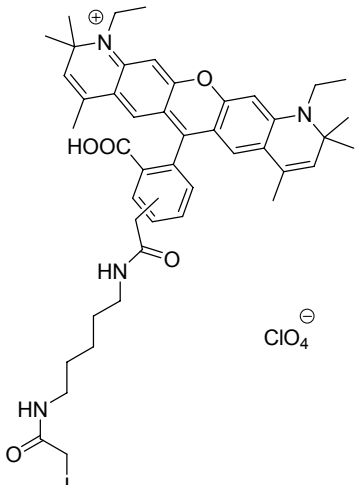
Absorption and emission maxima were determined in either ethanol or methanol and are consistent with the data provided by the supplier. Concentrations were determined by the dilution in a defined volume and validated *via* dilution in ethanol and UV-measurement. The concentrations were then calculated *via* the Lambert-Beer law

$$A = \epsilon cd$$

A: absorption; c: concentration; d: thickness of the measuring cell; ϵ : extinction coefficient.

Table 18: Data of all fluorescent dyes.

Name	Structure	λ_{abs} [nm]	λ_{em} [nm]	ϵ [M ⁻¹ cm ⁻¹]	FW [g mol ⁻¹]
invitrogen Alexa Fluor® 532 C ₅ - maleimide		528	552	78000	812.88 found: 791.18
invitrogen BODIPY® TMR C ₅ -maleimide		544	570	60000	562.42
Dy-649 hydrazide maleimide		653	676	250000	1049.20 found 1049.25
ATTO-TEC Atto 532 maleimide	Exact structure not revealed due to a pending patent. 	532	553	115000	1063 found 768.14

Name	Structure	λ_{abs} [nm]	λ_{em} [nm]	ϵ [M ⁻¹ cm ⁻¹]	FW [g mol ⁻¹]
Dyomics Dy-547 maleimide		557	574	150000	761.23
Dyomics Dy-649 maleimide		653	676	250000	1032.16
ATTO-TEC Atto 590 iodoacetamide		594	624	120000	970 found 857.25

6.1.15 Fluorescent labeling reactions of oligonucleotides

All labeling reactions were performed in Eppendorf tubes. Before starting the reaction the solution was vortexed and started by the addition of the respective dye and incubated on a thermo shaker at 650 rpm. The excess of dye was removed with DyeEx™ (Qiagen) according to the provided protocol. If the reactions were not directly purified by DyeEx the reaction was stopped by the addition of stop-mix. All reactions were analyzed on an 18% PAGE, using a loading buffer without xylencyanol to lower the fluorescent background signal. The gels were analyzed by scanning for autoradiography and fluorescence at the corresponding wavelength and subsequently stained with SYBR Gold and scanned again. Data was processed with ImageQuant or ImageJ.

Labeling protocol in the dipartite Diels-Alderase assay

For the Diels-Alder reaction catalyzed *in cis* the 38mer and the 11mer RNA anthracene-conjugate were hybridized in a ratio of 1:2. The strands were heated at 65°C in buffer without MgCl₂ for 2 min, MgCl₂ was added and slowly cooled to r.t. to ensure hybridization and folding of the two strands. The reaction was incubated at 25°C for 30 min.

Table 19: Protocol for fluorescent labeling of oligonucleotides *via* the dipartite Diels-Alderase assay.

Chemicals	Volume [μ L]	Final
Diels-Alder buffer (5 x)	2.0	1 x
38mer (2.5 μ M)	0.8	0.2 μ M
11mer AHEG (1 μ M)	1.0	0.1 μ M
11mer AHEG α^{32} -pCp labeled	1.0	doped
Dye (500 μ M)	1.0	50 μ M
MgCl ₂ (800 mM)	1.0	80 mM
H ₂ O	3.2	
Σ	10	

Labeling protocol monopartite Diels-Alderase assay

For the catalyzed Diels-Alder reaction *in trans* the Diels-Alderase ribozyme was heated at 65°C in buffer without MgCl₂ for 2 min, MgCl₂ was added and slowly cooled to r.t.. The reaction was incubated at 25°C for 30 min up to 2 h.

Table 20: Protocol for fluorescent labeling of oligonucleotides *via* monopartite Diels-Alderase assay.

Chemicals	Volume [μ L]	Final
Diels-Alder buffer (5 x)	4.0	1 x
ODN (100 μ M)	10.0	50 μ M
Diels-Alderase (70 μ M)	2.0	7 μ M
Dye (2 mM)	0.5	50 μ M
MgCl ₂ (800 mM)	2.0	80 mM
H ₂ O	1.5	
Σ	20	

Labeling of thiol modified oligonucleotides with maleimide dyes or iodoacetamide dyes

Thiol modified oligonucleotides have to be treated with a reduction reagent beforehand the actual labeling reaction. The reaction mixture was incubated with TCEP for 30 min to 1 h at 25°C and 650 rpm on a thermo shaker. After addition of the dye the reaction was incubated at 25°C for 2 h or at 4°C over night.

Atto 580 iodoacetamide is insoluble in water and therefore 20% EtOH had to be added during the reaction.

Table 21: Protocol for fluorescent labeling of thiolated oligonucleotides.

Chemicals	Volume [μ L]	Final
Tris buffer pH 7.2 (5x) or Diels-Alder buffer (5x)	4.0	1 x
ODN (100 μ M)	10.0	50 μ M
TECP (2 mM)	1.0	100 μ M
Dye (20 mM)	1.0	1 mM
H ₂ O	4.0	
Σ	20	

Bioorthogonal bi-functionalization of oligonucleotides with two fluorescent dyes

The oligonucleotide was incubated with TCEP for 30 min to 1 h at 25°C and 650 rpm on a thermo shaker. After addition of the iodoacetamide dye the reaction was incubated at 25°C for 2 h or at 4°C over night. Due to the insolubility of the iodoacetamide dye EtOH was added but evaporated before Diels-Alderase ribozyme catalyzed labeling with the maleimide dye.

Table 22: Protocol for the bis-functionalization of oligonucleotides with two different fluorescent dyes.

Chemicals	Volume [μL]	Final
Tris buffer pH 7.2 (5x) or Diels-Alder buffer (5x)	4.0	1 x
ODN (100 μ M)	10.0	50 μ M
TECP (2 mM)	1.0	100 μ M
Iodoacetamide dye (20 mM)	1.0	1 mM
Maleimide dye (2 mM)	0.5	50 μ M
Diels-Alderase (140 μ M)	1.0	7 μ M
MgCl ₂ (800 mM)	2.0	80 mM
H ₂ O	0.5	
Σ	20	

6.2 Synthetic procedures

6.2.1 General

All reagents were purchased from Sigma-Aldrich, Acros, AlfaAesar, ABCR and AppliChem and were, unless indicated otherwise, used without further purification.

Acid free dichloromethane was obtained by storing the solvent on K_2CO_3 for at least one night. Reactions with air-sensitive compounds were performed under argon atmosphere using standard Schlenk techniques.

TLC was carried out on silica gel plates Polygram Sil G/UV₂₅₄ (40 × 80 mm) from Macherey-Nagel, Düren. Compounds were made visible by using UV light at 254 nm, or staining reagents **a**) blue shift (0.1 g $Ce(SO_4)$, 2.1 g phosphomolybdic acid, 50 mL H_2O , 3.1 mL conc. H_2SO_4), **b**) Potassium Permanganate (1 g $KMnO_4$, 2.5 g K_2CO_3 in 50 mL H_2O), **c**) DNPH (1 g 1-(2,4-dinitrophenyl)hydrazine, 25 mL ethanol, 8 mL H_2O , 5 mL conc. H_2SO_4) **d**) ninhydrin (15 g ninhydrin, 0.15 mL acetic acid, 50 mL ethanol), **e**) vanillin (3 g vanillin, 0.75 mL conc. H_2SO_4 , 50 mL ethanol).

Flash chromatography was carried out on silica gel 40-63 μm from J.T. Baker. Preparative reverse phase column chromatography was carried out on LiChroprep RP – 18 (40–63 μm) columns using a mechanical pump. Alternatively an IntelliFlash 310 chromatography system from Varian, Darmstadt was used with columns from Varian: SuperFlash C18, 18% carbon, end capped on 50 μm particles,

NMR spectra were recorded on a Varian Mercury Plus 300 MHz spectrometer. 1H and $^{13}C\{^1H\}$ NMR spectra were calibrated to TMS on the basis of the relative chemical shift of the solvent as an internal standard. $^{31}P\{^1H\}$ NMR spectra were calibrated to an external standard (85% H_3PO_4). Abbreviations used are as follows: s = singlet, d = doublet, t = triplet, m = multiplet.

Infrared spectroscopy was carried out a Bruker EQUINOX 55, the absorption is measured in cm^{-1} and the intensities indicated as follows: s = strong, m = medium, b = broad.

FAB and EI mass spectra were recorded on a JEOL JMS-700 sector field mass spectrometer.

MALDI-TOF mass spectra were recorded on a Bruker BIFLEX III spectrometer.

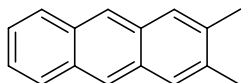
HR-ESI mass spectra were recorded on a Bruker MicroTOF-Q II spectrometer.

Melting points, if determined, were measured on a Reichert Jung Model No. 561C-H1.

6.3 Synthetic procedures for compounds of chapter 2

6.3.1 Synthetic procedures of the initiator nucleotides

2,3-Dimethylantracene (9)



2,3-Dimethyl-9,10-anthraquinone (502 mg, 2.12 mmol) was suspended in 7 mL H₂O and 10 mL 25% NH₃ (aq.) in an 150 mL autoclave. The suspension was cooled down in an ice/water bath and granular zinc (4.0 g, 61.2 mmol, 28.9 eq.) was added slowly. The autoclave was closed and the reaction was slowly allowed to warm up and later heated at 75°C for 23 h. The reaction was followed by TLC, turning from yellow to red and was then diluted with DCM (50 mL) and water (50 mL). The organic layer was decanted from the solid zinc. The aqueous layer was extracted with DCM (2 x 30 mL) and the combined organic layers were dried over MgSO₄. The solvent was removed under reduced pressure to yield a yellow solid. The product was diluted in isopropanol (20 mL), conc. HCl (2.0 mL) was added and heated at 95°C for 4 h. The reaction mixture was cooled to r.t. and stored at -20°C to crystallize the crude product. The product was purified by column chromatography (Hex : EtOAc 98 : 2, R_f = 0.37) on silica and again recrystallized from *n*-hexane to afford a yellow solid (120.3 mg, 28%).

C₁₆H₁₄ (206.28 g mol⁻¹).

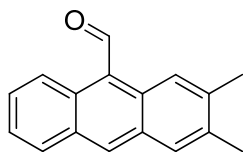
m.p. 202-210 °C.

¹H NMR (300 MHz, CDCl₃, 295 K): δ = 8.28 (s, 2H, Ar-H), 7.96 (dd, 2H, *J*(H,H) = 3.17 Hz, *J*(H,H) = 3.39 Hz, Ar-H), 7.65 (s, 2H, Ar-H), 7.37 (dd, 2H, *J*(H,H), 3.29 *J*(H,H) = 3.20 Hz, Ar-H), 2.29 (s, 6H, CH₃).

¹³C{¹H} NMR (75 MHz, CDCl₃, 295 K): δ = 135.55 (2C, Ar-CH₃), 131.33 (2C, Ar-H), 131.13 (2C, Ar-H), 128.06 (2C, Ar-C), 126.91 (2C, Ar-C), 124.76 (4C, Ar-H), 20.42 (2C, CH₃).

IR (KBr): (= 2932 (s), 1629 (s), 1456 (s), 899 (s).

MS (FAB) m/z (rel. Int. %): 207 (M+1) (5), 206 (15), 154 (100), 138 (30), 136 (74), 120 (12), 107 (26), 102 (22), 89 (24), 77 (26).

2,3-dimethylantracene-9-carbaldehyde (10)

In a Schlenk flask under argon were dissolved 2,3-dimethylantracene **9** (488.5 mg, 2.7 mmol) in 10 mL dry DMF. The solution was cooled to 0°C with an ice/water bath, and phosphorus(V) oxychloride (2.2 mL, 23.4 mmol) added dropwise to give a yellow suspension. The reaction mixture was allowed to warm up and heated at 95°C for 20 h. The mixture was basified by the addition of NH₃ (aq.) and DCM was added (400 mL). The aqueous layer was extracted with DCM (2 x 30 mL) and the organic layer was washed with brine (2 x 30 mL) and H₂O (2 x 50 mL). The organic extracts were combined, dried over MgSO₄ and the solvent was removed under reduced pressure. The crude product was purified by column chromatography (DCM : Hex 9 : 1, R_f = 0.55) over silica gel to afford a yellow solid 513.7 mg (93%).

C₁₇H₁₄O (234.29 g mol⁻¹).

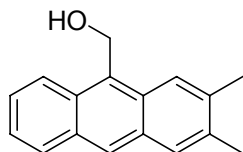
m.p. 116-117 °C.

¹H NMR (300 MHz, CDCl₃, 295 K): δ = 11.50 (s, 1H, COH), 8.98 (dd, 1H, *J*(H,H) = 0.9 Hz, *J*(H,H) = 9.0 Hz, Ar-H), 8.79 (s, 1H, Ar-H), 8.57 (s, 1H, Ar-H), 8.03 (dt, 1H, *J*(H,H) = 0.7 Hz, *J*(H,H) = 8.4 Hz, Ar-H), 7.80 (d, 1H, *J*(H,H) = 0.5 Hz, Ar-H), 7.64 (dt, 1H, *J*(H,H) = 1.5 Hz, *J*(H,H) = 7.8 Hz, Ar-H), 7.51 (dt, 1H, *J*(H,H) = 1.1 Hz, *J*(H,H) = 6.6 Hz, Ar-H), 2.54 (d, 3H, *J*(H,H) = 0.7 Hz, CH₃), 2.49 (d, 3H, *J*(H,H) = 0.9 Hz, CH₃).

¹³C{¹H} NMR (75 MHz, CDCl₃, 295 K): δ = 193.01 (1C, CHO), 140.18 (2C, Ar-H), 134.07 (1C, Ar-C), 131.92 (1C, Ar-CH₃), 131.71 (1C, Ar-CH₃), 130.68 (1C, Ar-C), 129.21 (1C, Ar-COH), 128.62 (1C, Ar-C), 128.01 (1C, Ar-H), 125.17 (2C, Ar-H), 123.42 (2C, Ar-H), 122.51 (1C, Ar-H), 21.25 (1C, CH₃), 20.13 (1C, CH₃).

IR (KBr): (= 2911 (s), 1675 (m), 1552 (s), 1450 (s), 1384 (s), 1257 (s).

MS (FAB) *m/z* (rel. Int. %): 235, 1 (M+1) (27), 234 (26), 167 (14), 154 (100), 149 (55), 136 (71), 107 (25), 89 (24), 71 (26), 57 (42).

(2,3-dimethylanthracen-9-yl)methanol (11)

Sodium borohydride (105 mg, 2.76 mmol, 1.25 eq.) were added to a solution of the 2,3-dimethylanthracene-9-carbaldehyde **10** (513,7 mg, 2,19 mmol) in 30 mL abs. THF and stirred overnight at room temperature. The solution was filtered to remove the excess of sodium borohydride and the solvent was removed under reduced pressure. The crude product was purified by dissolving it in DCM and recrystallizing the impurities by adding ice cold *n*-hexane. The impurities could be removed by filtration to afford a yellow solid 472.8 mg (92%).

$C_{17}H_{16}O$ (236.32 g mol⁻¹)

m.p. 158-159 °C.

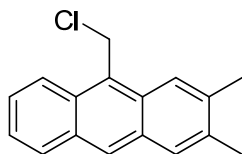
R_f: 0.30 (CH₂Cl₂).

¹H-NMR (300 MHz, CDCl₃, 295 K): δ = 8.36 (dd, 1H, J (H,H) = 0.8 Hz, J (H,H) = 8.70 Hz, Ar-H), 8.32 (s, 1H, Ar-H), 8.14 (s, 1H, Ar-H), 7.98 (dt, 1H, J (H,H) = 8.8 Hz, J (H,H) = 0.7 Hz, Ar-H), 7.76 (s, 1H, Ar-H), 7.52 (dt, 1H, J (H,H) = 1.4 Hz, J (H,H) = 7.6 Hz, Ar-H), 7.44 (dt, 1H, J (H,H) = 1.2 Hz, J (H,H) = 7.4 Hz, Ar-H), 5.63 (d, 2H, J (H,H) = 5.6 Hz, CH₂), 2.52 (d, 3H, J (H,H) = 3.8 Hz, CH₃), 2.48 (d, 3H, J (H,H) = 0.8 Hz, CH₃), 1.73 (t, 1H, J (H,H) = 5.6 Hz, OH).

¹³C{¹H} NMR (75 MHz, CDCl₃, 295 K): δ = 136.79 (1C, Ar-CH₂), 135.28 (1C, Ar-C), 131.01 (2C, Ar-CH₃), 129.64 (2C, Ar-C), 129.60 (1C, Ar-C), 129.03 (1C, Ar-H), 127.87 (1C, Ar-H), 126.95 (1C, Ar-H), 125.91 (1C, Ar-H), 124.52 (1C, Ar-H), 123.69 (1C, Ar-H), 122.75 (1C, Ar-H), 57.45 (1C, CH₂), 20.98 (1C, CH₃), 20.16 (1C, CH₃).

IR (KBr): ν = 3400 (b), 2912 (s), 1630 (b), 1451 (b), 1039 (s), 985 (s).

MS (FAB) *m/z* (rel. Int. %): 237,1 (M+1) (11), 236 (34), 219 (26), 181 (22), 165 (28), 154 (100), 137 (53), 136 (70), 107 (26), 89 (26), 77 (29), 57 (23).

9-(Chloromethyl)-2,3-dimethlanthracen (12b)

To (2,3-dimethylantracen-9-yl)methanol **11** (472.8 mg, 2.0 mmol) was added 20 mL abs. toluene and to the resulting suspension thionyl chloride (0.19 mL, 2.5 mmol, 1.25 eq.) dropwise. The reaction was heated to 90°C for 20 h. The solvent was removed under reduced pressure to yield a brown solid 471.0 mg (93%). The product could be used for synthesis without further purification.

C₁₇H₁₅Cl (254.75 g mol⁻¹)

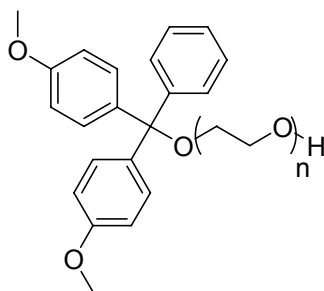
R_f: 0 – 0.7 (CH₂Cl₂).

¹H-NMR (300 MHz, CDCl₃, 295 K): δ = 8.36 (s, 1H, Ar-H), 8.28 (dd, 1H, *J* (H,H) = 0.9 Hz, *J* (H,H) = 8.9 Hz, Ar-H), 8.04 (s, 1H, Ar-H), 7.99 (d, 1H, *J* (H,H) = 8.4 Hz, Ar-H), 7.77 (s, 1H, Ar-H), 7.57 (dt, 1H, *J* (H,H) = 1.4 Hz, *J* (H,H) = 7.7 Hz, Ar-H), 7.46 (dt, 1H, *J* (H,H) = 1.1 Hz, *J* (H,H) = 7.5 Hz, Ar-H), 5.60 (s, 2H, CH₂), 2.55 (s, 3H, CH₃), 2.48 (s, 3H, CH₃).

¹³C{¹H} NMR (75 MHz, CDCl₃, 295 K): δ = 137.40 (1C, Ar-CH₂), 135.45 (1C, Ar-C), 131.10 (1C, Ar-CH₃), 130.93 (1C, Ar-CH₃), 129.69 (1C, Ar-C), 129.19 (1C, Ar-C), 129.02 (1C, Ar-C), 128.04 (1C, Ar-H), 127.86 (1C, Ar-H), 126.36 (1C, Ar-H), 126.24 (1C, Ar-H), 124.67 (1C, Ar-H), 123.29 (1C, Ar-H), 122.34 (1C, Ar-H), 39.27 (1C, CH₂), 21.12 (1C, CH₃), 20.15 (1C, CH₃).

MS (EI) *m/z* (rel. Int. %): 254 (M) (30), 219 (100), 202 (13), 189 (7), 178 (4).

IR (KBr): ν = 2916 (s), 1447 (s), 1244 (s), 1025 (s).

(4,4'-Dimethoxytrityl)-polyethylene glycol (13)

PEG 600 (8.93 mL, 16.7 mmol) was dried by coevaporation with toluene (3 x 25 mL) and suspended in acid free DCM (stored over K_2CO_3). TEA (0.86 mL, 6.18 mmol, 0.37 eq.) and 4-dimethylaminopyridine (DMAP) (20 mg, 0.17 mmol, 0.01 eq.) were added. A solution of 4,4'-dimethoxytriphenylmethylchloride (454 mg, 1.34 mmol, 0.08 eq.) in 13 mL acid free DCM was slowly added by a syringe pump over 5 hours 10 min at r.t.. The solution was then diluted with DCM and washed with 5% NaHCO_3 (50 mL), water (50 mL), and brine (50 mL), dried over Na_2SO_4 and the solvent removed under reduced pressure. The crude PEG protected PEG was purified by column chromatography (EtOAc : EtOH 9 : 1, preconditioned with the eluent containing 1% Et_3N , $R_f = 0-0.2$) on silica to afford a yellow oil (893.7 mg, 75%).

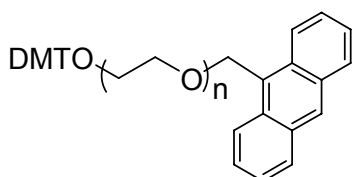
$^1\text{H-NMR}$ (300 MHz, $(\text{CD}_3)_2\text{CO}$, 295 K): $\delta = 7.51-6.6$ (m, 13H, Ar-H), 5.62 (s, 1H, OH), 3.79 (s, 6H, CH_3), 3.76-3.52 (m, CH_2).

$^{13}\text{C}\{^1\text{H}\}$ NMR (75 MHz, $(\text{CD}_3)_2\text{CO}$, 295 K): $\delta = 160.51$ (2C, Ar-O CH_3), 147.40 (1C, Ar-C), 138.18 (2C, Ar-C), 131.91 (4C, Ar-H), 130.02 (2C, Ar-H), 129.50 (2C, Ar-H), 128.41 (1C, Ar-H), 114.81 (4C, Ar-H), 87.60 (1C, Ar $_3$ CO), 74.54 (1C, CH_2OH), 65.11 (CH_2), 65.11 (3C, CH_3), 63.00 (3C, CH_3).

MALDI MS: m/z 915 $[\text{M}+\text{Na}]^+$ (calculated for $[\text{C}_{47}\text{H}_{72}\text{O}_{16}+\text{Na}]^+$ 915.47), m/z 931 $[\text{M}+\text{K}]^+$ (calculated for $[\text{C}_{47}\text{H}_{72}\text{O}_{16}+\text{K}]^+$ 931.45).

n	Calculated [M+Na] ⁺	Found [M+Na] ⁺	Calculated [M+K] ⁺	Found [M+K] ⁺	Formula
8	695.34	695.2	711.31	-	C ₃₇ H ₅₂ O ₁₁
9	739.37	739.2	755.34	-	C ₃₉ H ₅₆ O ₁₂
10	783.39	783.3	799.37	799.2	C ₄₁ H ₆₀ O ₁₃
11	827.42	827.3	843.39	843.2	C ₄₃ H ₆₄ O ₁₄
12	871.45	871.2	887.42	887.2	C ₄₅ H ₆₈ O ₁₅
13	915.47	915.3	931.45	931.2	C ₄₇ H ₇₂ O ₁₆
14	959.50	959.3	975.47	975.2	C ₄₉ H ₇₆ O ₁₇
15	1003.52	1003.3	1019.50	1019.2	C ₅₁ H ₈₀ O ₁₈
16	1048.55	1047.3	1063.52	-	C ₅₃ H ₈₄ O ₁₉
17	1091.58	1091.3	1107.55	-	C ₅₅ H ₈₈ O ₂₀
18	1135.60	1135.3	1151.58	-	C ₅₇ H ₉₂ O ₂₁

(Anthracen-9-yl-methoxy)-polyethylene glycol-DMT (15a)



General procedure I

The DMT-protected polyethylene glycol **13** (1.3 g, 1.46 mmol) was dried by coevaporation with toluene (3x25 mL) and dissolved in 8 mL dry ACN under argon. Sodium hydride (93 mg 60% in oil, 2.33 mmol, 1.6 equiv.) was added. The reaction mixture was stirred for 5 min at r.t. before the addition of 9-(chloromethyl)anthracene (362 mg, 1.6 mmol, 1.1 equiv.) and NaI (262 mg, 1.75 mmol, 1.2 equiv.). The reaction mixture was stirred for another 40 min at 40°C. The reaction was closely followed by TLC. The reaction mixture was quenched with 9 mL of water and extracted with EtOAc (80 mL) and additional water (40 mL). The organic layer was then washed with water (2 x 40 mL) and brine (2 x 40 mL), dried over Na₂SO₄ and the solvent removed under reduced pressure. The crude product was purified by column chromatography (gradient EtOAc : MeOH 98 : 2 to 8 : 2, column preconditioned with the eluent containing 1% Et₃N) over silica gel to afford a pale yellow oil (700 mg, 46%).

$R_f = 0.2$ (EtOAc : MeOH 98:2).

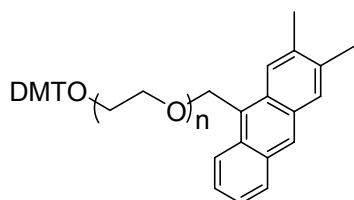
$^1\text{H NMR}$ (300 MHz, $(\text{CD}_3)_2\text{CO}$, 295 K): $\delta = 8.57$ (s, 1H, Ar-H), 8.52 (d, $J(\text{H,H}) = 8.4$ Hz, 2H, Ar-H), 8.09 (d, $J(\text{H,H}) = 8.4$ Hz, 2H, Ar-H), 7.60-7.48 (m, 6H, Ar-H), 7.36 (d, $J(\text{H,H}) = 9.0$ Hz, 5H, Ar-H), 7.30-7.23 (m, 2H, Ar-H), 6.88 (d, $J(\text{H,H}) = 8.7$ Hz, 4H, Ar-H), 5.56 (s, 2H, OCH_2Ar_A), 3.86 (t, $J(\text{H,H}) = 5.1$ Hz, 2H, PEG CH_2OCH_2), 3.77 (s, 6H, DMT- CH_3), 3.70-3.52 (m, PEG CH_2), 3.17 (**11**) (t, $J(\text{H,H}) = 5.1$ Hz, 2H, DMTO CH_2).

$^{13}\text{C}\{^1\text{H}\}$ NMR (75 MHz, $(\text{CD}_3)_2\text{CO}$, 295 K): $\delta = 160.51, 147.40, 138.18, 133.43-126.67, 114.81, 87.60, 72.24, 56.50$.

MALDI MS: m/z 1105.7 $[\text{M}+\text{Na}]^+$ (calculated for $[\text{C}_{62}\text{H}_{84}\text{O}_{16}+\text{Na}]^+$ 1105.58), m/z 1121.7 $[\text{M}+\text{K}]^+$ (calculated for $[\text{C}_{62}\text{H}_{84}\text{O}_{16}+\text{K}]^+$ 1121.69).

n	Calculated $[\text{M}+\text{Na}]^+$	Found $[\text{M}+\text{Na}]^+$	Calculated $[\text{M}+\text{K}]^+$	Found $[\text{M}+\text{K}]^+$	Formula
8	885.43	885.6	901.54	-	$\text{C}_{52}\text{H}_{62}\text{O}_{11}$
9	929.46	929.6	945.57	-	$\text{C}_{54}\text{H}_{66}\text{O}_{12}$
10	973.49	973.6	989.60	989.6	$\text{C}_{56}\text{H}_{70}\text{O}_{13}$
11	1017.52	1017.7	1033.63	1033.6	$\text{C}_{58}\text{H}_{74}\text{O}_{14}$
12	1061.55	1061.7	1077.66	1077.6	$\text{C}_{60}\text{H}_{80}\text{O}_{15}$
13	1105.58	1105.7	1121.69	1121.7	$\text{C}_{62}\text{H}_{84}\text{O}_{16}$
14	1149.61	1149.7	1165.72	1165.7	$\text{C}_{64}\text{H}_{88}\text{O}_{17}$
15	1193.64	1193.7	1209.75	1209.7	$\text{C}_{66}\text{H}_{92}\text{O}_{18}$
16	1237.67	1237.8	1253.78	1253.8	$\text{C}_{68}\text{H}_{96}\text{O}_{19}$
17	1281.7	1281.8	1297.81	1297.8	$\text{C}_{70}\text{H}_{100}\text{O}_{20}$
18	1325.73	1325.9	1341.84	-	$\text{C}_{72}\text{H}_{104}\text{O}_{21}$

2-((2,3-Dimethylantracen-9-yl)-methoxy)-polyethylene glycol-DMT (**15b**)



Product **15b** was prepared according to general procedure **I** from DMT-protected polyethylene glycol **13** (2.05 g, 2.30 mmol), 9-(chloromethyl)-2,3-dimethylantracene **12b** (645 mg, 2.53 mmol), sodium hydride (160.4 mg 60% in oil, 2.33 mmol, 1.6 equiv.) and NaI

(421.2 mg, 2.81 mmol). The crude product was purified by column chromatography (gradient EtOAc : MeOH 98 : 2 to 8 : 2, column preconditioned with the eluent containing 1% Et₃N) over silica gel to afford a yellow oil (1.83 g, 75%).

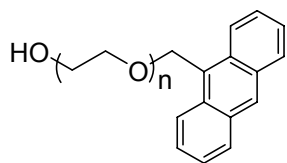
R_f = 0.2 (EtOAc : MeOH 98:2).

¹H NMR (300 MHz, (CD₃)₂CO, 295 K): δ = 8.57 (s, 1H, Ar-H), 8.52 (d, *J*(H,H) = 8.4 Hz, 2H, Ar-H), 8.09 (d, *J*(H,H) = 8.4 Hz, 2H, Ar-H), 7.60-7.48 (m, 6H, Ar-H), 7.36 (d, *J*(H,H) = 9.0 Hz, 5H, Ar-H), 7.30-7.23 (m, 2H, Ar-H), 6.88 (d, *J*(H,H) = 8.7 Hz, 4H, Ar-H), 5.56 (s, 2H, OCH₂Ar_A), 3.86 (t, *J*(H,H) = 5.1 Hz, 2H, PEG CH₂OCH₂), 3.77 (s, 6H, DMT-CH₃), 3.70-3.52 (m, PEG CH₂), 3.17 (11) (t, *J*(H,H) = 5.1 Hz, 2H, DMTOCH₂).

¹³C{¹H} NMR (75 MHz, (CD₃)₂CO, 295 K): δ = 160.51, 147.40, 138.18, 133.43-126.67, 114.81, 87.60, 72.24, 56.50.

MALDI MS: m/z 1105.7 [M+Na]⁺ (calculated for [C₆₂H₈₄O₁₆+Na]⁺ 1105.58), m/z 1121.7 [M+K]⁺ (calculated for [C₆₂H₈₄O₁₆+K]⁺ 1121.69).

n	Calculated [M+Na] ⁺	Found [M+Na] ⁺	Calculated [M+K] ⁺	Found [M+K] ⁺	Formula
8	913.45	913.4	929.42	-	C ₅₄ H ₆₆ O ₁₁
9	957.47	957.5	973.44	973.5	C ₅₆ H ₇₀ O ₁₂
10	1001.49	1001.5	1017.46	1017.5	C ₅₈ H ₇₄ O ₁₃
11	1045.51	1045.5	1061.48	1061.5	C ₆₀ H ₇₈ O ₁₄
12	1089.53	1089.5	1105.50	1105.5	C ₆₂ H ₈₂ O ₁₅
13	1133.55	1133.6	1149.52	1149.6	C ₆₄ H ₈₆ O ₁₆
14	1177.57	1177.6	1193.54	1193.6	C ₆₆ H ₉₀ O ₁₇
15	1221.59	1221.7	1237.56	1237.6	C ₆₈ H ₉₄ O ₁₈
16	1265.61	1265.7	1281.58	1281.6	C ₇₀ H ₉₈ O ₁₉
17	1309.63	1309.8	1325.60	1325.6	C ₇₂ H ₁₀₂ O ₂₀
18	1353.65	1354.8	1369.62	-	C ₇₄ H ₁₀₆ O ₂₁

(Anthracen-9-yl-methoxy)-polyethylene glycol (16a)**General procedure II**

1-(4,4'-Dimethoxytrityl) (9-anthracenemethoxy) polyethylene glycol **15a** (700 mg, 0.67 mmol) was dissolved in 16.8 mL solution of a 3% trifluoro acetic acid in dichloroethane at r.t. After 5 min stirring, the reaction mixture was quenched by pouring it in 25 mL NaHCO₃ and extracted with 30 mL of CH₂Cl₂. The organic layer was washed with 25 mL brine, dried over Na₂SO₄ and the solvent removed under reduced pressure. The crude product was purified by column chromatography (2 x 20, EtOAc : EtOH 9 : 1, R_f = 0-0.2) on silica gel to afford a pale yellow oil 380 mg (82%).

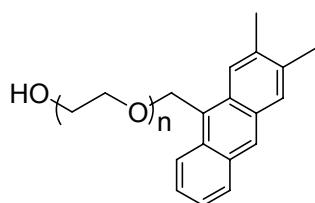
¹H NMR (300 MHz, (CD₃)₂CO, 295 K): δ = 8.56 (s, 1H, Ar-H), 8.52 (d, J(H,H) = 8.7 Hz, 2H, Ar-H), 8.09 (d, J(H,H) = 7.8 Hz, 2H, Ar-H), 7.61-7.49 (m, 4H, Ar-H), 5.57 (s, 2H, Ar-CH₂), 3.85 (t, J(H,H) = 4.8 Hz, 2H, PEG CH₂OH), 3.69 (t, J(H,H) = 5.1 Hz, 2H, PEG CH₂OCH₂), 3.60-3.52 (m, PEG CH₂), 2.81 (s, 1H, OH).

¹³C{¹H} NMR (75 MHz, (CD₃)₂CO, 295 K): δ = 133.42 (1C, Ar-H), 132.85 (1C, Ar-CH₂), 131.53 (1C, Ar-C), 130.68 (1C, Ar-H), 129.84 (1C, Ar-C), 127.89 (1C, Ar-H), 126.88 (1C, Ar-H), 126.67 (1C, Ar-H), 74.52 (Ar-CH₂), 72.22 (CH₂O PEG CH₂), 71.58 (PEG CH₂OH), 66.71 (PEG CH₂O CH₂).

MALDI MS: m/z 759.7 [M+Na]⁺ (calculated for [C₃₉H₆₀O₁₃+Na]⁺ 759.44), m/z 775.7 [M+K]⁺ (calculated for [C₃₉H₆₀O₁₃+K]⁺ 775.55).

n	Calculated [M+Na] ⁺	Found [M+Na] ⁺	Calculated [M+K] ⁺	Found [M+K] ⁺	Formula
8	583.32	583.5	599.43	-	C ₃₁ H ₄₄ O ₉
9	627.35	627.6	643.46	643.6	C ₃₃ H ₄₈ O ₁₀
10	671.38	671.6	687.49	687.6	C ₃₅ H ₅₂ O ₁₁
11	715.41	715.6	731.52	731.7	C ₃₇ H ₅₆ O ₁₂
12	759.44	759.7	775.55	775.7	C ₃₉ H ₆₀ O ₁₃
13	803.47	803.8	819.58	819.7	C ₄₁ H ₆₄ O ₁₄
14	847.50	847.8	863.61	863.8	C ₄₃ H ₆₈ O ₁₅
15	891.53	891.8	907.64	907.8	C ₄₅ H ₇₂ O ₁₆
16	935.56	935.8	951.67	-	C ₄₇ H ₇₆ O ₁₇

2-((2,3-Dimethylantracene-9-yl)-methoxy)-polyethylene glycol (16b)



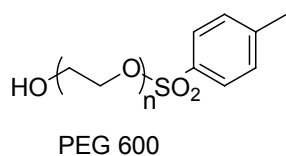
Product **16a** was prepared according to general procedure **II** from 2-((2,3-dimethylantracene-9-yl)-methoxy)-polyethylene glycol-DMT **15b** (1.83 g, 1.12 mmol) and 50 mL solution of a 3% trifluoro acetic acid in dichloroethane. The crude product was purified by column chromatography (gradient EtOAc : MeOH 100 : 0 to 98 : 2 to 8 : 2, preconditioned with the eluent containing 1% Et₃N) over silica gel to afford a yellow oil (719 mg, 84%).

¹H-NMR: (300 MHz, (CD₃)₂CO, 295 K): δ = 8.45 (d, 1H, *J* (H,H) = 8.4 Hz, Ar-H), 8.42 (s, 1H, Ar-H), 8.26 (s, 1H, Ar-H), 8.03 (dd, 1H, *J* (H,H) = 1.5 Hz, *J* (H,H) = 9.1 Hz, Ar-H), 7.82 (s, 1H, Ar-H), 7.55-7.30 (m, 2H, Ar-H), 5.53 (s, 2H, Ar-CH₂), 3.50-3.70 (m, PEG CH₂), 2.53 (s, 3H, CH₃), 2.47 (s, 3H, CH₃).

MALDI MS: *m/z* 655 [M+Na]⁺ (calculated for [C₃₅H₅₂O₁₀+Na]⁺ 655.35), *m/z* 671 [M+K]⁺ (calculated [C₃₅H₅₂O₁₀+K]⁺ 671.32).

n	Calculated [M+Na] ⁺	Found [M+Na] ⁺	Calculated [M+K] ⁺	Found [M+K] ⁺	Formula
8	611.33	-	627.30	-	C ₃₃ H ₄₈ O ₉
9	655.35	655.5	671.32	671.5	C ₃₅ H ₅₂ O ₁₀
10	699.37	699.5	715.34	715.5	C ₃₇ H ₅₆ O ₁₁
11	743.39	743.6	759.36	759.5	C ₃₉ H ₆₀ O ₁₂
12	787.41	787.6	803.38	803.6	C ₄₁ H ₆₄ O ₁₃
13	831.43	831.6	847.40	847.6	C ₄₁ H ₆₈ O ₁₄
14	875.45	875.6	891.42	891.6	C ₄₃ H ₇₂ O ₁₅
15	919.47	919.7	935.44	935.6	C ₄₅ H ₇₆ O ₁₆
16	963.49	963.7	979.46	979.7	C ₄₇ H ₈₀ O ₁₇
17	1007.51	1007.7	1023.48	1023.7	C ₄₉ H ₈₄ O ₁₈
18	1051.53	1051.7	1067.50	-	C ₅₁ H ₈₈ O ₁₉

Polyethylene glycol-*p*-toluenesulfonate PEG 600 (26c)



General procedure III

160 g PEG 600 (266.66 mmol, 10 eq.) was dried by coevaporation with toluene (3 x 25 mL) and dissolved in 50 mL dry DCM and DMAP (25.2 mg, 0.21 mmol, 0.05 eq.) and TEA (13.8 mL, 98.19 mmol, 0.37 eq.) were added. TsCl (5.1 g, 26.69 mmol) was dissolved in 200 mL dry DCM and added via a dropping funnel. The reaction was complete after 13.5 h. The solution was washed with 5% NaHCO₃ (3 x 200 mL), water (6 x 150 mL), and brine (3 x 300 mL), dried over Na₂SO₄ and the solvent removed under reduced pressure. The obtained yellow oil presented itself as pure product (13.9 g, 74%).

R_f: 0.15 (EtOH : MeOH 9 : 1).

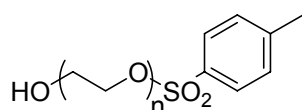
¹H NMR (300 MHz, (CD₃)₂CO, 295 K): δ = 7.82 (d, *J*(H,H) = 7.2 Hz, 2H, Ar-H), 7.49 (d, *J*(H,H) = 7.5 Hz, 2H, Ar-H), 4.18-3.57 (m, PEG CH₂), 2.79 (s, 1H, OH), 2.46 (s, 3H, CH₃).

¹³C{¹H} NMR (75 MHz, (CD₃)₂CO, 295 K): δ = 146.74 (1C, Ar-CH₃), 135.35 (1C, Ar-SO₂), 131.82 (2C, Ar-H), 129.72 (2C, Ar-H), 74.54-63.00 (PEG CH₂), 22.53 (1C, CH₃).

MALDI MS: m/z 723.4 $[M+Na]^+$ (calculated for $[C_{31}H_{56}O_{15}S]^+$ 723.37), m/z not observed for $[M+K]^+$ (calculated $[C_{31}H_{56}O_{15}S + Na]^+$ 739.48).

n	Calculated $[M+Na]^+$	Found $[M+Na]^+$	Formula
8	547.59	547.3	$C_{23}H_{40}O_{11}S$
9	591.64	591.3	$C_{25}H_{44}O_{12}S$
10	635.69	635.3	$C_{27}H_{48}O_{13}S$
11	679.74	679.4	$C_{29}H_{52}O_{14}S$
12	723.79	723.5	$C_{31}H_{56}O_{15}S$
13	767.84	767.5	$C_{33}H_{60}O_{16}S$
14	811.89	811.5	$C_{35}H_{64}O_{17}S$
15	855.94	855.6	$C_{37}H_{68}O_{18}S$
16	899.99	899.6	$C_{39}H_{72}O_{19}S$
17	944.04	943.6	$C_{41}H_{76}O_{20}S$
18	988.09	987.7	$C_{43}H_{80}O_{21}S$

Polyethylene glycol *p*-toluenesulfonate PEG 1500 (26d)



PEG 1500

Product **26d** was prepared according to general procedure **III** from PEG 1500 (100 g, 66.67 mmol, 10 eq.) dried by coevaporation (2 x 200 mL) in 95 mL dry DC, DMAP (6.3 mg, 0.052 mmol) and TEA (3.45 mL, 25 mmol). *p*-TsOCl (1.27 g, 6.67 mmol) in 18 mL dry DCM were added *via* a syringe pump over 7 h and 10 min and stirred over night. The reaction mixture was washed with 5% $NaHCO_3$ (3 x 50 mL), H_2O (6 x 250 mL) and brine (3 x 250 mL), dried over Na_2SO_4 and the solvent removed under reduced pressure to afford a white solid. As compared to PEG 600 the tosylated product of PEG 1500 was solid (10.5 g, 96%).

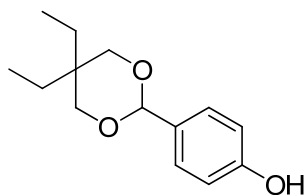
1H NMR (300 MHz, $(CD_3)_2CO$, 295 K): δ = 8.01 (d, $J(H,H)$ = 8.5 Hz, 2 H, Ar-H), 7.61 (d, $J(H,H)$ = 8.0 Hz, 2 H, Ar-H), 3.58 (m, PEG CH_2), 2.53 (s, 3 H, CH_3).

$^{13}\text{C}\{^1\text{H}\}$ NMR (75 MHz, $(\text{CD}_3)_2\text{CO}$, 295 K): δ = 147.94 (1C, Ar-CH₃), 141.69 (1C, Ar-SO₂), 130.90 (2C, Ar-H), 129.09 (2C, Ar-H), 72.88 00 (PEG CH₂), 70.62 (PEG CH₂), 61.23 (PEG CH₂OH), 21.06 (1C, CH₃).

MALDI MS: m/z 1581.8 $[\text{M}+1]^+$ (calculated for $[\text{C}_{71}\text{H}_{136}\text{O}_{35}\text{S}+1]^+$ 1581.98), m/z not observed for $[\text{M}+\text{Na}]^+$ (calculated $[\text{C}_{33}\text{H}_{60}\text{O}_{16}\text{S}+\text{Na}]^+$ 1605.97).

n	Calculated [M] ⁺	Found [M] ⁺	Formula
23	1184.71	1185.6	C ₅₃ H ₁₀₀ O ₂₆ S
24	1228.74	1229.6	C ₅₅ H ₁₀₄ O ₂₇ S
25	1272.77	1273.7	C ₅₇ H ₁₀₈ O ₂₈ S
26	1316.8	1317.7	C ₅₉ H ₁₁₂ O ₂₉ S
27	1360.83	1361.7	C ₆₁ H ₁₁₆ O ₃₀ S
28	1404.86	1405.7	C ₆₃ H ₁₂₀ O ₃₁ S
29	1448.89	1449.8	C ₆₅ H ₁₂₄ O ₃₂ S
30	1492.92	1493.8	C ₆₇ H ₁₂₈ O ₃₃ S
31	1536.95	1537.8	C ₆₉ H ₁₃₂ O ₃₄ S
32	1580.98	1581.8	C ₇₁ H ₁₃₆ O ₃₅ S
33	1625.01	1625.8	C ₇₃ H ₁₄₀ O ₃₆ S
34	1669.04	1669.8	C ₇₅ H ₁₄₄ O ₃₇ S
35	1713.07	1713.8	C ₇₇ H ₁₄₈ O ₃₈ S
36	1757.10	1757.9	C ₇₉ H ₁₅₂ O ₃₉ S
37	1801.13	1801.9	C ₈₁ H ₁₅₆ O ₄₀ S
38	1845.16	1845.9	C ₈₃ H ₁₆₀ O ₄₁ S
39	1889.19	1889.9	C ₈₅ H ₁₆₄ O ₄₂ S
40	1933.22	1933.9	C ₈₇ H ₁₆₈ O ₄₃ S
41	1977.25	1978.9	C ₈₉ H ₁₇₂ O ₄₄ S
42	2021.28	2021.9	C ₉₁ H ₁₇₆ O ₄₅ S
43	2065.31	2066.9	C ₉₃ H ₁₈₀ O ₄₆ S
44	2109.34	2109.9	C ₉₅ H ₁₈₄ O ₄₇ S
45	2153.37	2154.9	C ₉₇ H ₁₈₈ O ₄₈ S
46	2197.40	2198.8	C ₉₈ H ₁₉₂ O ₄₉ S

4-(5,5-diethyl-1,3-dioxan-2-yl)phenol (19)



4-Hydroxybenzaldehyde (10 g, 81.89 mmol), 2,2-diethyl-1,3-propanediol (12.8 g, 103.90 mmol, 1.27 eq.) and *p*-toluenesulfonic acid (0.78 g, 4.10 mmol, 0.05 eq.) as catalyst were suspended in 40 mL toluene and heated to reflux at 85°C for 3.5 h. The reaction mixture was extracted with diethyl ether (2 x 50 mL) and washed with H₂O (3 x 50 mL) and brine (3 x 30 mL), the combined organic layers were dried over Na₂SO₄ and the organic solvents removed under reduced pressure. The crude product was purified with column chromatography (Hex : EA 8 : 2, R_f = 0.15) on silica to afford a white solid (11.7 g, 61%).

C₁₄H₂₀O₃ (236.31 g mol⁻¹).

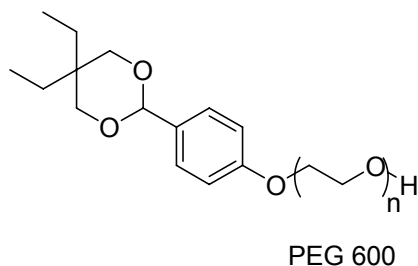
m.p. 56 °C.

¹H NMR (300 MHz, (CD₃)₂CO, 295 K): δ = 7.28 (d, *J*(H,H) = 8.3 Hz, 2H, Ar-H), 6.80 (d, *J*(H,H) = 8.7 Hz, 2H, Ar-H), 5.32 (s, 1H, Ar-CH), 3.87 (d, *J*(H,H) = 11.4 Hz, 2H, OCH₂a), 3.58 (d, *J*(H,H) = 11.4 Hz, 2H, OCH₂b), 1.80 (q, *J*(H,H) = 7.6 Hz, 2H, CH₂ a), 1.14 (q, *J*(H,H) = 7.4 Hz, 2H, CH₂b), 0.87 (t, *J*(H,H) = 7.6 Hz, 4H, CH₃a), 0.80 (t, *J*(H,H) = 7.6 Hz, 3H, CH₃b).

¹³C{¹H} NMR (75 MHz, (CD₃)₂CO, 295 K): δ = 159.31 (1C, Ar-OH), 132.28 (1C, Ar-CH), 129.28 (2C, Ar-H), 116.24 (2C, Ar-H), 103.54 (1C, Ar-CH), 75.98 (2C, OCH₂), 36.16 (1C, CH), 25.79 (1C, CH₂a), 24.19 (1C, CH₂b), 8.77 (1C, CH₃a), 7.85 (1C, CH₃b).

MS (FAB) *m/z* (rel. Int. %): 237 (M+1) (60), 236 (M) (11), 35 (M-1) (24), 154 (18), 143 (12), 137 (10), 136 (17), 124 (10), 123 (100), 121 (29), 107 (13), 97 (19), 77 (13), 69 (17), 57 (16), 43 (18), 41 (23), 39 (12), 29 (11).

IR (KCl): ν = 3339 (s), 2969 (s), 2870 (m), 2360 (w), 1615 (m), 1523 (m), 1456 (w), 1398 (s), 1270 (m), 1213 (m), 1167 (m), 1097 (s), 1057(m), 1000 (m), 955 (s), 917 (m).

2-(4-(5,5-Diethyl-1,3-dioxan-2-yl)phenoxy) polyethylene glycol PEG 600 (25c)**General procedure IV**

Under argon the protected aldehyde 4-(5,5-Diethyl-1,3-dioxan-2-yl)phenol **19** (6.97 g, 29.52 mmol, 1.3 eq.) was dissolved in 35 mL dry ACN, cooled down in an ice /water bath to 0°C and NaH (1.29 g, 29.52 mmol 1.3 eq.) was added and stirred for 10 min before allowing the reaction mixture to warm up to r.t.. Polyethylene glycol *p*-toluenesulfonate PEG 600 **26c** (13.9 g, 22.71 mmol) was coevaporated with toluene (3 x 50 mL) and dissolved in 160 mL dry acetonitrile and the reaction mixture was heated to reflux at 95°C for 3 days. TLC analysis showed that the reaction was not complete and the reaction mixture was heated to 95°C for 2 d. The reaction mixture was diluted with 100 mL DCM, washed with 5% NaHCO₃ (3 x 150 mL), H₂O (6 x 200 mL), brine (3 x 200 mL), dried over Na₂SO₄ and the solvent removed under reduced pressure. The crude product was purified with column chromatography (gradient: EA : Hex 9 : 1, EtOAc : EtOH 1 : 1, R_f = 0.42) on silica to afford a colorless yellow oil (8.3 g, 44%).

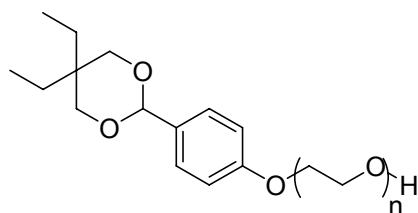
¹H NMR (300 MHz, (CD₃)₂CO, 295 K): δ = 7.38 (d, *J*(H,H) = 8.7 Hz, 2H, Ar-H), 6.92 (d, *J*(H,H) = 8.7 Hz, 2H, Ar-H), 5.36 (s, 1H, Ar-CH), 4.13 (t, *J*(H,H) = 5.1, 2H, OCH₂a), 3.81 (t, *J*(H,H) = 4.8, 2H, OCH₂b), 3.67-3.57 (m, PEGCH₂), 2.79 (s, 1H, OH), 1.81 (q, *J*(H,H) = 7.5 Hz, 2H, CH₂a), 1.17 (q, *J*(H,H) = 7.8 Hz, 2H, CH₂b), 0.88 (t, *J*(H,H) = 7.5 Hz, 3H, CH₃a), 0.81 (t, *J*(H,H) = 7.5 Hz, 3H, CH₃b).

¹³C{¹H} NMR (75 MHz, (CD₃)₂CO, 295 K): δ = 161.06 (1C, Ar-O), 133.80 (1C, Ar-CH), 129.38 (2C, Ar-H), 115.70 (2C, Ar-H), 103.45 (1C, Ar-CH), 76.13-69.36 (PEGCH₂+CH₂O), 36.35 (1C, CH), 25.94 (1C, CH₂CH₃a), 24.36 (1C, CH₂CH₃b), 8.83 (1C, CH₃a), 7.90 (1C, CH₃b).

MALDI MS: m/z 743.7 [M+Na]⁺ (calculated for [C₃₆H₆₄O₁₆+Na]⁺ 743.85).

n	Calculated [M+Na] ⁺	Found [M+Na] ⁺	Formula
7	567.65	567.4	C ₂₈ H ₄₈ O ₁₂
8	611.70	611.5	C ₃₀ H ₅₂ O ₁₃
9	655.75	655.6	C ₃₂ H ₅₆ O ₁₄
10	699.80	699.6	C ₃₄ H ₆₀ O ₁₅
11	743.85	743.7	C ₃₆ H ₆₄ O ₁₆
12	787.90	787.7	C ₃₈ H ₆₈ O ₁₅
13	831.95	831.8	C ₄₀ H ₇₂ O ₁₆
14	876.00	875.8	C ₄₂ H ₇₆ O ₁₇
15	920.05	919.8	C ₄₄ H ₈₀ O ₁₈
16	964.10	963.9	C ₄₆ H ₈₄ O ₁₉
17	1008.15	1007.9	C ₄₈ H ₈₈ O ₂₀
18	1052.20	1052.0	C ₅₀ H ₉₂ O ₂₁
19	1096.25	1096.0	C ₅₂ H ₉₆ O ₂₂
20	1140.30	1138.0	C ₅₄ H ₁₀₀ O ₂₃

2-(4-(5,5-Diethyl-1,3-dioxan-2-yl)phenoxy)polyethylene glycol PEG 1500 (25d)



PEG 1500

According to general procedure **IV** 4-(5,5-Diethyl-1,3-dioxan-2-yl)phenol **19** (2.38 g, 10.07 mmol, 1.1 eq.) was dissolved in 15 mL dry ACN, and deprotonated with NaH (241.77 mg, 10.07 mmol, 1.1 eq.). Polyethylene glycol *p*-toluenesulfonate PEG 1500 **25d** (14.5 g, 9.16 mmol) in 80 mL dry acetonitrile were added and refluxed for 2 days. The reaction mixture was diluted with 150 mL DCM, washed with H₂O (3 x 200 mL), 5% NaHCO₃ (3 x 150 mL), brine (3 x 200 mL). Purification on silica (gradient: DCM : Hex 6 : 4, DCM : Hex 8 : 2, EA : Hex 1 : 1, DCM : EtOH 1 : 1) on silica to afford a colorless oil 4 g, 27%).

^1H NMR (300 MHz, $(\text{CD}_3)_2\text{CO}$, 295 K): δ = 7.39 (d, $J(\text{H,H})$ = 8.7 Hz, 2H, Ar-**H**), 6.94 (d, $J(\text{H,H})$ = 8.7 Hz, 2H, Ar-**H**), 5.36 (s, 1H, Ar-**CH**), 4.14 (t, $J(\text{H,H})$ = 5.1, 2H, **OCH₂a**), 3.82 (t, $J(\text{H,H})$ = 4.8, 2H, **OCH₂b**), 3.59 (m, PEG**CH₂**), 3.28 (s, 1H, **OH**), 1.80 (q, $J(\text{H,H})$ = 7.5 Hz, 2H, **CH₂a**), 1.17 (q, $J(\text{H,H})$ = 7.8 Hz, 2H, **CH₂b**), 0.88 (t, $J(\text{H,H})$ = 7.5 Hz, 3H, **CH₃a**), 0.81 (t, $J(\text{H,H})$ = 7.5 Hz, 3H, **CH₃b**).

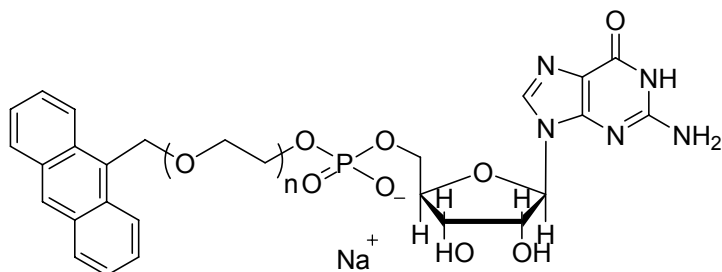
$^{13}\text{C}\{^1\text{H}\}$ NMR (75 MHz, $(\text{CD}_3)_2\text{CO}$, 295 K): δ = 159.98 (1C, Ar-**O**), 134.13 (1C, Ar-**CH**), 129.71 (2C, Ar-**H**), 116.62 (2C, Ar-**H**), 108.18 (1C, Ar-**CH**), 67.68 (PEG**CH₂**+**CH₂O**), 31.60 (1C, **CH**), 26.57 (1C, **CH₂CH₃**), 10.65 (1C, **CH₃**).

MALDI MS: m/z 1623.9 $[\text{M}+\text{Na}]^+$ (calculated for $[\text{C}_{48}\text{H}_{82}\text{O}_{20}+\text{Na}]^+$ 1624.10), 1639.8 $[\text{M}+\text{K}]^+$ (calculated for $[\text{C}_{48}\text{H}_{82}\text{O}_{20}+\text{K}]^+$ 1640.03).

n	Calculated $[\text{M}+\text{Na}]^+$	Found $[\text{M}+\text{Na}]^+$	Calculated $[\text{M}+\text{K}]^+$	Found $[\text{M}+\text{K}]^+$	Formula
22	1227.79	1227.5	1243.76	1245.6	$\text{C}_{58}\text{H}_{108}\text{O}_{25}$
23	1271.82	1271.6	1287.79	1289.6	$\text{C}_{30}\text{H}_{50}\text{O}_{12}$
24	1315.85	1315.6	1331.82	1333.6	$\text{C}_{32}\text{H}_{54}\text{O}_{13}$
25	1389.88	1359.6	1375.85	1377.6	$\text{C}_{34}\text{H}_{58}\text{O}_{14}$
26	1403.91	1403.7	1419.88	1421.7	$\text{C}_{36}\text{H}_{62}\text{O}_{15}$
27	1447.96	1447.7	1463.91	1465.7	$\text{C}_{38}\text{H}_{66}\text{O}_{16}$
28	1492.01	1791.8	1507.94	1509.7	$\text{C}_{40}\text{H}_{70}\text{O}_{17}$
29	1536.04	1535.8	1551.97	1553.8	$\text{C}_{42}\text{H}_{74}\text{O}_{18}$
30	1580.07	1579.8	1596.00	1597.8	$\text{C}_{44}\text{H}_{78}\text{O}_{19}$
31	1624.10	1623.9	1640.03	1639.8	$\text{C}_{48}\text{H}_{82}\text{O}_{20}$
32	1668.13	1667.9	1684.06	1683.9	$\text{C}_{50}\text{H}_{86}\text{O}_{21}$
33	1712.16	1711.9	1728.09	1727.9	$\text{C}_{52}\text{H}_{90}\text{O}_{22}$
34	1756.19	1756.0	1772.12	1772.0	$\text{C}_{54}\text{H}_{94}\text{O}_{23}$
35	1800.22	1800.0	1816.15	1816.0	$\text{C}_{28}\text{H}_{46}\text{O}_{11}$
36	1844.25	1844.1	1860.18	1860.0	$\text{C}_{30}\text{H}_{50}\text{O}_{12}$
37	1888.28	1888.1	1904.21	1904.0	$\text{C}_{32}\text{H}_{54}\text{O}_{13}$
38	1932.31	1932.1	1948.24	1948.0	$\text{C}_{34}\text{H}_{58}\text{O}_{14}$
39	1976.34	1976.1	1992.27	1992.1	$\text{C}_{36}\text{H}_{62}\text{O}_{15}$
40	2020.37	2020.2	2036.3	2036.1	$\text{C}_{38}\text{H}_{66}\text{O}_{16}$
41	2064.4	2064.2	2080.33	2080.2	$\text{C}_{40}\text{H}_{70}\text{O}_{17}$

Initiator nucleotides

Initiator nucleotide (7a)



General procedure V

(Anthracen-9-yl-methoxy)-polyethylene glycol **16a** (380 mg, 0.55 mmol) was dried by coevaporation with toluene (3×5 mL). A solution of 8 mL 0.1 M of phosphoramidite **17** (470 mg, 0.66 mmol, 1.2 eq.) in dry THF were added under argon and 4,5-dicyanoimidazole was added as activator (65 mg, 0.55 mmol, 1.0 eq.) and the reaction was stirred at r.t. for 1 h. The coupling reaction was then stopped by addition of 0.55 mL *t*-butyl hydroperoxide (3.3 mmol, 10 eq.). The reaction mixture was stirred for 30 min at r.t and all volatiles were removed under vacuum using Schlenk technique. To remove the TBDMS protection groups of the guanosine the residue was taken up in 3.3 mL 1 M TBAF in THF (3.3 mmol, 6 equiv) under argon and stirred for 3 h at r.t.. Reaction control was performed on TLC RP-18 plates (ACN : H₂O 1 : 1). The THF was removed under vacuum and the residue was taken up in water, filtered over a 0.22 μ M membrane filter, and purified by preparative reverse phase chromatography using a chromatography pump (gradient ACN : H₂O 2 : 8 to 1 : 1) the product was collected and lyophilized. Tetra butylammonium cations were exchanged for sodium ions on a DOWEX® 50WX8-200 resin (sodium form) according to standard protocol with water as eluent. The aqueous solution could then be directly submitted again to the preparative reverse phase as described above. The product was collected and lyophilized to afford a yellow solid.

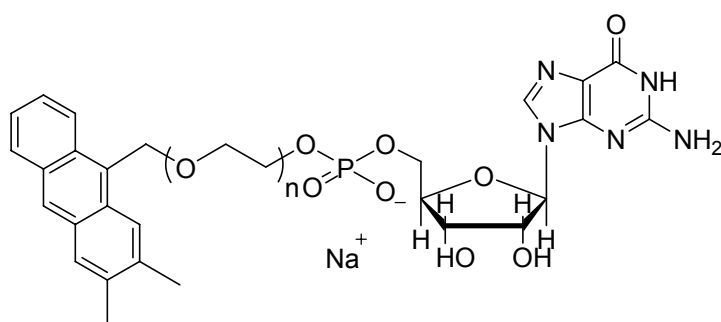
¹H-NMR (500 MHz, CD₃OH, 295 K): δ = 8.58 (s, 1H), 8.40 (m, 2H), 8.10 (m, 3H), 7.68 (m, 4H), 5.88 (m, 2H), 4.49 (m, 2H), 3.96-3.88 (m, 3H), 3.74-3.37 (m, nH, PEGCH₂).

³¹P-NMR (500 MHz, D₂O, 295 K): δ = 0.23 (s).

MALDI MS: m/z 1038.5 $[M]^+$ (calculated for $[C_{47}H_{67}N_5O_{19}P]^+$ 1036.46), m/z 1060.5 $[M+Na]^+$ (calculated for $[C_{47}H_{67}N_5O_{19}P + Na]^+$ 1059.45).

n	Calculated [M] ⁺	Found [M] ⁺	Calculated [M+Na] ⁺	Found [M+Na]	Formula
8	904.37	903.5	927.36	-	C ₄₁ H ₅₅ N ₅ O ₁₆ P ⁺
9	948.40	950.5	971.39	972.5	C ₄₃ H ₅₉ N ₅ O ₁₇ P ⁺
10	992.43	994.5	1015.42	1016.5	C ₄₅ H ₆₃ N ₅ O ₁₈ P ⁺
11	1036.46	1038.5	1059.45	1060.5	C ₄₇ H ₆₇ N ₅ O ₁₉ P ⁺
12	1080.49	1082.5	1103.48	1104.5	C ₄₉ H ₇₁ N ₅ O ₂₀ P ⁺
13	1124.52	1126.5	1147.51	1148.5	C ₅₁ H ₇₅ N ₅ O ₂₁ P ⁺
14	1168.55	1170.6	1191.54	1192.5	C ₅₃ H ₇₉ N ₅ O ₂₂ P ⁺
15	1212.56	1214.6	1235.57	1238.6	C ₅₅ H ₈₃ N ₅ O ₂₃ P ⁺
16	1256.61	1258.6	1279.60	1282.5	C ₅₇ H ₈₇ N ₅ O ₂₄ P ⁺
17	1300.64	1302.6	1323.63	-	C ₅₉ H ₉₁ N ₅ O ₂₅ P ⁺

Initiator nucleotide (7b)



Initiator nucleotide **7b** was synthesized according to general procedure **V** from 2-((2,3-Dimethylanthracen-9-yl)methoxy)-polyethylene glycol **16b** (710.7 mg 0.93 mmol), 14.1 mL 0.1 M of phosphoramidite **17** (470 mg, 0.66 mmol, 1.2 eq.) in dry THF, 4,5-dicyanoimidazole (125 mg, 1.06 mmol, 1.0 eq.). The coupling reaction was stopped with 1.18 mL *t*-butylhydroperoxide (9.4 mmol, 10 eq.), after evaporation of the reaction mixture the residue was taken up in TBAF in THF (5.7 mL, 5.58 mmol, 6 eq.). Half of the crude product was purified by preparative reverse phase chromatography using a chromatography pump (gradient: 1) ACN: H₂O 2:8 400 mL, 2) ACN: H₂O 3:7 200 mL, 3) ACN: H₂O 4:6 200 mL, 4) ACN: H₂O 1:1 600 mL) to yield a yellow solid (125.2 mg, 24%).

¹H-NMR (500 MHz, D₂O, 295 K): δ = 8.09 (d, 1H, J (H,H) = 4.2 Hz), 8.04 (s, 1H), 7.75 (s, 1H), 7.44 (s, 1H), 7.38 (d, 1H, J (H,H) = 7.8 Hz), 7.33 (d, 1H, J (H,H) = 0.4 Hz), 7.17 (s, 1H), 6.88 (s, 1H), 5.86 – 5.79 (12 x s, 12 x 2H), 5.07 (s, 2H), 4.75 (m), 4.49 (d, 1H, J (H,H) = 1 Hz), 4.31 (s, 1H), 4.12 (d, 2H, J (H,H) = 3.5 Hz), 3.93 (dd, 2H, J (H,H) = 1.8 Hz, J (H,H) = 2.9 Hz), 3.70 – 3.30 (m, nH, PEGCH₂), 2.14 (s, 3H), 1.96 (s, 3H).

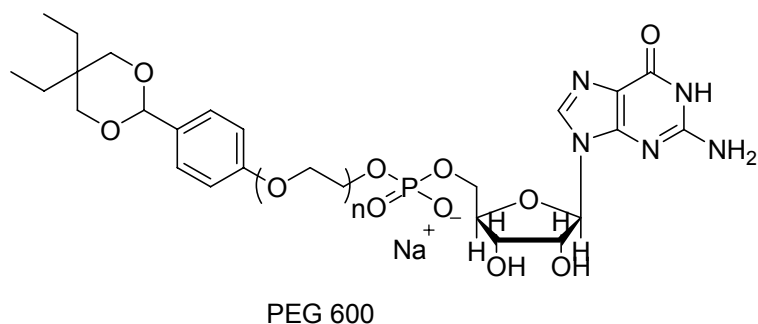
³¹P-NMR (500 MHz, D₂O, 295 K): δ = 0,231 (s).

¹³C{¹H} NMR (75 MHz, D₂O, 295 K) δ = 159.74, 138.33, 136.92, 132.26, 132.09, 132.07, 131.69, 131.68, 131.47, 131.46, 130.08, 128.75, 128.31, 127.27, 127.26, 125.98, 125.98, 125.96, 125.26, 125.24, 124.09, 124.07, 117.58, 117.57, 114.33, 104.99, 88.47, 85.34, 85.23, 85.20, 85.18, 85.17, 85.15, 75.02, 75.01, 74.99, 72.01, 71.97, 71.47, 71.46, 71.43, 71.03, 70.43, 66.02, 65.95, 21.36, 20.50.

MALDI MS: m/z 1154.5 [$M+Na$]⁺ (calculated for [$C_{53}H_{79}N_5O_{21}P+Na$]⁺ 1154.47), m/z 1176.5 [$M+K$]⁺ (calculated for [$C_{53}H_{79}N_5O_{21}P+K$]⁺ 1176.45).

n	Calculated [$M+Na$] ⁺	Found [$M+Na$] ⁺	Calculated [$M+K$] ⁺	Found [$M+K$] ⁺	Formula
8	934.37	-	956.35	-	C ₄₃ H ₅₉ N ₅ O ₁₆ P ⁻
9	978.39	978.3	1000.37	1000.3	C ₄₅ H ₆₃ N ₅ O ₁₇ P ⁻
10	1022.41	1022.4	1044.39	1044.4	C ₄₇ H ₆₇ N ₅ O ₁₈ P ⁻
11	1066.43	1066.4	1088.41	1088.4	C ₄₉ H ₇₁ N ₅ O ₁₉ P ⁻
12	1110.45	1110.4	1132.43	1132.4	C ₅₁ H ₇₅ N ₅ O ₂₀ P ⁻
13	1154.47	1154.5	1176.45	1176.5	C ₅₃ H ₇₉ N ₅ O ₂₁ P ⁻
14	1198.49	1198.5	1220.47	1220.5	C ₅₅ H ₈₃ N ₅ O ₂₂ P ⁻
15	1242.51	1242.6	1264.49	1264.6	C ₅₇ H ₈₇ N ₅ O ₂₃ P ⁻
16	1286.53	1286.6	1308.51	1308.7	C ₅₉ H ₉₁ N ₅ O ₂₄ P ⁻
17	1330.55	1330.7	1352.53	1354.7	C ₆₁ H ₉₅ N ₅ O ₂₅ P ⁻
18	1374.57	1374.7	1396.55	-	C ₆₃ H ₉₉ N ₅ O ₂₆ P ⁻

Initiator nucleotide (7c)



Initiator nucleotide **7c** was synthesized according to general procedure **V** from 2-(4-(5,5-diethyl-1,3-dioxan-2-yl)phenoxy)polyethylene glycol PEG 600 **25c** (960 mg, 2.61 mmol), 14.1 mL 0.1 M of phosphoramidite **17** (990 mg, 3.13 mmol, 1.2 eq.) in dry THF, 4,5-dicyanoimidazole (140 g, 2.61 mmol, 1.0 eq.). The coupling reaction was stopped after 50 min with 1.17 mL *t*-butyl hydroperoxide (26.10 mmol, 10 eq.), after evaporation of the reaction mixture the residue was taken up in TBAF in THF (5.7 mL, 5.58 mmol, 6 eq.) and stirred for 16h at r.t.. 246.46 mg of the crude product was purified with reversed phase chromatography system with two pumps, using the following gradient with acetonitrile and water.

Time [min]	ACN [%]
0	15
15	40
50	60
65	80
70	100
75	50
80	50

After ion exchange and reverse phase chromatography was carried out as described above 26.7 mg (20%) clean product could be obtained out of the initially loaded 246.46 mg.

¹H NMR (500 MHz, D₂O, 295 K): δ = 8.10 (s, 1H), 7.43 (s, 2H), 7.03 (s, 2H), 5.92 (d, *J*(H,H) = 5.5 Hz, 1H), 5.50 (m, 1H), 4.51 (t, *J*(H,H) = 5 Hz, 1H), 4.32 (s, 1H), 4.13 (t, *J*(H,H) = 4.5 Hz, 2H), 3.96 (d, *J*(H,H) = 11 Hz, 2H), 3.92 (m, 4H), 3.78-3.61 (m, nH, PEGCH₂), 1.79 (q,

$J(\text{H,H}) = 7.5 \text{ Hz}$, 2H), 1.17 (q, $J(\text{H,H}) = 7.5 \text{ Hz}$, 2H), 0.89 (t, $J(\text{H,H}) = 7.5 \text{ Hz}$, 3H), 0.80 (t, $J(\text{H,H}) = 7.5 \text{ Hz}$, 3H).

$^{13}\text{C}\{^1\text{H}\}$ NMR (75 MHz, D_2O , 295 K): $\delta = 163.22, 156.15, 151.78, 147.32, 137.40, 130.39, 127.71, 114.64, 104.64, 101.66, 86.82, 74.50, 73.38, 70.37, 69.69, 69.50, 68.98, 34.46, 23.41, 22.10, 6.65, 5.79$.

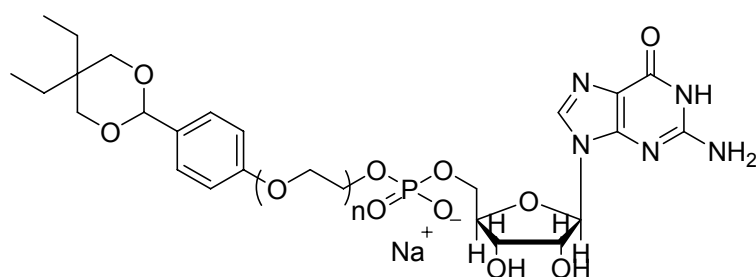
^{31}P -NMR (121.5 MHz, D_2O , 295K): $\delta = 0.25$ (s).

MS HR-ESI: m/z 1064.47 (calculated for $[\text{C}_{46}\text{H}_{75}\text{O}_{21}\text{N}_5\text{P}]^+$ 1064.51).

MALDI MS: m/z 1067.3 $[\text{M}]^+$ (calculated for $[\text{C}_{46}\text{H}_{75}\text{O}_{21}\text{N}_5\text{P}]^+$ 1064.51), m/z 1089.4 $[\text{M}+\text{Na}]^+$ (calculated for $[\text{C}_{46}\text{H}_{75}\text{O}_{21}\text{N}_5\text{P} + \text{Na}]^+$ 1087.50).

n	Calculated $[\text{M}]^+$	Found $[\text{M}]^+$	Calculated $[\text{M}+\text{Na}]^+$	Found $[\text{M}+\text{Na}]^+$	Formula
7	888.39	891.2	911.38	-	$\text{C}_{38}\text{H}_{59}\text{O}_{17}\text{N}_5\text{P}^-$
8	932.42	935.2	955.41	-	$\text{C}_{40}\text{H}_{63}\text{O}_{18}\text{N}_5\text{P}^-$
9	976.45	979.2	999.44	1001.4	$\text{C}_{42}\text{H}_{67}\text{O}_{19}\text{N}_5\text{P}^-$
10	1020.48	1023.3	1043.47	1045.4	$\text{C}_{44}\text{H}_{71}\text{O}_{20}\text{N}_5\text{P}^-$
11	1064.51	1067.3	1087.50	1089.4	$\text{C}_{46}\text{H}_{75}\text{O}_{21}\text{N}_5\text{P}^-$
12	1108.54	1111.4	1131.53	1133.5	$\text{C}_{48}\text{H}_{79}\text{O}_{22}\text{N}_5\text{P}^-$
13	1152.57	1155.5	1175.56	1177.5	$\text{C}_{50}\text{H}_{83}\text{O}_{23}\text{N}_5\text{P}^-$
14	1196.6	1199.6	1219.59	1221.6	$\text{C}_{52}\text{H}_{87}\text{O}_{24}\text{N}_5\text{P}^-$
15	1240.63	1243.6	1263.62	1265.6	$\text{C}_{54}\text{H}_{91}\text{O}_{25}\text{N}_5\text{P}^-$
16	1284.66	1287.7	1307.65	1309.6	$\text{C}_{56}\text{H}_{95}\text{O}_{26}\text{N}_5\text{P}^-$
17	1328.69	1331.8	1351.68	1353.7	$\text{C}_{58}\text{H}_{99}\text{O}_{27}\text{N}_5\text{P}^-$
18	1372.72	1375.9	1395.71	-	$\text{C}_{60}\text{H}_{103}\text{O}_{28}\text{N}_5\text{P}^-$
19	1416.75	1419.9	1439.74	-	$\text{C}_{62}\text{H}_{107}\text{O}_{29}\text{N}_5\text{P}^-$

Initiator nucleotide (7d)



PEG 1500

Initiator nucleotide **7d** was synthesized according to general procedure **V** from 2-(4-(5,5-diethyl-1,3-dioxan-2-yl)phenoxy)polyethylene glycol PEG 1500 **25d** (1 g 0.58 mmol), 8 mL 0.1 M of phosphoramidite **17** (493 mg, 0.69 mmol, 1.2 eq.) in dry THF, 4,5-dicyanoimidazole (69 mg, 0.58 mmol, 1.0 eq.). The coupling reaction was stopped with 0.58 mL *t*-butyl hydroperoxide (5.8 mmol, 10 eq.), after evaporation of the reaction mixture the residue was taken up in TBAF in THF (3.48 mL, 3.48 mmol, 6 eq.). The solvent was removed under reduced pressure and HPLC followed by MALDI MS analysis revealed that only one TBDMS protection group had been removed. Another 3.48 mL TBAF was added and stirred over night. The product was purified on a reverse phase LC chromatography system IntelliFlash gradient with acetonitrile and water. The product was eluted between 14-16 min.

Time [min]	ACN [%]
0	10
10	20
25	65
30	70

After ion exchange and chromatography as described 16 mg clean product could be obtained out of the initially loaded 150 mg.

¹H NMR (500 MHz, D₂O, 295 K): δ = 8.11 (s, 1H), 7.48 (s, 2H), 7.08 (s, 2H), 5.93 (d, $J(\text{H,H})$ = 5.5 Hz, 1H), 5.55 (d, $J(\text{H,H})$ = 5.0 Hz, 1H), 4.52 (t, $J(\text{H,H})$ = 4.5 Hz, 1H), 4.25 (s, 1H), 4.11 (t, $J(\text{H,H})$ = 4.5 Hz, 2H), 3.97 (d, $J(\text{H,H})$ = 11 Hz, 2H), 3.93 (m, 4H), 3.77-3.62 (m, nH, PEGCH₂), 1.81 (m, 2H), 1.18 (m, 2H), 0.91 (t, $J(\text{H,H})$ = 7.5 Hz, 3H), 0.81 (t, $J(\text{H,H})$ = 7.5 Hz, 3H).

¹³C{¹H} NMR (75 MHz, D₂O, 295 K): δ = 158.83, 151.83, 146.94, 138.20, 127.78, 114.72, 109.99, 101.66, 86.79, 83.66, 74.53, 69.71, 69.53, 69.48, 67.17, 34.49, 23.43.

³¹P NMR (121.5 MHz, D₂O, 295K): δ = 0.25 (s).

MS HR-ESI: m/z 1856.97 (calculated for [C₈₂H₁₄₇O₃₉N₅P] 1857.05).

MALDI MS: m/z 1771.6 [M+Na]⁺ (calculated for [C₇₈H₁₃₉O₃₇N₅P+Na]⁺ 1768.99).

n	Calculated [M+Na]⁺	Found [M+Na]⁺	Formula
17	1328.06	1330.2	C ₅₈ H ₈₉ O ₂₇ N ₅ P
18	1372.09	1374.2	C ₆₀ H ₉₃ O ₂₈ N ₅ P
19	1416.12	1418.3	C ₆₂ H ₉₇ O ₂₉ N ₅ P
20	1460.15	1462.3	C ₆₄ H ₁₁₁ O ₃₀ N ₅ P
21	1504.81	1506.4	C ₆₆ H ₁₁₅ O ₃₁ N ₅ P
22	1548.84	1550.4	C ₆₈ H ₁₁₉ O ₃₂ N ₅ P ⁻
23	1592.87	1594.4	C ₇₀ H ₁₂₃ O ₃₃ N ₅ P
24	1636.90	1638.5	C ₇₂ H ₁₂₇ O ₃₄ N ₅ P
25	1680.93	1683.5	C ₇₄ H ₁₃₁ O ₃₅ N ₅ P
26	1724.96	1727.5	C ₇₆ H ₁₃₅ O ₃₆ N ₅ P
27	1768.99	1771.6	C ₇₈ H ₁₃₉ O ₃₇ N ₅ P
28	1813.02	1815.9	C ₈₀ H ₁₄₃ O ₃₈ N ₅ P
29	1857.05	1859.9	C ₈₂ H ₁₄₇ O ₃₉ N ₅ P
30	1901.08	1904.0	C ₈₄ H ₁₅₁ O ₄₀ N ₅ P
31	1945.11	1948.1	C ₈₆ H ₁₅₅ O ₄₁ N ₅ P
32	1989.14	1992.1	C ₈₈ H ₁₅₉ O ₄₂ N ₅ P
33	2033.17	2036.3	C ₉₀ H ₁₆₃ O ₄₃ N ₅ P
34	2077.20	2080.4	C ₉₂ H ₁₆₇ O ₄₄ N ₅ P
35	2121.23	2124.5	C ₉₄ H ₁₇₁ O ₄₅ N ₅ P
36	2165.26	2168.6	C ₉₆ H ₁₇₅ O ₄₆ N ₅ P
37	2209.29	2212.7	C ₉₈ H ₁₇₉ O ₄₇ N ₅ P
38	2253.32	2256.7	C ₁₀₀ H ₁₈₃ O ₄₈ N ₅ P
39	2297.35	2230.7	C ₁₀₂ H ₁₈₇ O ₄₉ N ₅ P

6.3.2 Analysis of the initiator nucleotides

High-performance liquid chromatography of the initiator nucleotides

The purity of the initiator nucleotides A-D was confirmed by analytical HPLC. For initiator nucleotide **7a** and **b** gradient I1 was used, initiator nucleotides **7c** and **d** were analysed using gradient I2.

Gradient I1		Gradient I2	
Time [min]	Buffer B [%]	Time [min]	Buffer B [%]
0	5	0	15
25	40	15	40
40	80	50	60
45	100	55	100
60	100	60	100
65	5	65	15

Table 23 : Retention time of the initiator nucleotides 7a-d.

Initiator nucleotide	Gradient	Retention time R_t [min]
a	I1	32.7-35.4
b	I1	36.0-37.7
c	I2	26.7-33.4
d	I2	39.6-44.4

MALDI TOF Mass spectrometry of the initiator nucleotides

The samples for analysis were prepared using the dried droplet method with dithranol in 1:10 v/v water/ acetone as matrix solutions; detection in the positive mode.

6.3.3 Alternative procedures towards the synthesis of initiator nucleotides

(4,4'-Dimethoxytrityl)-polyethylene glycol PEG 1500 (13d)



PEG 1500

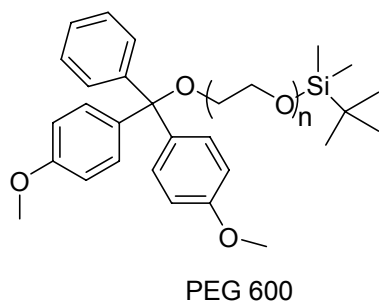
PEG 1500 (50 g, 33 mmol) was dried by coevaporation with toluene (3 x 100 mL) and suspended in 25 mL acid free CH_2Cl_2 (stored over K_2CO_3). Triethylamine (1.7 mL, 12.33 mmol, 0.37 eq.) and 4-dimethylaminopyridine (DMAP) (40 mg, 0.33 mmol, 0.01 eq.) were added. A solution of 4,4'-dimethoxytriphenylmethylchloride (902 mg, 2.66 mmol, 0.08 eq.) in 9 mL acid free CH_2Cl_2 was slowly added by a syringe pump over 3 h 35 min at r.t.. The solution was then diluted with 75 mL CH_2Cl_2 and washed with 5% NaHCO_3 (2 x 75 mL), water (3 x 75 mL), and brine (2 x 75 mL), dried over Na_2SO_4 and the solvent removed under reduced pressure. The crude PEG protected polyethylene glycol was purified by column chromatography (gradient pure EtOH, EtOH : DCM 1 : 1, preconditioned with EtOH containing 1% Et_3N , $R_f = 0.2$ (EtOH)) on silica to afford a yellow oil (3.6 g, 75%).

^1H NMR (300 MHz, $(\text{CD}_3)_2\text{CO}$, 295 K): $\delta = 7.44$ (m, 1H, Ar-H), 7.33 (m, 2H, Ar-H), 7.26 (m, 4H, Ar-H), 7.16 (m, 2H, Ar-H), 6.08 (m, 4H, Ar-H), 3.79 (t, $J(\text{H,H}) = 4.2$ Hz, 6H, CH_3), 3.63 (m, PEG CH_2).

$^{13}\text{C}\{^1\text{H}\}$ NMR (75 MHz, $(\text{CD}_3)_2\text{CO}$, 295 K): $\delta = 158.8$ (2C, Ar-O), 139.7 (2C, Ar-H), 136.5 (2C, Ar-C), 130.4 (2C, Ar-H), 129.1 (2C, Ar-H), 128.3 (1C, Ar-H), 128.0 (2C, Ar-H), 113.4 (2C, Ar-H), 86.1 (1C, Ar_3CO), 70.8 (PEG CH_2), 62.0 (PEG CH_2), 55.5 (CH_3).

MALDI MS: m/z 1884.8 $[\text{M}+\text{Na}]^+$ (calculated for $[\text{C}_{91}\text{H}_{160}\text{O}_{38}+\text{Na}]^+$ 1884.18).

n	Calculated [M+Na]⁺	Found [M+Na]⁺	Formula
19	1179.7	1180.1	C ₅₉ H ₉₆ O ₂₂
20	1223.73	1224.1	C ₆₁ H ₁₀₀ O ₂₃
21	1267.76	1268.1	C ₆₃ H ₁₀₄ O ₂₄
22	1311.79	1312.2	C ₆₅ H ₁₀₈ O ₂₅
23	1355.82	1356.2	C ₆₇ H ₁₁₂ O ₂₆
24	1399.85	1400.3	C ₆₉ H ₁₁₆ O ₂₇
25	1443.88	1444.3	C ₇₁ H ₁₂₀ O ₂₈
26	1487.91	1488.4	C ₇₃ H ₁₂₄ O ₂₉
27	1531.94	1532.5	C ₇₅ H ₁₂₈ O ₃₀
28	1575.97	1576.5	C ₇₇ H ₁₃₂ O ₃₁
29	1620.00	1620.6	C ₇₉ H ₁₃₆ O ₃₂
30	1664.03	1664.6	C ₈₁ H ₁₄₀ O ₃₃
31	1707.06	1708.7	C ₈₃ H ₁₄₄ O ₃₄
32	1752.09	1752.7	C ₈₅ H ₁₄₈ O ₃₅
33	1796.12	1797.7	C ₈₇ H ₁₅₂ O ₃₆
34	1840.15	1840.8	C ₈₉ H ₁₅₆ O ₃₇
35	1884.18	1884.8	C ₉₁ H ₁₆₀ O ₃₈
36	1928.21	1928.8	C ₉₃ H ₁₆₄ O ₃₉
37	1972.24	1973.9	C ₉₅ H ₁₇₀ O ₄₀
38	2016.27	2017.9	C ₉₇ H ₁₇₄ O ₄₁
39	2060.30	2063.0	C ₉₉ H ₁₇₈ O ₄₂
40	2104.33	2106.0	C ₁₀₁ H ₁₈₂ O ₄₃
41	2148.36	2150.0	C ₁₀₃ H ₁₈₆ O ₄₄

DMT and TBDMS protected PEG 600 (20c)**General procedure VI**

Mono DMT protected polyethylene glycol PEG 600 13a (7.34 g, 8.23 mmol) was dissolved in 60 mL dry DMF under argon and TBDMS-Cl (1.5 g, 9.9 mmol, 1.2 eq.) and imidazole (1.68 g, 24.7 mmol, 3 eq.) were added and stirred over night. The reaction mixture was diluted with 60 mL DCM and 100 mL H₂O. The aqueous solution was extracted with DCM (2 x 50 mL) and the combined organic layers were washed with 5% NaHCO₃ (50 mL), H₂O (4 x 50 mL) and brine (60 mL), dried over Na₂SO₄ and the solvent removed under reduced pressure. The crude product was purified by column chromatography (pure EtOH, preconditioned with the EtOH containing 1% Et₃N, R_f = 0.93 -0.51, (EA : EtOH 7 : 3) on silica to afford a yellow oil (6.3 g, 76%).

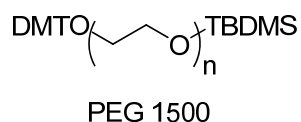
¹H NMR (300 MHz, (CD₃)₂CO, 295 K): δ = 7.50 (d, *J*(H,H) = 7.1 Hz, 2H, Ar-H), 7.36 (d, *J*(H,H) = 9.0 Hz, 4H, Ar-H), 7.30 (d, *J*(H,H) = 7.8 Hz, 2H, Ar-H), 7.21 (t, *J*(H,H) = 7.2 Hz, 1H, Ar-H), 6.88 (d, *J*(H,H) = 8.9 Hz, 4H, Ar-H), 3.79 (s, 6H, OCH₃), 3.57 (m, PEG CH₂), 0.90 (s, 9H, C(CH₃)₃), 0.07 (s, 6H, Si(CH₃)₂).

¹³C{¹H} NMR (75 MHz, (CD₃)₂CO, 295 K): δ = 160.49 (2C, Ar-O), 147.40 (1C, Ar-C), 138.16 (1C, Ar-C), 131.91 (4C, Ar-H), 130.00 (2C, Ar-H), 129.50 (2C, Ar-H), 128.40 (1C, Ar-H), 114.79 (4C, Ar-H), 87.57 (1C, Ar₃CO), 72.23 (PEG CH₂), 63.08 (2C, OCH₃), 27.28 (3C, C(CH₃)₃), 19.85 (1C, C(CH₃)₃), -4.07 (2C, Si(CH₃)₂).

MALDI MS: m/z 1030.0 [M+Na]⁺ (calculated for [C₅₃H₈₆O₁₆Si +Na]⁺ 1029.56), m/z 1046.0 [M+K]⁺ (calculated for [C₅₃H₈₆O₁₆Si +K]⁺ 1045.67).

n	Calculated [M+Na] ⁺	Found [M+Na] ⁺	Calculated [M+K] ⁺	Found [M+K] ⁺	Formula
10	897.47	898.0	913.58	914.0	C ₄₇ H ₇₄ O ₁₃ Si
11	941.50	942.0	957.61	958.0	C ₄₉ H ₇₈ O ₁₄ Si
12	985.53	986.0	1001.64	1002.1	C ₅₁ H ₈₂ O ₁₅ Si
13	1029.56	1030.0	1045.67	1046.0	C ₅₃ H ₈₆ O ₁₆ Si
14	1073.59	1074.1	1089.70	1090.0	C ₅₅ H ₉₀ O ₁₇ Si
15	1117.62	1118.1	1133.73	1134.1	C ₅₇ H ₉₄ O ₁₈ Si
16	1161.65	1162.1	1177.76	1178.1	C ₅₉ H ₉₈ O ₁₉ Si
17	1205.68	1206.2	-	-	C ₆₁ H ₁₀₂ O ₂₀ Si
18	1249.71	1250.3	-	-	C ₆₃ H ₁₀₄ O ₂₁ Si
19	1293.74	1295.1	-	-	C ₆₅ H ₁₀₈ O ₂₂ Si

DMT and TBDMS protected PEG 1500 (20d)



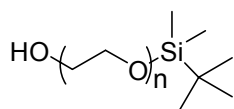
Compound 20d was synthesized from polyethylene glycol PEG 1500 13d (3.6 g, 2.0 mmol), TBDMS-Cl (0.38 g, 2.5 mmol, 1.25 eq.) and imidazole (0.41 g, 6.0 mmol, 3 eq.) in 45 mL dry DMF. For workup the reaction mixture was diluted with DCM (200 mL) and washed with 5% NaHCO₃ (3 x 50 mL), H₂O (4 x 75 mL) and brine (3 x 75 mL), dried over Na₂SO₄ and the solvent removed under reduced pressure. The crude product was purified by column chromatography (EtOH : DCM 1 : 1, preconditioned with the EtOH containing 1% Et₃N, R_f = 0.8 DCM : EtOH 1 : 1) on silica to afford a yellow oil (2.7 g, 70%).

¹H NMR (300 MHz, (CD₃)₂CO, 295 K): δ = 7.33 (m, 9 H, Ar-H), 6.87 (d, *J*(H,H) = 8.9 Hz, 4 H, Ar-H), 3.62 (m, PEG CH₂), 1.1 (t, *J*(H,H) = 7.0 Hz, 9 H, m, PEG CH₂), 0.07 (s, 4 H).

¹³C{¹H} NMR (75 MHz, (CD₃)₂CO, 295 K): δ = 160.3, 147.2, 137.9, 129.8, 129.4, 128.3, 114.7, 87.4, 72.1, 64.9, 56.4, 27.4, 19.7.

MALDI MS: *m/z* 1664.01 [M+Na]⁺ (calculated for [C₈₁H₁₄₂O₃₅Si+K+2H]⁺ 1665.1).

n	Calculated	Found	Calculated	Found	Formula
	[M+K+2H] ⁺	[M+K+2H] ⁺	[M+K+Li] ⁺	[M+K+Li] ⁺	
14	1091.62	1097.6	1096.62	1097.6	C ₅₅ H ₉₀ O ₁₇ Si
15	1135.65	1335.7	1140.65	1141.7	C ₅₇ H ₉₄ O ₂₄ Si
16	1179.68	1185.7	1184.68	1185.7	C ₅₉ H ₉₈ O ₂₅ Si
17	1223.71	1223.7	1228.71	1229.7	C ₆₁ H ₁₀₂ O ₂₆ Si
18	1267.74	1273.8	1272.74	1273.8	C ₆₃ H ₁₀₆ O ₂₆ Si
19	1311.77	1311.8	1316.77	1317.8	C ₆₅ H ₁₁₀ O ₂₇ Si
20	1355.80	1361.8	1360.80	1361.8	C ₆₇ H ₁₁₄ O ₂₈ Si
21	1399.83	1405.9	1404.83	1405.9	C ₆₉ H ₁₁₈ O ₂₉ Si
22	1443.86	1449.9	1448.86	1449.9	C ₇₁ H ₁₂₂ O ₃₀ Si
23	1487.89	1494.0	1492.89	1494.0	C ₇₃ H ₁₂₆ O ₃₁ Si
24	1531.92	1532.0	1536.92	1538.0	C ₇₅ H ₁₃₀ O ₃₂ Si
25	1575.95	1576.0	1580.95	1582.1	C ₇₇ H ₁₃₄ O ₃₃ Si
26	1619.98	1620.0	1624.98	1626.1	C ₇₉ H ₁₃₈ O ₃₄ Si
27	1664.01	1665.1	1669.01	1670.1	C ₈₁ H ₁₄₂ O ₃₅ Si
28	1708.04	1708.1	1713.04	1714.2	C ₈₃ H ₁₄₆ O ₃₆ Si
29	1752.07	1752.2	1757.07	1758.2	C ₈₅ H ₁₅₀ O ₃₇ Si
30	1796.10	1796.2	1801.10	1803.3	C ₈₇ H ₁₅₄ O ₃₈ Si
31	1840.13	1841.2	1845.13	1846.3	C ₈₉ H ₁₅₈ O ₃₉ Si
32	1884.16	1884.3	1889.16	1890.3	C ₉₁ H ₁₆₂ O ₄₀ Si
33	1928.19	1929.3	1933.19	1935.3	C ₉₃ H ₁₆₆ O ₄₁ Si
34	1972.22	1972.3	1977.22	1978.4	C ₉₅ H ₁₇₀ O ₄₂ Si
35	2016.25	2017.4	2021.25	2022.4	C ₉₇ H ₁₇₄ O ₄₃ Si
36	2060.28	2061.4	2065.28	2067.4	C ₉₉ H ₁₇₈ O ₄₄ Si
37	2104.31	2105.4	2109.31	-	C ₁₀₁ H ₁₈₂ O ₄₅ Si
38	2148.34	2149.4	2153.34	-	C ₁₀₃ H ₁₈₆ O ₄₆ Si
39	2192.37	2193.5	2197.37	-	C ₁₀₅ H ₁₉₀ O ₄₇ Si
40	2236.40	2237.5	2241.40	-	C ₁₀₇ H ₁₉₄ O ₄₈ Si
41	2280.43	2281.6	2285.43	-	C ₁₀₉ H ₁₉₈ O ₄₉ Si

t-Butyl dimethylsilyl polyethylene glycol PEG 600 (22c)

PEG 600

General procedure VII

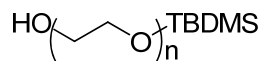
DMT and TBDMS protected PEG 600 **21c** (6.3 g, 6.26 mmol) were dissolved in 143.3 mL 3% TCA in DCE. The reaction mixture was stirred for 5 min at r.t. before it was quenched by 200 mL saturated NaHCO₃ solution and extracted with 250 mL DCM. The combined organic layers were washed with brine (2 x 120 mL), dried over Na₂SO₄ and the solvent removed under reduced pressure. The crude product was purified by column chromatography (gradient EtOAc : MeOH 98 : 2, EtOAc : MeOH : CH₂Cl₂ 77 : 15 : 8) on silica to afford a pale yellow oil (2.2 g, 50%).

¹H NMR (300 MHz, (CD₃)₂CO, 295 K): δ = 3.58 (m, PEG CH₂), 2.82 (s, 1H, OH), 0.90 (s, 9H, C(CH₃)₃), 0.07 (s, 6H, Si(CH₃)₂).

¹³C{¹H} NMR (75 MHz, (CD₃)₂CO, 295 K): δ = 72.26 (PEG CH₂), 64.54 (PEG CH₂), 27.30 (3C, C(CH₃)₃), 19.87 (1C, C(CH₃)₃), -4.06 (2C, Si(CH₃)₂).

MALDI MS: m/z 683.5 [M+Na]⁺ (calculated for C₃₀H₆₄O₁₃Si+Na)⁺ 683.40), m/z 699.5 [M+K]⁺ (calculated for [C₃₀H₆₄O₁₃Si+K]⁺ 699.51).

n	Calculated [M+Na] ⁺	Found [M+Na] ⁺	Calculated [M+K] ⁺	Found [M+K] ⁺	Formula
8	507.28	507.3	523.39	523.3	C ₂₂ H ₄₆ O ₉ Si
9	551.31	551.3	567.42	567.3	C ₂₄ H ₅₀ O ₁₀ Si
10	595.34	595.4	611.45	611.4	C ₂₆ H ₅₄ O ₁₁ Si
11	639.37	639.5	655.48	655.4	C ₂₈ H ₆₀ O ₁₂ Si
12	683.40	683.5	699.51	699.5	C ₃₀ H ₆₄ O ₁₃ Si
13	727.43	727.5	743.54	743.5	C ₃₂ H ₆₈ O ₁₄ Si
14	771.46	771.6	787.57	787.5	C ₃₄ H ₇₂ O ₁₅ Si
15	815.49	815.6	-	-	C ₃₆ H ₇₆ O ₁₆ Si

***t*-Butyl dimethylsilyl polyethylene glycol PEG 600 (22d)**

PEG 1500

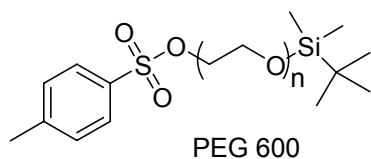
Compound **22d** was synthesized by deprotecting DMT and TBDMS protected PEG 600 **21d** (2.6 g, 1.5 mmol) with 34 mL 3% TCA in DCE for 7.5 min and quenched by 45 mL saturated NaHCO₃ solution and extracted with 55 mL DCM. The combined organic layers were washed with brine (45 mL), dried over Na₂SO₄ and the solvent removed under reduced pressure. The crude product was purified by column chromatography (gradient EtOAc : MeOH 98 : 2, EtOH : CH₂Cl₂ 1 : 1) on silica to afford a white solid (1.7 g, 78 %).

¹H NMR (300 MHz, (CD₃)₂CO, 295 K): δ = 3.58 (m, PEG CH₂), 2.80 (s, 1H, OH), 0.90 (s, 9H, C(CH₃)₃), 0.07 (s, 6H, Si(CH₃)₂).

¹³C{¹H} NMR (75 MHz, (CD₃)₂CO, 295 K): δ = 70.6 (PEG CH₂), 61.3 (PEG CH₂), 25.7 (3C, C(CH₃)₃), 20.7 (1C, C(CH₃)₃), -4.07 (2C, Si(CH₃)₂).

MALDI MS: m/z not observed [M+Na]⁺ (calculated for C₇₀H₁₄₄O₃₂Si+Na)⁺ 1547.93), m/z 1582.3 [M+K+2H]⁺ (calculated for [C₇₀H₁₄₄O₃₂S+K+2H)⁺ 1582.03).

n	Calculated [M+K+2H]⁺	Found [M+K+2H]⁺	Formula
20	1053.67	1053.8	C ₄₆ H ₈₆ O ₂₀ Si
21	1097.7	1097.8	C ₄₈ H ₁₀₀ O ₂₁ Si
22	1141.73	1141.9	C ₅₀ H ₁₀₄ O ₂₂ Si
23	1185.76	1185.9	C ₅₂ H ₁₀₈ O ₂₃ Si
24	1229.79	1229.9	C ₅₄ H ₁₁₂ O ₂₄ Si
25	1273.82	1274.0	C ₅₆ H ₁₁₆ O ₂₅ Si
26	1317.85	1318.0	C ₅₈ H ₁₂₀ O ₂₆ Si
27	1361.88	1362.1	C ₆₀ H ₁₂₄ O ₂₇ Si
28	1405.91	1406.1	C ₆₂ H ₁₂₈ O ₂₈ Si
29	1449.94	1450.1	C ₆₄ H ₁₃₂ O ₂₉ Si
30	1493.97	1494.2	C ₆₆ H ₁₃₆ O ₃₀ Si
31	1538.00	1538.2	C ₆₈ H ₁₄₀ O ₃₁ Si
32	1582.03	1582.3	C ₇₀ H ₁₄₄ O ₃₂ Si
33	1626.06	1626.3	C ₇₂ H ₁₄₈ O ₃₃ Si
34	1670.09	1670.3	C ₇₄ H ₁₅₂ O ₃₄ Si
35	1714.12	1714.3	C ₇₆ H ₁₅₆ O ₃₅ Si
36	1758.15	1758.4	C ₇₈ H ₁₆₀ O ₃₆ Si
37	1802.18	1802.4	C ₈₀ H ₁₆₄ O ₃₇ Si
38	1846.21	1847.4	C ₈₂ H ₁₇₀ O ₃₈ Si
39	1890.24	1891.4	C ₈₄ H ₁₇₄ O ₃₉ Si
40	1934.27	1935.4	C ₈₆ H ₁₇₈ O ₄₀ Si
41	1978.30	1979.4	C ₈₈ H ₁₈₂ O ₄₁ Si
42	2022.33	2023.4	C ₉₀ H ₁₈₆ O ₄₂ Si
43	2066.36	2067.5	C ₉₂ H ₁₉₀ O ₄₃ Si
44	2110.39	2111.5	C ₉₄ H ₁₉₄ O ₄₄ Si
45	2154.42	2154.5	C ₉₆ H ₁₉₈ O ₄₅ Si

***t*-Butyldimethylsilyl polyethylen glycol *p*-toluolsulfonat PEG 600 (23c)****General procedure VIII**

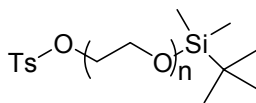
TBDMS protected PEG 600 **22c** (1.7 g, 2.41 mmol) was coevaporated with toluene (3 x 50 mL), dissolved under argon in 15 mL dry DCM. DMAP (14.7 mg, 0.12 mmol, 0.05 eq.) and triethylamine (1.2 mL, 7.23 mmol, 3 eq) were added, cooled down to 0°C in an ice/ water bath to add TsCl (0.51 g, 2.65 mmol, 1.1 eq.). The reaction mixture was allowed to warm up and stirred for 12 h at r.t.. The reaction mixture was diluted with 50 mL EtOAc, washed with 5% NaHCO₃ (2 x 75 mL), H₂O (2 x 50 mL) and brine (2 x 50 mL), dried over Na₂SO₄ and the solvent removed under reduced pressure to yield a pale yellow oil (1.8 g, 87%).

¹H NMR (300 MHz, (CD₃)₂CO, 295 K): δ = 7.82 (d, *J*(H,H) = 8.4 Hz, 2H, Ar-H), 7.49 (d, *J*(H,H) = 8.0 Hz, 2H, Ar-H), 3.58 (m, PEG CH₂), 2.46 (s, 3H, Ar-CH₃), 0.89 (s, 9H, C(CH₃)₃), 0.07 (s, 6H, Si(CH₃)₂).

¹³C{¹H} NMR (75 MHz, (CD₃)₂CO, 295 K): δ = 146.75 (1C, Ar-CH₃), 135.34 (1C, Ar-SO₂), 131.82 (2C, Ar-H), 129.71 (2C, Ar-H), 72.23 (PEG CH₂), 27.28 (3C, C(CH₃)₃), 22.53 (1C, Ar-CH₃), 19.85 (1C, C(CH₃)₃), -4.07 (2C, Si(CH₃)₂).

MALDI MS: *m/z* 837.4 [M+Na]⁺ (calculated for C₃₇H₇₀O₁₅SSi+Na]⁺ 837.41), *m/z* 853.4 [M+K]⁺ (calculated for [C₃₇H₇₀O₁₅SSi+K]⁺ 853.52).

n	Calculated [M+Na] ⁺	Found [M+Na] ⁺	Calculated [M+K] ⁺	Found [M+K] ⁺	Formula
9	705.32	705.3	721.43	721.3	C ₃₁ H ₅₈ O ₁₂ SSi
10	749.35	749.3	765.46	765.3	C ₃₃ H ₆₂ O ₁₃ SSi
11	793.38	793.4	809.49	809.3	C ₃₅ H ₆₆ O ₁₄ SSi
12	837.41	837.4	853.52	853.4	C ₃₇ H ₇₀ O ₁₅ SSi
13	881.44	881.4	897.55	897.4	C ₃₉ H ₇₄ O ₁₆ SSi
14	925.47	925.4	941.58	941.4	C ₄₁ H ₇₈ O ₁₇ SSi
15	969.50	969.4	-	-	C ₄₃ H ₈₂ O ₁₈ SSi

***t*-Butyl dimethylsilyl polyethylene glycol *p*-toluenesulfonate PEG 1500 (23d)**

PEG 1500

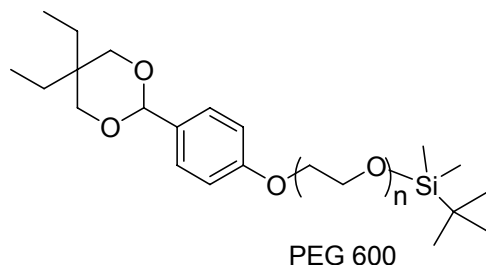
Compound **23d** was synthesized according to general procedure **VIII** from *t*-butyl dimethylsilyl polyethylene glycol PEG 1500 **22d** (1.7 g, 1.04 mmol) in 5.5 mL dry DCM, DMAP (6.3 mg, 0.052 mmol, 0.05 eq.) and TEA (0.44 mL, 3.12 mmol, 3 eq.). For the work up the reaction was diluted with EtOAc (25 mL) and washed with 5% NaHCO₃ (2 x 35 mL), H₂O (2 x 25 mL) and brine (2 x 25 mL) to yield a white solid (1.4 g, 75%).

¹H NMR (300 MHz, (CD₃)₂CO, 295 K): δ = 7.82 (d, *J*(H,H) = 8.4 Hz, 2H, Ar-H), 7.49 (d, *J*(H,H) = 8.0 Hz, 2H, Ar-H), 3.59 (m, PEG CH₂), 2.47 (s, 3H, Ar-CH₃), 0.90 (s, 9H, C(CH₃)₃), 0.07 (s, 6H, Si(CH₃)₂).

¹³C{¹H} NMR (75 MHz, (CD₃)₂CO, 295 K): δ = 146.7 (1C, Ar-CH₃), 136.2 (1C, Ar-SO₂), 131.82 (2C, Ar-H), 129.71 (2C, Ar-H), 72.3 (PEG CH₂), 70.3 (PEG CH₂), 22.5 (3C, C(CH₃)₃), 22.50 (1C, Ar-CH₃), 15.5 (1C, C(CH₃)₃), -4.07 (2C, Si(CH₃)₂).

MALDI MS: *m/z* not observed [M+Na]⁺ (calculated for C₇₇H₁₅₀O₃₅SSi+Na]⁺ 1695.06), *m/z* 1709.2 [M+K]⁺ (calculated for [C₃₇H₇₀O₁₅SSi+2 Li]⁺ 1709.09).

n	Calculated [M+2Li]⁺	Found [M+2Li]⁺	Formula
22	1268.79	1268.8	C ₅₇ H ₁₁₀ O ₂₅ SSi
23	1312.82	1312.8	C ₅₉ H ₁₁₄ O ₂₆ SSi
24	1356.85	1356.8	C ₆₁ H ₁₁₈ O ₂₇ SSi
25	1400.88	1400.9	C ₆₃ H ₁₂₂ O ₂₈ SSi
26	1444.91	1444.9	C ₆₅ H ₁₂₆ O ₂₉ SSi
27	1488.94	1489.0	C ₆₇ H ₁₃₀ O ₃₀ SSi
28	1532.97	1533.0	C ₆₉ H ₁₃₄ O ₃₁ SSi
29	1577.00	1577.1	C ₇₁ H ₁₃₈ O ₃₂ SSi
30	1621.03	1621.1	C ₇₃ H ₁₄₂ O ₃₃ SSi
31	1665.06	1665.1	C ₇₅ H ₁₄₆ O ₃₄ SSi
32	1709.09	1709.2	C ₇₇ H ₁₅₀ O ₃₅ SSi
33	1753.12	1753.2	C ₇₉ H ₁₅₄ O ₃₆ SSi
34	1797.15	1797.3	C ₈₁ H ₁₅₈ O ₃₇ SSi
35	1841.18	1841.3	C ₈₃ H ₁₆₂ O ₃₈ SSi
36	1885.21	1885.3	C ₈₅ H ₁₆₆ O ₃₉ SSi
37	1929.24	1930.4	C ₈₇ H ₁₇₀ O ₄₀ SSi
38	1973.27	1973.4	C ₈₉ H ₁₇₄ O ₄₁ SSi
39	2017.30	2017.4	C ₉₁ H ₁₇₈ O ₄₂ SSi
40	2061.33	2067.3	C ₉₃ H ₁₈₂ O ₄₃ SSi
41	2105.36	2105.3	C ₉₅ H ₁₈₆ O ₄₄ SSi
42	2149.39	2155.3	C ₉₇ H ₁₉₀ O ₄₅ SSi
43	2193.42	2193.4	C ₉₉ H ₁₉₄ O ₄₆ SSi
44	2237.45	2243.4	C ₁₀₁ H ₁₉₈ O ₄₇ SSi

TBDMS protected 2-(4-(5, 5-Diethyl-1, 3-dioxan-2-yl)phenoxy) polyethylene glycol PEG 600 (24c)

General procedure IX

Under argon 4-(5,5-diethyl-1,3-dioxan-2-yl)phenol **19** (0.68 g, 2.88 mmol, 1.8 eq.) were dissolved in 25 mL dry ACN and cooled in an ice/ water bath to 0°C. NaH (128 mg 60% in oil, 3.2 mmol, 2 eq.) were added and the reaction stirred for 10 min at 0 °C before allowing it to warm up to r.t. The reaction mixture was stirred for another 15 min at r.t. before *t*-butyl dimethylsilyl polyethylene glycol *p*-toluenesulfonate PEG 600 **23d** (1.4 g, 1.6 mmol), which had been coevaporated with toluene (3 x 20 mL) was added dropwise *via* a dropping funnel in 50 mL dry ACN. The reaction mixture was stirred for 90 h and diluted with 100 mL DCM, washed with H₂O (3 x 150 mL), 5% NaHCO₃ (3 x 150 mL) and brine (3 x 150 mL), dried over Na₂SO₄ and the solvent removed under reduced pressure. The curd product was purified by column chromatography (gradient EtOAc : EtOH 8 : 2, DCM : EtOH 1 : 1, R_f = 0.48 (Hexan : EtOH 8 : 2)) on silica to afford a pale yellow oil (0.9 g, 61%).

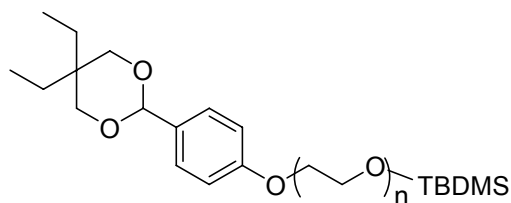
¹H NMR (300 MHz, (CD₃)₂CO, 295 K): δ = 7.37 (d, *J*(H,H) = 8.7 Hz, 2H, Ar-H), 6.92 (d, *J*(H,H) = 8.8 Hz, 2H, Ar-H), 5.36 (s, 1H, CH), 3.57 (m, (PEGCH₂+CH₂O)), 1.80 (q, *J*(H,H) = 7.6 Hz, 2H, CH₂a), 1.15 (q, *J*(H,H) = 7.5 Hz, 2H, CH₂b), 0.90 (s, 9H, C(CH₃)₃), 0.88 (t, *J*(H,H) = 7.6 Hz, 3H, CH₃a), 0.81 (t, *J*(H,H) = 7.6 Hz, 3H, CH₃b), 0.07 (s, 6H, Si(CH₃)₂).

¹³C{¹H} NMR (75 MHz, (CD₃)₂CO, 295 K): δ = 161.08 (1C, Ar-O), 129.73 (1C, Ar-CH), 129.39 (2C, Ar-H), 115.71 (2C, Ar-H), 103.45 (1C, Ar-CH), 76.14 (PEGCH₂), 74.34 (11), 72.26 (PEGCH₂), 36.35 (1C, C), 27.30 (3C, C(CH₃)₃), 25.94 (2C, CH₂O), 24.37 (1C, C(CH₃)₃), 7.91 (2C, CH₃) -4.05 (2C, Si(CH₃)₂).

MALDI MS: m/z 901.5 [M+Na]⁺ (calculated for C₄₄H₈₂O₁₅Si+Na)⁺ 901.53), m/z 917.4 [M+K]⁺ (calculated for [C₄₄H₈₂O₁₅Si+K)⁺ 917.64).

n	Calculated [M+Na] ⁺	Found [M+Na] ⁺	Calculate [M+K] ⁺	Found [M+K] ⁺	Formula
9	769.44	769.4	-	-	C ₃₈ H ₇₀ O ₁₂ Si
10	813.47	813.4	-	-	C ₄₀ H ₇₄ O ₁₃ Si
11	857.50	857.5	873.61	873.4	C ₄₂ H ₇₈ O ₁₄ Si
12	901.53	901.5	917.64	917.4	C ₄₄ H ₈₂ O ₁₅ Si
13	945.56	945.5	961.67	961.5	C ₄₆ H ₈₆ O ₁₆ Si
14	989.59	989.5	-	-	C ₄₈ H ₉₀ O ₁₇ Si
15	1033.62	1033.5	-	-	C ₅₀ H ₉₄ O ₁₈ Si

TBDMS protected 2-(4-(5, 5-Diethyl-1, 3-dioxan-2-yl)phenoxy) polyethylene glycol PEG 1500 (24d)



PEG 1500

Compound **24d** was synthesized according to general procedure **IX** from 4-(5,5-diethyl-1,3-dioxan-2-yl)phenol **19** (130 mg, 0.55 mmol, 1.8 eq.) in 25 mL dry ACN, NaH (13 mg 60% in oil, 0.55 mmol, 1.1 eq.), *t*-butyl dimethylsilyl polyethylene glycol *p*-toluenesulfonate PEG 1500 **23d** (1.4 g, 0.50 mmol) in 12 mL dry ACN. The reaction mixture was stirred for 48 min and diluted with 50 mL DCM, washed with H₂O (3 x 75 mL), 5% NaHCO₃ (3 x 75 mL) and brine (3 x 75 mL), dried over Na₂SO₄ and the solvent removed under reduced pressure. The crude product was purified by column chromatography (gradient EtOAc : EtOH 8 : 2, DCM . EtOH 1 : 1) on silica to afford a white solid (0.9 g, 99%).

¹H NMR (300 MHz, (CD₃)₂CO, 295 K): δ = 7.28 (d, *J*(H,H) = 8.5 Hz, 2H, Ar-H), 6.81 (d, *J*(H,H) = 8.5 Hz, 2H, Ar-H), 5.62 (s, 1H, CH), (s, 1H), 3.59 (m, (PEGCH₂+CH₂O)), 1.80 (q, *J*(H,H) = 7.6 Hz, 2H, CH₂a), 1.15 (q, *J*(H,H) = 7.6 Hz, 2H, CH₂b),), 0.90 (s, 9H, C(CH₃)₃), 0.88 (t, *J*(H,H) = 7.6 Hz, 3 H, CH₃a), 0.81 (t, *J*(H,H) = 7.6 Hz, 3 H CH₃b), 0.07 (s, 6H, Si(CH₃)₂).

$^{13}\text{C}\{^1\text{H}\}$ NMR (75 MHz, $(\text{CD}_3)_2\text{CO}$, 295 K): $\delta = 159.4$ (1C, Ar-O), 131.7 (1C, Ar-CH), 129.3 (2C, Ar-H), 116.3 (2C, Ar-H), 103.5 (1C, Ar-CH), 75.9 (PEGCH₂), 72.1 (PEGCH₂), 36.2 (1C, C), 25.8 (3C, C(CH₃)₃), 24.2 (2C, CH₂O), 22.4 (1C, C(CH₃)₃), 8.7 (2C, CH₃) -4.05 (2C, Si(CH₃)₂).

MALDI MS: m/z 1758.1 $[\text{M}]^+$ (calculated for $\text{C}_{84}\text{H}_{162}\text{O}_{35}\text{Si}^+$ 1759.18), m/z 1774.4 $[\text{M}+2\text{Li}]^+$ (calculated for $[\text{C}_{84}\text{H}_{82}\text{O}_{15}\text{Si}+2\text{Li}]^+$ 1773.22), m/z 1780.5 $[\text{M}+\text{Na}]^+$ (calculated for $[\text{C}_{44}\text{H}_{82}\text{O}_{15}\text{Si}+\text{Na}]^+$ 1782.18).

n	Calculated $[\text{M}]^+$	Found $[\text{M}]^+$	Calculated $[\text{M}+2\text{Li}]^+$	Found $[\text{M}+2\text{Li}]^+$	Calculated $[\text{M}+\text{Na}]^+$	Found $[\text{M}+\text{Na}]^+$	Formula
20	1230.82	1229.9	1244.86	-	1253.82	1251.9	$\text{C}_{60}\text{H}_{114}\text{O}_{23}\text{Si}$
21	1274.85	1273.9	1288.89	-	1297.85	1295.9	$\text{C}_{62}\text{H}_{118}\text{O}_{24}\text{Si}$
22	1318.88	1317.9	1332.92	-	1341.88	1339.9	$\text{C}_{64}\text{H}_{122}\text{O}_{25}\text{Si}$
23	1362.91	1362.0	1376.95	-	1385.91	1384.0	$\text{C}_{66}\text{H}_{126}\text{O}_{26}\text{Si}$
24	1406.94	1406.0	1420.98	-	1429.94	1428.0	$\text{C}_{68}\text{H}_{130}\text{O}_{27}\text{Si}$
25	1450.97	1450.1	1465.01	-	1473.97	1472.1	$\text{C}_{70}\text{H}_{134}\text{O}_{28}\text{Si}$
26	1495.00	1494.1	1509.04	1510.1	1518.00	1516.2	$\text{C}_{72}\text{H}_{138}\text{O}_{29}\text{Si}$
27	1539.03	1538.1	1553.07	1554.1	1562.03	1560.3	$\text{C}_{74}\text{H}_{142}\text{O}_{30}\text{Si}$
28	1583.06	1582.2	1597.10	1599.2	1606.06	1604.3	$\text{C}_{76}\text{H}_{146}\text{O}_{31}\text{Si}$
29	1627.09	1626.3	1641.13	1642.3	1650.09	1648.3	$\text{C}_{78}\text{H}_{150}\text{O}_{32}\text{Si}$
30	1671.12	1670.3	1685.16	1686.3	1694.12	1692.4	$\text{C}_{80}\text{H}_{154}\text{O}_{33}\text{Si}$
31	1715.15	1714.3	1729.19	1730.4	1738.15	1736.4	$\text{C}_{82}\text{H}_{158}\text{O}_{34}\text{Si}$
32	1759.18	1758.1	1773.22	1774.4	1782.18	1780.5	$\text{C}_{84}\text{H}_{162}\text{O}_{35}\text{Si}$
33	1803.21	1802.4	1817.25	1819.4	1826.21	1824.5	$\text{C}_{86}\text{H}_{166}\text{O}_{36}\text{Si}$
34	1847.24	1846.5	1861.28	1868.5	1870.24	1868.5	$\text{C}_{88}\text{H}_{170}\text{O}_{37}\text{Si}$
35	1891.27	1890.5	1905.31	1906.6	1914.27	1912.6	$\text{C}_{90}\text{H}_{174}\text{O}_{38}\text{Si}$
36	1935.30	1934.6	1949.34	1951.6	1958.30	1956.6	$\text{C}_{92}\text{H}_{178}\text{O}_{39}\text{Si}$
37	1979.33	1978.6	1993.37	1995.6	2002.33	1998.6	$\text{C}_{94}\text{H}_{182}\text{O}_{40}\text{Si}$
38	2023.36	2022.7	2037.40	2039.7	2046.36	2043.7	$\text{C}_{96}\text{H}_{186}\text{O}_{41}\text{Si}$
39	2067.39	2066.7	2081.43	2083.7	2090.39	2087.2	$\text{C}_{98}\text{H}_{190}\text{O}_{42}\text{Si}$
40	2111.42	2107.8	2125.46	2127.7	2134.42	2130.7	$\text{C}_{100}\text{H}_{194}\text{O}_{43}\text{Si}$
41	2155.45	2151.8	2169.49	2171.7	2178.45	2175.8	$\text{C}_{102}\text{H}_{198}\text{O}_{44}\text{Si}$
42	2199.48	2195.8	2213.52	2215.7	2222.48	-	$\text{C}_{104}\text{H}_{202}\text{O}_{45}\text{Si}$
43	2243.51	2239.9	2257.55	2259.8	2266.51	-	$\text{C}_{106}\text{H}_{206}\text{O}_{46}\text{Si}$
44	2287.54	2283.9	2301.58	2303.8	2310.54	-	$\text{C}_{108}\text{H}_{210}\text{O}_{47}\text{Si}$

Deprotection of 2-(4-(5, 5-Diethyl-1, 3-dioxan-2-yl)phenoxy) polyethylene glycol (25c / d)**Procedure A**

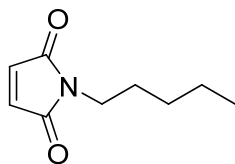
2-(4-(5, 5-Diethyl-1, 3-dioxan-2-yl)phenoxy) polyethylene glycol **25c/d** (0.9g, 0.59 mmol) was stirred in 1 M TBAF in THF (1.18 mL, 1.18 mmol, 2 eq.) for 1 h at r.t. and evaporated to dryness. The crude product was purified with column chromatography (gradient EtOAc : EtOH 8 : 2, DCM : EtOH 1 : 1) on silica followed by ion exchange column to exchange TBA⁺ against Na⁺ ions, followed by another column chromatography (gradient EtOAc : Hex : DCM 7 : 2 : 1, DCM : EtOH 1 : 1). MALDI-TOF analysis revealed that the product had only partially been deprotected.

Procedure B

2-(4-(5, 5-Diethyl-1, 3-dioxan-2-yl)phenoxy) polyethylene glycol **25c/d** (20 mg, 0.013 mmol) was stirred with 3 HF x TEA (32 μ L, 0.320 mmol), 0.6 mL THF and 0.1 mL TEA for 24 h. The reaction mixture was diluted with 15 mL EtOAc (15 ml) washed with saturated NaHCO₃-solution (3 x 25 mL) dried over Na₂SO₄ and the solvent removed under reduced pressure. MALDI-TOF MS analysis confirmed that the product had only partially been deprotected.

6.4 Synthetic procedures for compounds chapter 4

N-Pentylmaleimide (31b)



General procedure X

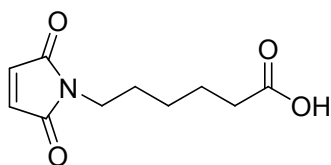
N-Pentylamine **30b** (6.7 mL, 57.48 mmol) and maleic anhydride **29** (6.2 g, 63.23 mmol 1.1 eq.) were suspended in 320 mL toluene and stirred at 30°C for 1h. Hexamethyldisilazane (HMDS) (10.58 mL, 86.22 mmol, 1.5 eq.) in 35 mL toluene and ZnBr₂ (14.24 g, 63.23 mmol, 1.1 eq.) were added and the reaction mixture refluxed for 3 h. The heating source was removed and the mixture stirred over night. The reaction mixture was poured into 150 mL 0.5 M HCl. The organic layer was separated and the aqueous phase was re-extracted with EtOAc (2x 170 mL). The combined organic layers were washed with saturated NaHCO₃ (2 x 170 mL) and brine (2 x 170 mL), dried over Na₂SO₄ and the solvent was removed under reduced pressure. The crude product was purified by column chromatography (DCM : MeOH 99 : 1, R_f = 0.68) on silica to afford a slightly brown crystalline solid (7.88 g, 82%).

C₉H₁₃NO₂ (167.09 g mol⁻¹).

¹H NMR (300 MHz, CDCl₃, 295 K): δ = 6.67 (s, 2 H, CH), 3.49 (t, *J*(H,H) = 7.5 Hz, 2H, NCH₂), 1.58 (quint., *J*(H,H) = 7.5 Hz, 2H, CH₂), 1.28 (m, 4H, CH₂), 0.87 (t, *J*(H,H) = 7.2 Hz, 2H, CH₂).

¹³C{¹H} NMR (75 MHz, CDCl₃, 295 K): δ = 170.85 (2C, CO), 134.08 (2C, CH), 37.86 (1C, CH₂), 28.81 (1C, CH₂), 28.17 (1C, CH₂), 22.16 (1C, CH₂), 13.88 (1C, CH₃).

HR-ESI MS: 168.1019 m/z [M]⁺ (calculated for [C₉H₁₃NO₂]⁺ 167.09).

6-Maleimidocaproic acid (31c)

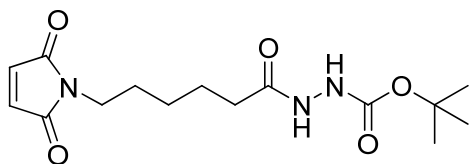
Analogue to general procedure **X** aminocaproic acid **31a** (2.6 g, 20.4 mmol) and maleic anhydride **29** (2.2 g, 22.4 mmol 1.1 eq.), suspended in a mixture of 110 mL toluene and 60 mL ACN were reacted with HMDS (3.75 mL, 30.6 mmol, 1.5 eq.) in 10 mL toluene and ZnBr₂ (5 g, 22.4 mmol, 1.1eq.). Work up was carried out as described accept the aqueous phase was acidified with concentrated HCl before extraction. A white solid was obtained (3.5 g, 74%).

C₁₀H₁₃NO₄ (211.08 g mol⁻¹).

¹H NMR (300 MHz, CDCl₃, 295 K): δ = 11.28 (s, 1H, OH), 6.67 (s, 2 H, CH), 3.49 (t, *J*(H,H) = 7.2 Hz, 2H, NCH₂), 2.32 (t, *J*(H,H) = 7.5 Hz, 2H, CH₂), 1.61 (m, 4H, CH₂), 1.31 (m, 2H, CH₂).

¹³C{¹H} NMR (75 MHz, CDCl₃, 295 K): δ = 179.33 (2C, COOH), 170.83 (2C, CO), 134.04 (2C, CH), 37.56 (1C, CH₂), 33.71 (1C, CH₂), 28.13 (1C, CH₂), 26.08 (1C, CH₂), 24.06 (1C, CH₃).

HR-ESI MS: 210.0791 m/z [M] (calculated for [C₁₀H₁₃NO₄] 211.08).

Boc-protected 6-maleimidocaproic acid (32)

6-Maleimidocaproic acid **31a** (500 mg, 2.39 mmol) was dissolved in 30 mL acetonitrile and *N*-Ethyl-*N'*-(3-dimethylaminopropyl)carbodiimide hydrochloride (EDC-HCl) (504 mg, 2.63 mmol, 1.1 eq.) and *t*-butyl carbazate (379 mg, 2.87 mmol, 1.2 eq.) were added and stirred over night. The reaction mixture was separated between EtOAc (25 mL) and 0.5 M HCl (25 mL). The combined organic layers were washed with H₂O (3 x 25 mL) and brine (3 x 25 mL), dried over Na₂SO₄ and the solvent removed under reduced pressure. The crude product was

purified by column chromatography (pure EtOAc, $R_f = 0.7$) on silica to afford a yellow oil (310 mg, 61%).

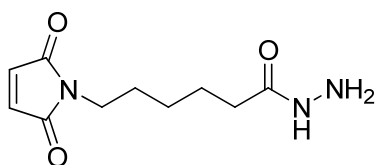
$C_{15}H_{23}N_3O_5$ (325.16 g mol⁻¹).

¹H NMR (300 MHz, CDCl₃, 295 K): $\delta = 7.20$ (s, 1H, NH), 6.67 (s, 2 H, CH), 6.46 (s, 1H, NH), 3.50 (t, $J(H,H) = 7.2$ Hz, 2H, NCH₂), 2.21 (t, $J(H,H) = 4.5$ Hz, 2H, CH₂), 1.79 (m, 2H, CH₂), 1.60 (m, 2H, CH₂), 1.47 (s, 9H, CH₃), 1.35 (m, 2H, CH₂).

¹³C{¹H} NMR (75 MHz, CDCl₃, 295 K): $\delta = 172.14$ (1C, CH₂CONH), 170.84 (2C, CO), 155.40 (1C, COC(CH₃)₃), 134.04 (2C, CH), 81.83 (1C, C(CH₃)₃), 37.50 (1C, CH₂), 33.77 (1C, CH₂), 28.25 (1C, CH₂), 28.14 (3C, CH₃)₃, 26.14 (1C, CH₂), 24.51(1C, CH₂).

MALDI MS: m/z 348.0 [M]⁺ (calculated for [C₁₅H₂₃N₃O₅+Na]⁺ 348.15).

6-Maleimidocaproic acid hydrazide (33)



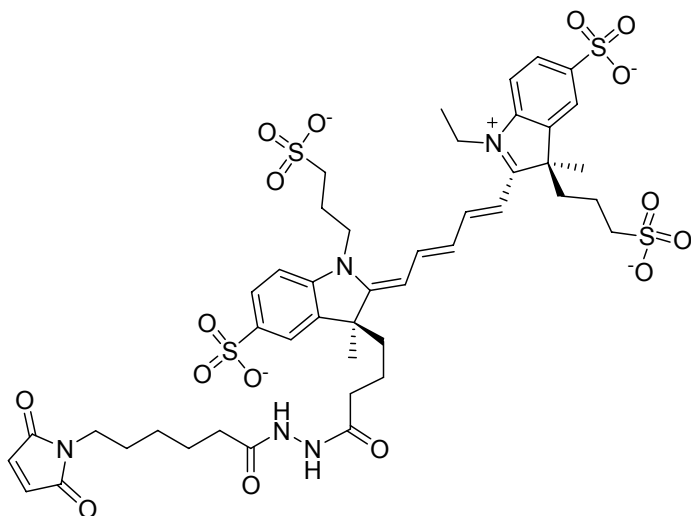
Boc-protected 6-maleimidocaproic acid hydrazide **32** (269 mg, 2.39 mmol) was dissolved in dichloromethane under semi dry conditions and cooled on an ice bath. TFA was added to a 10% v/v and the reaction mixture was allowed to warm up to r.t., stirred for 17 h and evaporated to yield a yellow solid, the reaction could not be further purified and yielded the TFA salt, which has a molecular weight of 339.10 g mol⁻¹ (395 mg, 93%).

$C_{10}H_{15}N_3O_3$ (225.11 g mol⁻¹).

¹H NMR (300 MHz, CDCl₃, 295 K): $\delta = 9.18$ (s, 1H, NH), 6.69 (s, 2 H, CH), 6.49 (s, 1H, NH), 3.51 (m, 2H, NCH₂), 2.35 (m, 2H, CH₂), 1.74 (m, 4H, CH₂), 1.31 (m, 2H, CH₂).

¹³C{¹H} NMR (75 MHz, CDCl₃, 295 K): $\delta = 171.04$ (1C, CH₂CONH), 170.97 (2C, CO), 134.09 (2C, CH), 37.32 (1C, CH₂), 33.63 (1C, CH₂), 27.83 (1C, CH₂), 25.77 (1C, CH₂), 24.33(1C, CH₂).

MALDI MS: m/z 248.0 [M+Na]⁺ (calculated for [C₁₅H₂₃N₃O₅+Na]⁺ 248.10).

DY 649 as maleimidocaproic acid hydrazide (34)

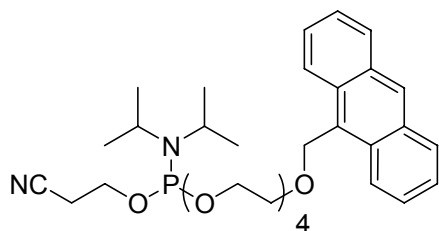
A stock solution of 6-maleimidocaproic acid hydrazide was prepared in abs. DMF. 10 μL 6-maleimidocaproic acid hydrazide (1.984 μmol , 2.0 eq.) of this solution were transferred into a solution of the DY 649 NHS ester (0.992 μmol) in 50 μL DMF. 1.38 μL triethylamine (9.92 μmol , 10 eq.) were added and the reaction vial placed in a thermo shaker at 650 rpm at 25°C for 1 h. MALDI-TOF analysis showed that no reaction had taken place. 0.28 μL DIPEA (2.96 μmol , 3 eq.) were added and the reaction incubated for additional 36 h at 25°C. The progress of the reaction was monitored by MALDI-TOF analysis. After 36 h most of the product had reacted but starting material could still be observed as well as some hydrolysis product of the dye. The reaction was evaporated and purified by semi-preparative HPLC chromatography. The integrity of the dye was only determined by HPLC and mass analysis, because the reaction was only performed in mg scale.

$\text{C}_{45}\text{H}_{54}\text{N}_5\text{O}_{16}\text{S}_4^{3-}$ (1049.20 g mol^{-1}).

MS HR-ESI: m/z 1049.2528 $[\text{M}]^+$ (calculated for $[\text{C}_{45}\text{H}_{54}\text{N}_5\text{O}_{16}\text{S}_4^{3-}]^+$ 1049.20), m/z 1071.2352 $[\text{M}+\text{K}]^+$ (calculated for $[\text{C}_{45}\text{H}_{54}\text{N}_5\text{O}_{16}\text{S}_4^{3-}+\text{Na}]^+$ 1072.19).

HPLC: Phenomenex® Luna 5 μm C18 (4.6 \times 250 mm), 1 mL/min, 25 °C, t_{R} = 8 min, λ local max 256 nm.

Time [min]	Acetonitrile [%]
0	5
25	40
30	100
35	100

ATEG-(β -cyanoethyl-*N,N*-diisopropylphosphoramidite) (27a)**General procedure XI**

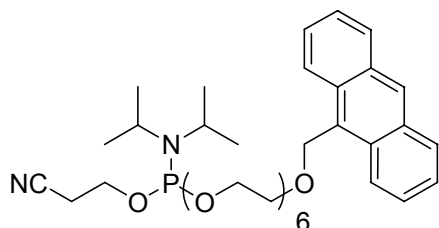
ATEG (190 mg, 0.40 mmol) was suspended in 3 mL of dichloromethan under argon and ethyl diisopropylamine (224 μ L, 1.28 mmol, 3 eq.) were added. The mixture was cooled to 0°C in an ice /water bath before addition of 2-cyanoethyl-*N,N*-diisopropylchlorophosphoramidite (93 μ L, 0.42 mmol, 1.04 eq.). The reaction mixture was stirred for 1 h, during which the temperature was slowly raised to r.t. and followed closely by TLC. After about 1 h the reaction mixture was directly submitted to column chromatography (pure EtOAc, R_f = 0.4) afford afforded the clean product as yellow oil (178 mg, 71%).

$C_{32}H_{45}N_2O_6P$ (584.31 g mol⁻¹).

¹H NMR (500 MHz, CDCl₃, 295 K): δ = 8.43 (m, 3H, Ar-H), 8.01 (m, 2H, Ar-H), 7.53 (m, 2H, Ar-H), 7.47 (m, 2H, Ar-H), 5.55 (s, 2H, CH₂Ar), 3.80-6.62 (m, 22H, PEG CH₂, CH₂ and CH), 1.16 (m, 12 H, CH₃).

³¹P NMR (500 MHz, CDCl₃, 295 K): δ = 148.48 (s).

MALDI MS: m/z 623.3 [M+K]⁺ (calculated for [C₃₂H₄₅N₂O₆P +K]⁺ 623.47).

AHEG-(β -cyanoethyl-*N,N*-diisopropylphosphoramidite)

Compound **27b** was synthesized according to general procedure **XI** AHEG (260 mg, 0.55 mmol), ethyl diisopropylamine (290 μ L, 1.65 mmol, 3 eq.) and 2-cyanoethyl-*N,N*-diisopropylchlorophosphoramidite (150 μ L, 0.66 mmol, 1.2 eq.) to yield a clean product after column chromatography (pure EtOAc, R_f = 0.7) as yellow oil (309 mg, 84%).

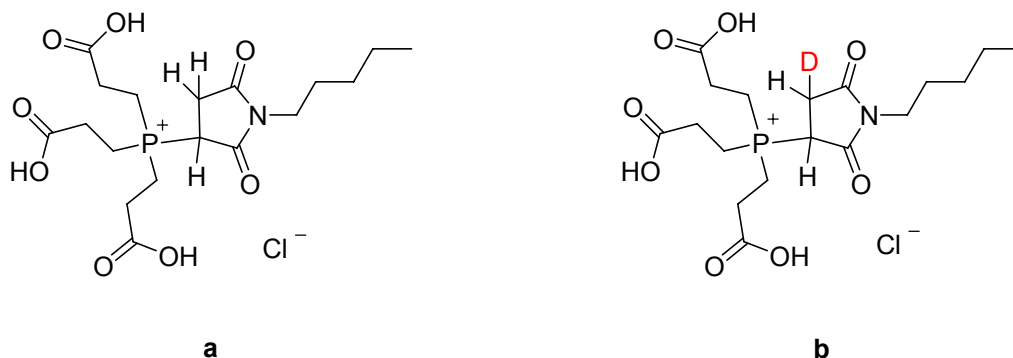
$C_{36}H_{53}N_2O_8P$ (672.47 g mol⁻¹).

¹H NMR (500 MHz, CDCl₃, 295 K): δ = 8.43 (t, $J(H,H)$ = 6.6 Hz, 3H, Ar-H), 8.00 (d, $J(H,H)$ = 5.6 Hz, 2H, Ar-H), 7.54 (m, 2H, Ar-H), 7.47 (m, 2H, Ar-H), 5.55 (s, 2H, CH₂Ar), 3.80-6.61 (m, 22H, PEG CH₂, CH₂ and CH), 1.17 (m, 12 H, CH₃).

¹³C{¹H} NMR (75 MHz, CDCl₃, 295 K): δ = 172.14 (1C, CH₂CONH), 170.84 (2C, CO), 155.40 (1C, COC(CH₃)₃), 134.04 (2C, CH), 81.83 (1C, C(CH₃)₃), 37.50 (1C, CH₂), 33.77 (1C, CH₂), 28.25 (1C, CH₂), 28.14 (3C, CH₃)₃, 26.14 (1C, CH₂), 24.51 (1C, CH₂).

³¹P NMR (500 MHz, CDCl₃, 295 K): δ = 148.48 (s).

MALDI MS: m/z 673.4 [M+1]⁺ (calculated for [C₃₆H₅₃N₂O₈P+1]⁺ 673.41), m/z 695.4 [M+Na]⁺ (calculated for [C₃₆H₅₃N₂O₈P+Na]⁺ 695.41).

Addition-product tris(2-carboxyethyl)phosphine and *N*-pentylmaleimide (35a/b)

Tris(2-carboxyethyl)phosphine hydrochloride (17.15 mg, 59.85 μmol) was dissolved in 1 mL water, respectively deuterium oxide and *N*-pentylmaleimide (10 mg, 59.85 μmol) was added, vortexed well and placed in a thermo shaker for 1 h at 25°C and 650 rpm, to best mimic the reaction conditions in the labeling reaction. The reaction in water was lyophilized and dissolved in deuterium oxide for NMR analysis, while from the reaction in D₂O 700 μL were directly submitted to NMR analysis. The remaining reaction mixture was lyophilized and submitted to mass analysis.

35a:

C₁₈H₂₉NO₈P (418.16 g mol⁻¹).

¹H NMR (500 MHz, D₂O, 295 K): δ = 3.55 (t, $J(\text{H,H})$ = 7.0 Hz, 3H, CH₂N), 3.37 (m, 1H, CHP), 2.89 (m, 14H, CH₂), 1.57 (quint., $J(\text{H,H})$ = 7.5 Hz, 2H, CH₂), 1.29 (m, 4 H, CH₂), 0.87 (t, $J(\text{H,H})$ = 7.5 Hz, 3H, CH₃).

¹³C{¹H} NMR (75 MHz, D₂O, 295 K): δ = 176.17 (1C, COOH), 174.23 (1C, CO), 173.14 (1C, CO), 39.96 (1C, CH₂), 29.31 (1C, CH), 26.18 (1C, CH₂), 25.93 (1C, CH₂), 25.90 (1C, CH₂), 21.44 (1C, CH₂), 14.62 (1C, CH₂), 14.22 (1C, CH₂), 13.07 (1C, CH₃).

³¹P NMR (500 MHz, D₂O, 295 K): δ = 39.12 (s).

HR-ESI MS: 418.1550 m/z [M] (calculated for [C₁₈H₂₉NO₈P] 418.1625).

35b:

C₁₈H₂₈DNO₈P (419.17 g mol⁻¹).

¹H NMR (500 MHz, D₂O, 295 K): δ = 3.55 (t, $J(\text{H,H})$ = 7.0 Hz, 3H, CH₂N), 3.37 (m, 1H, CHP), 2.87 (m, 14H, CH₂), 1.57 (quint., $J(\text{H,H})$ = 7.5 Hz, 2H, CH₂), 1.29 (m, 4 H, CH₂), 0.87 (t, $J(\text{H,H})$ = 7.5 Hz, 3H, CH₃),

¹³C{¹H} NMR (75 MHz, D₂O, 295 K): δ = 176.17 (1C, COOH), 174.21 (1C, CO), 173.15 (1C, CO), 39.96 (1C, CH₂), 28.25 (1C, CH), 26.19 (1C, CH₂), 25.91 (1C, CH₂), 25.88 (1C, CH₂), 21.44 (1C, CH₂), 14.61 (1C, CH₂), 14.21 (1C, CH₂), 13.07 (1C, CH₃).

³¹P NMR (500 MHz, D₂O, 295 K): δ = 39.12 (s).

HR-ESI MS: 419.1611 m/z [M] (calculated for [C₁₈H₂₈DNO₈P] 419.1688).

6.5 Oligonucleotides, buffers and material

Oligonucleotides

Oligonucleotides were either synthesized by automated solid-phase synthesis on an Expedite 8909 automated synthesizer by Applied Biosystems or ordered from IBA (Goettingen, Germany), NOXXON (Berlin, Germany), Eurofins MWG Operon (Ebersberg, Germany) or CSS – Chemical Synthesis Services (East Lothian, Scotland).

Purchased oligonucleotides were HPLC purified and in case of the 49mer Diels-Alderase ribozyme desalted.

49 nt Ribozyme:

wt

5'- GGA GCU CGC UUC GGC GAG GCC GUG CCA GCU CUU CGG AGC AAU ACU CGG C -3'

Mutants

5'- GGA GCU CGC UUC GGC GAG GCC GUG CCA GCU CUU CGG AGC AA**C** ACU CGG C -3'

5'- GGA GCU CGC UUC GGC GAG GCC GUG CCA GCU CUU CGG AGC AA**iC** ACU CGG C -3'

49 nt Ribozym as bipartite system:

38 nt: 5'- GGG CGA GGC CGU GCC AGC UCUUCGGAGCAAUACUCGGC -3'

11 nt: 5'- GGA GCU CGC CC -3'

11 nt modified:

5'- AHEG-GGA GCU CGC CC -3'

Primers:

Primer A

5'-TCT AAT ACG ACT CAC TAT AGG AGC TCA GCC TTC ACT GC -3'

Primer B

5'-GTG GAT CCG ACC GTG GTG CC -3'

109 nt ssDNA pool with randomized 70 nt region

5'-GGA GCT CAG CCT TCA CTG C- N₇₀-GGC ACC ACG GTC GGA TCC AC-3'

128 nt dsDNA pool with randomized 70 nt region and promoter region

5'- TCT AAT ACG ACT CAC TAT AGG GGA GCT CAG CCT TCA CTG C- N₇₀-GGC ACC ACG GTC
GGA TCC AC-3'

25 nt sense

5'- TCT AAT ACG ACT CAC TAT AGG AGC TCA GCC TAC GAG CCT GAG CC-3'

25 nt antisense

5'- GGC TCA GGC TCG TAG GCT GAG CTC CTA TAG TGA GTC GTA TTA GA-3'

Transcript

5'-GG AGC UCA GCC UAC GAG CCU GAG CC-3'

19 nt sense

5' - GGA GCT CAG CCT TCA CTG C -3'

19 nt antisense

5' -GCA GTG AAG GCT GAG CTC C -3'

Modified 19 nt

5' **AHEG**-GGA GCT CAG CCT TCA CTG C-3'

5' **SH C₆**- GGA GCT CAG CCT TCA CTG C -3'

15 nt sense

5' -GTA CAG TCT GAA GTG-3'

15 nt antisense

5' -CAC TTC AGA CTG TAC-3'

Modified 15 nt

5' **AHEG**-GTA CAG TCT GAA GTG-3'

5' **ATEG**-GTA CAG TCT GAA GTG-3'

5' **SH C₆**-GTA CAG TCT GAA GTG-3'

5' **AHEG**-GTA CAG TCT GAA GTG- **SH C₃** 3'

Standard buffers

Diels-Alderase buffer	30 mM Tris HCl pH 7.4 300 mM NaCl 80 mM MgCl ₂
Transcription buffer	40 mM Tris HCl pH 8.1 22 mM MgCl ₂ 1 mM Spermidine 0.01 % Triton X-100
Buffer A	0.1 M TEAA pH 7.0
Buffer B	0.1 M TEAA pH 7.0 80% ACN
Caccodylate buffer	50 mM Sodium Cacodylate pH 7.5
Loading buffer denaturing standard	90% Formamide 9.8% TBE 0.1% Xylencyanol 0.1% Bromphenol blue
Stopmix standard	100 mM β -Mercaptoethanol 20 mM EDTA 80% Formamide

Enzymes

T7 RNA polymerase	In-house
T4 Polynucleotide Kinase (T4 PNK)	Fermentas, St. Leon-Rot
T4 RNA Ligase	Fermentas, St. Leon-Rot
BioTherm DNA-Polymeras, 5 u / μ l	Rapidozym, Berlin
dNTPs	Rapidozym, Berlin
radioactive nucleotides	Hartmann Analytic, Braunschweig

Standard reagents

UltraPure™ Agarose	Invitrogen, Karlsruhe
High resolution Agarose	Invitrogen, Karlsruhe
Ethidium bromide solution	Carl-Roth, Karlsruhe
SYBR®Gold	Molecular Probes®, Invitrogen,
GeneRuler™ 100 bp DNA Ladder	Fermentas, St. Leon-Rot
GeneRuler™ Ultra Low Range DNA Ladder	Fermentas, St. Leon-Rot
Rotiphorese® Ready-to-Use Gel Solutions	Carl Roth, Karlsruhe

Kits and devices

DyeEx 2.0 Spin Kit 250	Qiagen, Hilden
Eppendorf tubes	siliconized Carl Roth, Karlsruhe
Filtertips	Sarstedt, Nümbrecht
Greiner tubes	Greiner Bio-One, Frickenhausen
Nanaosep® MF Centrifugal Devices	PALL® Life Science
NAP columns	Sephadex G-25 GE Healthcare
PCR tubes	Thermo Scientific, Schwerte
PCR wells	Thermo Scientific, Schwerte
QIAquick PCR Purification Kit	Qiagen, Hilden
RNeasy MinElute Cleanup Kit	Qiagen, Hilden
TranscriptAid™ T7 High Yield Transcription Kit	Fermentas, St. Leon-Rot
ZipTip	Millipore, Schwalbach

Instruments

Analytical balance	AX 204 and B3001-S Mettler Toledo
Centrifuges	Eppendorf 5804 R and Mikro 120 Hettich
Electrophoresis chamber	GIBCO BRL Sequencing System
Freeze dryer	BenchTop K Series, VirTis Ismatec
Gel Documentation equipment	AlphaImager TM 2200 Alpha Innotech
Flourescence spectrometer	Jasco
HPLC	Agilent 1100 Series
HPLC Columns	Luna C18, 5 μ m, 4.6 250 mm and 15.0 \times 250 mm
IntelliFlash 310	Varian
Mass Spectrometer	MALDI-TOF Bruker BIFLEX III
	FAB and EI JEOL JMS-700
	Bruker MicroTOF-QII
	LIFDI JEOL JMS-700 magnetic sector
Minicentrifuges	Kiesker
NMR Spectrometer	Mercury Plus 300, Varian VNMR S 500
pH-Meter	MP 220 Mettler Toledo
Phosphorimager	Typhoon 9400 Amersham Biosciences
Pipettes Abimed	P2, P20, P200, P1000
Scintillation counter	Beckman LS 6500
Speed vac	Univapo 100 ECH
Synthesizer	Applied Biosystems Expedite TM 8909
Syringe filters PTFE	13 mm, 0.2 μ m, Carl Roth
Thermomixer	Eppendorf, Thermomixer 5436
Ultrapure Water Purification System	Milli-Q, Millipore
UV Cuvettes Quarzglas	HELLMA
UV-Lamp 254 nm	Benda NU-8 KL
UV-Transilluminator	254 nm, 300 \times 200 mm Carl Roth
UV/VIS Spectrophotometer	Ultrospec 2100 pro Amersham
	NanoDrop ND-1000 Peqlab Biotechnologie
	Cary 100 Bio Varian

6.6 List of Abbreviations

A	Adenosine; Peak area
Å	Ångström
A ₂₆₀	Absorbance at 260 nm
Ac	Acetyl
ACN	Acetonitrile
AHEG	9-anthracenylmethyl hexaethylene glycol
APS	Ammonium persulfate
ATEG	9-anthracenylmethyl tetraethylene glycol
ATP	Adenosine-5'-triphosphate
Boc	<i>tert</i> -butyloxycarbonyl
br	Broad (IR)
BSA	Bovine serum albumin
Bu	Butyl
c	Concentration
C	Cytidine
cDNA	Complementary DNA
CEP-Cl	2-Cyanoethyl diisopropylphosphoramidochloridite
Ci	Curie; 1Ci = 37 MBq
CPG	Controlled pore glass
cpm	Counts per minute (radioactive decay)
CTP	Cytidine-5'-triphosphate
Cy3/5	Cyanine 3/5
d	Doublet (NMR)
DAD	Diode array detector
DCI	4,5-Dicyanoimidazole
DCM	Dichloromethane
DEA	Diethylamine
DIPA	Diisopropylamine
DMAP	4-(Dimethylamino)pyridine
DMF	<i>N,N'</i> -Dimethylformamide
DMSO	Dimethyl sulfoxide
DMT	4,4'-Dimethoxytrytil
DNA	Deoxyribonucleic acid
dNTP	Deoxynucleoside 5'-triphosphate
ds	Double stranded
DTT	dithiothreitol
EA	Ethyl acetate
EDC-HCl	<i>N</i> -(3-Dimethylaminopropyl)- <i>N'</i> -ethylcarbodiimide hydrochloride

EDTA	Ethylenediaminetetraacetic acid
EI	Electron impact
EPR	Electron paramagnetic resonance
equiv	Equivalent
ESI	Electro spray ionization
EtBr	Ethidium bromide
EtOH	Ethanol
FAB	Fast atomic bombardment
FAD	Fluorescence array detector
FRET	Förster resonance energy transfer
FT-ICR	Fourier-transform ion cyclotron resonance
FW	Formula weight (Molecular weight)
g	Gram
G	Guanosine
GMP	Guanosine-5'-monophosphate
GTP	Guanosine-5'-triphosphate
h	Hour
HEPES	4-(2-Hydroxyethyl)-1-piperazineethanesulfonic acid
Hex	Hexane
HOMO	Highest-energy occupied molecular orbital
HPLC	High Performance Liquid Chromatography
Hz	Hertz
<i>i</i>	iso
I	Light intensity
<i>I</i>	Spin quantum number
IR	Infrared
<i>J</i>	Coupling constant
<i>K</i>	Reaction rate constant
<i>l</i>	Length of the light path
L	Liter
LIFDI	liquid injection field desorption ionization
LUMO	lowest-energy unoccupied molecular orbital
m	Multiplet (NMR), medium (IR), meter
M	Mol/L; Molar
m.p.	melting point
M ⁺	molecular ion (MS)
mA	Milli Ampere
MALDI-TOF	Matrix assisted laser desorption ionization time-of-flight
MBq	Mega Becquerel
Me	Methyl
MHz	Megahertz

min	Minute
mol	Mol
MOPS	3-morpholinopropane-1-sulfonic acid (buffer)
MS	Mass spectrometry
n	Polyethylene glycol units
n	stretching vibration
NHS	<i>N</i> -hydroxysuccinimide, <i>N</i> -hydroxysuccinimidyl
nm	Nanometer
NMR	Nuclear magnetic resonance
nt	Nucleotide
NTP	Nucleoside 5'-triphosphate
OD	Optical density
ORN	Oligoribonucleotide
ODN	Oligodeoxynucleotide
PAGE	Polyacrylamide gel electrophoresis
PBS	Phosphate buffered saline
PCR	Polymerase chain reaction
pCp	Cytidine 3',5'-bisphosphate
PEG	polyethylene glycole
PNA	Peptide nucleic acid
PNK	Polynucleotide kinase
ppm	Parts per million
q	Quartet (NMR)
quint.	Quintet (NMR)
rel int	Relative intensity
R _f	Retention factor (TLC)
RNA	Ribonucleic acid
RNAP	RNA polymerase
rpm	Rotations per minute
RT	Reverse transcription
rt	Room temperature
s	Singlet (NMR); strong (IR)
SDS	Sodiumdodecyl sulfate
sec	Second
SELEX	Systematic evolution of ligands by exponential enrichment
ss	Single stranded
t, <i>t</i>	Triplet, tert
T	Thymidine; Temperature
TBAF	Tetra- <i>n</i> -butylammonium fluoride
TAMRA	Tetramethyl-6-Carboxyrhodamine
TBDMS-Cl	<i>tert</i> -butyldimethylsilyl chloride

TBE	Tris-borate-EDTA buffer
TCA	Trichloroacetic acid
TCEP	Tris(2-carboxyethyl)phosphine
TEA	Triethylamine
TEAA	Triethylammonium acetate
TEMED	Tetramethylethylenediamine
TFA	Trifluoroacetic acid
THF	Tetrahydrofuran
TLC	Thin layer chromatography
T_m	Melting temperature (nucleic acids)
TOCSY	Total correlated spectroscopy (NMR)
t_R	Retention time (HPLC)
Tris	Trishydroxymethylaminomethane; 2-amino-2-hydroxymethyl-1,3-propanediol
U	Uridine; Unit
UTP	Uridine 5'-triphosphate
UV	Ultraviolet
V	Volt
W	Watt
w	Weak (IR)
wt	Wild type
δ	Chemical shift (NMR), bending vibration (IR)
ϵ	Molar extinction coefficient
λ	Wavelength
λ_{abs}	Absorption maximum
λ_{em}	Emission maximum
λ_{max}	Maximum absorption
f	femto
p	pico
n	nano
μ	micro
m	milli

6.7 Appendix

Thermal denaturation studies of the Diels-Alderase ribozyme

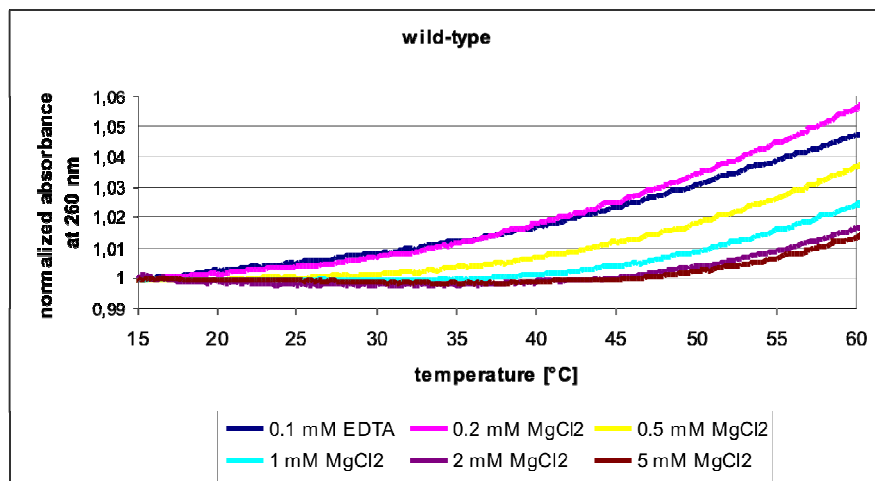


Figure 40: Absorption of the wild-type at different MgCl₂ concentrations respectively with EDTA.

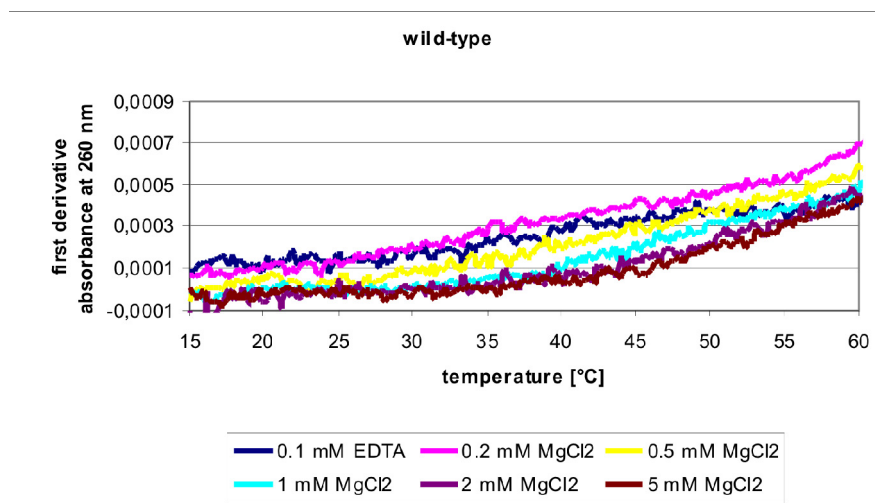


Figure 41: First derivative absorbance at 260 nm of the wild-type at different MgCl₂ concentrations respectively with EDTA.

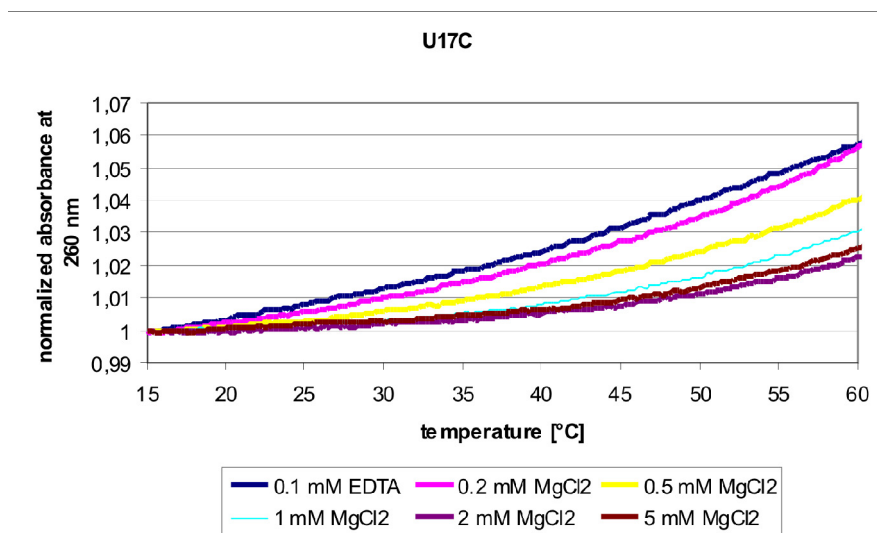


Figure 42: Absorption of the mutant U17C at different $MgCl_2$ concentrations respectively with EDTA.

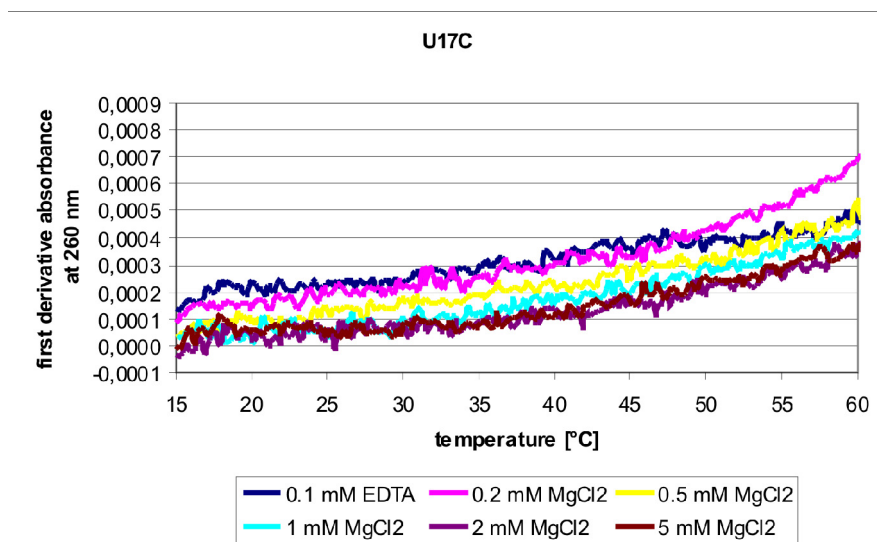


Figure 43: First derivative absorbance at 260 nm of the mutant U17C at different $MgCl_2$ concentrations respectively with EDTA.

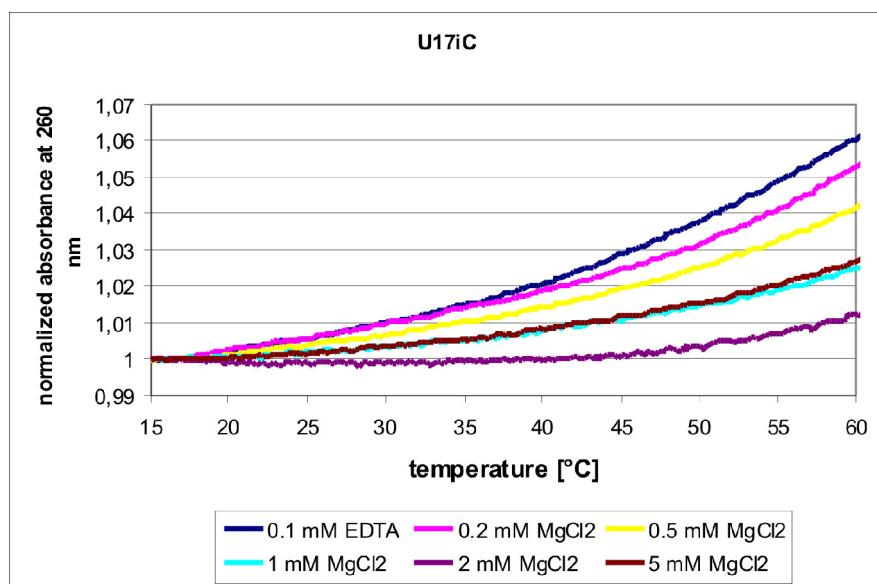


Figure 44: Absorption of the mutant U17iC at different MgCl₂ concentrations respectively with EDTA.

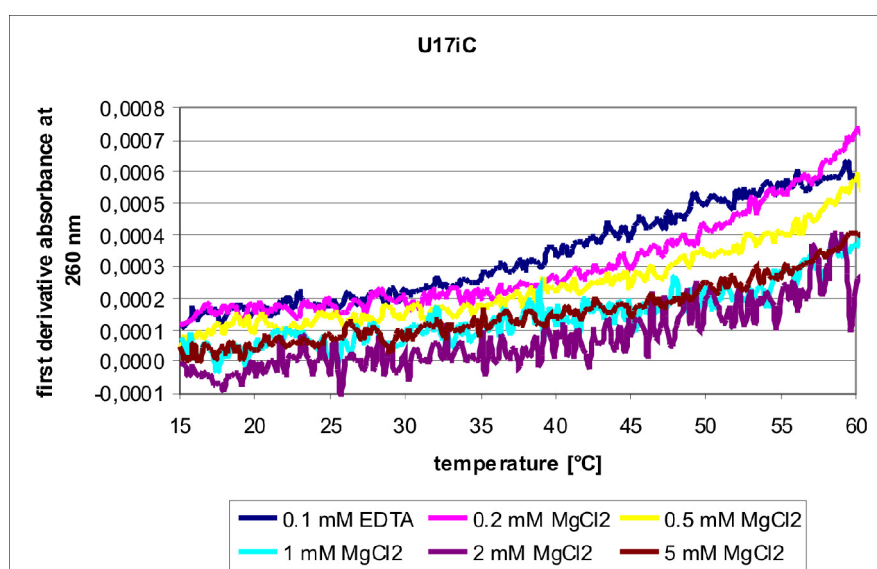


Figure 45: First derivative absorbance at 260 nm of the mutant U17iC at different MgCl₂ concentrations respectively with EDTA.

Bioorthogonal and orthogonal labeling of oligonucleotides

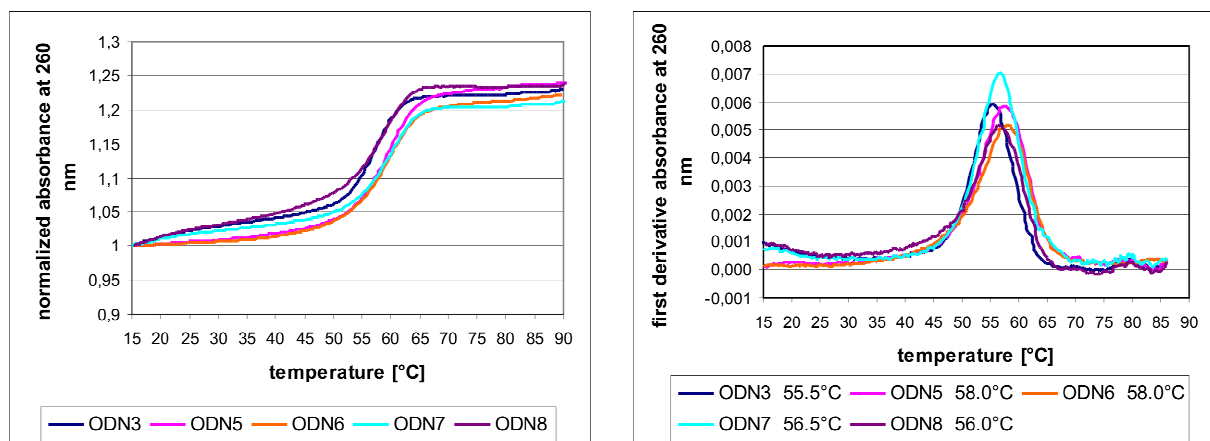


Figure: Determination of the melting temperature of the modified 15mer oligonucleotides. T_m was measured in 25 mM sodium cacodylate buffer pH 7.5 with 7.5 mM $MgCl_2$.

7 Bibliography

- [1] W. Gilbert - *Origin of life: The RNA world*, Nature **1986**, 319, 618.
- [2] F. H. Crick - *The origin of the genetic code*, J. Mol. Biol. **1968**, 38, 367-379.
- [3] K. Kruger, P. J. Grabowski, A. J. Zaug, J. Sands, D. E. Gottschling, T. R. Cech - *Self-splicing RNA: autoexcision and autocyclization of the ribosomal RNA intervening sequence of Tetrahymena*, Cell **1982**, 31, 147-157.
- [4] T. R. Cech, A. J. Zaug, P. J. Grabowski - *In vitro splicing of the ribosomal RNA precursor of Tetrahymena: involvement of a guanosine nucleotide in the excision of the intervening sequence*, Cell **1981**, 27, 487-496.
- [5] T. R. Cech - *Nobel lecture. Self-splicing and enzymatic activity of an intervening sequence RNA from Tetrahymena*, Biosci. Rep. **1990**, 10, 239-261.
- [6] C. Guerrier-Takada, K. Gardiner, T. Marsh, N. Pace, S. Altman - *The RNA moiety of ribonuclease P is the catalytic subunit of the enzyme*, Cell **1983**, 35, 849-857.
- [7] S. Altman - *The road to RNase P*, Nat. Struct. Biol. **2000**, 7, 827-828.
- [8] S. Altman - *Nobel lecture. Enzymatic cleavage of RNA by RNA*, Biosci. Rep. **1990**, 10, 317-337.
- [9] E. Puerta-Fernandez, C. Romero-Lopez, A. Barroso-delJesus, A. Berzal-Herranz - *Ribozymes: recent advances in the development of RNA tools*, FEMS Microbiol. Rev. **2003**, 27, 75-97.
- [10] A. C. Forster, R. H. Symons - *Self-cleavage of plus and minus RNAs of a virusoid and a structural model for the active sites*, Cell **1987**, 49, 211-220.
- [11] A. Hampel, R. Tritz - *RNA catalytic properties of the minimum (-)sTRSV sequence*, Biochemistry **1989**, 28, 4929-4933.
- [12] D. M. Lilley - *The Varkud satellite ribozyme*, RNA **2004**, 10, 151-158.
- [13] M. Y. Kuo, L. Sharmeen, G. Dinter-Gottlieb, J. Taylor - *Characterization of self-cleaving RNA sequences on the genome and antigenome of human hepatitis delta virus*, J. Virol. **1988**, 62, 4439-4444.
- [14] F. Crick, *The RNA world*, 1st, Cold Spring Harbor Laboratory Press, Cold Spring Harbor, New York, **1993**.
- [15] S. J. Klug, M. Famulok - *All you wanted to know about SELEX*, Mol. Biol. Rep. **1994**, 20, 97-107.
- [16] A. D. Ellington, J. W. Szostak - *In vitro selection of RNA molecules that bind specific ligands*, Nature **1990**, 346, 818-822.
- [17] G. F. Joyce - *Amplification, mutation and selection of catalytic RNA*, Gene **1989**, 82, 83-87.
- [18] C. Tuerk, L. Gold - *Systematic evolution of ligands by exponential enrichment: RNA ligands to bacteriophage T4 DNA polymerase*, Science **1990**, 249, 505-510.
- [19] D. L. Robertson, G. F. Joyce - *Selection in vitro of an RNA enzyme that specifically cleaves single-stranded DNA*, Nature **1990**, 344, 467-468.
- [20] D. P. Bartel, J. W. Szostak - *Isolation of new ribozymes from a large pool of random sequences*, Science **1993**, 261, 1411-1418.
- [21] M. Levy, K. E. Griswold, A. D. Ellington - *Direct selection of trans-acting ligase ribozymes by in vitro compartmentalization*, RNA **2005**, 11, 1555-1562.
- [22] J. J. Agresti, B. T. Kelly, A. Jäschke, A. D. Griffiths - *Selection of ribozymes that catalyze multiple-turnover Diels-Alder cycloadditions by using in vitro compartmentalization*, Proc. Natl. Acad. Sci. U S A **2005**, 102, 16170-16175.
- [23] T. Tuschl, P. A. Sharp, D. P. Bartel - *Selection in vitro of novel ribozymes from a partially randomized U2 and U6 snRNA library*, EMBO J. **1998**, 17, 2637-2650.

- [24] J. B. Thomson, S. T. Sigurdsson, A. Zeuch, F. Eckstein - *In vitro selection of hammerhead ribozymes containing a bulged nucleotide in stem II*, Nucleic Acids Res. **1996**, *24*, 4401-4406.
- [25] B. Sargueil, J. M. Burke - *In vitro selection of hairpin ribozymes*, Methods Mol. Biol. **1997**, *74*, 289-300.
- [26] B. Zhang, T. R. Cech - *Peptide bond formation by in vitro selected ribozymes*, Nature **1997**, *390*, 96-100.
- [27] D. H. Burke, L. Gold - *RNA aptamers to the adenosine moiety of S-adenosyl methionine: structural inferences from variations on a theme and the reproducibility of SELEX*, Nucleic Acids Res. **1997**, *25*, 2020-2024.
- [28] J. C. Cox, A. Hayhurst, J. Hesselberth, T. S. Bayer, G. Georgiou, A. D. Ellington - *Automated selection of aptamers against protein targets translated in vitro: from gene to aptamer*, Nucleic Acids Res. **2002**, *30*, e108.
- [29] J. R. Lorsch, J. W. Szostak - *In vitro selection of RNA aptamers specific for cyanocobalamin*, Biochemistry **1994**, *33*, 973-982.
- [30] M. Sassanfar, J. W. Szostak - *An RNA motif that binds ATP*, Nature **1993**, *364*, 550-553.
- [31] M. Famulok, J. W. Szostak - *Stereospecific recognition of tryptophan agarose by in vitro selected RNA*, J. Am. Chem. Soc. **1992**, *114*, 3990-3991.
- [32] G. J. Connell, M. Illangsekare, M. Yarus - *Three small ribooligonucleotides with specific arginine sites*, Biochemistry **1993**, *32*, 5497-5502.
- [33] L. A. Holeman, S. L. Robinson, J. W. Szostak, C. Wilson - *Isolation and characterization of fluorophore-binding RNA aptamers*, Fold Des. **1998**, *3*, 423-431.
- [34] J. Tang, R. R. Breaker - *Structural diversity of self-cleaving ribozymes*, Proc. Natl. Acad. Sci. U S A **2000**, *97*, 5784-5789.
- [35] M. Illangsekare, G. Sanchez, T. Nickles, M. Yarus - *Aminoacyl-RNA synthesis catalyzed by an RNA*, Science **1995**, *267*, 643-647.
- [36] M. Illangsekare, M. Yarus - *Specific, rapid synthesis of Phe-RNA by RNA*, Proc. Natl. Acad. Sci. U S A **1999**, *96*, 5470-5475.
- [37] E. H. Eklund, J. W. Szostak, D. P. Bartel - *Structurally complex and highly active RNA ligases derived from random RNA sequences*, Science **1995**, *269*, 364-370.
- [38] S. Fusz, A. Eisenfuhr, S. G. Srivatsan, A. Heckel, M. Famulok - *A ribozyme for the aldol reaction*, Chem. Biol. **2005**, *12*, 941-950.
- [39] J. Tsang, G. F. Joyce - *Specialization of the DNA-cleaving activity of a group I ribozyme through in vitro evolution*, J. Mol. Biol. **1996**, *262*, 31-42.
- [40] T. Pan, O. C. Uhlenbeck - *A small metalloribozyme with a two-step mechanism*, Nature **1992**, *358*, 560-563.
- [41] B. Seelig, A. Jäschke - *A small catalytic RNA motif with Diels-Alderase activity*, Chem. Biol. **1999**, *6*, 167-176.
- [42] T. M. Tarasow, S. L. Tarasow, B. E. Eaton - *RNA-catalysed carbon-carbon bond formation*, Nature **1997**, *389*, 54-57.
- [43] T. J. Kang, H. Suga - *In vitro selection of a 5'-purine ribonucleotide transferase ribozyme*, Nucleic Acids Res. **2007**, *35*, 4186-4194.
- [44] N. K. Vaish, P. A. Heaton, O. Fedorova, F. Eckstein - *In vitro selection of a purine nucleotide-specific hammerheadlike ribozyme*, Proc. Natl. Acad. Sci. U S A **1998**, *95*, 2158-2162.
- [45] A. Eisenfuhr, P. S. Arora, G. Sengle, L. R. Takaoka, J. S. Nowick, M. Famulok - *A ribozyme with michaelase activity: synthesis of the substrate precursors*, Bioorg. Med. Chem. **2003**, *11*, 235-249.
- [46] E. A. Curtis, D. P. Bartel - *New catalytic structures from an existing ribozyme*, Nat. Struct. Mol. Biol. **2005**, *12*, 994-1000.

- [47] T. W. Wiegand, R. C. Janssen, B. E. Eaton - *Selection of RNA amide synthases*, Chem. Biol. **1997**, *4*, 675-683.
- [48] L. Sun, Z. Cui, R. L. Gottlieb, B. Zhang - *A selected ribozyme catalyzing diverse dipeptide synthesis*, Chem. Biol. **2002**, *9*, 619-628.
- [49] X. Dai, A. De Mesmaeker, G. F. Joyce - *Cleavage of an amide bond by a ribozyme*, Science **1995**, *267*, 237-240.
- [50] F. Huang, M. Yarus - *5'-RNA self-capping from guanosine diphosphate*, Biochemistry **1997**, *36*, 6557-6563.
- [51] D. Nieuwlandt, M. West, X. Cheng, G. Kirshenheuter, B. E. Eaton - *The first example of an RNA urea synthase: selection through the enzyme active site of human neutrophil elastase*, Chembiochem **2003**, *4*, 651-654.
- [52] E. H. Eklund, D. P. Bartel - *RNA-catalysed RNA polymerization using nucleoside triphosphates*, Nature **1996**, *382*, 373-376.
- [53] C. Wilson, J. W. Szostak - *In vitro evolution of a self-alkylating ribozyme*, Nature **1995**, *374*, 777-782.
- [54] S. Tsukiji, S. B. Pattnaik, H. Suga - *Reduction of an aldehyde by a NADH/Zn²⁺ - dependent redox active ribozyme*, J. Am. Chem. Soc. **2004**, *126*, 5044-5045.
- [55] M. Wecker, D. Smith, L. Gold - *In vitro selection of a novel catalytic RNA: characterization of a sulfur alkylation reaction and interaction with a small peptide*, RNA **1996**, *2*, 982-994.
- [56] S. Tsukiji, S. B. Pattnaik, H. Suga - *An alcohol dehydrogenase ribozyme*, Nat. Struct. Biol. **2003**, *10*, 713-717.
- [57] M. M. Conn, J. R. Prudent, P. G. Schultz - *Porphyrin metalation catalyzed by a small RNA molecule*, J. Am. Chem. Soc. **1996**, *118*, 7012-7013.
- [58] P. A. Lohse, J. W. Szostak - *Ribozyme-catalysed amino-acid transfer reactions*, Nature **1996**, *381*, 442-444.
- [59] A. Jenne, M. Famulok - *A novel ribozyme with ester transferase activity*, Chem. Biol. **1998**, *5*, 23-34.
- [60] Y. Ryu, K. J. Kim, C. A. Roessner, A. I. Scott - *Decarboxylative Claisen condensation catalyzed by in vitro selected ribozymes*, Chem. Commun. (Camb) **2006**, 1439-1441.
- [61] D. S. Wilson, J. W. Szostak - *In vitro selection of functional nucleic acids*, Annu. Rev. Biochem. **1999**, *68*, 611-647.
- [62] O. Diels, K. Alder - *Synthesen in der hydroaromatischen Reihe*, Ann. Chem. **1928**, *460*, 98-122.
- [63] K. Fukui, T. Yonezawa, H. A. Shingu - *A molecular orbital theory of reactivity in aromatic hydrocarbons*, J. Chem. Phys. **1952**, *20*, 722-725.
- [64] R. B. Woodward, R. Hoffmann - *Conservation of Orbital Symmetry*, Angew. Chem. Int. Ed. Engl. **1969**, *8*, 781-853.
- [65] T. M. Tarasow, B. E. Eaton - *The Diels-Alder reaction and biopolymer catalysis*, Cell. Mol. Life Sci. **1999**, *55*, 1463-1472.
- [66] O. Diels, K. Alder - *Synthesen in der hydroaromatischen Reihe. XII. Mitteilung. („Dien-Synthesen“ sauerstoffhaltiger Heteroringe. 2. Dien-Synthesen des Furans.)*, Ann. Chem. **1931**, *490*, 243-257.
- [67] R. B. Woodward, H. Baer - *The Reaction of Furan with Maleic Anhydride*, J. Am. Chem. Soc. **1948**, *70*, 1161-1166.
- [68] T. A. Eggelte, H. d. Koning, H. O. Huisman - *Diels-Alder reaction of furan with some dienophiles*, Tetrahedron **1973**, *29*, 2491-2493.
- [69] D. C. Rideout, R. Breslow - *Hydrophobic acceleration of Diels-Alder reactions*, J. Am. Chem. Soc. **1980**, *102*, 7816-7817.
- [70] S. Otto, J. B. Engberts - *Hydrophobic interactions and chemical reactivity*, Org. Biomol. Chem. **2003**, *1*, 2809-2820.

- [71] L. Pauling - *Chemical achievement and hope for the future*, American Scientist **1948**, 36, 51-58.
- [72] W. P. Jencks, *Catalysis in Chemistry and Enzymology* McGraw Hill Book Co. Inc., New York, **1969**.
- [73] A. Tramontano, K. D. Janda, R. A. Lerner - *Catalytic antibodies*, Science **1986**, 234, 1566-1570.
- [74] E. Keinan, R. A. Lerner - *The First Decade of Antibody Catalysis: Perspective and Prospects.*, Isr. J. Chem. **1996**, 113-119.
- [75] R. A. Lerner, S. J. Benkovic - *Principles of antibody catalysis*, BioEssays **1988**, 9, 107-112.
- [76] V. E. Gouverneur, K. N. Houk, B. de Pascual-Teresa, B. Beno, K. D. Janda, R. A. Lerner - *Control of the exo and endo pathways of the Diels-Alder reaction by antibody catalysis*, Science **1993**, 262, 204-208.
- [77] D. Hilvert, K. W. Hill, K. D. Nared, M. T. M. Auditor - *Antibody catalysis of the Diels-Alder reaction*, J. Am. Chem. Soc. **1989**, 111, 9261-9262.
- [78] J. Chen, Q. Deng, R. Wang, K. Houk, D. Hilvert - *Shape complementarity, binding-site dynamics, and transition state stabilization: a theoretical study of Diels-Alder catalysis by antibody 1E9*, Chembiochem **2000**, 1, 255-261.
- [79] G. Pohnert - *Diels-Alderase*, Chembiochem **2001**, 2, 873-875.
- [80] S. Laschat - *Pericyclic Reactions in Biological Systems - Does Nature Know About the Diels-Alder Reaction?* Angew. Chem. Int. Ed. Engl. **1996**, 35, 289-291.
- [81] H. Oikawa, T. Tokiwano - *Enzymatic catalysis of the Diels-Alder reaction in the biosynthesis of natural products*, Nat. Prod. Rep. **2004**, 21, 321-352.
- [82] K. Auclair, A. Sutherland, J. Kennedy, D. J. Witter, J. P. V. d. Heever, C. R. Hutchinson, J. C. Vederas - *Lovastatin Nonaketide Synthase Catalyzes an Intramolecular Diels-Alder Reaction of a Substrate Analogue*, J. Am. Chem. Soc. **2000**, 122, 11519-11520.
- [83] K. Watanabe, T. Mie, A. Ichihara, H. Oikawa, M. Honma - *Detailed reaction mechanism of macrophomate synthase. Extraordinary enzyme catalyzing five-step transformation from 2-pyrone to benzoates*, J. Biol. Chem. **2000**, 275, 38393-38401.
- [84] J. M. Serafimov, D. Gillingham, S. Kuster, D. Hilvert - *The putative Diels-Alderase macrophomate synthase is an efficient aldolase*, J. Am. Chem. Soc. **2008**, 130, 7798-7799.
- [85] T. Ose, K. Watanabe, T. Mie, M. Honma, H. Watanabe, M. Yao, H. Oikawa, I. Tanaka - *Insight into a natural Diels-Alder reaction from the structure of macrophomate synthase*, Nature **2003**, 422, 185-189.
- [86] M. Linder, A. Hermansson, J. Liebeschuetz, T. Brinck - *Computational design of a lipase for catalysis of the Diels-Alder reaction*, J. Mol. Model. **2010**, doi:10.1007/s00894-010-0775-8.
- [87] D. J. Tantillo - *How an enzyme might accelerate an intramolecular Diels-Alder reaction: theozymes for the formation of salvileucalin B*, Org. Lett. **2010**, 12, 1164-1167.
- [88] J. B. Siegel, A. Zanghellini, H. M. Lovick, G. Kiss, A. R. Lambert, J. L. St Clair, J. L. Gallaher, D. Hilvert, M. H. Gelb, B. L. Stoddard, K. N. Houk, F. E. Michael, D. Baker - *Computational design of an enzyme catalyst for a stereoselective bimolecular Diels-Alder reaction*, Science **2010**, 329, 309-313.
- [89] A. Zanghellini, L. Jiang, A. M. Wollacott, G. Cheng, J. Meiler, E. A. Althoff, D. Rothlisberger, D. Baker - *New algorithms and an in silico benchmark for computational enzyme design*, Protein Sci. **2006**, 15, 2785-2794.
- [90] M. Chandra, S. K. Silverman - *DNA and RNA can be equally efficient catalysts for carbon-carbon bond formation*, J. Am. Chem. Soc. **2008**, 130, 2936-2937.

- [91] B. Seelig, S. Keiper, F. Stuhlmann, A. Jäschke - *Enantioselective Ribozyme Catalysis of a Bimolecular Cycloaddition Reaction*, *Angew. Chem. Int. Ed. Engl.* **2000**, *39*, 4576-4579.
- [92] S. Keiper, D. Bebenroth, B. Seelig, E. Westhof, A. Jäschke - *Architecture of a Diels-Alderase ribozyme with a preformed catalytic pocket*, *Chem. Biol.* **2004**, *11*, 1217-1227.
- [93] A. Serganov, S. Keiper, L. Malinina, V. Tereshko, E. Skripkin, C. Hobartner, A. Polonskaia, A. T. Phan, R. Wombacher, R. Micura, Z. Dauter, A. Jäschke, D. J. Patel - *Structural basis for Diels-Alder ribozyme-catalyzed carbon-carbon bond formation*, *Nat. Struct. Mol. Biol.* **2005**, *12*, 218-224.
- [94] D. W. Staple, S. E. Butcher - *Pseudoknots: RNA structures with diverse functions*, *PLoS Biol.* **2005**, *3*, e213.
- [95] S. Keiper - *Inaugural-Dissertation: Funktionelle und strukturelle Charakterisierung von Ribozymen für eine Diels-Alder-Reaktion*, Universität Heidelberg **2003**.
- [96] F. Stuhlmann, A. Jäschke - *Characterization of an RNA active site: Interactions between a Diels-Alderase ribozyme and its substrates and products*, *J. Am. Chem. Soc.* **2002**, *124*, 3238-3244.
- [97] E. A. Arn, J. Abelson, in *RNA Structure and Function* (Eds.: R. W. Simons, M. Grunberg-Manago), Cold Spring Harbor Laboratory Press, Cold Spring Harbor, NY, **1998**, 695-726.
- [98] J. R. Sampson, O. C. Uhlenbeck - *Biochemical and physical characterization of an unmodified yeast phenylalanine transfer RNA transcribed in vitro*, *Proc. Natl. Acad. Sci. U S A* **1988**, *85*, 1033-1037.
- [99] M. Samuels, A. Fire, P. A. Sharp - *Dinucleotide priming of transcription mediated by RNA polymerase II*, *J. Biol. Chem.* **1984**, *259*, 2517-2525.
- [100] R. K. Gaur, G. Krupp, *Chemical and Enzymatic Approaches to Construct Modified RNAs*, Humana Press Inc., Totowa, New Jersey, **1997**.
- [101] A. B. Burgin, N. R. Pace - *Mapping the active site of ribonuclease P RNA using a substrate containing a photoaffinity agent*, *EMBO J.* **1990**, *9*, 4111-4118.
- [102] J. C. Schlatterer, A. Jäschke - *Universal initiator nucleotides for the enzymatic synthesis of 5'-amino- and 5'-thiol-modified RNA*, *Biochem. Biophys. Res. Commun.* **2006**, *344*, 887-892.
- [103] L. Zhang, L. Sun, Z. Cui, R. L. Gottlieb, B. Zhang - *5'-sulfhydryl-modified RNA: initiator synthesis, in vitro transcription, and enzymatic incorporation*, *Bioconjug. Chem.* **2001**, *12*, 939-948.
- [104] D. Williamson, M. J. Cann, D. R. Hodgson - *Synthesis of 5'-amino-5'-deoxyguanosine-5'-N-phosphoramidate and its enzymatic incorporation at the 5'-termini of RNA molecules*, *Chem. Commun. (Camb)* **2007**, 5096-5098.
- [105] S. Pfander, R. Fiamengo, S. I. Kirin, N. Metzler-Nolte, A. Jäschke - *Reversible site-specific tagging of enzymatically synthesized RNAs using aldehyde-hydrazine chemistry and protease-cleavable linkers*, *Nucleic Acids Res.* **2007**, *35*, e25.
- [106] S. Fusz, S. G. Srivatsan, D. Ackermann, M. Famulok - *Photocleavable initiator nucleotide substrates for an aldolase ribozyme*, *J. Org. Chem.* **2008**, *73*, 5069-5077.
- [107] <http://www.trilinkbiotech.com>
- [108] F. Huang, G. Wang, T. Coleman, N. Li - *Synthesis of adenosine derivatives as transcription initiators and preparation of 5' fluorescein- and biotin-labeled RNA through one-step in vitro transcription*, *RNA* **2003**, *9*, 1562-1570.
- [109] N. Li, C. Yu, F. Huang - *Novel cyanine-AMP conjugates for efficient 5' RNA fluorescent labeling by one-step transcription and replacement of [gamma-32P]ATP in RNA structural investigation*, *Nucleic Acids Res.* **2005**, *33*, e37.

- [110] F. Huang, J. He, Y. Zhang, Y. Guo - *Synthesis of biotin-AMP conjugate for 5' biotin labeling of RNA through one-step in vitro transcription*, Nat. Protoc. **2008**, 3, 1848-1861.
- [111] B. Seelig, A. Jäschke - *Ternary conjugates of guanosine monophosphate as initiator nucleotides for the enzymatic synthesis of 5'-modified RNAs*, Bioconjug. Chem. **1999**, 10, 371-378.
- [112] M. Helm, M. Petermeier, B. Ge, R. Fiammengo, A. Jäschke - *Allosterically activated Diels-Alder catalysis by a ribozyme*, J. Am. Chem. Soc. **2005**, 127, 10492-10493.
- [113] D. K. Willkomm, R. K. Hartmann, *Handbook of RNA Biochemistry*, WILEY-VCH Verlag GmbH & Co. KGaA, Weinheim, **2005**.
- [114] A. J. Svoboda, E. H. McConkey - *Crosslinking of proteins to ribosomal RNA in HeLa cell polysomes by sodium periodate*, Biochem. Biophys. Res. Commun. **1978**, 81, 1145-1152.
- [115] R. E. Hileman, K. M. Parkhurst, N. K. Gupta, L. J. Parkhurst - *Synthesis and Characterization of Conjugates Formed between Periodate-Oxidized Ribonucleotides and Amine-Containing Fluorophores*, Bioconjug. Chem. **1994**, 5, 436-444.
- [116] T. C. Chu, K. Y. Twu, A. D. Ellington, M. Levy - *Aptamer mediated siRNA delivery*, Nucleic Acids Res. **2006**, 34, e73.
- [117] C. J. Sanderson, D. V. Wilson - *A simple method for coupling proteins to insoluble polysaccharides*, Immunology **1971**, 20, 1061-1065.
- [118] P. R. Whitfeld, R. Markham - *Natural Configuration of the Purine Nucleotides in Ribonucleic Acids: Chemical Hydrolysis of the Dinucleoside Phosphates*, Nature **1953**, 171, 1151-1152.
- [119] F. Hansske, F. Cramer, *Modification of the 3' terminus of tRNA by periodate oxidation and subsequent reaction with hydrazides*, Methods Enzymol. **1979**, 59, 172-181.
- [120] D. Proudnikov, A. Mirzabekov - *Chemical methods of DNA and RNA fluorescent labeling*, Nucleic Acids Res. **1996**, 24, 4535-4542.
- [121] C. Hobartner, P. I. Pradeepkumar, S. K. Silverman - *Site-selective depurination by a periodate-dependent deoxyribozyme*, Chem. Commun. (Camb) **2007**, 2255-2257.
- [122] K. Lu, Q. P. Duan, L. Ma, D. X. Zhao - *Chemical strategies for the synthesis of peptide-oligonucleotide conjugates*, Bioconjug. Chem. **2010**, 21, 187-202.
- [123] D. M. Rosenbaum, D. R. Liu - *Efficient and sequence-specific DNA-templated polymerization of peptide nucleic acid aldehydes*, J. Am. Chem. Soc. **2003**, 125, 13924-13925.
- [124] R. E. Kleiner, Y. Brudno, M. E. Birnbaum, D. R. Liu - *DNA-templated polymerization of side-chain-functionalized peptide nucleic acid aldehydes*, J. Am. Chem. Soc. **2008**, 130, 4646-4659.
- [125] Y. Brudno, M. E. Birnbaum, R. E. Kleiner, D. R. Liu - *An in vitro translation, selection and amplification system for peptide nucleic acids*, Nat. Chem. Biol. **2010**, 6, 148-155.
- [126] G. T. Hermanson, *Bioconjugate Techniques*, Academic Press, Inc., San Diego, CA, **1996**.
- [127] M. Oberhuber, G. F. Joyce - *A DNA-templated aldol reaction as a model for the formation of pentose sugars in the RNA world*, Angew. Chem. Int. Ed. Engl. **2005**, 44, 7580-7583.
- [128] Z. J. Gartner, M. W. Kanan, D. R. Liu - *Expanding the reaction scope of DNA-templated synthesis*, Angew. Chem. Int. Ed. Engl. **2002**, 41, 1796-1800.
- [129] J. Fan, G. Sun, C. Wan, Z. Wang, Y. Li - *Investigation of DNA as a catalyst for Henry reaction in water*, Chem. Commun. (Camb) **2008**, 32, 3792-3794.
- [130] J. Dambachera, W. Zhaoa, A. El-Battaa, R. Annessa, C. Jianga, M. Bergdahl - *Water is an efficient medium for Wittig reactions employing stabilized ylides and aldehydes*, Tetrahedron Lett. **2005**, 46, 4473-4477.

- [131] Z. J. Gartner, R. Grubina, C. T. Calderone, D. R. Liu - *Two enabling architectures for DNA-templated organic synthesis*, *Angew. Chem. Int. Ed. Engl.* **2003**, *42*, 1370-1375.
- [132] M. L. McKee, P. J. Milnes, J. Bath, E. Stulz, A. J. Turberfield, R. K. O'Reilly - *Multistep DNA-templated reactions for the synthesis of functional sequence controlled oligomers*, *Angew. Chem. Int. Ed. Engl.* **2010**, *49*, 7948-7951.
- [133] I. Ugi, C. Steinbrückner - *Über ein neues Kondensations-Prinzip*, *Angew. Chem.* **1960**, *72*, 267-268.
- [134] S. Marcaccini, T. Torroba - *The use of the Ugi four-component condensation*, *Nat. Protoc.* **2007**, *2*, 632 - 639.
- [135] M. C. Pirrung, K. D. Sarma - *Multicomponent reactions are accelerated in water*, *J. Am. Chem. Soc.* **2004**, *126*, 444-445.
- [136] M. Waki, J. Meienhofer - *Peptide synthesis using the four-component condensation (Ugi reaction)*, *J. Am. Chem. Soc.* **1977**, *99*, 6075-6082.
- [137] C. Baldoli, S. Maiorana, E. Licandro, G. Zinzalla, D. Perdicchia - *Synthesis of chiral chromium tricarbonyl labeled thymine PNA monomers via the Ugi reaction*, *Org. Lett.* **2002**, *4*, 4341-4344.
- [138] N. S. Joshi, L. R. Whitaker, M. B. Francis - *A three-component Mannich-type reaction for selective tyrosine bioconjugation*, *J. Am. Chem. Soc.* **2004**, *126*, 15942-15943.
- [139] L. F. Fieser, J. L. Hartwell, J. E. Jones, J. H. Wood, R. W. Bost - *9-anthraaldehyde, 2-ethoxy-1-naphthaldehyde*, *Org. Synth.* **1940**, *20*, 11.
- [140] R. Fiammengo, K. Musilek, A. Jäschke - *Efficient preparation of organic substrate-RNA conjugates via in vitro transcription*, *J. Am. Chem. Soc.* **2005**, *127*, 9271-9276.
- [141] F. W. Kotch, V. Sidorov, Y. F. Lam, K. J. Kayser, H. Li, M. S. Kaucher, J. T. Davis - *Water-mediated association provides an ion pair receptor*, *J. Am. Chem. Soc.* **2003**, *125*, 15140-15150.
- [142] X.-F. Zhu, H. J. Williams, A. I. Scott - *Facile and highly selective 5'-desilylation of multisilylated nucleosides*, *J. Chem. Soc., Perkin Trans. 1* **2000**, 2305-2306.
- [143] Y. Hayakawa, M. Kataoka - *Facile synthesis of oligodeoxyribonucleotides via the phosphoramidite method without nucleoside base protection*, *J. Am. Chem. Soc.* **1998**, *120*, 12395-12401.
- [144] B. M. Choudary, N. S. Chowdari, M. L. Kantam - *Montmorillonite clay catalyzed tosylation of alcohols and selective monotosylation of diols with p-toluenesulfonic acid: An enviro-economic route*, *Tetrahedron* **2000**, *56*, 7291-7298.
- [145] A. Bouzide, G. Sauve - *Silver(I) oxide mediated highly selective monotosylation of symmetrical diols. Application to the synthesis of polysubstituted cyclic ethers*, *Org. Lett.* **2002**, *4*, 2329-2332.
- [146] M. A. Petersen, L. G. Yin, E. Kokkoli, M. A. Hillmyer - *Synthesis and characterization of reactive PEO-PMCL polymersomes*, *Polym. Chem.* **2010**, *1*, 1281-1290.
- [147] J. W. Bae, E. Lee, K. M. Park, K. D. Park - *Vinyl Sulfone-Terminated PEG-PLLA Diblock Copolymer for Thiol-Reactive Polymeric Micelle*, *Macromolecules* **2009**, *42*, 3437-3442.
- [148] D. Shenoy, W. Fu, J. Li, C. Crasto, G. Jones, C. DiMarzio, S. Sridhar, M. Amiji - *Surface functionalization of gold nanoparticles using hetero-bifunctional poly(ethylene glycol) spacer for intracellular tracking and delivery*, *Int. J. Nanomedicine* **2006**, *1*, 51-57.
- [149] Y. K. Wu, P. Ahlberg - *Preparation of 4,4-Dimethoxybutyl Iodide from 1,4-Butanediol Via the Corresponding Tosylate*, *J. Org. Chem.* **1994**, *59*, 5076-5077.
- [150] H. Bauer, F. Stier, C. Petry, A. Knorr, C. Stadler, H. A. Staab - *Electron donor-acceptor compounds, 52. Phenothiazine-bipyridinium cyclophanes*, *Eur. J. Org. Chem.* **2001**, 3255-3278.

- [151] S. Ciampi, T. Bocking, K. A. Kilian, J. B. Harper, J. J. Gooding - *Click chemistry in mesoporous materials: functionalization of porous silicon rugate filters*, *Langmuir* **2008**, *24*, 5888-5892.
- [152] K. Shimada, R. Nagahata, S. Kawabata, S. Matsuyama, T. Saito, S. Kinugasa - *Evaluation of the quantitiveness of matrix-assisted laser desorption/ionization time-of-flight mass spectrometry using an equimolar mixture of uniform poly(ethylene glycol) oligomers*, *J. Mass. Spectrom.* **2003**, *38*, 948-954.
- [153] G. Montaudo, R. P. Lattimer, *Mass Spectrometry of Polymers*, CRC Press, Boca Raton, Florida, **2002**.
- [154] H. Togashi - *Competitive attachment of alkali cations to poly(ethylene glycol) and poly(propylene glycol) oligomers in matrix-assisted laser desorption/ionization process*, *Chem. Lett.* **2000**, *6*, 704-705.
- [155] J. Gross, oral presentation, **2007**.
- [156] J. F. Milligan, D. R. Groebe, G. W. Witherell, O. C. Uhlenbeck - *Oligoribonucleotide synthesis using T7 RNA polymerase and synthetic DNA templates*, *Nucleic Acids Res.* **1987**, *15*, 8783-8798.
- [157] J. F. Milligan, O. C. Uhlenbeck - *Synthesis of small RNAs using T7 RNA polymerase*, *Methods Enzymol.* **1989**, *180*, 51-62.
- [158] R. Fiammengo, personal communication, **2005**.
- [159] O. C. Musgrave - *Oxidation of alkyl aryl ethers*, *Chem. Rev.* **1969**, *69*, 499-531.
- [160] H. Kotani, K. Ohkubo, S. Fukuzumi - *Photocatalytic oxygenation of anthracenes and olefins with dioxygen via selective radical coupling using 9-mesityl-10-methylacridinium ion as an effective electron-transfer photocatalyst*, *J. Am. Chem. Soc.* **2004**, *126*, 15999-16006.
- [161] S. S. Sastry, B. M. Ross - *Nuclease activity of T7 RNA polymerase and the heterogeneity of transcription elongation complexes*, *J. Biol. Chem.* **1997**, *272*, 8644-8652.
- [162] R. T. Batey, R. P. Rambo, J. A. Doudna - *Tertiary Motifs in RNA Structure and Folding*, *Angew. Chem. Int. Ed. Engl.* **1999**, *38*, 2326-2343.
- [163] B. Felden - *RNA structure: experimental analysis*, *Curr. Opin. Microbiol.* **2007**, *10*, 286-291.
- [164] A. M. Pyle - *Ribozymes: a distinct class of metalloenzymes*, *Science* **1993**, *261*, 709-714.
- [165] J. H. Cate, R. L. Hanna, J. A. Doudna - *A magnesium ion core at the heart of a ribozyme domain*, *Nat. Struct. Biol.* **1997**, *4*, 553-558.
- [166] I. Tinoco, Jr., J. S. Kieft - *The ion core in RNA folding*, *Nat. Struct. Biol.* **1997**, *4*, 509-512.
- [167] R. Das, K. J. Travers, Y. Bai, D. Herschlag - *Determining the Mg²⁺ stoichiometry for folding an RNA metal ion core*, *J. Am. Chem. Soc.* **2005**, *127*, 8272-8273.
- [168] V. L. Pecoraro, J. D. Hermes, W. W. Cleland - *Stability constants of Mg²⁺ and Cd²⁺ complexes of adenine nucleotides and thionucleotides and rate constants for formation and dissociation of MgATP and MgADP*, *Biochemistry* **1984**, *23*, 5262-5271.
- [169] D. Lambert, D. Leipply, R. Shiman, D. E. Draper - *The influence of monovalent cation size on the stability of RNA tertiary structures*, *J. Mol. Biol.* **2009**, *390*, 791-804.
- [170] D. E. Draper - *RNA folding: thermodynamic and molecular descriptions of the roles of ions*, *Biophys. J.* **2008**, *95*, 5489-5495.
- [171] J. B. Murray, A. A. Seyhan, N. G. Walter, J. M. Burke, W. G. Scott - *The hammerhead, hairpin and VS ribozymes are catalytically proficient in monovalent cations alone*, *Chem. Biol.* **1998**, *5*, 587-595.
- [172] J. Schnabl, R. K. Sigel - *Controlling ribozyme activity by metal ions*, *Curr. Opin. Chem. Biol.* **2010**, *14*, 269-275.

- [173] M. Egli, G. Minasov, L. Su, A. Rich - *Metal ions and flexibility in a viral RNA pseudoknot at atomic resolution*, Proc. Natl. Acad. Sci. U S A **2002**, *99*, 4302-4307.
- [174] D. Grilley, A. M. Soto, D. E. Draper - *Mg²⁺-RNA interaction free energies and their relationship to the folding of RNA tertiary structures*, Proc. Natl. Acad. Sci. U S A **2006**, *103*, 14003-14008.
- [175] A. Y. Kobitski, A. Nierth, M. Helm, A. Jäschke, G. U. Nienhaus - *Mg²⁺-dependent folding of a Diels-Alderase ribozyme probed by single-molecule FRET analysis*, Nucleic Acids Res. **2007**, *35*, 2047-2059.
- [176] N. Kisseleva, S. Kraut, A. Jäschke, O. Schiemann - *Characterizing multiple metal ion binding sites within a ribozyme by cadmium-induced EPR silencing*, HFSP J. **2007**, *1*, 127-136.
- [177] T. Berezniak, M. Zahran, P. Imhof, A. Jäschke, J. C. Smith - *Magnesium-dependent active-site conformational selection in the Diels-Alderase ribozyme*, J. Am. Chem. Soc. **2010**, *132*, 12587-12596.
- [178] E. Bebenroth - *Inaugural-Dissertation: Über Struktur-Funktions-Beziehungen zur Architektur von Ribozymen für eine Diels-Alder-Reaktion*, Universität Heidelberg, **2007**.
- [179] S. Kraut, A. Jäschke, personal communication, **2010**.
- [180] J. D. Puglisi, I. Tinoco, Jr. - *Absorbance melting curves of RNA*, Methods Enzymol. **1989**, *180*, 304-325.
- [181] J. A. Jaeger, J. SantaLucia, Jr., I. Tinoco, Jr. - *Determination of RNA structure and thermodynamics*, Annu. Rev. Biochem. **1993**, *62*, 255-287.
- [182] J. L. Mergny, L. Lacroix - *Analysis of thermal melting curves*, Oligonucleotides **2003**, *13*, 515-537.
- [183] J. Santalucia, in *Spectrophotometry and Spectrofluorimetry: A Practical Approach* (Ed.: M. G. Gore), Oxford, Oxford University Press, **2000**.
- [184] J. M. Thomas, M. E. Hodes - *A new discontinuous buffer system for the electrophoresis of cationic proteins at near-neutral pH*, Anal. Biochem. **1981**, *118*, 194-196.
- [185] K. J. Ellis, J. F. Morrison - *Buffers of constant ionic strength for studying pH-dependent processes*, Methods Enzymol. **1982**, *87*, 405-426.
- [186] J. Sambrook, D. Russell, *Molecular Cloning: A Laboratory Manual*, Cold Spring Harbor Laboratory Press, Cold Spring Harbor, New York, **2001**.
- [187] H. Fukada, K. Takahashi - *Enthalpy and heat capacity changes for the proton dissociation of various buffer components in 0.1 M potassium chloride*, Proteins: Struct., Funct., Bioinf. **1998**, *33*, 159-166.
- [188] P. L. Nixon, C. A. Theimer, D. P. Giedroc - *Thermodynamics of stabilization of RNA pseudoknots by cobalt(III) hexaammine*, Biopolymers **1999**, *50*, 443-458.
- [189] L. I. Willems, M. Verdoes, B. I. Florea, G. A. van der Marel, H. S. Overkleeft - *Two-Step Labeling of Endogenous Enzymatic Activities by Diels-Alder Ligation*, ChemBiochem **2010**, *11*, 1769-1781.
- [190] J. C. Jewett, C. R. Bertozzi - *Cu-free click cycloaddition reactions in chemical biology*, Chem. Soc. Rev. **2010**, *39*, 1272-1279.
- [191] R. T. Ranasinghe, T. Brown - *Fluorescence based strategies for genetic analysis*, Chem. Commun. (Camb) **2005**, 5487-5502.
- [192] V. V. Didenko - *DNA probes using fluorescence resonance energy transfer (FRET): designs and applications*, Biotechniques **2001**, *31*, 1106-1116, 1118, 1120-1101.
- [193] S. Weiss - *Measuring conformational dynamics of biomolecules by single molecule fluorescence spectroscopy*, Nat. Struct. Biol. **2000**, *7*, 724-729.
- [194] A. N. Kapanidis, T. Strick - *Biology, one molecule at a time*, Trends Biochem. Sci. **2009**, *34*, 234-243.

- [195] A. Bayer - *Ueber eine neue Klasse von Farbstoffen*, Ber. Dtsch. Chem. Ges. **1871**, 4, 555-558.
- [196] L. J. Kricka, P. Fortina - *Analytical Ancestry: "Firsts" in Fluorescent Labeling of Nucleosides, Nucleotides, and Nucleic Acids*, Clin. Chem. **2009**, 55, 670-683.
- [197] J. C. Schulhof, D. Molko, R. Teoule - *The Final Deprotection Step in Oligonucleotide Synthesis Is Reduced to a Mild and Rapid Ammonia Treatment by Using Labile Base-Protecting Groups*, Nucleic Acids Res. **1987**, 15, 397-416.
- [198] S. Berndt, N. Herzig, P. Kele, D. Lachmann, X. H. Li, O. S. Wolfbeis, H. A. Wagenknecht - *Comparison of a Nucleosidic vs Non-Nucleosidic Postsynthetic "Click" Modification of DNA with Base-Labile Fluorescent Probes*, Bioconjug. Chem. **2009**, 20, 558-564.
- [199] P. M. Gramlich, C. T. Wirges, A. Manetto, T. Carell - *Postsynthetic DNA modification through the copper-catalyzed azide-alkyne cycloaddition reaction*, Angew. Chem. Int. Ed. Engl **2008**, 47, 8350-8358.
- [200] S. H. Weisbrod, A. Marx - *Novel strategies for the site-specific covalent labelling of nucleic acids*, Chem. Commun. **2008**, 5675-5685.
- [201] P. C. Jocelyn, *Biochemistry of the SH Group*, Academic Press, New York, **1972**.
- [202] K. Shimada, K. Mitamura - *Derivatization of thiol-containing compounds*, J. Chromatogr. B. Biomed. Appl. **1994**, 659, 227-241.
- [203] B. A. Connolly, P. Rider - *Chemical synthesis of oligonucleotides containing a free sulphhydryl group and subsequent attachment of thiol specific probes*, Nucleic Acids Res. **1985**, 13, 4485-4502.
- [204] R. Zuckermann, D. Corey, P. Schultz - *Efficient methods for attachment of thiol specific probes to the 3'-ends of synthetic oligodeoxyribonucleotides*, Nucleic Acids Res. **1987**, 15, 5305-5321.
- [205] M. E. Levison, A. S. Josephson, D. M. Kirschenbaum - *Reduction of Biological Substances by Water-Soluble Phosphines: ζ -Globulin (Igg)*, Experientia **1969**, 25, 126-127.
- [206] U. T. Rügge, J. Rudinger, *Cleavage of disulfide bonds in proteins*, Academic Press, San Diego, **1977**.
- [207] J. A. Burns, J. C. Butler, J. Moran, G. M. Whitesides - *Selective Reduction of Disulfides by Tris(2-Carboxyethyl)Phosphine*, J. Org. Chem. **1991**, 56, 2648-2650.
- [208] J. C. Han, G. Y. Han - *A Procedure for Quantitative-Determination of Tris(2-Carboxyethyl)Phosphine, an Odorless Reducing Agent More Stable and Effective Than Dithiothreitol*, Anal. Biochem. **1994**, 220, 5-10.
- [209] D. E. Shafer, J. K. Inman, A. Lees - *Reaction of tris(2-carboxyethyl)phosphine (TCEP) with maleimide and alpha-haloacyl groups: Anomalous elution of TCEP by gel filtration*, Anal. Biochem. **2000**, 282, 161-164.
- [210] K. Tyagarajan, E. Pretzer, J. E. Wiktorowicz - *Thiol-reactive dyes for fluorescence labeling of proteomic samples*, Electrophoresis **2003**, 24, 2348-2358.
- [211] E. B. Getz, M. Xiao, T. Chakrabarty, R. Cooke, P. R. Selvin - *A comparison between the sulphhydryl reductants tris(2-carboxyethyl)phosphine and dithiothreitol for use in protein biochemistry*, Anal. Biochem. **1999**, 273, 73-80.
- [212] R. Breslow - *Hydrophobic Effects on Simple Organic-Reactions in Water*, Accounts Chem. Res. **1991**, 24, 159-164.
- [213] S. Otto, F. Bertocin, J. B. Engberts - *Lewis acid catalysis of a Diels-Alder reaction in water*, J. Am. Chem. Soc. **1996**, 118, 7702-7707.
- [214] W. Blokzijl, J. B. Engberts - *Enforced Hydrophobic Interactions and Hydrogen-Bonding in the Acceleration of Diels-Alder Reactions in Water*, Structure and Reactivity in Aqueous Solution, ACS Symposium Series **1994**, 568, 303-317.

- [215] A. D. de Araujo, J. M. Palomo, J. Cramer, M. Kohn, H. Schroder, R. Wacker, C. Niemeyer, K. Alexandrov, H. Waldmann - *Diels-Alder ligation and surface immobilization of proteins*, *Angew. Chem. Int. Ed. Engl.* **2005**, *45*, 296-301.
- [216] A. D. de Araujo, J. M. Palomo, J. Cramer, O. Seitz, K. Alexandrov, H. Waldmann - *Diels-Alder ligation of peptides and proteins*, *Chemistry* **2006**, *12*, 6095-6109.
- [217] V. Marchan, A. Grandas - *Synthesis of Peptide-oligonucleotide conjugates by Diels-Alder cycloaddition in water*, *Curr. Protoc. Nucleic. Acid. Chem.* **2007**, *Chapter 4*, Unit 4.32.
- [218] V. Steven, D. Graham - *Oligonucleotide conjugation to a cell-penetrating (TAT) peptide by Diels-Alder cycloaddition*, *Org. Biomol. Chem.* **2008**, *6*, 3781-3787.
- [219] V. Borsenberger, S. Howorka - *Diene-modified nucleotides for the Diels-Alder-mediated functional tagging of DNA*, *Nucleic Acids Res.* **2009**, *37*, 1477-1485.
- [220] A. H. El-Sagheer, V. V. Cheong, T. Brown - *Rapid chemical ligation of oligonucleotides by the Diels-Alder reaction*, *Org. Biomol. Chem.* **2011**, *9*, 232-235.
- [221] K. W. Hill, J. Taunton-Rigby, J. D. Carter, E. Kropp, K. Vagle, W. Pieken, D. P. C. McGee, G. M. Husar, M. Leuck, D. J. Anziano, D. P. Sebesta - *Diels-Alder bioconjugation of diene-modified oligonucleotides*, *J. Org. Chem.* **2001**, *66*, 5352-5358.
- [222] D. Graham, A. Grondin, C. McHugh, L. Fruk, W. E. Smith - *Internal labeling of oligonucleotide probes by Diels-Alder cycloaddition*, *Tetrahedron Lett.* **2002**, *43*, 4785-4788.
- [223] D. L. J. Sauer, A. Mielert, - *The Order of Reactivity of Dienes towards Maleic Anhydride in the Diels-Alder Reaction*, *Angew. Chem. Int. Ed. Engl.* **1962**, *74*, 268-269.
- [224] H. Vorbrueggen - *Adventures in silicon - Organic chemistry*, *Accounts Chem. Res.* **1995**, *28*, 509-520.
- [225] P. Y. Reddy, S. Kondo, T. Toru, Y. Ueno - *Lewis acid and hexamethyldisilazane-promoted efficient synthesis of N-alkyl- and N-arylimide derivatives*, *J. Org. Chem.* **1997**, *62*, 2652-2654.
- [226] F. Ilhan, D. S. Tyson, D. J. Stasko, K. Kirschbaum, M. A. Meador - *Twisted, Z-shaped perylene bisimide*, *J. Am. Chem. Soc.* **2006**, *128*, 702-703.
- [227] S. S. Newaz - *TCEP a reagent of choice in both Proteomics and nucleic acid chemistry*, www.polyorganix.com.
- [228] E. Pretzer, J. E. Wiktorowicz - *Saturation fluorescence labeling of proteins for proteomic analyses*, *Anal. Biochem.* **2008**, *374*, 250-262.
- [229] C. Da Pieve, P. Williams, D. M. Haddleton, R. M. Palmer, S. Missailidis - *Modification of thiol functionalized aptamers by conjugation of synthetic polymers*, *Bioconjug. Chem.* **2010**, *21*, 169-174.
- [230] D. G. Nickens, N. Bardiya, J. T. Patterson, D. H. Burke - *Template-directed ligation of tethered mononucleotides by t4 DNA ligase for kinase ribozyme selection*, *PLoS One* **2010**, *5*, e12368.
- [231] A. Bugaut, J. J. Toulme, B. Rayner - *SELEX and dynamic combinatorial chemistry interplay for the selection of conjugated RNA aptamers*, *Org. Biomol. Chem.* **2006**, *4*, 4082-4088.
- [232] *Data 28-9416-50 AA*, GE Healthcare.
- [233] Thermo Fisher Scientific Inc., **2008**.
- [234] K. L. Berkner, W. R. Folk - *Polynucleotide kinase exchange reaction: quantitative assay for restriction endonuclease-generated 5'-phosphoroyl termini in DNA*, *J. Biol. Chem.* **1977**, *252*, 3176-3184.
- [235] R. I. Gumport, O. C. Uhlenbeck - *T4 RNA ligase as a nucleic acid synthesis and modification reagent*, *Gene Amplif. Anal.* **1981**, *2*, 313-345.

- [236] T. E. England, O. C. Uhlenbeck - *3'-terminal labelling of RNA with T4 RNA ligase*, Nature **1978**, 275, 560-561.
- [237] S. L. Beaucage, R. P. Iyer - *The functionalization of oligonucleotides via phosphoramidite derivatives*, Tetrahedron **1993**, 49, 1925.
- [238] M. H. Caruthers, A. D. Barone, S. L. Beaucage, D. R. Dodds, E. F. Fisher, L. J. McBride, M. Matteucci, Z. Stabinsky, J. Y. Tang - *Chemical synthesis of deoxyoligonucleotides by the phosphoramidite method*, Methods Enzymol. **1987**, 154, 287-313.

Affidavit for dissertation

I hereby declare that this thesis has been written only by the undersigned and without any assistance from third parties. Furthermore, I confirm that no sources have been used in the preparation of this thesis other than those indicated in the thesis itself.

Florentine Wahl